CRCLEME
Cooperative Research Centre for
Landscape Evolution & Mineral Exploration

CSIRO
EXPLORATION
AND MINING

AMIRA
Australian Mineral Industries Research Association Limited ACN 004 448 266

OPEN FILE
REPORT
SERIES

REPORT ON LATERITE GEOCHEMISTRY IN THE CSIRO-AGE DATABASE FOR THE SOUTHERN MURCHISON REGION

(Yalgoo, Kirkalocka, Perenjori, Ninghan sheets)

E.C. Grunsky, J. Innes, R.E. Smith and J.L. Perdrix

CRC LEME OPEN FILE REPORT 8

October 1998

(CSIRO Division of Exploration Geoscience Report 2R, 1988.
Second impression 1998)

AMIRA
Australian Mineral Industries Research Association Limited ACN 004 448 266

CRCLEME
Cooperative Research Centre for
Landscape Evolution & Mineral Exploration

CSIRO
EXPLORATION
AND MINING

REPORT ON LATERITE GEOCHEMISTRY IN THE CSIRO-AGE DATABASE FOR THE SOUTHERN MURCHISON REGION (Yalgoo, Kirkalocka, Perenjori, Ninghan sheets)

E.C. Grunsky, J. Innes, R.E. Smith and J.L. Perdrix

CRC LEME OPEN FILE REPORT 8

October 1998

(CSIRO Division of Exploration Geoscience Report 2R, 1988.
Second impression 1998)

CRC LEME is an unincorporated joint venture between The Australian National University,
University of Canberra, Australian Geological Survey Organisation and CSIRO Exploration and Mining
Headquarters: CRC LEME c/o CSIRO Exploration and Mining, Private Bag, PO Wembley, Western Australia, 6014

RESEARCH ARISING FROM CSIRO/AMIRA REGOLITH GEOCHEMISTRY PROJECTS 1987-1993

In 1987, CSIRO commenced a series of multi-client research projects in regolith geology and geochemistry which were sponsored by companies in the Australian mining industry, through the Australian Mineral Industries Research Association Limited (AMIRA). The initial research program, "Exploration for concealed gold deposits, Yilgarn Block, Western Australia" (1987-1993) had the aim of developing improved geological, geochemical and geophysical methods for mineral exploration that would facilitate the location of blind, buried or deeply weathered gold deposits. The program included the following projects:

P240: Laterite geochemistry for detecting concealed mineral deposits (1987-1991). Leader: Dr R.E. Smith.
Its scope was development of methods for sampling and interpretation of multi-element laterite geochemistry data and application of multi-element techniques to gold and polymetallic mineral exploration in weathered terrain. The project emphasised viewing laterite geochemical dispersion patterns in their regolith-landform context at local and district scales. It was supported by 30 companies.

P241: Gold and associated elements in the regolith - dispersion processes and implications for exploration (1987-1991). Leader: Dr C.R.M. Butt.
The project investigated the distribution of ore and indicator elements in the regolith. It included studies of the mineralogical and geochemical characteristics of weathered ore deposits and wall rocks, and the chemical controls on element dispersion and concentration during regolith evolution. This was to increase the effectiveness of geochemical exploration in weathered terrain through improved understanding of weathering processes. It was supported by 26 companies.

These projects represented "an opportunity for the mineral industry to participate in a multi-disciplinary program of geoscience research aimed at developing new geological, geochemical and geophysical methods for exploration in deeply weathered Archaean terrains". This initiative recognised the unique opportunities, created by exploration and open-cut mining, to conduct detailed studies of the weathered zone, with particular emphasis on the near-surface expression of gold mineralisation. The skills of existing and specially recruited research staff from the Floreat Park and North Ryde laboratories (of the then Divisions of Minerals and Geochemistry, and Mineral Physics and Mineralogy, subsequently Exploration Geoscience and later Exploration and Mining) were integrated to form a task force with expertise in geology, mineralogy, geochemistry and geophysics. Several staff participated in more than one project. Following completion of the original projects, two continuation projects were developed.

P240A: Geochemical exploration in complex lateritic environments of the Yilgarn Craton, Western Australia (1991-1993). Leaders: Drs R.E. Smith and R.R. Anand.
The approach of viewing geochemical dispersion within a well-controlled and well-understood regolith-landform and bedrock framework at detailed and district scales continued. In this extension, focus was particularly on areas of transported cover and on more complex lateritic environments typified by the Kalgoorlie regional study. This was supported by 17 companies.

P241A: Gold and associated elements in the regolith - dispersion processes and implications for exploration. Leader: Dr. C.R.M. Butt.
The significance of gold mobilisation under present-day conditions, particularly the important relationship with pedogenic carbonate, was investigated further. In addition, attention was focussed on the recognition of primary lithologies from their weathered equivalents. This project was supported by 14 companies.

Although the confidentiality periods of the research reports have expired, the last in December 1994, they have not been made public until now. Publishing the reports through the CRC LEME Report Series is seen as an appropriate means of doing this. By making available the results of the research and the authors' interpretations, it is hoped that the reports will provide source data for future research and be useful for teaching. CRC LEME acknowledges the Australian Mineral Industries Research Association and CSIRO Division of Exploration and Mining for authorisation to publish these reports. It is intended that publication of the reports will be a substantial additional factor in transferring technology to aid the Australian Mineral Industry.

This report (CRC LEME Open File Report 8) is a Second impression (second printing) of CSIRO, Division of Exploration Geoscience Restricted Report 002R, first issued in 1988, which formed part of the CSIRO/AMIRA Project P240.

Copies of this publication can be obtained from:
The Publication Officer, c/- CRC LEME, CSIRO Exploration and Mining, PMB, Wembley, WA 6014, Australia. Information on other publications in this series may be obtained from the above or from http://leme.anu.edu.au/
Cataloguing-in-Publication:

Report on laterite geochemistry in the CSIRO-AGE Database for the Southern Murchison Region (Yalgoo, Kirkalocka, Perenjori, Ninghan Sheets)
ISBN 0 642 28238 2
1. Geochemistry 2. Laterite 3. Western Australia - Murchison Region.
I. Grunsky, E.C. II. Title
CRC LEME Open File Report 8.
ISSN 1329-4768

CONTENTS

Figures

Diskette

ABSTRACT

A multi-element geochemical study largely based upon laterite sampling covering parts of the main greenstone belts of the Perenjori, Ninghan, Yalgoo, and Kirkalocka 1:250 000 map sheets has outlined the following geochemical features:

a) district-scale (30 to 50 km in length) patterns in the distribution of Cu + Zn + Ni + Co ± Cr; V + Sn;, and Zr + Nb; each pattern appearing to relate to dominant characteristics of varying bedrock associations;

b) an As + Sb association in the Yalgoo-Singleton Greenstone Belt, most prominent in a central regional north-south trend (referred to as a chalcophile corridor, Smith , 1987) passing through Golden Grove and extending south to Mt. Gibson;

c) isolated anomalies on the 2 to 5 km scale showing associations of Bi + Mo + W ± Ge ± Sn;

d) several anomalies at the 1 km scale that require follow-up sampling in exploration in order to assess their continuity and significance;

e) The study also provides knowledge of the element abundance levels and variation of laterite geochemistry that complements information arising from orientation studies about mineral deposits.

Sporadic Au anomalies also occur. However, the general sample spacing of 3 km with fill-in sampling at 1 km is too wide for reliable interpretation of Au patterns in laterites. Laterite geochemistry at these low sample densities generally requires the use of intermediate zonal targets such as anomalous chalcophile envelopes which can occur about individual deposits.

The sampling arose as part of a combined research programme at CSIRO and an experimental exploration programme (the AGE Joint Venture Programme) during the period 1983 to 1986.

In the region covered by the present report a total of 721 samples were analyzed for 31 elements. Summary statistics, histograms, and maps of the percentile classes, are presented for selected elements in laterites and some very iron-rich materials from partly eroded profiles which have been referred to as ferricretes. A principal components analysis was also carried out with the resulting component scores plotted up for the first five components. The results of the analysis confirm the presence of some broad regional geochemical trends that are related to bedrock lithologies and regional alteration processes.

INTRODUCTION

This report summarizes the results of some of the progress of an on-going project to assess the geochemistry of laterites and associated materials for the purposes of developing and improving exploration concepts, sampling strategies, and isolation of potentially mineralized areas. The report presents the results of reconnaissance-scale laterite geochemistry on the KIRKALOCKA, NINGHAN, PERENJORI, and YALGOO 1:250,000 map sheets. The sampling was carried out in the 1983-1986 period as part of an application feasibility test of laterite geochemistry for mineral exploration. This work was collaborative between the AGE Joint Venture (Greenbushes Ltd., St. Joe Minerals, and later Sons of Gwalia, NL) and CSIRO.

Regional geochemical databases have been developed for a variety of uses in several countries. Their ultimate aim has been to define geochemical provinces in which the bedrock sequences contain anomalous populations of specific elements that can be related to zones of mineralization.

The results of this report are part of larger geochemical database that covers wide areas of the Yilgarn Block of Western Australia, and forms part of the foundations for on-going research into the use of laterite geochemistry in mineral exploration. The project has focused on the sampling and analysis of the laterite cover that is extensively but variably developed throughout the Yilgarn Block.

The area forms part of the Archaean Yilgarn Block which is composed of synformal arcuate sequences of metamorphosed supracrustal volcanic and sedimentary assemblages intruded by felsic plutons. Large regional domains of gneissic terrain occur throughout the area and represent assimilated supracrustal areas. Four consistently recognized stratigraphic sequences occur within the supracrustal rocks (Baxter and Lipple, 1985).

The region was sampled at 3 km triangular spacing intervals with follow-up sampling at closer spacings. A variety of lateritic materials were sampled and classified as to the type of sample. Most samples belong to the nodular and pisolithic laterite category for which geochemical maps are produced in this report.

Concept and Scope

The research objectives of establishing a regional geochemical database were:

- To provide knowledge of regional variations in laterite geochemistry that may be due to regional changes in climate or landform characteristics.
- To establish the types of variation in laterite composition encountered in areas away from orientation studies about specific ore deposits.
- To relate laterite composition to both regional and local geological variation.
- To test, and further develop the most efficient sampling strategies that will allow cost effective exploration.

Background to the Study

Primary and secondary haloes can develop, persist, or be greatly enhanced in size through the development of lateritic profiles as documented by Smith et al (1979) who found kilometre-scale chalcophile element haloes in the pisolithic laterite cover associated with the Golden Grove Cu-Zn orebodies.

These observations together with Mazzuchelli and James (1966) and Zeegers et al (1981) provided the rationale for sampling various lateritic materials and analyzing a suite of chalcophile and associated elements as well as additional indicator elements. By concisely defining the geochemical characteristics of the various lateritic materials it is expected that better control can be established on classifying the characteristics of unknown suites of samples with the ability to recognize geochemical anomalies that may be associated with mineralization.

Physiography and Climate

The study area of 64,000 square kilometres includes part of the Swanland and Salinaland physiographic divisions of Jutson (1950). The boundary between the two domains is the topographic divide separating drainages flowing west to the Indian Ocean across the Perth Basin, underlain largely by Phanerozoic sediments, and those of

an internal drainage system, largely dismembered into saline playas, flowing east across the Archaean craton of the Yilgarn Block. Most of the area falls in the catchment area of the intermittent saline Lake Moore drainage basin of Mann (1982).

Jutson (1950) regarded Salinaland as comprising a "new plateau", a consequence of an arid erosional cycle, on which stand mesa- and butte-like remnants of the "old plateau" with the transition between the two being marked by lines of scarp retreat or "breakaways". The height differential between the two surfaces is of the order of 10 to 60 metres. The "old plateau" is part of the Great Plateau of Western Australia (Jutson, 1950). Relief on the Yilgarn Block ranges generally from 150 to 550 m.

In the Jutson model, laterite was restricted to the "old plateau" whereas in fact it has formed and may still be forming on surfaces of the "new plateau". More recent workers attempted to explain the laterite distribution in terms of partial stripping of the laterite profile and development of lateritic etchplains (Finkl and Churchward, 1973) or, alternately, as an alternating cycle of etchplanation and pediplanation resulting in a sawtooth landscape whereby the occurrence of laterites on topographic highs is seen largely as a consequence of relief inversion (e.g. Ollier et al., 1988).

The area falls within a semi-desert Mediterranean climatic regime with mild winters and hot summers with most rain falling in the cooler months of April-September although cyclonic systems cause heavy falls in the summer months. The 250 mm isohyet passes through the region. Temperature ranges from a winter period mean of 16° C to a summer period mean of 28° C in the Yalgoo district although summer maxima in excess of 38° C are common.

To the south-west of Mullewa on the YALGOO sheet area, vegetation comprises forest woodland with varieties of mallee with species of Acacia and Grevillea common. The eastern two- thirds of the study area is characterized by xerophytic and halophytic vegetation, mainly Acacia sp., dense heath scrub (mainly on sandplains) with scattered forests of Eucalyptus sp., the latter mainly salmon gum and York gum. The area is sparsely settled with land use relating mainly to pastoral leases and mining except for some cultivation for wheat in the south-west portion.

GEOLOGICAL SETTING AND MINERALIZATION

Regional Geology

The four 1:250,000 map sheets comprising the study area form part of the southern Murchison Province within the cratonic Archaean Yilgarn Block of Western Australia. A generalized geological map is shown in Figure 1. Arcuate north to northwesterly-trending belts of thick synclinorial sequences of Archaean supracrustal rocks comprising the Murchison Supergroup are preserved within a gneissic terrain intruded by Archaean granitoids. Within the belts, the lithologic successions can be divided into associations of either mafic volcanic or sedimentary affiliation as recognized by Hallberg (1976) following Muhling and Low (1973). Four such lithologic associations were established by regional 1:250,000 scale mapping of the YALGOO, KIRKALOCKA, NINGHAN and PERENJORI sheet areas (Muhling and Low, 1977; Lipple et al., 1983; Baxter et al., 1983 and Baxter and Lipple, 1985). The sequence of these lithological associations is repeated from belt to belt with an apparent consistency of stratigraphic order. The four associations in order of decreasing age are:

Lower mafic volcanic association (Murrouli Basalt, Golconda Formation and Gabanintha Formation (in part) in the Luke Creek Group) - comprises mainly tholeiitic metabasalts and dolerites with mafic and ultramafic intrusives. Pillow and vesicular textures are common. Banded iron formation and minor felsic (mainly dacitic) volcanics are present in cyclic alternation with the mafic flows. This association hosts the largest proportion of historical gold producers in the southern Murchison Province.

Lower sedimentary-volcanic association (mainly Windaning Formation in Luke Creek Group, also Gabanintha Formation in part) - comprises mainly fine-grained sediments with banded iron formation and volcaniclastic rocks. Minor felsic volcanics, constrained to local sub-aerial or sub-aqueous eruptive centres, are also present. The association is intruded by both mafic and ultramafic rocks. Lower units within this association host economic syngenetic base metal sulphide - gold/silver mineralization.

Upper mafic volcanic association (Singleton and Wadgingarra Basalts, Camberathunun Formation in Mount Farmer Group) - resembles the lower mafic volcanic association

generally but differs in having a lower proportion of banded iron formation and a higher proportion of pyroclastic rocks and high-magnesium (komatiitic) basalts. Local dacitic to rhyodacitic volcanics are present.

Upper sedimentary association (Mougooderra Formation in Mount Farmer Group) - comprises mainly shale and siltstone with interbedded polymictic and oligomictic conglomerate with sandstone and minor banded iron formation towards the base of the sequence. This association unconformably overlies the Luke Creek Group rocks.

All four associations are most extensively developed in the Warriedar Fold Belt and its southerly prolongation into the Ninghan, Yandhanoo and Retaliation Fold Belts, together forming the Yalgoo-Singleton greenstone belt. Similar or identical associations are present in the Tallering, Gullewa, and Koolanooka greenstone belts to the west and in the Paynes Find, Wydgee and Magnet greenstone belts to the east. Formal stratigraphic terms have only recently been applied (Watkins et al, in press) to the supracrustal units within the study area.

In the case of the Warriedar Fold Belt, upwards of an 5 kilometre thickness of supracrustal rocks comprising the above associations is preserved in synformal structures. Metamorphic grades within the belts are typically greenschist to amphibolite- transition facies although there is a general increase in grade to the western part of the YALGOO and PERENJORI sheet areas where amphibolite and local granulite facies grades are developed. Contact metamorphic facies of hornfels facies may be developed at the supracrustal-granitoid margins. Regional structures within the greenstone fold belts appear to have been controlled by the emplacement of the granitoid batholiths with folds being variably close or open with a heterogeneous structural fabric varying with rock type and proximity to the margins of the fold belts. Five phases of deformation initiated by recumbent folding and thrusting of the Luke Creek Group rocks are defined by Watkins and Hickman (1988).

A complex and largely undeciphered sequence of granitoid intrusion is developed regionally. Variably porphyritic, equigranular, foliated or undeformed granite, adamellite, trondhjemite and tonalite exhibit marginal gneissic or migmatitic zones with zones of mixed granitoid types occurring between adjacent intrusions. High level (epizonal) granitoids generally exhibit less intense deformation and are associated with pegmatoid and quartz vein swarms in shallow overlying supracrustal roof pendants. Four phases of intrusion of siliceous plutons are recognized by Watkins and Hickman (1988), two phases being pre/syn-kinematic/metamorphic and the others being post-folding.

Geochronological data suggest that the volcanic component of the supracrustal belts in the southern Murchison Province formed at ca. 3.0 Ga. and were metamorphosed at ca. 2.7 Ga. Browning et al. (1987) have shown that galenas contained in syngenetic volcanogenic base-metal mineralization at the Scuddles and Gossan Hill deposits in the Warriedar Fold Belt gave Pb model ages consistent with Sm-Nd, Pb-Pb and U-Pb zircon ages for the greenstone belts. The majority of galenas associated with gold mineralization in the southern Murchison Province gave Pb model ages of ca. 2.75 to 2.85 Ga., implying that epigenetic gold mineralization in the region was synchronous with regional metamorphism of the supracrustal belts although Phillips (1985) has shown that, in some cases at least, peak metamorphism had outlasted the mineralizing event. Sm-Nd data from metavolcanic rocks from the Warriedar Fold Belt gave original isochron ages of 2.98 Ga. (Fletcher et al., 1984). Rb-Sr whole rock isochrons for a variety of syntectonic and post-tectonic granitoid batholiths distributed across the southern Murchison Province gave a spread of ages from 2.5 to 2.7 Ga. (Browning et al., 1987). Arriens (1971), however, found evidence of an older crustal component in the 2.8 to 3.1 Ga. ages in gneisses from the Koolanooka Hills and Morawa-Mullewa areas on the western edge of the southern Murchison Province.

Large, deformed gabbroic complexes in the eastern and north-eastern parts of the region (the Windimurra and Narndee complexes) are intruded by granitoids and are believed to be older than 2.6 Ga. (Baxter et al., 1983). Differentiated Stillwater-type sills and magnetite-bearing complexes are common in both the lower mafic volcanic and the lower sedimentary- volcanic associations (Hallberg, 1976).

In the extreme western part of the region, the Darling Fault, marking the eastern edge of the Perth Basin, brings Phanerozoic marine and continental sediments and glacial deposits into fault contact with the Archaean rocks of the Yilgarn Block.

Cainozoic deposits are widespread and extensively developed in the region, mantling variably stripped Archaean surfaces, and encompass a variety of lithotypes. Muhling and Low (1977) recognized two "sandplain" units during mapping of the YALGOO 1:250,000 sheet area and which were found to occur rather widely distributed on adjacent sheet areas viz: (a) a red-brown/yellow sand overlying laterite or weathered bedrock, occurring as isolated remnants on topographically higher areas and overlapping onto (b) a yellow/buff coloured sand with ferruginous gravels which overlies stripped granitic surfaces or granitic detritus. Most of the region was subject to a period of lateritization during a warm, humid climatic regime followed by a period of stripping and etching continuing to the present during a period of aridity (Johnstone et al., 1973). Extensive and deeply developed lateritic weathering profiles remain, in some cases buried beneath alluvial and colluvial units, and are the subject of the current study.

Slope-wash and valley-fill colluvium may grade down-drainage into an indurated, red-brown hardpan up to 5 metres in thickness which, in turn, may grade downslope into calcrete in trunk drainages which are largely eviscerated, formerly east-draining systems having degenerated into a system of saline closed drainage sumps or playas. Thin kankar sheets and caliche may develop in the lower portions of hardpan and in the upper parts of laterite profiles. Aeolian red-brown sands overlie various other Cainozoic units and may form dunes on the edges of saline playas and drainage sumps. Saline and gypseous fine-grained sediments are developed on the floors and margins of such depressions.

Mineralization

Historically, mines in the YALGOO, KIRKALOCKA, NINGHAN and PERENJORI 1:250,000 sheet areas have produced in excess of 67,369 kg (to 1985) of gold, mainly from deposits in the Magnet Fold Belt, where the Hill 50 mine was the major producer. Most deposits are hosted by tholeiitic basalts or dolerites although banded iron formations, ultramafic rocks and granitoids also feature. Most deposits are viewed as epigenetic and many shears and mineralized vein systems are associated with CO_2, soda and potash metasomatism, the mineralizing fluids conceivably being derived by progressive metamorphic dewatering of mafic and ultramafic sequences in the supracrustal pile (e.g. Browning et al., 1987). Hallberg (1976) notes that on a gross scale, gold producers were virtually restricted to deposits within the two older supracrustal associations noted above and particularly within para-amphibolites, ultramafic schists and banded iron formations grouped into the lower mafic volcanic association. A more recent study by Hickman and Watkins (1988) suggests that there are both regional and local controls on the formation of gold deposits in the area. Regional controls included proximity of the deposits to large regional fault systems, a general occurrence within 2 km of granitoid-greenstone contacts, and concentration of deposits in the upper three formations of the Luke Creek Group. Local controls include structures, ore-fluid composition, temperature-pressure conditions, and host rock compositions.

Operations at the Mt. Gibson lateritic gold deposit of Forsayth N.L. and Reynolds Australia Mines Pty. Ltd. commenced in November 1986, resulting in production of 2,300 kg of gold to November 1987. At Mt. Gibson, gold occurs finely dispersed through various units of the regolith profile (overlying the Windaning Formation), both residual and transported, particularly in pisolithic and nodular laterite, in lateritic duricrust and to a lesser extent in hardpan containing lateritic materials. At the Midway North prospect, 4.5 km north of the Mt. Gibson mine plant, an in situ geological resource of 1.5 Mt @ 6.0 g/t Au associated with Pb-Zn-Ag mineralisation has been reported from a plunging sequence of altered and sheared felsic and mafic volcanics (Gold Gazette, October, 1988). Similar prospective volcanogenic base/precious metal mineralization has been recognized in felsic volcanics in the Narndee complex (Marston, 1979)

Within the Warriedar Fold Belt, significant resources of polymetallic base-metal mineralization of syngenetic volcanogenic association have been proven at Golden

Grove; specifically at the Scuddles and Gossan Hill deposits. These deposits are sited in a unit of felsic pyroclastic and volcaniclastic rocks near the base of a pile of mixed volcano-sedimentary rocks, mafic volcanic rocks and banded iron formation belonging to the lower sedimentary-volcanic association (Gabanintha and Windaning Formations). The Gossan Hill deposit occurs in a proximal portion of a felsic volcanic complex comprised of rhyolitic to dacitic ash and lapilli tuffs and agglomerates and mineralization was emplaced at the close of a volcano-effusive cycle marked by hanging-wall cherts (Marston, 1979). The complex is intruded by leucocratic adamellite and granophyre. Discrete ore shoots are located within a broadly conformable mineralized zone which is up to 550 by 130 metres in surface dimensions. The ores are zoned with a cupriferous centre and with both lead and zinc increasing stratigraphically upwards and distally. Marston (1979) records the primary mineral assemblage as magnetite-pyrite-chalcopyrite-pyrrhotite with subordinate sphalerite, galena and traces of cubanite, arsenopyrite, tennantite, valleriite, pentlandite and tellurobismuthite. Iron and Mg metasomatism of the wall rocks is marked. Published resources at Scuddles total 10.5 Mt @ 11.7% Zn, 1.2% Cu, 89 g/t Ag and 1.1 g/t Au while the Gossan Hill deposit has a possible resource of 14 Mt @ 3.8% Cu with minor silver values (Mining Journal, August 19, 1988, V. 311, No. 7982, p. 137,139).

Other metal commodities have been produced in significant quantity from the region. Mining of supergene enriched banded iron formation at Koolanooka Hill resulted in production of 6.7 Mt of iron ore. Molybdenum, Bi, Be, Ta and Li have been produced from pegmatites and quartz veins in supracrustal metamorphic rocks roofing granitoid intrusives (in the Noongal area) and emplaced in border-facies rocks associated with high-level granite intrusions at several localities through the region. A resource of 1.6 Mt. of 0.649% WO_3 (Baxter, 1978) has been established in a greisen sheet in a high-level leucogranite stock intruding rocks of the lower mafic volcanic association at Mulgine Hill in the Warriedar Fold Belt. In the vicinity of the Mt. Gibson mine, wolframite has been produced from quartz veins intruding sediments of the Mougoodorra Formation in the Yandhanoo Fold Belt.

Figure 2 shows a map with some of the significant past and present mineral producers in the area.

THE SAMPLING PROGRAMME

Sampling

A 3 km spaced triangular sampling grid was used over most of the sampled area, with limitations caused by the distribution of access roads, the extent of erosional dissection of the laterite cover, the extent of cover by younger alluvium/colluvium, and the extent of mining and other land tenements. Various follow-up and fill-in samples were also taken, usually closing the sample spacing to 1 km, in some cases to 330m; the locations of follow-up sampling being obvious in the plots showing sample sites, for example at 1:250,000 scale or more detailed. Figure 3 shows the distribution of the samples collected throughout the area.

The intention was to sample the cemented pisolithic laterite blanket, and/or the loose lateritic pisoliths which had been released from the duricrust by natural disaggregation. Lateritic nodules and pisoliths in the range of 1cm to 2cm diameter were sought in order to avoid the possibility of skewing the sample characteristics if very coarse material were collected and to aid sample preparation by providing suitable feed for the disk grinding stage (avoiding coarse crushing). Sampling was typically carried out over a 10 metre radius in order to suppress any unforseen local variation. A 1 kg sample was collected for crushing, grinding and analysis of an aliquot. A separate 1 kg sample was collected for permanent reference. Other sample types were collected where the prime media were not available. A breakdown of the number of samples collected is given in Table 1. Where available, 1:50,000 photomosaics were used in selecting sample sites and for recording the locations. All samples were allocated AMG coordinates.

The classification used in this report is the scheme adopted during the AGE study of 1983-1986. A more comprehensive and, in due course, genetic classification scheme is currently under development within the CSIRO/AMIRA Laterite Geochemistry Project. It is likely that some of the terms used in this report will be

modified, although the main categories still stand. The main change will be a replacement for the various "ferricretes" as used here so as to avoid confusion with the very broad use of "ferricrete" in the French literature.

I LATERITE SAMPLE TYPES

Samples belonging to the laterite family (often occurring geomorphically above breakaways (i.e. a relatively complete laterite profile):

Loose Pisoliths (LP) and Cemented Pisoliths (CP) - Ferruginous particles with high sphericity, 2mm - 3cm in diameter, and a concretionary iron coating. Internal concentric banding is common. This sample type commonly forms a blanket deposit, whether loose or cemented, up to a few metres in thickness. Also forms redistributed colluvium.

Loose Nodular Laterite (LN) Cemented Nodular Laterite (CN) - Ferruginous particles with low sphericity but rounded. Commonly 1 - 4 cm across and a goethitic "skin". Lateritic nodules and pisoliths form a continuous series and commonly occur together.

Vermiform or Vermicular Laterite (VL) - Iron-rich cemented mottled zone saprolite containing sinuous worm-like tunnels, holes or clay zones. May contain spaced pisoliths, nodules or sporadic rock fragments.

Plinthite (PN) - Grit cemented by goethite, with visible quartz grains. Plinthite fragments do not have a concretionary goethite "skin".

Mottled Zone Scree (MS) - Loose, locally derived scree or float derived from iron-rich mottles within the lateritic weathering profile.

II FERRICRETE SAMPLE TYPES

Samples belonging to the ferricrete family (typically occurring in situations where the nodular of pisolithic laterite has been removed by erosion, but stripping has not cut deeply into saprolite. These include:

Massive Ferricrete (MF) - Iron rich material lacking pisolith- nodule texture, commonly has a botryoidal texture.

Ferricrete Fragments (FF) - Rounded fragments of Fe-rich material often showing relict internal structure but has NO Fe-rich concretionary skin.

Cemented Pebbly Ferricrete (PF) - Dense black Fe-rich material with pebbly texture, and irregular shape. This type normally occurs at the top of a full laterite profile.

Ferricrete Pellets (PE) - Particles of Fe-rich material with moderate to high sphericity, up to 1.5cm across and no Fe-rich concretionary "skin".

III OTHER CATEGORIES

Various categories that are treated individually include:

Loose Ooliths (OL) - Ferruginous particles with high sphericity <2mm in size with a definite concretionary iron-rich coating. Commonly they are black or very dark brown. May occur in soil, as surface lag or may be cemented. They do not form blanket deposits.

Recemented Fe-rich Colluvium (RC) - Fe-rich angular to sub-rounded rock fragments in a fine Fe-rich matrix.

Lateritized Rock (LR) - Saprolite that is enriched in Fe-bearing weathering minerals; goethite and hematite.

Other (OT) - Unclassified materials, the descriptions of which are recorded in the archived field sheet records.

Figure 4 shows the distribution of the lateritic sample materials (LN, LP, CN, CP, MS) and Figure 5 shows the distribution of the ferricrete materials (FF, MF, PF, RC). Sampling of ferricretes is more widespread in the northern part of the area, whilst sampling of loose nodules dominates the southern part of the area.

Table 1: Sample Type, Abbreviation, and Number of Samples

Sample type	Code	Number of Samples
Lateritic Types		
Loose Pisoliths	'LP'	335
Cemented Pisoliths	'CP'	32
Loose Nodules	'LN'	221
Cemented Nodules	'CN'	9
Vermicular Laterite	'VL'	1
Plinthite	'PN'	16
Mottled Zone Scree	'MS'	2
Ferricrete Types		
Massive Ferricrete	'MF'	52
Ferricrete Fragments	'FF'	8
Cemented Pebbly Ferricrete	'PF'	12
Ferricrete Pellets	'PE'	7
Miscellaneous Types		
Oolites Loose	'OL'	9
Re-cemented Fe-rich Colluvium	'RC'	3
Lateritized Rock	'LR'	14
Other	'OT'	0

Sample Preparation

The samples were prepared using non-metallic sample preparation methods described by Smith (1987). Oversized material from 1 kg samples is reduced to minus 8 mm by crushing between zirconia plates in an automated hydraulic press. The crushed oversized material together with the direct feed material is then fed to an epoxy-resin lined disc grinder with alumina plates and further reduced to minus 1 mm. Final milling is done in an agate or alumina mill. Cleaning of the equipment is performed by a combination of air- and sand-blasting and the passage of a quartz blank.

Analytical Methods

A total 721 samples were analyzed by Amdel Ltd. (Adelaide) for 25 elements. An additional 13 elements were analyzed by the CSIRO analytical facilities on 40% of the samples. Au was analyzed by Analabs (Perth) on about half of the samples. The methods of analysis are outlined in Table 2. Tin and Bi were analyzed by two methods because of their perceived importance in laterite geochemistry and to provide a consistent gauge of confidence in the results. At this point, the following elements have been analyzed by the methods outlined in Table 2: SiO_2, Fe_2O_3, MgO, CaO, TiO_2, Au,

Mn, Cr, V, Cu, Pb, Zn, Ni, Co, As, Sb, Bi, Cd, Mo, Ag, Sn, Ge, Ga, W, Ba, Zr, Nb, Ta, Se, and, Be. Additional elements will be analyzed later on.

Samples analyzed by CSIRO were carried out on an Inductively Coupled Plasma Spectrometer (ICP) using a lithium metaborate fusion dissolved in nitric acid. Gold was analyzed by Analabs Laboratories using Atomic Absorption Spectroscopy (Graphite Furnace) after aqua-regia dissolution of 50g samples.

Analytical Quality Control

Each batch of samples submitted for analysis contained three control samples that represent a spectrum of multi-element values. These control samples were submitted in a scrambled numerical sequence. The samples were also subjected to replicate analysis both by the CSIRO analytical facilities and by an independent laboratory. Problems of between-batch variation could usually be detected by examination of maps of the plotted data. If any clustering or unusual patterns were noted, the duplicated samples were submitted for assay.

DATA PRESENTATION AND ANALYSIS

The geochemical data that accompanies this report is contained on a 5.25" floppy diskette which can be found in the back pocket of the report. Appendix 1 provides the detail regarding the format of the data.

Summary Tables

A summary of the multi-element geochemical data is listed in Tables 3 - 6. The tables list the number of samples analyzed for each element, the 1, 5, 10, 25, 50, 75, 90, 95, and 99th percentiles, minimum, maximum, mode, mean values, and the standard deviation.

Material that was classified as loose nodules (LN), loose pisoliths (LP), cemented nodules (CN) and cemented pisoliths (CP) are known to be compatible sample media and were therefore grouped together. These samples, placed in the laterite family, total 599, and their statistics are shown in Table 3. Similarly, samples of the ferricrete categories, FF, MF, PF, and RC were grouped together, totalling 75 samples, and their statistics are listed in Table 4. Statistics on Plinthite (PN), are shown in Table 5, and Massive Ferricrete (MF) as a separate sub-category in Table 6.

Many samples were analyzed for elements whose values were below the detection limit. In these cases, the value of the variable was set to one third of the detection limit as the default minimum values. Subsequent statistical and numerical procedures used this minimum value. All samples have not been analyzed for the same set of elements, at this stage. In such cases, for calculations of statistics the number of samples used to compute the statistic was reduced. The number of samples used, for the calculations of the statistics, for each element is indicated in the tables.

Barium must be interpreted with caution as the method of sample preparation (from alumina disks) adds an average of about 100 ppm of Ba depending on the hardness of the sample.

Bismuth and Sn include two methods of analysis one by OES and the other by XRF. Both methods confirm consistency of the results.

Some of the elements such as SiO2, Al2O3, Fe2O3 (ICP), MgO, CaO, Mn (ICP),Cr (ICP), V (ICP), Cu (ICP), Ni (ICP), are listed in the summary tables but are not considered further. Cd were not considered further because of its very low levels of abundance.

Histograms

Histograms of the data were plotted for selected elements of specific sample types. These plots are shown in figures 6 - 30. The histograms were computed using 40 class divisions based on the minimum and maximum values of the variables. For presentation purposes, the minimum and maximum values were truncated at the mean ± three standard deviations. Above each histogram is a box and whisker plot that shows the median (50th percentile), left hinge (25th percentile), right hinge (75th percentile)

TABLE 2
ANALYTICAL METHODS AND LOWER LIMITS OF DETECTION

Element	Reported as	Detection Limit	Laboratory	Analysis	Digestion Method
SIO2	WT%	0.1	CSIRO	ICP FS	
AL2O3	WT%	0.1	CSIRO	ICP FS	
FE2O3	WT%	0.1	CSIRO	ICP FS	
FE2O3	WT%	0.1	AMDEL	AAS	HF
MGO	WT%	0.05	CSIRO	ICP FS	
CAO	WT%	0.05	CSIRO	ICP FS	
TIO2	WT%	0.003	CSIRO	ICP FS	
MN2	PPM	5	AMDEL	AAS	HF
MN4	PPM	20	CSIRO	ICP FS	
CR1	PPM	50	CSIRO	ICP FS	
CR3	PPM	5	AMDEL	XRF	
V1	PPM	50	CSIRO	ICP FS	
V3	PPM	10	AMDEL	XRF	
CU1	PPM	50	CSIRO	ICP FS	
CU4	PPM	2	AMDEL	AAS	HF
PB3	PPM	4	AMDEL	XRF	
ZN3	PPM	2	AMDEL	AAS	HF
NI1	PPM	50	CSIRO	ICP FS	
NI3	PPM	5	AMDEL	AAS	HF
CO3	PPM	5	AMDEL	AAS	HF
AS4	PPM	2	AMDEL	XRF	
SB2	PPM	2	AMDEL	XRF	
BI1	PPM	1	AMDEL	OES	
BI3	PPM	1	AMDEL	XRF	
CD2	PPM	1	AMDEL	AAS	HF
MO2	PPM	2	AMDEL	XRF	
AG1	PPM	0.1	AMDEL	OES	
SN1	PPM	1	AMDEL	OES	
SN5	PPM	1	AMDEL	XRF	
GE1	PPM	1	AMDEL	OES	
GA	PPM	1	AMDEL	OES	
W2	PPM	10	AMDEL	XRF	
BA1	PPM	100	CSIRO	ICP FS	
ZR1	PPM	50	CSIRO	ICP FS	
NB3	PPM	3	AMDEL	XRF	
TA3	PPM	3	AMDEL	XRF	
SE2	PPM	1	AMDEL	XRF	
BE1	PPM	1	AMDEL	OES	
AU	PPB	1	ANALABS	Carbon Rod	Aqua Regia

Legend: AAS Atomic Absorption Spectroscopy
XRF X-ray Fluoresence
ICP FS Inductively Coupled Plasma Fusion
OES Optical Emmission Spectroscopy

Note: The numerical suffix associated with each elements distinguishes between different laboratories and analytical methods used by the Laterite Geochemistry Group. For example, for Chromium, two methods used were:

CR1 = ICP FS (CSIRO)
CR3 = XRF (AMDEL)

Table 3: STATISTICS FOR SOUTH MURCHISON AREA

LATERITIC SAMPLE TYPES:
MS (Mottled Zone Scree)
CN (Cemented Nodules)
CP (Cemented Pisoliths)
LN (Loose Nodules)
LP (Loose Pisoliths)

ELEMENT	LAB	METHOD	#SAMPLES	PERCENTILES												
				1%	5%	10%	25%	50%	75%	90%	95%	99%	MINIMUM	MAXIMUM	MODE	MEAN	STD. DEV.
SiO_2 WT%	CSIRO	ICP FS	217	3.69	7.98	12.29	15.75	23.56	40.34	51.40	55.00	60.14	2.87	64.23	23.52	28.13	15.08
Al_2O_3 WT%	CSIRO	ICP FS	217	7.15	8.40	10.32	12.33	15.68	19.09	21.68	24.09	32.68	5.87	36.13	15.67	16.01	4.98
Fe_2O_3 WT%	CSIRO	ICP FS	218	14.67	19.32	21.18	32.57	48.56	58.19	64.73	67.69	76.08	12.27	80.21	48.51	45.57	15.98
Fe_2O_3 WT%	AMDEL	AAS HF	599	4.30	8.50	11.10	18.70	30.80	39.90	47.20	50.50	58.10	2.90	70.20	30.80	29.82	13.31
MGO WT%	CSIRO	ICP FS	218	0.02	0.02	0.02	0.02	0.05	0.08	0.13	0.17	0.32	0.02	3.97	0.05	0.08	0.28
CAO WT%	CSIRO	ICP FS	217	0.02	0.02	0.02	0.02	0.05	0.07	0.10	0.12	0.20	0.02	0.58	0.05	0.05	0.05
TiO_2 WT%	CSIRO	ICP FS	224	0.32	0.42	0.48	0.63	0.84	1.15	1.55	1.92	3.38	0.26	3.80	0.83	0.95	0.53
$AG1^2$ PPM	AMDEL	AAS HF	599	0.03	0.03	0.03	0.03	0.03	0.10	0.30	0.60	1.00	0.03	6.00	0.03	0.14	0.35
MN2 PPM	AMDEL	AAS HF	599	9.0	18.0	25.0	47.0	107.0	210.0	450.0	935.0	3627.0	1.7	9999.0	106.0	261.6	681.6
MN4 PPM	CSIRO	ICP FS	216	6.7	6.7	30.0	60.0	118.0	209.0	332.0	569.0	1391.0	6.7	4958.0	117.0	195.9	393.4
CR1 PPM	CSIRO	ICP FS	219	124.0	166.0	216.0	294.0	580.0	1684.0	4911.0	8516.0	14324.0	87.0	17388.0	578.0	1720.2	2890.1
CR3 PPM	AMDEL	XRF	599	95.0	166.0	200.0	310.0	570.0	1640.0	5150.0	9712.0	9999.0	56.0	9999.0	570.0	1641.5	2485.1
V1 PPM	CSIRO	ICP FS	219	169.0	269.0	317.0	434.0	633.0	914.0	1143.0	1290.0	1521.0	137.0	1727.0	629.0	690.8	324.3
V3 PPM	AMDEL	XRF	599	32.0	116.0	170.0	313.0	582.0	969.0	1384.0	1571.0	2020.0	3.3	2180.0	581.0	687.9	462.4
CU1 PPM	CSIRO	ICP FS	144	7.0	11.0	14.0	16.7	39.0	97.0	154.0	211.0	767.0	5.0	2096.0	39.0	84.8	192.4
CU4 PPM	AMDEL	AA HF	598	4.0	6.0	8.0	15.0	33.0	64.0	107.0	142.0	330.0	2.0	2033.0	33.0	53.5	100.5
PB3 PPM	AMDEL	XRF	599	0.7	0.7	5.0	14.0	25.0	40.0	58.0	74.0	166.0	0.7	309.0	25.0	30.8	28.3
ZN3 PPM	AMDEL	AA HF	599	6.0	8.0	11.0	16.0	24.0	33.0	46.0	58.0	110.0	4.0	268.0	24.0	27.7	20.0
NI1 PPM	CSIRO	ICP FS	216	16.7	27.0	35.0	53.0	90.0	149.0	360.0	541.0	1926.0	16.7	3334.0	89.0	173.4	336.2
NI3 PPM	AMDEL	AA HF	599	1.7	1.7	5.0	14.0	28.0	50.0	123.0	270.0	820.0	1.0	2000.0	28.0	69.1	177.5
CO3 PPM	AMDEL	AA HF	599	1.7	1.7	1.7	1.7	6.0	14.0	37.0	47.0	74.0	1.7	170.0	6.0	13.0	17.8
AS4 PPM	AMDEL	XRF	599	3.0	6.0	9.0	17.0	28.0	48.0	93.0	179.0	541.0	0.7	987.0	28.0	51.1	92.6
SB2 PPM	AMDEL	XRF	599	0.7	0.7	0.7	0.7	0.7	4.0	7.0	11.0	35.0	0.7	115.0	0.7	3.6	7.7
BI1 PPM	AMDEL	OES	598	0.3	0.3	0.3	0.3	0.3	0.3	1.0	2.0	6.0	0.3	50.0	0.3	0.6	2.2
BI3 PPM	AMDEL	XRF	599	0.3	0.3	0.3	0.3	0.3	2.0	3.0	4.0	7.0	0.3	75.0	0.3	1.2	3.4
CD2 PPM	AMDEL	AAS HF	599	0.3	0.3	0.3	0.3	0.3	0.3	1.0	2.0	3.0	0.3	3.0	0.3	0.5	0.6
MO2 PPM	AMDEL	XRF	599	0.7	0.7	0.7	0.7	0.7	5.0	8.0	11.0	25.0	0.7	63.0	0.7	3.3	4.9
SN1 PPM	AMDEL	OES	598	0.3	0.3	0.3	0.3	0.3	2.0	3.0	6.0	10.0	0.3	60.0	0.3	1.6	3.1
SN5 PPM	AMDEL	XRF	597	0.3	0.3	0.3	0.3	3.0	5.0	7.0	9.0	13.0	0.3	72.0	3.0	3.5	4.1
GE1 PPM	AMDEL	OES	598	0.3	0.3	0.3	0.3	0.3	1.0	2.0	2.0	6.0	0.3	20.0	0.3	0.8	1.3
GA PPM	AMDEL	OES	599	3.0	6.0	10.0	15.0	20.0	30.0	30.0	40.0	60.0	2.0	80.0	20.0	22.4	10.3
W2 PPM	AMDEL	XRF	599	3.3	3.3	3.3	3.3	3.3	3.3	14.0	25.0	76.0	3.3	5884.0	3.3	19.0	247.8
BA1 PPM	CSIRO	ICP FS	213	33.3	33.3	51.0	106.0	140.0	203.0	379.0	811.0	1879.0	33.3	4317.0	139.0	247.5	438.1
ZR1 PPM	CSIRO	ICP FS	219	147.0	189.0	211.0	242.0	309.0	408.0	763.0	962.0	1244.0	125.0	1592.0	308.0	394.2	246.6
NB3 PPM	AMDEL	XRF	594	1.3	1.3	5.0	9.0	12.0	18.0	24.0	29.0	44.0	1.3	125.0	12.0	14.1	9.6
TA3 PPM	AMDEL	XRF	594	1.0	1.0	1.0	1.0	1.0	1.0	1.0	4.0	7.0	1.0	10.0	1.0	1.3	1.1
SE2 PPM	AMDEL	XRF	599	0.3	0.3	0.7	2.0	4.0	6.0	7.0	9.0	10.0	0.3	13.0	4.0	4.1	2.5
BE1 PPM	AMDEL	OES	596	0.3	0.3	0.3	0.3	0.3	0.3	0.3	0.3	1.0	0.3	3.0	0.3	0.4	0.2
AU PPB	ANALABS	334	268	0.3	0.3	0.3	2.0	3.0	8.0	15.0	20.0	40.0	0.3	192.0	3.0	6.7	13.5

Table 4: STATISTICS FOR SOUTH MURCHISON AREA

FERRICRETE SAMPLE TYPES
FF (Ferricrete Fragments)
MF (Massive Ferricrete)
PF (Cemented Pebbly Ferricrete)
RC (Recemented Fe-rich Colluvium)

ELEMENT	LAB	METHOD	#SAMPLES	PERCENTILES													
				1%	5%	10%	25%	50%	75%	90%	95%	99%	MINIMUM	MAXIMUM	MODE	MEAN	STD. DEV.
SiO_2 WT%	CSIRO	ICP FS	25	4.54	5.15	5.67	9.80	14.89	19.52	31.72	41.85	50.48	4.54	50.48	14.28	16.70	10.93
Al_2O_3 WT%	CSIRO	ICP FS	25	5.27	6.65	6.99	8.18	10.41	11.43	15.66	16.41	21.75	5.27	21.75	9.82	10.46	3.49
Fe_2O_3 WT%	CSIRO	ICP FS	25	37.78	43.12	45.31	57.84	65.29	68.95	73.38	74.03	77.96	37.78	77.96	64.09	62.52	10.29
Fe_2O_3 WT%	AMDEL	AAS HF	75	3.90	8.10	19.60	33.60	41.40	48.80	54.30	61.30	72.60	3.90	72.60	40.40	39.66	13.83
MGO WT%	CSIRO	ICP FS	25	0.02	0.03	0.03	0.05	0.07	0.10	0.13	0.13	0.18	0.02	0.18	0.06	0.07	0.04
CAO WT%	CSIRO	ICP FS	25	0.02	0.02	0.02	0.06	0.08	0.11	0.24	0.26	0.37	0.02	0.37	0.08	0.11	0.09
TiO_2 WT%	CSIRO	ICP FS	25	0.24	0.25	0.34	0.55	0.92	1.63	2.99	3.38	4.54	0.24	4.54	0.84	1.27	1.08
AG1 PPM	AMDEL	AAS HF	75	0.03	0.03	0.03	0.03	0.03	0.10	0.20	0.30	0.60	0.03	0.60	0.03	0.08	0.10
MN2 PPM	AMDEL	AAS HF	75	1.7	33.0	53.0	94.0	174.0	426.0	1100.0	2100.0	6800.0	1.7	6800.0	168.0	476.2	973.1
MN4 PPM	CSIRO	ICP FS	25	6.7	98.0	119.0	148.0	220.0	326.0	593.0	884.0	914.0	6.7	914.0	198.0	280.7	223.1
CR1 PPM	CSIRO	ICP FS	25	141.0	193.0	202.0	278.0	525.0	1006.0	1517.0	1761.0	7943.0	141.0	7943.0	446.0	941.5	1532.0
CR3 PPM	AMDEL	XRF	75	100.0	159.0	255.0	351.0	880.0	2037.0	4440.0	9999.0	9999.0	100.0	9999.0	840.0	1834.2	2549.2
V1 PPM	CSIRO	ICP FS	25	217.0	290.0	352.0	442.0	622.0	927.0	1165.0	1332.0	1552.0	217.0	1552.0	610.0	710.7	339.4
V3 PPM	AMDEL	XRF	75	30.0	108.0	200.0	351.0	624.0	880.0	1180.0	1243.0	1662.0	30.0	1662.0	618.0	656.2	371.9
CU1 PPM	CSIRO	ICP FS	20	16.0	27.0	32.0	43.0	69.0	115.0	124.0	186.0	723.0	16.0	723.0	60.0	103.1	151.4
CU4 PPM	AMDEL	AA HF	75	7.0	11.0	16.0	36.0	64.0	130.0	245.0	308.0	971.0	7.0	971.0	64.0	113.6	155.0
PB3 PPM	AMDEL	XRF	75	0.7	0.7	0.7	6.0	21.0	35.0	55.0	77.0	341.0	0.7	341.0	18.0	27.6	42.3
ZN3 PPM	AMDEL	AA HF	75	14.0	17.0	21.0	27.0	39.0	75.0	130.0	320.0	1121.0	14.0	1121.0	38.0	90.8	180.0
NI1 PPM	CSIRO	ICP FS	25	37.0	46.0	46.0	58.0	82.0	109.0	135.0	144.0	317.0	37.0	317.0	75.0	91.4	56.8
NI3 PPM	AMDEL	AA HF	75	1.7	1.7	8.0	14.0	35.0	73.0	507.0	810.0	1500.0	1.7	1500.0	35.0	140.0	289.2
CO3 PPM	AMDEL	AA HF	75	1.7	1.7	1.7	5.0	9.0	25.0	45.0	55.0	240.0	1.7	240.0	9.0	23.0	41.4
AS4 PPM	AMDEL	XRF	75	0.7	0.7	2.0	8.0	20.0	53.0	182.0	315.0	2595.0	0.7	2595.0	20.0	85.2	308.5
SB2 PPM	AMDEL	XRF	75	0.7	0.7	0.7	0.7	3.0	6.0	9.0	13.0	212.0	0.7	212.0	3.0	6.7	24.3
BI1 PPM	AMDEL	OES	75	0.3	0.3	0.3	0.3	0.3	0.3	0.3	2.0	3.0	0.3	3.0	0.3	0.5	0.5
BI3 PPM	AMDEL	XRF	75	0.3	0.3	0.3	0.3	0.3	2.0	4.0	6.0	12.0	0.3	12.0	0.3	1.4	2.1
CD2 PPM	AMDEL	AAS HF	75	0.3	0.3	0.3	0.3	0.3	0.3	0.3	2.0	2.0	0.3	2.0	0.3	0.4	0.4
MO2 PPM	AMDEL	XRF	75	0.7	0.7	0.7	0.7	2.0	4.0	10.0	15.0	46.0	0.7	46.0	0.7	4.2	6.9
SN1 PPM	AMDEL	OES	75	0.3	0.3	0.3	0.3	0.3	1.0	2.0	3.0	6.0	0.3	6.0	0.3	0.8	1.0
SN5 PPM	AMDEL	XRF	75	0.3	0.3	0.3	0.3	2.0	6.0	8.0	8.0	14.0	0.3	14.0	2.0	3.3	3.1
GE1 PPM	AMDEL	OES	75	0.3	0.3	0.3	0.3	0.3	1.0	2.0	2.0	4.0	0.3	4.0	0.3	0.7	0.7
GA PPM	AMDEL	OES	75	0.3	0.3	5.0	6.0	10.0	15.0	25.0	25.0	30.0	0.3	30.0	10.0	11.9	7.4
W2 PPM	AMDEL	XRF	75	3.3	3.3	3.3	3.3	3.3	13.0	18.0	41.0	145.0	3.3	145.0	3.3	11.9	23.1
BA1 PPM	CSIRO	ICP FS	25	131.0	132.0	133.0	139.0	160.0	211.0	569.0	661.0	725.0	131.0	725.0	158.0	232.9	170.5
ZR1 PPM	CSIRO	ICP FS	25	170.0	217.0	221.0	236.0	287.0	336.0	427.0	468.0	475.0	170.0	475.0	284.0	300.9	78.2
NB3 PPM	AMDEL	XRF	75	1.3	1.3	1.3	5.0	10.0	14.0	17.0	27.0	29.0	1.3	29.0	10.0	10.0	7.0
TA3 PPM	AMDEL	XRF	75	1.0	1.0	1.0	1.0	1.0	1.0	1.0	4.0	18.0	1.0	18.0	1.0	1.5	2.2
SE2 PPM	AMDEL	XRF	75	0.3	0.3	0.3	0.3	2.0	5.0	7.0	8.0	10.0	0.3	10.0	2.0	2.9	2.6
BE1 PPM	AMDEL	OES	75	0.3	0.3	0.3	0.3	0.3	0.3	0.3	0.3	1.0	0.3	1.0	0.3	0.3	0.1
AU PPB	ANALABS	334	30	0.3	0.3	1.0	2.0	2.7	6.0	14.0	40.0	183.0	0.3	183.0	2.7	11.2	33.3

Table 5: STATISTICS FOR SOUTH MURCHISON AREA

SAMPLE TYPE: PN (Plinthite)

ELEMENT	LAB	METHOD	#SAMPLES	PERCENTILES												
				1%	5%	10%	25%	50%	75%	90%	95%	99%	MINIMUM	MAXIMUM	MODE	MEAN	STD. DEV.
SiO_2 WT%	CSIRO	ICP FS	9	18.42	18.42	18.42	34.42	49.06	57.63	72.38	72.38	72.38	18.42	72.38	41.64	46.86	16.38
Al_2O_3 WT%	CSIRO	ICP FS	9	7.98	7.98	7.98	12.44	16.68	17.56	23.04	23.04	23.04	7.98	23.04	14.18	15.41	4.48
Fe_2O_3 WT%	CSIRO	ICP FS	9	9.19	9.19	9.19	19.49	22.21	42.22	50.58	50.58	50.58	9.19	50.58	19.92	29.04	14.81
Fe_2O_3 WT%	AMDEL	AAS HF	16	6.10	6.10	6.20	11.80	15.00	29.30	33.20	33.60	33.60	6.10	33.60	15.00	17.94	9.97
MGO WT%	CSIRO	ICP FS	9	0.02	0.02	0.02	0.02	0.02	0.06	0.08	0.08	0.08	0.02	0.08	0.02	0.04	0.03
CAO WT%	CSIRO	ICP FS	9	0.02	0.02	0.02	0.02	0.02	0.05	0.08	0.08	0.08	0.02	0.08	0.02	0.04	0.03
TiO_2 WT%	CSIRO	ICP FS	9	0.43	0.43	0.43	0.60	0.79	0.87	1.45	1.45	1.45	0.43	1.45	0.75	0.80	0.31
AG1 PPM	AMDEL	AAS HF	16	0.03	0.03	0.03	0.03	0.03	0.20	0.20	1.00	1.00	0.03	1.00	0.03	0.14	0.24
MN2 PPM	AMDEL	AAS HF	16	15.0	15.0	25.0	25.0	85.0	160.0	166.0	167.0	167.0	15.0	167.0	35.0	81.6	62.0
MN4 PPM	CSIRO	ICP FS	7	31.0	31.0	31.0	31.0	87.0	187.0	240.0	240.0	240.0	31.0	240.0	47.0	112.1	84.1
CR1 PPM	CSIRO	ICP FS	9	97.0	97.0	97.0	227.0	251.0	303.0	3029.0	3029.0	3029.0	97.0	3029.0	237.0	548.6	932.9
CR3 PPM	AMDEL	XRF	16	88.0	88.0	105.0	190.0	236.0	298.0	375.0	3697.0	3697.0	88.0	3697.0	220.0	438.9	872.2
V1 PPM	CSIRO	ICP FS	9	147.0	147.0	147.0	357.0	386.0	509.0	923.0	923.0	923.0	147.0	923.0	363.0	446.4	247.8
V3 PPM	AMDEL	XRF	16	38.0	38.0	83.0	121.0	294.0	504.0	861.0	905.0	905.0	38.0	905.0	270.0	336.2	270.4
CU1 PPM	CSIRO	ICP FS	4	11.0	11.0	11.0	38.0	72.0	119.0	119.0	119.0	119.0	11.0	119.0	38.0	60.0	46.6
CU4 PPM	AMDEL	AA HF	16	4.0	4.0	4.0	6.0	10.0	26.0	50.0	130.0	130.0	4.0	130.0	8.0	21.1	31.7
PB3 PPM	AMDEL	XRF	16	7.0	7.0	12.0	20.0	25.0	34.0	55.0	137.0	137.0	7.0	137.0	25.0	32.9	30.3
ZN3 PPM	AMDEL	AA HF	16	6.0	6.0	6.0	8.0	14.0	34.0	44.0	47.0	47.0	6.0	47.0	10.0	18.1	14.1
NI1 PPM	CSIRO	ICP FS	9	16.7	16.7	16.7	45.0	52.0	58.0	470.0	470.0	470.0	16.7	470.0	52.0	99.3	141.0
NI3 PPM	AMDEL	AA HF	16	1.7	1.7	5.0	10.0	20.0	25.0	40.0	88.0	88.0	1.7	88.0	15.0	20.9	20.8
CO3 PPM	AMDEL	AA HF	16	1.7	1.7	1.7	1.7	5.0	10.0	11.0	25.0	25.0	1.7	25.0	5.0	6.9	6.0
AS4 PPM	AMDEL	XRF	16	11.0	11.0	11.0	16.0	28.0	39.0	55.0	178.0	178.0	11.0	178.0	18.0	34.3	40.3
SB2 PPM	AMDEL	XRF	16	0.7	0.7	0.7	0.7	0.7	5.0	9.0	10.0	10.0	0.7	10.0	0.7	2.5	3.2
BI1 PPM	AMDEL	OES	16	0.3	0.3	0.3	0.3	0.3	1.0	2.0	2.0	2.0	0.3	2.0	0.3	0.6	0.6
BI3 PPM	AMDEL	XRF	16	0.3	0.3	0.3	0.3	0.3	1.0	3.0	4.0	4.0	0.3	4.0	0.3	1.0	1.2
CD2 PPM	AMDEL	AAS HF	16	0.3	0.3	0.3	0.3	0.3	0.3	0.3	2.0	2.0	0.3	2.0	0.3	0.4	0.4
MO2 PPM	AMDEL	XRF	16	0.7	0.7	0.7	0.7	3.0	4.0	10.0	11.0	11.0	0.7	11.0	3.0	3.5	3.1
SN1 PPM	AMDEL	OES	16	0.3	0.3	0.3	0.3	2.0	3.0	4.0	6.0	6.0	0.3	6.0	1.0	1.8	1.6
SN5 PPM	AMDEL	XRF	16	0.3	0.3	0.3	2.0	4.0	6.0	7.0	8.0	8.0	0.3	8.0	3.0	3.5	2.5
GE1 PPM	AMDEL	OES	16	0.3	0.3	0.3	0.3	0.3	0.3	1.0	1.0	1.0	0.3	1.0	0.3	0.4	0.2
GA PPM	AMDEL	OES	16	10.0	10.0	15.0	20.0	25.0	30.0	30.0	30.0	30.0	10.0	30.0	25.0	23.7	6.2
W2 PPM	AMDEL	XRF	16	3.3	3.3	3.3	3.3	3.3	13.0	16.0	27.0	27.0	3.3	27.0	3.3	7.0	7.1
BA1 PPM	CSIRO	ICP FS	7	33.3	33.3	33.3	45.0	196.0	225.0	1090.0	1090.0	1090.0	33.3	1090.0	148.0	277.5	366.3
ZR1 PPM	CSIRO	ICP FS	9	214.0	214.0	214.0	231.0	252.0	439.0	865.0	865.0	865.0	214.0	865.0	246.0	380.2	226.0
NB3 PPM	AMDEL	XRF	16	6.0	6.0	10.0	11.0	13.0	30.0	37.0	58.0	58.0	6.0	58.0	13.0	18.7	13.5
TA3 PPM	AMDEL	XRF	16	1.0	1.0	1.0	1.0	1.0	1.0	4.0	7.0	7.0	1.0	7.0	1.0	1.6	1.6
SE2 PPM	AMDEL	XRF	16	0.3	0.3	0.3	3.0	3.0	6.0	7.0	9.0	9.0	0.3	9.0	3.0	3.8	2.5
BE1 PPM	AMDEL	OES	16	0.3	0.3	0.3	0.3	0.3	0.3	1.0	1.0	1.0	0.3	1.0	0.3	0.4	0.2
AU PPB	ANALABS	334	10	0.3	0.3	0.3	1.0	2.0	3.0	4.0	5.0	5.0	0.3	5.0	1.0	2.1	1.6

Table 6: STATISTICS FOR SOUTH MURCHISON AREA

SAMPLE TYPE: MF (Massive Ferricrete)

ELEMENT	LAB	METHOD	#SAMPLES	PERCENTILES								MINIMUM	MAXIMUM	MODE	MEAN	STD. DEV.
				1%	5%	10%	25%	50%	75%	90%	95%	99%					
SiO_2 WT%	CSIRO	ICP FS	10	9.38	9.38	9.80	13.55	19.55	31.72	41.85	50.48	50.48	9.38	50.48	19.52	23.58	13.83
Al_2O_3 WT%	CSIRO	ICP FS	10	6.65	6.65	7.82	8.18	10.60	11.40	11.59	16.41	16.41	6.65	16.41	10.41	10.37	2.68
Fe_2O_3 WT%	CSIRO	ICP FS	10	37.78	37.78	43.12	45.31	57.84	61.43	66.36	72.75	72.75	37.78	72.75	53.19	54.60	11.10
Fe_2O_3 WT%	AMDEL	AAS HF	52	3.90	7.20	17.90	30.40	38.90	43.20	50.50	53.60	55.40	3.90	55.40	38.20	35.61	13.15
MGO WT%	CSIRO	ICP FS	10	0.05	0.05	0.05	0.06	0.08	0.10	0.11	0.13	0.13	0.05	0.13	0.08	0.08	0.03
CAO WT%	CSIRO	ICP FS	10	0.02	0.02	0.02	0.07	0.09	0.11	0.16	0.17	0.17	0.02	0.17	0.08	0.09	0.05
TiO_2 WT%	CSIRO	ICP FS	10	0.25	0.25	0.43	0.51	0.83	1.17	1.43	1.63	1.63	0.25	1.63	0.66	0.83	0.45
AG1 PPM	AMDEL	AAS HF	52	0.03	0.03	0.03	0.03	0.03	0.03	0.20	0.30	0.60	0.03	0.60	0.03	0.08	0.11
MN2 PPM	AMDEL	AAS HF	52	1.7	27.0	47.0	66.0	168.0	423.0	1100.0	2216.0	6800.0	1.7	6800.0	160.0	539.0	1147.1
MN4 PPM	CSIRO	ICP FS	10	6.7	6.7	98.0	152.0	252.0	398.0	884.0	914.0	914.0	6.7	914.0	198.0	339.9	313.9
CR1 PPM	CSIRO	ICP FS	10	202.0	202.0	226.0	292.0	525.0	766.0	1006.0	1517.0	1517.0	202.0	1517.0	446.0	602.9	416.7
CR3 PPM	AMDEL	XRF	52	100.0	135.0	250.0	335.0	840.0	1840.0	3536.0	4492.0	9999.0	100.0	9999.0	730.0	1416.4	1872.8
V1 PPM	CSIRO	ICP FS	10	217.0	217.0	290.0	352.0	540.0	905.0	927.0	1165.0	1165.0	217.0	1165.0	404.0	577.2	319.2
V3 PPM	AMDEL	XRF	52	30.0	100.0	138.0	310.0	540.0	861.0	1131.0	1180.0	1420.0	30.0	1420.0	510.0	584.6	357.3
CU1 PPM	CSIRO	ICP FS	9	44.0	44.0	44.0	70.0	88.0	115.0	723.0	723.0	723.0	44.0	723.0	85.0	159.2	213.0
CU4 PPM	AMDEL	AA HF	52	7.0	13.0	27.0	45.0	95.0	177.0	280.0	370.0	971.0	7.0	971.0	94.0	142.1	176.9
PB3 PPM	AMDEL	XRF	52	0.7	0.7	0.7	4.0	18.0	35.0	57.0	79.0	341.0	0.7	341.0	17.0	27.9	49.0
ZN3 PPM	AMDEL	AA HF	52	14.0	16.0	22.0	30.0	46.0	102.0	259.0	323.0	1121.0	14.0	1121.0	45.0	112.8	212.3
NI1 PPM	CSIRO	ICP FS	10	37.0	37.0	58.0	65.0	105.0	122.0	135.0	144.0	144.0	37.0	144.0	96.0	95.4	34.6
NI3 PPM	AMDEL	AA HF	52	1.7	1.7	8.0	14.0	37.0	75.0	507.0	673.0	1400.0	1.7	1400.0	35.0	130.6	260.0
CO3 PPM	AMDEL	AA HF	52	1.7	1.7	1.7	6.0	10.0	35.0	50.0	170.0	240.0	1.7	240.0	10.0	27.6	48.3
AS4 PPM	AMDEL	XRF	52	0.7	0.7	0.7	7.0	20.0	53.0	199.0	476.0	2595.0	0.7	2595.0	19.0	105.3	367.4
SB2 PPM	AMDEL	XRF	52	0.7	0.7	0.7	0.7	3.0	6.0	8.0	13.0	212.0	0.7	212.0	3.0	7.5	29.2
BI1 PPM	AMDEL	OES	52	0.3	0.3	0.3	0.3	0.3	0.3	0.3	2.0	3.0	0.3	3.0	0.3	0.5	0.6
BI3 PPM	AMDEL	XRF	52	0.3	0.3	0.3	0.3	0.3	1.0	3.0	4.0	6.0	0.3	6.0	0.3	1.0	1.3
CD2 PPM	AMDEL	AAS HF	52	0.3	0.3	0.3	0.3	0.3	0.3	0.3	2.0	2.0	0.3	2.0	0.3	0.5	0.5
MO2 PPM	AMDEL	XRF	52	0.7	0.7	0.7	0.7	0.7	3.0	4.0	9.0	15.0	0.7	15.0	0.7	2.2	3.0
SN1 PPM	AMDEL	OES	52	0.3	0.3	0.3	0.3	0.3	0.3	3.0	3.0	6.0	0.3	6.0	0.3	0.9	1.2
SN5 PPM	AMDEL	XRF	52	0.3	0.3	0.3	0.3	2.0	6.0	8.0	8.0	14.0	0.3	14.0	2.0	3.3	3.1
GE1 PPM	AMDEL	OES	52	0.3	0.3	0.3	0.3	0.3	1.0	2.0	2.0	3.0	0.3	3.0	0.3	0.6	0.6
GA PPM	AMDEL	OES	52	0.3	0.3	6.0	6.0	10.0	20.0	25.0	25.0	30.0	0.3	30.0	10.0	12.1	7.5
W2 PPM	AMDEL	XRF	52	3.3	3.3	3.3	3.3	3.3	3.3	11.0	14.0	18.0	3.3	18.0	3.3	4.7	3.6
BA1 PPM	CSIRO	ICP FS	10	131.0	131.0	132.0	136.0	197.0	283.0	413.0	569.0	569.0	131.0	569.0	161.0	239.3	145.7
ZR1 PPM	CSIRO	ICP FS	10	170.0	170.0	225.0	236.0	287.0	298.0	332.0	336.0	336.0	170.0	336.0	273.0	271.7	50.6
NB3 PPM	AMDEL	XRF	52	1.3	1.3	1.3	6.0	11.0	14.0	16.0	27.0	29.0	1.3	29.0	11.0	10.6	6.8
TA3 PPM	AMDEL	XRF	52	1.0	1.0	1.0	1.0	1.0	1.0	1.0	4.0	7.0	1.0	7.0	1.0	1.2	1.0
SE2 PPM	AMDEL	XRF	52	0.3	0.3	0.3	0.7	3.0	5.0	7.0	9.0	10.0	0.3	10.0	3.0	3.1	2.7
BE1 PPM	AMDEL	OES	52	0.3	0.3	0.3	0.3	0.3	0.3	0.3	0.3	1.0	0.3	1.0	0.3	0.3	0.1
AU PPB	ANALABS	334	16	0.3	0.3	2.0	2.7	5.0	10.0	40.0	183.0	183.0	0.3	183.0	5.0	18.4	44.9

and range (minimum and maximum values) of the data. Outliers are most easily expressed using this type of presentation of the data distribution. Each histogram also indicates the mode, left hinge, right hinge, minimum value, maximum value, mean, and standard deviation in a numerical form at the right hand side of the figure.

Each figure is comprised of two histograms; the lateritic materials group (CN, CP, LN, LP, MS), and the ferricrete group (FF, MF, PC, RC). The lateritic materials display some differences in their distribution relative to the ferricrete group samples although at this stage it is difficult to test quantitatively. Because none of the variables exhibit normal distributions, a topic for further research, it is difficult to apply standard statistical tests to compare sample types or groups of data. Thus, a detailed analysis of the distribution of the sample populations is not attempted in this report. Subsequent investigations will examine the differences between materials.

Some general trends can be observed from the histograms. Generally, the ferricretes show a greater range of abundances than the lateritic materials. This can be seen most clearly in the box and whisker plots where the hinge lines (25^{th} and 75^{th} percentiles) are more widely spaced in the ferricretes as opposed to the laterites. This could suggest that ferricretes may contain a geochemical pattern that reflects residual abundances of materials. Although the range of the data is broader for the ferricretes, the maximum values between the two sample mediums are similar. Thus, there is no sample medium preference for high relative abundances (anomalous values). A comparison of the means and modes between the lateritic and ferricrete materials for many of the elements shows that there is not much difference between the two groups. However, some elements such as Fe_2O_3, Mn Cu, Zn, Ni, Co, and Zr display distinctively different means between the lateritic and ferricrete samples types. However, a greater number of ferricrete samples would be required, coupled with further investigation, in order to characterize differences. Such research is currently underway within the Laterite Geochemistry Project.

At least three distinct populations are observed in the data. The distributions of the variables, Fe Ti, Cr, V, Zn, Zr, and Nb appear to be comprised of two or more modes as seen in Figures 7, 8, 10, 11, 14, 29, and 30. For these elements the two apparent populations may represent differences between the supracrustal volcanic host rocks (basalts vs. rhyolites, etc.), and/or differences in weathered materials, and/or anomalous abundances associated with mineralization. Zinc (Figure 14) is unique in that it can reflect both compositional variation of the original volcanic rocks and abundances that reflect proximity to base metal accumulations (Wolfe, 1977). Iron (Fe_2O_3), appears to be bi-modally distributed (Figure 7) and it may reflect compositional differences between the weathered materials (nodules/pisoliths vs. ferricrete).

Elements such as Au, Ag, As, Sb, Bi, Sn, W, Mn, and Ni are log-normal in their distribution (see Figures 6, 9, 15, 17, 18, 19, 20, 22, 23, 24, and 27). For many of these histograms, positively skewed values represent anomalous values that are potentially associated with various types of mineralization.

Element Maps

The abundances of a selected group of elements are shown in Figures 31-55.

Typically, the elements in lateritic and other weathered materials are not normally distributed. In this case, one approach that provides a good representation of the distribution of the data, is the use of percentiles of the ranked data. Thus, the relative position of the data values with respect to the maximum and minimum can be plotted with some knowledge of the true distribution of the data.

Because the sample sites are not distributed uniformly over the map area, methods of data presentation such as contour maps are not appropriate for describing the spatial variation of the data at the scale presented. However, the data can be conveniently presented by using symbols whose sizes are based on the percentile ranking of the data. A commonly used method of expressing concentrations over irregularly sampled areas is expression of each concentration by a symbol whose size is proportional to its magnitude (Howarth, 1983, p.124). The use of such symbols can be employed to indicate areas that are enriched or depleted. However, caution is advised in the interpretation of these proportionally sized symbols. Symbol size does not necessarily reflect anomalously low or high values, rather it reflects the maximum and

minimum values of the data which may or may not be "anomalous" with respect to zones of mineralization.
The size of the symbols is not a linear function of concentration of the elements. For visual ease and assistance in the recognition of outlier data the symbol sizes are defined as:

$$\text{Map Symbol Size} = \text{Minimum Symbol Size for Map} + \text{Constant Symbol Size} * (\text{Percentile}/100)^4$$

where the percentile is the percentile ranking of the sample for the particular element being considered. This quartic function enhances the size of the symbols for the high end outliers of the data whilst making the samples that fit in the rankings of less than 75 percentile range more equal in size. This non-linear distribution of symbol sizes assists in a faster visual assessment of anomalous values.

Interpretation of the Geochemical Distributions

Interpretation of the geochemical maps requires some knowledge of the geological processes that have acted, or are still acting within an area. Inference about the geological environment can be made from many of the geochemical maps and can assist in refining geological models. Hallberg (1984) has shown that within the saprolitic laterite profile, ratios of Ti, Cr, and Zr retain characteristics of the original lithologies. Titanium, and Cr ratios, commonly outline the mafic volcanic or mafic volcanic derived sedimentary assemblages, whilst Zr is useful in outlining the Zr enriched felsic volcanics. Maps of these elements must be interpreted with caution as the abundances of the elements may have been modified by several processes, particularly during weathering. Fractionated igneous rocks tend to show enrichment in Mo, Be, W, Ga, and Sn and laterite geochemistry on a regional scale could be expected to reflect such effects.

Several patterns emerge from a careful examination of the element maps. One of the most dominant patterns is that shown by Fe, Cr, Cu, Zn, Ni, and Co. These elements all show high relative abundance in the eastern and central part of the map sheets as shown in Figures 32, 35, 37, 39, 40, and 41. The abundances of these elements in laterite can reflect mafic-ultramafic bedrock lithologies. The increased relative abundances are associated with mafic volcanic and intrusive rocks in the south-east part of the Yalgoo-Singleton Greenstone Belt and north-easterly into the Wydgee and Magnet Fold Belts. Part of the abundances increase may be due to sampling bias, namely more of the samples were collected over mafic and ultramafic lithologies in the eastern part of the area, although it would appear that these three greenstone areas have a significant amount of mafic material in common. An opposing increase in Ga is noted in the west of the area which may reflect sampling of felsic volcanics, felsic sediments, or felsic plutonic rocks.

Another striking trend is the common association of As and Sb as shown in Figures 42 and 43. Several isolated As and Sb anomalies occur throughout the map, however, a noticeable "corridor" trends northwesterly through the Yalgoo-Singleton greenstone belt from the Mt. Gibson area to the Noongal area. This zone contains significant enrichment of As, Sb, and accompanying Au (Figure 31). Many of the higher relative abundances of As and Sb lie close to major faults in the Yalgoo-Singleton area. This suggests that there is an association between some of the fault zones and gold associated elements.

Gold (Figure 31) shows sporadic variation throughout the area based on reconnaissance sampling. Closer sample spacing, for example at 300m is more appropriate for establishing Au distribution.

Niobium, Pb and Zr as shown in Figures 38, 54, and 55 show similar relative increases at the west end of the Red Hill area, the Koolanooka Fe area, and the migmatite zone that occurs in the south east part of the Perenjori map sheet. This pattern may result from fractionation products (i.e. pegmatites) of the surrounding intrusive rocks. Nb also shows an increase near the Rothsay area and in the gneiss terrains to the southwest.

Manganese shows increased relative abundance in the areas where the greenstone belts are narrow, notably the Mt. Magnet, Koolanooka, and west Yalgoo areas.

The relative abundance pattern of V (Figure 36) is high in the Koolanooka and Gullewa areas. This increase is possibly associated with a corresponding Fe enrichment within oxide facies ironstones.

Tin (Figures 48 and 49) shows a relative increase in the Koolanooka and the Golden Grove areas. At Golden Grove, Sn is associated with dispersion from the base metal sulphide deposits (Smith and Perdrix, 1983). Other Sn patterns in the area may be related to magmatic enrichment from the syn-kinematic granitic rocks.

Bismuth, Mo, and W (Figures 44, 45 46, and 52) show enrichment in the Magnet Fold Belt area, the Red Hill area, Golden Grove, and the Noongal area. Relative abundance increases of these elements suggests a felsic magmatic origin that is associated at the margins of the fold belts or through veins that invade the country rock.

Increased abundance levels of Cu, Zn, Pb, and Ni (Figures 37-40) are most notable in the Red Hill, Koolanooka, and Yalgoo areas. The locations of these anomalies appear to be associated closely with lithologic differences within the supracrustal rocks. Such elements can also represent dispersion patterns from sulphide mineral deposits.

Germanium (Figure 50) shows a relative increase pattern in the area north of the Mt. Gibson Au deposits and in the Noongal, and Red Hill areas. This could reflect associated Si enrichment from intruding veins from granitic sources, or be related to sulphide-bearing mineralized environments.

Barium (Figure 52) displays a very large relative increase in the eastern part of the area south of Kirkalocka. The sample that shows the enrichment is situated in the granitic terrain and thus may not have any exploration significance.

Zirconium shows greater relative abundances in areas that were sampled over felsic rocks. Figure 54 shows the distribution of Zr in which the felsic volcanic and granitic gneisses have higher relative abundances.

Figure 56 summarizes the main geochemical trends in the lateritic materials. These trends are:

- the Fe, Co, Cr, Ni, Cu, Zn trend in the east side of the area (Figure 56a)
- the chalcophile corridor as defined primarily by As, and Sb (Figure 56b)
- the zone of relative abundance increases in V in the western part of the area with some local accompanying Sn increases (Figure 56c).
- the zones of Nb and Zr increases that reflect sampling of the more fractionated igneous rocks (Figure 56d),

Principal Components Analysis

Many of these trends discussed above can be determined by the use of systematic and statistical mean of data analysis. One such commonly used technique is principal components analysis which is now discussed.

A fundamental objective in the analysis of data is the extraction of meaningful information from which a reasonable interpretation can be made. As the number of variables increase the more detail is provided however this is at the expense of simplicity of interpretation. There are several good reviews that discuss the basics of multivariate data analysis techniques (e.g. Jöreskog et al, 1976; Davis, 1986).

In geological applications, and particularly within the study of igneous rocks, the foundation of petrology is based upon the systematic variation of the elements involved in magmatic fractionation. It is already known that the lithogeochemistry of igneous rocks contains a number of chemical variables that will correlate with one another. Because of this it would be easier to examine just a few critical elements to extract a meaningful interpretation. However, it is not always known what elements are involved in the magmatic process during fractionation of igneous rocks nor is it always known what subsequent alteration or metamorphism has occurred. Thus, there is uncertainty in choosing, a priori, which variables to include in a subsequent data analysis. A way to overcome this uncertainty is to apply some technique of data analysis that will assist in

reducing the number of variables based on correlations or covariances of the variables. Techniques such as factor analysis, principal components analysis, and cluster analysis, have been developed in response to these problems.

The objective of principal components analysis is to reduce the number of variables necessary to describe the observed variation within a set of data. This is done by forming linear combinations of the variables (components) that describe the distribution of the data. Ideally, to the geologist, each component might be interpreted as describing a geological process such as differentiation (partial melting, crystal fractionation, etc.) and alteration/mineralization (carbonatization, silicification, alkali depletion, metal associations and enrichments etc.).

A method of principal components analysis known as Simultaneous RQ-Mode Principal Components Analysis (Zhou et al, 1983) was carried out on the correlation matrix of the data. The results indicate similar geochemical trends as those discussed above. Table 7 shows the results of the analysis. Table 7a shows the correlation matrix of the variables; Table 7b lists the eigenvalues and corresponding variance accounted for. Table 7c lists the component loadings of the variables, and Table 7d lists the contribution that each variable makes to each component of the reduced variable space.

The geochemical data displays significant variation as indicated by the principal components analysis. The broad spread in the variation is explained by the fact that of the 721 samples consisting of 22 elements, only 70% of the data variation was explained by the first 10 components. The first component only accounts for 13.6% of the data variation. Significant variables for each component are underlined in Table 7. Both the component loadings and relative contributions are shown for all of the components. The relative contributions are defined as the percentage contribution that each variable makes to a given component over the entire reduced variable (component) space.

The first component is dominated by Co, Ni, Cr, Cu, Fe, and Zn. This supports the previously made observation of a common association of these elements. Figure 57 shows the large positive scores of the first component where the mafic rocks of the Magnet and Yalgoo-Singleton Greenstone Belts are outlined. As well Ga is opposed to the enrichment of these elements. The Ga enrichment is shown by the large asterisks in Figure 57. The enrichment of negative component scores compares with the Ga enrichment of Figure 51. As suggested above, a possible explanation of this relationship is the result of a relative Al increase with Ga in Al rich materials, felsic volcanics and other fractionated rocks that are depleted in Co, Ni, Cr, Cu, Zn, and Fe relative to the mafic volcanics and intrusives.

The second component is dominated by Sn, Bi, V, and Fe. This association is most significant in the Red Hill, Golden Grove, Magnet greenstone belts and northwest of the Koolanooka area (see Figure 58). There is a noticeable depletion of Mn within these areas which cannot be easily explained.

The third component outlines a Mn, Pb enrichment that Golden Grove, Koolanooka, Red Hill, Noongal and Gullewa (Figure 59). The significance of this component is, as of yet, not understood.

The fourth component (Figure 60) accounts for a strong association of Mo and W that is greatest at Red Hill and the southern part of Magnet Fold Belt. Greisen associations and other types of mineralization related to pegmatites and felsic intrusions can explain the associations of the variations in this component. A significant inverse relationship with Nb is noted but at this time cannot be explained.

The fifth component displays a very strong association of As, and Sb as outlined above and the pattern of the component scores in Figure 61 indicates the trend of the "chalcophile corridor" that these elements define. In the Warriedar Fold Belt As and Sb associations have been observed in outcrops of some weathered metapelites (R.E. Smith, unpublished data). As well, the strong As, Sb associations tend be associated with more felsic rocks as indicated by the negative association of Cr, Ni, and Co. The distinction of this significant component is further enhanced in that As, and Sb enriched materials are also depleted in Ga, and Nb as indicated in Table 7c (component loadings). An additional important consideration is the proximity of large positive component 5 scores to fault zones in the centre of the Yalgoo-Singleton greenstone belt.

TABLE 7: PRINCIPAL COMPONENTS ANALYSIS OF THE SOUTH MURCHISON AREA

OBSERVATIONS: 721
VARIABLES: 22

The following variables were used from the file SMURCH.SDF:
$Fe_2O_3$2, Ag1, Mn2, Cr3, V3, Cu4, Pb3, Zn3, Ni3, Co3,
As4, Sb2, Bi3, Mo2, Sn5, Ge1, Ga, W2, Nb3, Ta3, Se2, Be1

Table 7a: CORRELATION MATRIX

	Fe2O3	Ag	Mn	Cr	V	Cu	Pb	Zn	Ni	Co	As
Fe_2O_3	1.0000	0.0803	-0.0400	0.3832	0.5087	0.2340	-0.0597	0.2119	0.2136	0.2131	0.1407
Ag	0.0803	1.0000	0.0159	0.0327	0.1293	0.0546	0.1864	0.0606	0.0114	-0.0109	0.0309
Mn	-0.0400	0.0159	1.0000	0.0351	-0.1091	0.0170	0.3270	0.2711	0.1966	0.4053	-0.0399
Cr	0.3832	0.0327	0.0351	1.0000	0.2615	0.1945	-0.1291	0.0780	0.6040	0.2948	0.0728
V	0.5087	0.1293	-0.1091	0.2615	1.0000	0.1079	-0.0665	-0.0304	-0.0141	0.0111	-0.0412
Cu	0.2340	0.0546	0.0170	0.1945	0.1079	1.0000	-0.0976	0.3490	0.1955	0.3144	0.2554
Pb	-0.0597	0.1864	0.3270	-0.1291	-0.0665	-0.0976	1.0000	0.0956	-0.0752	-0.0821	0.0504
Zn	0.2119	0.0606	0.2711	0.0780	-0.0304	0.3490	0.0956	1.0000	0.2704	0.4694	0.0766
Ni	0.2136	0.0114	0.1966	0.6040	-0.0141	0.1955	-0.0752	0.2704	1.0000	0.5363	0.0187
Co	0.2131	-0.0109	0.4053	0.2948	0.0111	0.3144	-0.0821	0.4694	0.5363	1.0000	0.0672
As	0.1407	0.0309	-0.0399	0.0728	-0.0412	0.2554	0.0504	0.0766	0.0187	0.0672	1.0000
Sb	0.1056	0.0474	-0.0104	0.0465	0.0150	0.0469	0.2957	0.1095	0.0017	0.0124	0.2169
Bi	0.1222	0.0176	-0.0420	0.0344	-0.0151	0.0090	0.0102	-0.0109	0.0143	-0.0262	0.1044
Mo	0.0514	-0.0693	-0.0143	-0.0567	-0.0636	-0.0630	0.1463	-0.0476	-0.0269	-0.1243	-0.0499
Sn	0.1687	0.1587	-0.0956	-0.0402	0.1159	0.0016	0.0005	-0.0036	-0.0848	-0.0476	0.0891
Ge	0.2705	0.2326	-0.0441	0.0742	-0.0197	0.0332	-0.0201	0.0124	0.0384	-0.0077	0.0545
Ga	-0.1729	0.0362	-0.0689	-0.1419	0.1505	-0.2790	0.1060	-0.1969	-0.1718	-0.2098	-0.1098
W	0.0111	-0.0052	-0.0164	-0.0055	0.0416	0.0357	0.0603	-0.0141	-0.0090	-0.0107	-0.0148
Nb	-0.0787	0.0594	-0.0216	-0.1201	-0.0621	-0.1828	0.1319	-0.0466	-0.1193	-0.1167	-0.0646
Ta	0.0924	-0.0143	-0.0329	-0.0058	-0.0169	-0.0236	-0.0372	-0.0226	-0.0478	-0.0545	0.0168
Se	-0.0744	0.0343	-0.0345	-0.0758	0.0748	-0.0409	0.0376	-0.0320	-0.0278	-0.0644	0.0270
Be	-0.2164	-0.0532	0.1624	-0.1043	-0.1764	-0.0490	0.2124	-0.0108	-0.0521	-0.0076	-0.0490

	Sb	Bi	Mo	Sn	Ge	Ga	W	Nb	Ta	Se	Be
Fe_2O_3	0.1056	0.1222	0.0514	0.1687	0.2705	-0.1729	0.0111	-0.0787	0.0924	-0.0744	-0.2164
Ag	0.0474	0.0176	-0.0693	0.1587	0.2326	0.0362	-0.0052	0.0594	-0.0143	0.0343	-0.0532
Mn	-0.0104	-0.0420	-0.0143	-0.0956	-0.0441	-0.0689	-0.0164	-0.0216	-0.0329	-0.0345	0.1624
Cr	0.0465	0.0344	-0.0567	-0.0402	0.0742	-0.1419	-0.0055	-0.1201	-0.0058	-0.0758	-0.1043
V	0.0150	-0.0151	-0.0636	0.1159	-0.0197	0.1505	0.0416	-0.0621	-0.0169	0.0748	-0.1764
Cu	0.0469	0.0090	-0.0630	0.0016	0.0332	-0.2790	0.0357	-0.1828	-0.0236	-0.0409	-0.0490
Pb	0.2957	0.0102	0.1463	0.0005	-0.0201	0.1060	0.0603	0.1319	-0.0372	0.0376	0.2124
Zn	0.1095	-0.0109	-0.0476	-0.0036	0.0124	-0.1969	-0.0141	-0.0466	-0.0226	-0.0320	-0.0108
Ni	0.0017	0.0143	-0.0269	-0.0848	0.0384	-0.1718	-0.0090	-0.1193	-0.0478	-0.0278	-0.0521
Co	0.0124	-0.0262	-0.1243	-0.0476	-0.0077	-0.2098	-0.0107	-0.1167	-0.0545	-0.0644	-0.0076
As	0.2169	0.1044	-0.0499	0.0891	0.0545	-0.1098	-0.0148	-0.0646	0.0168	0.0270	-0.0490
Sb	1.0000	0.0857	-0.0469	0.0890	0.0383	-0.0729	-0.0028	-0.0746	-0.0306	-0.0156	-0.0643
Bi	0.0857	1.0000	0.2331	0.6051	0.0161	0.0466	0.0473	-0.0378	0.0475	0.0491	-0.0523
Mo	-0.0469	0.2331	1.0000	0.0514	0.0196	0.0070	0.4740	-0.0399	-0.0102	0.0280	0.0567
Sn	0.0890	0.6051	0.0514	1.0000	0.0892	0.1827	0.0527	0.2966	0.0361	0.0767	-0.0732
Ge	0.0383	0.0161	0.0196	0.0892	1.0000	-0.0347	0.0078	-0.0251	0.0136	-0.0308	-0.0548
Ga	-0.0729	0.0466	0.0070	0.1827	-0.0347	1.0000	-0.0357	0.4085	0.0099	0.1589	-0.0163
W	-0.0028	0.0473	0.4740	0.0527	0.0078	-0.0357	1.0000	-0.0494	-0.0102	0.1134	-0.0107
Nb	-0.0746	-0.0378	-0.0399	0.2966	-0.0251	0.4085	-0.0494	1.0000	0.0771	0.0180	0.0502
Ta	-0.0306	0.0475	-0.0102	0.0361	0.0136	0.0099	-0.0102	0.0771	1.0000	-0.0777	-0.0222
Se	-0.0156	0.0491	0.0280	0.0767	-0.0308	0.1589	0.1134	0.0180	-0.0777	1.0000	-0.0663
Be	-0.0643	-0.0523	0.0567	-0.0732	-0.0548	-0.0163	-0.0107	0.0502	-0.0222	-0.0663	1.0000

TABLE 7 (CONT'D) PRINCIPAL COMPONENTS ANALYSIS OF THE SOUTH MURCHISON AREA

Table 7b: EIGENVALUES (VARIANCE EXPLAINED)

	EIGENVALUES	% OF TRACE	Σ OF TRACE
1	2.9932	13.6054	13.6054
2	2.1380	9.7181	23.3235
3	1.7978	8.1720	31.4955
4	1.5692	7.1327	38.6282
5	1.4317	6.5079	45.1361
6	1.3179	5.9907	51.1268
7	1.1763	5.3466	56.4734
8	1.0804	4.9111	61.3845
9	1.0469	4.7588	66.1433
10	0.9486	4.3120	70.4553
11	0.8968	4.0762	74.5316
12	0.8593	3.9058	78.4373
13	0.7866	3.5756	82.0129
14	0.7089	3.2223	85.2352
15	0.6021	2.7369	87.9720
16	0.5812	2.6417	90.6137
17	0.5251	2.3870	93.0007
18	0.4115	1.8704	94.8711
19	0.3625	1.6475	96.5186
20	0.2705	1.2294	97.7481
21	0.2584	1.1747	98.9228
22	0.2370	1.0772	100.0000

TABLE 7 (CONT'D): PRINCIPAL COMPONENTS ANALYSIS OF THE SOUTH MURCHISON AREA

Table 7c: COMPONENT LOADINGS

	1	2	3	4	5	6	7	8	9	10	11
Fe_2O_3	0.5669	0.5176	-0.1199	-0.0212	-0.0159	0.2100	-0.1639	0.1543	-0.1915	-0.1231	0.0014
Ag	0.0769	0.2759	0.1998	-0.3149	0.1190	0.3845	-0.1880	-0.4224	0.1154	-0.0505	-0.0076
Mn	0.2671	-0.3959	0.5254	-0.1830	-0.2325	0.0569	-0.0379	0.0401	-0.0537	-0.1250	-0.2127
Cr	0.6343	0.1551	-0.2024	-0.0357	-0.2924	0.0717	-0.0642	0.2846	0.3253	0.1736	0.1934
V	0.2225	0.4872	-0.2947	-0.1429	-0.1907	0.4217	0.2060	0.2152	-0.2637	-0.3264	0.0928
Cu	0.5728	0.0357	0.0074	0.1002	0.2562	-0.0977	0.1608	-0.2400	-0.3297	-0.0342	0.3139
Pb	-0.1225	-0.0712	0.7024	-0.1466	0.1082	0.4116	-0.0074	0.2603	0.0147	-0.0055	-0.0116
Zn	0.5553	-0.1453	0.3508	-0.1243	0.0336	-0.0814	0.0902	-0.2033	-0.3499	-0.0558	-0.1439
Ni	0.6854	-0.1138	0.0258	-0.0392	-0.3811	-0.0949	-0.0235	0.0711	0.3453	0.2566	0.0317
Co	0.7142	-0.2323	0.1847	-0.1295	-0.2395	-0.1778	0.0788	-0.1022	-0.0660	0.0108	-0.0718
As	0.2357	0.1839	0.1501	0.0342	0.5385	-0.1384	0.1969	0.0560	-0.0079	0.3777	0.3589
Sb	0.1434	0.1626	0.3236	-0.0572	0.4998	0.1771	0.1791	0.4321	0.1900	0.1073	-0.1852
Bi	0.0101	0.5619	0.3362	0.1938	-0.0272	-0.5171	-0.0090	0.0614	0.2159	-0.2353	-0.1232
Mo	-0.1243	0.1845	0.3351	0.6899	-0.2702	0.1302	-0.1502	0.0370	-0.0475	0.0436	0.0397
Sn	-0.0779	0.7020	0.3190	-0.1355	-0.0574	-0.4171	0.0023	-0.0881	0.0355	-0.1724	0.0204
Ge	0.1494	0.2791	0.0062	-0.0595	0.1689	0.2504	-0.5206	-0.4258	0.2552	0.1512	-0.0366
Ga	-0.4706	0.2583	0.0711	-0.3901	-0.3729	0.0669	0.1744	0.0610	-0.0318	0.1589	0.1033
W	-0.0230	0.1634	0.2453	0.6456	-0.2600	0.2587	0.0406	-0.1062	-0.1825	0.2019	0.0649
Nb	-0.3514	0.1815	0.2100	-0.4867	-0.2864	-0.1264	-0.0847	-0.0147	-0.1963	0.2819	0.2493
Ta	-0.0376	0.1171	-0.0671	-0.0459	0.0346	-0.1875	-0.4474	0.2547	-0.4840	0.4119	-0.2539
Se	-0.1358	0.1638	0.0855	0.0355	-0.1524	0.1378	0.6100	-0.3098	0.0688	0.2832	-0.1362
Be	-0.1609	-0.3656	0.3361	0.0119	-0.0427	-0.0242	-0.2217	0.0834	0.0250	-0.2214	0.5816

	12	13	14	15	16	17	18	19	20	21	22
Fe_2O_3	0.0212	0.2801	0.0051	-0.0913	0.2065	0.0658	-0.0790	0.0746	-0.0570	-0.2890	0.1270
Ag	-0.1821	-0.5455	0.0610	-0.0031	0.0141	0.1691	-0.1157	-0.0733	-0.0365	-0.0621	0.0071
Mn	-0.1612	0.1579	0.3750	0.1675	0.0301	-0.1923	-0.0115	-0.2602	0.0787	-0.0809	-0.0173
Cr	-0.0797	-0.1264	-0.0351	-0.0539	0.0368	-0.1094	0.1763	-0.2178	-0.1730	0.1282	0.1324
V	-0.1284	0.0408	0.0493	0.0993	-0.0487	0.0518	-0.0019	-0.0048	0.0950	0.1782	-0.2048
Cu	0.0024	-0.1368	-0.0694	-0.1127	-0.2304	-0.4409	-0.0873	-0.0062	0.0129	-0.0445	0.0022
Pb	-0.0619	-0.0358	0.0450	-0.2304	0.0587	-0.1671	0.1412	0.3053	-0.0413	0.0895	0.0362
Zn	0.2035	0.0521	-0.2363	-0.2261	-0.0334	0.2818	0.2718	-0.1434	0.0151	0.0445	-0.0173
Ni	-0.0080	-0.1204	-0.0883	-0.0962	-0.0267	0.0353	-0.0143	0.1577	0.2815	-0.1114	-0.1371
Co	0.0547	0.0550	0.0460	0.2397	-0.0842	0.1390	-0.2614	0.2199	-0.1914	0.1473	0.0537
As	-0.0829	0.1061	0.4333	0.0178	0.0583	0.2231	0.0386	-0.0147	0.0366	0.0302	-0.0321
Sb	0.2144	-0.0190	-0.3266	0.2087	-0.1249	-0.0053	-0.1711	-0.1400	0.0162	-0.0340	-0.0266
Bi	-0.1677	-0.0222	0.0405	-0.0972	-0.1008	-0.0146	0.0593	0.0123	-0.1962	-0.0768	-0.2151
Mo	0.1209	0.0259	0.0730	-0.3035	-0.0373	0.0857	-0.2898	-0.1331	0.0616	0.1196	0.0369
Sn	0.0157	-0.0357	-0.0611	0.1819	0.1030	-0.0579	0.0489	0.0306	0.2210	0.1149	0.2166
Ge	0.0639	0.4458	-0.0495	0.0684	-0.1526	-0.1054	0.0572	0.0087	0.0064	0.0990	-0.0758
Ga	0.0922	0.0902	0.1085	-0.0586	-0.5264	0.0897	0.0293	-0.0057	-0.0187	-0.1107	0.0976
W	0.1329	-0.1506	-0.0197	0.4057	0.0018	-0.0064	0.2224	0.0586	-0.0447	-0.0958	-0.0270
Nb	0.3372	-0.0063	-0.0818	-0.0048	0.3086	-0.1179	-0.1063	-0.0682	-0.0800	0.0015	-0.1586
Ta	-0.4209	-0.1004	-0.0997	0.0255	-0.0916	-0.0031	-0.0153	0.0077	0.0214	0.0399	-0.0022
Se	-0.4405	0.2278	-0.2287	-0.0643	0.1471	-0.0439	-0.0641	-0.0343	-0.0284	-0.0017	0.0170
Be	-0.3429	0.1490	-0.3157	0.1155	-0.0378	0.1501	-0.0283	-0.0358	0.0026	-0.0446	-0.0010

Note: The most significant coefficients are underlined.

TABLE 7 (CONT'D): PRINCIPAL COMPONENTS ANALYSIS OF THE SOUTH MURCHISON AREA

Table 7d: RELATIVE CONTRIBUTIONS: VARIABLES

	1	2	3	4	5	6	7	8	9	10	11
Fe_2O_3	32.1425	26.7940	1.4382	0.0449	0.0251	4.4116	2.6862	2.3820	3.6675	1.5144	0.0002
Ag	0.5916	7.6104	3.9903	9.9145	1.4171	14.7815	3.5361	17.8440	1.3325	0.2551	0.0058
Mn	7.1365	15.6749	27.6022	3.3478	5.4065	0.3232	0.1436	0.1606	0.2882	1.5616	4.5222
Cr	40.2324	2.4071	4.0970	0.1274	8.5515	0.5144	0.4123	8.1008	10.5815	3.0127	3.7394
V	4.9528	23.7382	8.6824	2.0421	3.6366	17.7817	4.2444	4.6297	6.9546	10.6536	0.8608
Cu	32.8136	0.1276	0.0055	1.0038	6.5641	0.9540	2.5849	5.7612	10.8677	0.1169	9.8512
Pb	1.4998	0.5064	49.3390	2.1479	1.1699	16.9431	0.0054	6.7763	0.0217	0.0031	0.0134
Zn	30.8346	2.1105	12.3054	1.5446	0.1126	0.6628	0.8138	4.1336	12.2426	0.3117	2.0709
Ni	46.9828	1.2943	0.0665	0.1533	14.5263	0.9014	0.0552	0.5062	11.9215	6.5853	0.1005
Co	51.0029	5.3952	3.4129	1.6767	5.7341	3.1630	0.6209	1.0448	0.4358	0.0117	0.5156
As	5.5568	3.3833	2.2543	0.1173	28.9963	1.9153	3.8764	0.3137	0.0062	14.2677	12.8805
Sb	2.0560	2.6451	10.4742	0.3274	24.9816	3.1359	3.2081	18.6672	3.6095	1.1508	3.4293
Bi	0.0103	31.5741	11.3025	3.7573	0.0740	26.7357	0.0082	0.3764	4.6630	5.5363	1.5168
Mo	1.5441	3.4030	11.2288	47.5957	7.3019	1.6951	2.2548	0.1367	0.2254	0.1904	0.1579
Sn	0.6065	49.2869	10.1740	1.8356	0.3291	17.3960	0.0005	0.7766	0.1260	2.9725	0.0415
Ge	2.2329	7.7917	0.0039	0.3545	2.8537	6.2699	27.1024	18.1317	6.5113	2.2875	0.1340
Ga	22.1490	6.6722	0.5058	15.2145	13.9051	0.4478	3.0425	0.3721	0.1012	2.5235	1.0668
W	0.0527	2.6696	6.0166	41.6739	6.7614	6.6934	0.1652	1.1280	3.3294	4.0752	0.4208
Nb	12.3474	3.2928	4.4101	23.6880	8.2029	1.5976	0.7168	0.0217	3.8516	7.9475	6.2175
Ta	0.1417	1.3709	0.4507	0.2111	0.1195	3.5145	20.0180	6.4850	23.4216	16.9624	6.4484
Se	1.8430	2.6823	0.7303	0.1262	2.3218	1.8982	37.2150	9.6003	0.4732	8.0199	1.8543
Be	2.5893	13.3675	11.2942	0.0140	0.1826	0.0586	4.9150	0.6962	0.0625	4.9039	33.8290

	12	13	14	15	16	17	18	19	20	21	22
Fe_2O_3	0.0448	7.8456	0.0026	0.8332	4.2655	0.4330	0.6240	0.5564	0.3249	8.3499	1.6138
Ag	3.3143	29.7541	0.3718	0.0010	0.0198	2.8607	1.3390	0.5366	0.1331	0.3857	0.0051
Mn	2.5985	2.4940	14.0610	2.8050	0.0905	3.6981	0.0132	6.7684	0.6190	0.6551	0.0299
Cr	0.6355	1.5983	0.1233	0.2905	0.1356	1.1978	3.1070	4.7456	2.9939	1.6431	1.7529
V	1.6479	0.1665	0.2432	0.9867	0.2372	0.2685	0.0004	0.0023	0.9031	3.1739	4.1935
Cu	0.0006	1.8705	0.4819	1.2704	5.3096	19.4354	0.7620	0.0038	0.0166	0.1982	0.0005
Pb	0.3828	0.1285	0.2026	5.3062	0.3448	2.7914	1.9942	9.3204	0.1708	0.8009	0.1313
Zn	4.1412	0.2716	5.5829	5.1129	0.1115	7.9411	7.3878	2.0568	0.0228	0.1984	0.0298
Ni	0.0064	1.4502	0.7800	0.9254	0.0710	0.1246	0.0204	2.4875	7.9219	1.2407	1.8787
Co	0.2988	0.3030	0.2116	5.7435	0.7092	1.9319	6.8326	4.8356	3.6619	2.1702	0.2881
As	0.6866	1.1262	18.7706	0.0315	0.3396	4.9790	0.1490	0.0217	0.1338	0.0913	0.1028
Sb	4.5960	0.0362	10.6651	4.3565	1.5594	0.0029	2.9271	1.9593	0.0264	0.1153	0.0706
Bi	2.8138	0.0492	0.1643	0.9445	1.0163	0.0214	0.3522	0.0152	3.8511	0.5891	4.6283
Mo	1.4615	0.0671	0.5331	9.2127	0.1393	0.7351	8.3979	1.7719	0.3799	1.4313	0.1364
Sn	0.0248	0.1271	0.3731	3.3077	1.0609	0.3351	0.2391	0.0933	4.8820	1.3193	4.6922
Ge	0.4083	19.8710	0.2452	0.4681	2.3301	1.1116	0.3273	0.0076	0.0041	0.9792	0.5739
Ga	0.8506	0.8139	1.1782	0.3430	27.7071	0.8038	0.0857	0.0033	0.0349	1.2263	0.9527
W	1.7661	2.2675	0.0389	16.4566	0.0003	0.0040	4.9467	0.3428	0.2002	0.9179	0.0728
Nb	11.3673	0.0040	0.6683	0.0023	9.5239	1.3900	1.1293	0.4653	0.6401	0.0002	2.5154
Ta	17.7151	1.0089	0.9930	0.0651	0.8382	0.0010	0.0233	0.0059	0.0457	0.1593	0.0005
Se	19.4063	5.1884	5.2319	0.4136	2.1640	0.1925	0.4113	0.1176	0.0807	0.0003	0.0289
Be	11.7598	2.2213	9.9669	1.3344	0.1427	2.2541	0.0801	0.1282	0.0007	0.1988	0.0001

Note: The most significant coefficients are underlined.

The remaining component loadings are shown in Table 7c. Some of the linear combinations of the variables may not have any meaning. This may be the result of random variation of the data or some unrecognized process that has not been observed or understood. Further investigation is required in order to place any geological significance on many of the linear combinations that the principal components analysis produces. This will be the subject of future research.

Geochemical Anomalies

Each of the maps were compared with known mineral occurrences and anomalies that exist in the area. Figure 62 shows the locations of the previously defined geochemical anomalies arising during the AGE programme. Also indicated are additional anomalies as defined by the 95^{th} and 99^{th} percentile rankings of the data. All locations with values greater than the 99^{th} percentile level were indicated on the map for the elements, Mn, V, Cu, Pb, Zn, Co, As, Sb, Be, Mo, Ag, Sn, Ge, Ga, W, Ba, and Nb. For Au, values greater than the 95^{th} percentile level were indicated. Elements that were not plotted for all of the anomalies include Fe_2O_3, TiO_2, Cr Ni, and Zr.

Table 8 summarizes the anomalies and their associated anomalous elements. Elements marked with an asterisk are associated elements that show increased abundances at the 95^{th} percentile rank.

Some elements show increased abundances without any corresponding significant increases in other elements. These single element anomalies are not shown in Figure 62. In particular, there is an increase in Zr over the southern part of the Perenjori sheet that is probably related to the gneissic terrain that was sampled. As well, individual sites of Nb abundance increases were noted in the southern part of the Perenjori sheet. Local Cu increases were noted northwest of the Messenger Patch area. Isolated Sn, V, and Ag increases were also noted in the Gullewa area. An area of V abundance increases was noted in the Koolanooka fold belt. An isolated Sn increase was also noted northeast of Mt. Mulgine.

Table 9 lists the anomalies with their corresponding associations to the first five principal components. Anomalies can be associated with very high or very low principal component scores. Anomalies that are associated with a given component generally show close association to the elements that are most significant for that component. The associated elements for each component represent linear combinations of elements that account for the greatest magnitudes of the component scores. That is, if the first component shows that its large positive scores are the result of the dominance of Co, Ni, Cr, Fe, Cu, and Zn, then areas with large positive component scores will show an associated increase in those elements. Similarly, for the first component large negative scores are associated with Ga, and Nb. Thus areas that show large negative component scores will tend to show enrichment in those two elements. Also, those samples that are enriched with elements associated with positive scores will tend to be depleted with samples that are associated with elements with negative scores; and vice-versa. The positive or negative associations of the variables can be found in the component loadings part of Table 7. The significance of each variable is shown in percent form in the following table which shows the relative contributions.

The elemental associations shown in Table 8 may not be the same as shown in Table 9. This is because the anomalies were defined at the 99^{th} percentile level. If the anomaly threshold were dropped to a lower rank, most of the anomalies would have a corresponding greater number of associated elements.

Table 8
Anomalies as Determined from 95th* and 99th Percentile Ranking

Kirkalocka Sheet

Anomaly	Association
KL1,2	Au*, Zn, Ni, Co, Fe, Mn, Pb, Ba, Bi*, Mo*, Ag*
KL5	Au*, Zn
KL8	Bi, Mo, W, As*
KLA	Cu, Co, Ba, Mn, Zn, Ni
KLB	Au*, As, Co, Cu, Zn, Ni
KLC	Au*, Mo, Mn, Ga,
KLD	Ba, Au*, Bi*
KLE	Sb, Mn, Pb, Ti
KLF	Cu, Ni, Zn, Co, Mo, Ba
KLG	As, Cu

Yalgoo Sheet

Anomaly	Association
YL1	As, Mn, W
YL6	As, Sb, V
YL10	Zn, Pb, Ga, Bi, Be
YLA	Au*, W, Be, Mn, Zn, Co, Bi
YLB	Au*, Ag, Mn, W, Zn, Mo, Ga, Ba
YLC	Pb, Ga, Be
YLD	Zn, Ag
YLE	Bi, Pb
YLF	Sn, Ga

Perenjori Sheet

Anomaly	Association
PJ1	V, Cu, Zn, Sb, Bi, As*
PJ2	V, Sb, As*
PJ3	Au*, As, Bi, Sn, Mo, W, Cu, Zn, Fe, Ti, V, Ag, Ge, Nb, Ga, Ba, Be
PJ4	Au*, Ag, Sn
PJ6	Ag, Cu, Zn, Pb, Sn, Ge
PJ8	Au*, As, Sn, Ge, Nb
PJ9	Au*, Cr*, V, Pb, Zn*, Ni*, As, Sb, Ag, Sn, Nb
PJA	Nb, Bi

Ninghan Sheet

Anomaly	Association
NG1	As, Sb, Co*
NG2	Ti, As, Sb, Ga, Co*
NG3	Ti, Co, Zn*, Cu*, W*
NG4	Cu, As, Ag, Co, Zn*
NG5	As, Cu, Ag, Ge, Ni
NGA	Au*, Ag, Cu, Ag, Ni, Co
NGB	Au*, As, Ge, Ti

Table 9
Anomalies and Associated Elements as
Determined from Principal Components Analysis

Component 1
Positive scores (Co,Ni,Cr,Fe,Cu,Zn): KLA, KLB, KL1,2, NGA, PJ1,YLA
Negative scores: (Ga,Nb): PJA, YLB, YL10, YLC, PJ3

Component 2
Positive scores (Sn,Bi,V,Fe): KL8, PJ, Golden Grove
Negative scores (Be,Mn): YLA, KLA, KLB

Component 3
Positive scores (Pb,Mn): YLA, YLE, PJ1, PJ3, PJ6, Golden Grove
Negative scores (V): YL1

Component 4
Positive scores (Mo,W,Bi):KL8, PJ3
Negative scores (Nb,Ga,Ag): PJ9, PJ6, YLC, YLA, PJA

Component 5
Positive scores (As,Sb,Cu): KLG, KLE, NG1, PJ9, PJ6, PJ3, PJ1
Negative scores (Co,Cr,Ni,Nb,Ga): KLA, KL1,2, PJ3

Recommendations and Conclusions

The southern Murchison region is host to a number of mineral deposits, most significantly gold and base metal deposits. The laterite geochemistry presented here identifies several anomalous areas that need to be assessed for their possible relevance to Au, base metal or W-Mo type deposits. As well, the presence of a "chalcophile corridor" suggests that the mineral potential of the area may be strategically significant. Many of the geochemical patterns do not have an obvious explanation at this stage. This may be partly due to the scale of sampling. Also dispersion within the laterite profile can create anomalous zones that may be a mixture of adjacent geological situations, making interpretation difficult.

Gold mineralization is commonly associated with an increase in the abundance of a variety of elements, most commonly, As, Sb, W, Mo, B, Ag, Li, Ba, Rb, and Cr in the unweathered profile. As well, Cu, Zn, and Pb can be present in some gold deposits (Groves, 1988; Colvine et al, 1988). However, not all of these elements are present for all types of deposits. Pegmatite associated rare metal deposits can be indicated by enrichment of Bi, As, Sb, Mo, Sn, Ge, W, Nb, and Au. Any one or combination of these elements can be considered as possible pathfinders to a variety of ore deposits.

There appears to be several regional trends in the anomalous occurrences. A significant gold and base-metal trend occurs in the "chalcophile corridor", mentioned above, trending north-northwesterly through the Yalgoo-Singleton Greenstone belt from Mt. Gibson in the south, to Noongal in the north. This trend follows the trend of the belt and may be associated with large fracture zones that provided the conduits for mineralizing processes. In particular, the significance of anomalies, YLA, YL1, KLE, KLG, NGA, NG5, NG4, NG1, NG2, and NGB should be assessed due to their presence close to or within an inferred chalcophile corridor. The "corridor" trend is also supported by the results of the principal components analysis. The fifth component of the analysis shows that large component scores outline areas of increased abundances of As and Sb. These areas fall within the chalcophile corridor. The most significant component scores occur in the Chulaar Hill area of the Yalgoo-Singletown greenstone belt. These values also occur at or very close to known fault zones.

The Noongal area with associated W and Au may be diagnostic of Au and Sn or W deposits that are associated with late post-kinematic granitic stocks that post date peak metamorphism in the area. The anomalies PJ4, PJ8, PJ9, and PJ6 have scattered associations of chalcophile elements and anomalous Au and might be investigated with this type of model in mind.

The PJ3 anomaly at Red Hill has a diverse association of Au, As, Bi, Sn, Mo, W, Cu, Zn, Fe, Ti, V, Ag, Ge, Nb, Ga, Ba, and Be. Such a large anomaly comprised of contributions from so many elements may reflect multiple episodes of mineralization of varying styles. It warrants further study in order to determine the nature of the process(es) that have produced such a pattern.

Several anomalies are situated northeast of Mt. Mulgine. These occurrences reflect both base-metal and Au style anomalies that could be associated with the "chalcophile corridor" that trends north-northwesterly, or mineralization that is associated with the large north-northeasterly trending fault that intersects the Magnet Fold belt.

The northerly trending zone of anomalies that includes KL1,2, KL5, KL8, KLA, KLB, KLC, KLD, and KLF define a linear zone of varying degrees of chalcophile and precious metal enrichment. These anomalies are associated within a narrow greenstone belt that is surrounded by a large granitic terrain. Granophile type deposits or felsic intrusive hosted Au deposits as well as shear zone associated deposits might be associated with this type of geological environment.

REFERENCES

Arriens, P.A., 1971: Archaean geochronology of Australia. Geol. Soc. Aust. Spec. Publ., 3, 11-23.

Baxter, J.L., 1978: Molybdenum, tungsten, vanadium and chromium in Western Australia. Geol. Surv. W. Aust., Min. Resources Bull., 11, 140 pp.

Baxter, J.L. and Lipple, S.L., 1985: Perenjori, Western Australia, Geol. Surv. W. Aust. 1:250,000 Geol. Series Explan. Notes,. 32pp.

Baxter, J.L., Lipple, S.L. and Marston, R.J., 1983: Kirkalocka, Western Australia. Geol. Surv. W. Aust. 1:250,000 Geol. Series Explan Notes, 24pp.

Browning, P., Groves, D.I., Blockley, J.G. and Rosman, K.J.R., 1987: Lead isotope constraints on the age and source of gold mineralization in the Archaean Yilgarn Block, Western Australia. Econ. Geology, 82, 971-86.

Colvine, A.C. et al, 1988: Archaean Lode Gold Deposits in Ontario; Ontario Geological Survey Miscellaneous Paper 139, 136p.

Davis, J.C., 1986: Statistics and Data Analysis in Geology, John Wiley & Sons Inc., second edition, 646p.

Finkl, C.W. Jnr. and Churchward, H.M., 1973: The etched land surfaces of southwestern Australia. J. Geol.Soc.Aust., 20(3), 295-307.

Fletcher, I.R., Rosman, K.J.R., Williams, I.R., Hickman, A.H. and Baxter, J.L., 1984: Sm-Nd geochronology of greenstone belts in the Yilgarn Block, Western Australia. Precambr. Res., 26, 333-61.

Groves, D.I. 1988: Gold Mineralization in the Yilgarn Block, Western Australia, Bicentennial Gold 88, Extended Abstracts, Oral Programme, Geological Society of Australia Inc., Abstracts No. 22, p.13-23.

Hallberg, J.A., 1976: A petrochemical study of a portion of the western Yilgarn Block. CSIRO Div. of Mineralogy Rept. FP 13, 38pp.

Hallberg, J.A., 1984: A Geochemical Aid to Igneous Rock Type Identification in Deeply Weathered Terrain, Journal of Exploration Geochemistry, Vol. 20, p. 1-8.

Hickman, A.H., and Watkins, K.P., 1988: Gold Mineralization in the Murchison Province, Western Australia, in Bicentennial Gold 88, Extended Abstract, Poster Programme, Vol. 1, Geological Society of Australia Inc., Abstracts No. 23, p. 23-25.

Howarth, R.J., 1983: Statistics and Data Analysis in Geochemical Prospecting, edited by R.J. Howarth, Vol. 2, in Handbook of Exploration Geochemistry, edited by G.J.S. Govett, Elsevier, 437 p.

Johnstone, M.H., Lowry, D.C. and Quilty, P.G., 1973: The geology of southwestern Australia - a review. J. Roy. Soc. W. Aust., 56, 5-15.

Jöreskog, K.G., Klovan, J.E., Reyment, R.A., 1976. Geological Factor Analysis. Elsevier Scientific Publishing Company, New York, 178p.

Jutson, J.T., 1950: The physiography (geomorphology) of Western Australia. Geol. Surv. W. Aust., Bull. 95 (3rd ed.), 366pp.

Lipple, S.L., Baxter, L.J. and Marston, R.J., 1983: Ninghan, Western Australia. Geol. Surv. W. Aust. 1:250,000 Geol. Series Explan. Notes, 23pp.

Mann, A.W., 1982: Physical characteristics of the drainages of the Yilgarn Block, South Western Australia. CSIRO Div. of Mineralogy, Rpt. FP 25, 14pp.

Marston, R.J., 1979: Copper mineralization in Western Australia. Geol. Surv. W.Aust., Min. Resources Bull., 13, 208pp.

Mazzuchelli, R.H., and James, C.H., 1966: Arsenic as a guide to gold mineralization in laterite-covered areas of Western Australia., Trans. Inst. Min. Metall. Sect, B, 75: 285-294.

Muhling, P.C. and Low, G.H., 1973: Explanatory notes on the Yalgoo 1:250,000 geological sheet, W.A. Geol. Surv. W. Aust. Record 1973/6.

Muhling, P.C. and Low, G.H., 1977: Yalgoo, Western Australia. Geol. Surv. W. Aust. 1:250,000 Geol. Series Explan. Notes, 36pp.

Phillips, G.N., 1985: Interpretation of Big Bell/Hemlo-type gold deposits: precursors, metamorphism, melting and genetic constraints. Geol. Soc. S. Afr., Trans., 88, 159-73.

Ollier, C.D., Chan, R.A., Craig, M.A. and Gibson, D.L., 1988: Aspects of landscape history and regolith in the Kalgoorlie region, Western Australia. BMR J. Aust. Geol. and Geophys., 10, 309-321.

Smith, R.E. and Perdrix, J.L. 1983: Pisolitic laterite geochemistry in the Golden Grove massive sulphide district, Western Australia, J. Geochem. Explor., Vol. 18, p. 131-164.

Smith, R.E., Moeskops, P.G., and Nickel, E.H., 1979: Multi-element geochemistry at the Golden Grove Cu-Zn-Ag deposit. In: J.E. Glover, D.I. Groves, and R.E. Smith (Editors), Pathfinder and Multi-element Geochemistry in Mineral Exploration. Univ. W.Australia, Geol. Dept. Extension Service, Publ. 4, pp. 30-41.

Watkins, K.P., and Hickman, A.H., 1988: Geology of the Murchison Province: Locality Guide. Centennial Field Excursion Guide, Geol. Survey of Western Australia. 14pp.

Wolfe, W.J., 1977: Geochemical Exploration of Early Precambrian Sulphide Mineralization in Ben Nevis Township, District of Cochrane; Ontario Geological Survey Study 19, 39pp.

Zeegers, H., Goni, J. and Wilhem, E., 1981: Geochemistry of lateritic profiles over a disseminated Cu-Mo mineralization in Upper Volta (West Africa) - preliminary results. In M.K. Roychowdhury, B.P. Radhakrishna, R. Vaidyanadhan, P.K. Banerjee and K. Ranganathan (Editors), Lateritization Processes. Balkema Publishers, Rotterdam, pp. 359-368.

Zhou, D., Chang, T., Davis, J.C., 1983. Dual Extraction of R-Mode and Q-Mode Factor Solutions, Mathematical Geology, Vol. 15, #5, pp. 581-606.

APPENDIX 1

Data Format of the South Murchison Database

The data is contained on a double sided double density (360Kb) 5.25" floppy diskette that is formatted for an IBM PC or compatible computer running under DOS.

The name of the file that contains the data is: SMURCH.SDF
Refer to Table 2 for the meaning of the various element codes.
The data is recorded in ASCII format and each record of the file has the following attributes:

Field	Field Name	Type	Width	Dec
1	SAMPLE	Character	7	
2	SAMPLETYPE	Character	5	
3	GEOLOGY	Character	5	
4	MAPREF	Character	8	
5	EASTING	Numeric	6	
6	NORTHING	Numeric	7	
7	SI02	Numeric	6	2
8	AL203	Numeric	6	2
9	FE2031	Numeric	6	2
10	FE2032	Numeric	6	2
11	MGO	Numeric	6	3
12	CAO	Numeric	6	3
13	TI02	Numeric	6	3
14	AG1	Numeric	6	1
15	MN2	Numeric	6	
16	MN4	Numeric	6	
17	CR1	Numeric	6	
18	CR3	Numeric	6	
19	V1	Numeric	6	
20	V3	Numeric	6	
21	CU1	Numeric	6	
22	CU4	Numeric	6	
23	PB3	Numeric	6	
24	ZN3	Numeric	6	
25	NI1	Numeric	6	
26	NI3	Numeric	6	
27	CO3	Numeric	6	
28	AS4	Numeric	6	
29	SB2	Numeric	6	
30	BI1	Numeric	6	
31	BI3	Numeric	6	
32	CD2	Numeric	6	
33	MO2	Numeric	6	
34	SN1	Numeric	6	
35	SN5	Numeric	6	
36	GE1	Numeric	6	
37	GA	Numeric	6	
38	W2	Numeric	6	
39	BA1	Numeric	6	
40	ZR1	Numeric	6	
41	NB3	Numeric	6	
42	TA3	Numeric	6	
43	SE2	Numeric	6	
44	BE1	Numeric	6	
45	AU	Numeric	6	

For the variable, GEOLOGY, the following codes are used to define the geology of the areas where the samples were collected:

AVR - Acid Volcanic Rocks
BIF - Banded Iron Formation
FGM - Foliated Granite and Migmatite
GIR - Granitic Intrusions
LBU - Layered Basic and Ultrabasic Intrusions
MBU - Metabasic and Ultrabasic Rocks
MSR - Metasedimentary Rocks
UMG - Undifferentiated Massive Granitic Rocks

The codes were derived from the geological maps of the Western Australia Geological Survey.

A FORTRAN 77 format statement would read in the data in the following manner

```
      CHARACTER*7 SAMPLE
      CHARACTER*5 SAMTYP,GEOL
      CHARACTER*8 MAPREF
      REAL*4  EAST,NORTH,
     $        SIO2,AL2O3,FE2O31,FE2O32,MGO,CAO,TIO2,AG1,
     $        MN2,MN4,CR1,CR3,V1,V3,CU1,CU4,PB3,ZN3,NI1,NI3,
     $        CO3,AS4,SB2,BI1,BI3,CD2,MO2,SN1,SN5,GE1,GA,W2,
     $        BA1,ZR1,NB3,TA3,SE2,BE1,AU
      READ(5,10) SAMPLE,SAMTYP,GEOL,MAPREF,EAST,NORTH,
     $           SIO2,AL2O3,FE2O31,FE2O32,MGO,CAO,TIO2,AG1,
     $           MN2,MN4,CR1,CR3,V1,V3,CU1,CU4,PB3,ZN3,NI1,NI3,
     $           CO3,AS4,SB2,BI1,BI3,CD2,MO2,SN1,SN5,GE1,GA,W2,
     $           BA1,ZR1,NB3,TA3,SE2,BE1,AU
10    FORMAT(A7,2A5,A8,F6.0,F7.0,4F6.2,3F6.3,F6.1,31F6.0)
```

Negative values indicate less than detection limit.

Zero values indicate that no analysis was performed for that element.

Figure 1: (located in back pocket)

SOUTH MURCHISON PRESENT/PAST PRODUCERS

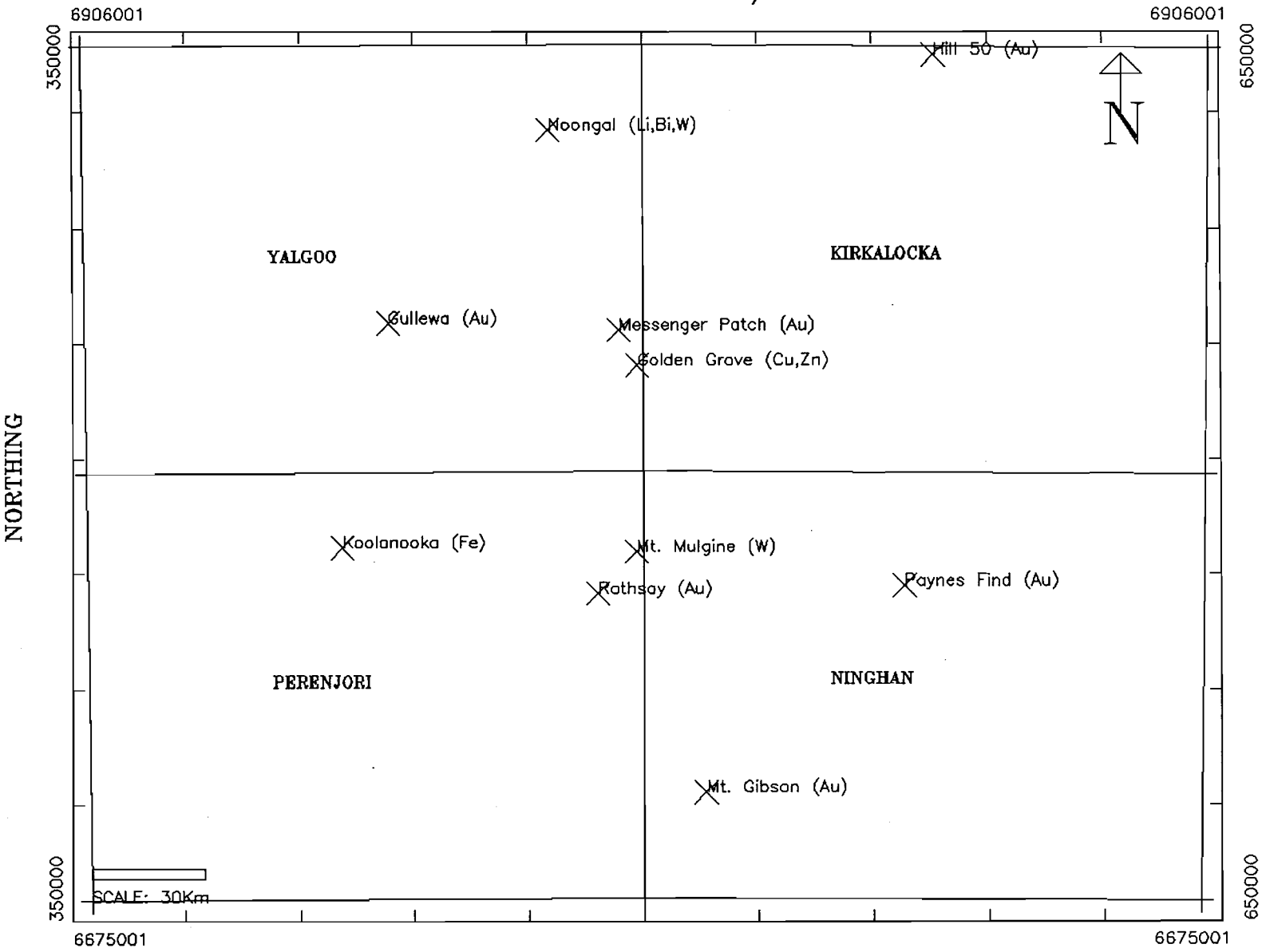

Figure 2

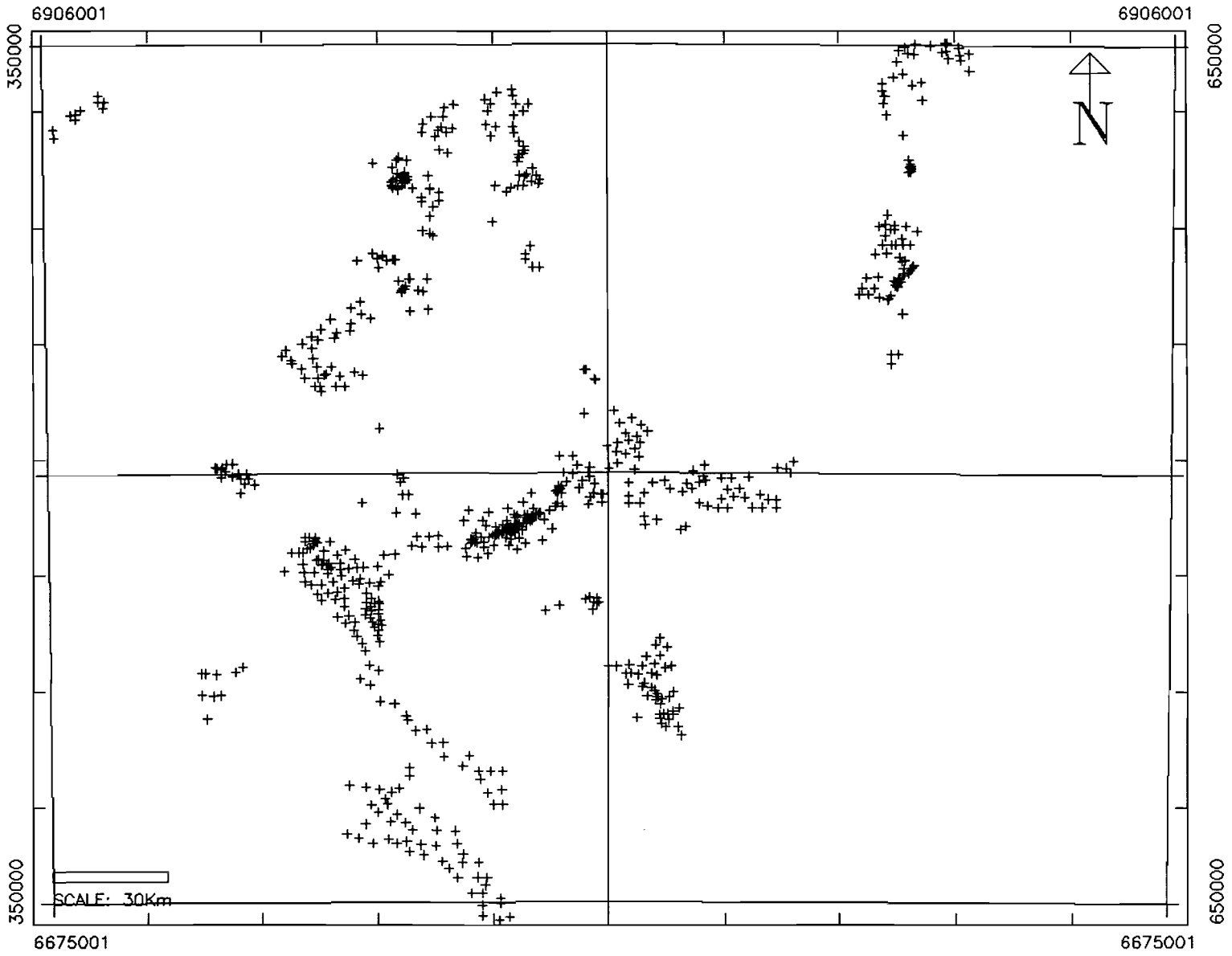
SOUTH MURCHISON MAIN SAMPLE SITES
6906001
6906001
350000
650000
N
NORTHING
SCALE: 30Km
350000
650000
6675001
6675001
EASTING
721 STATIONS PLOTTED

Figure 3

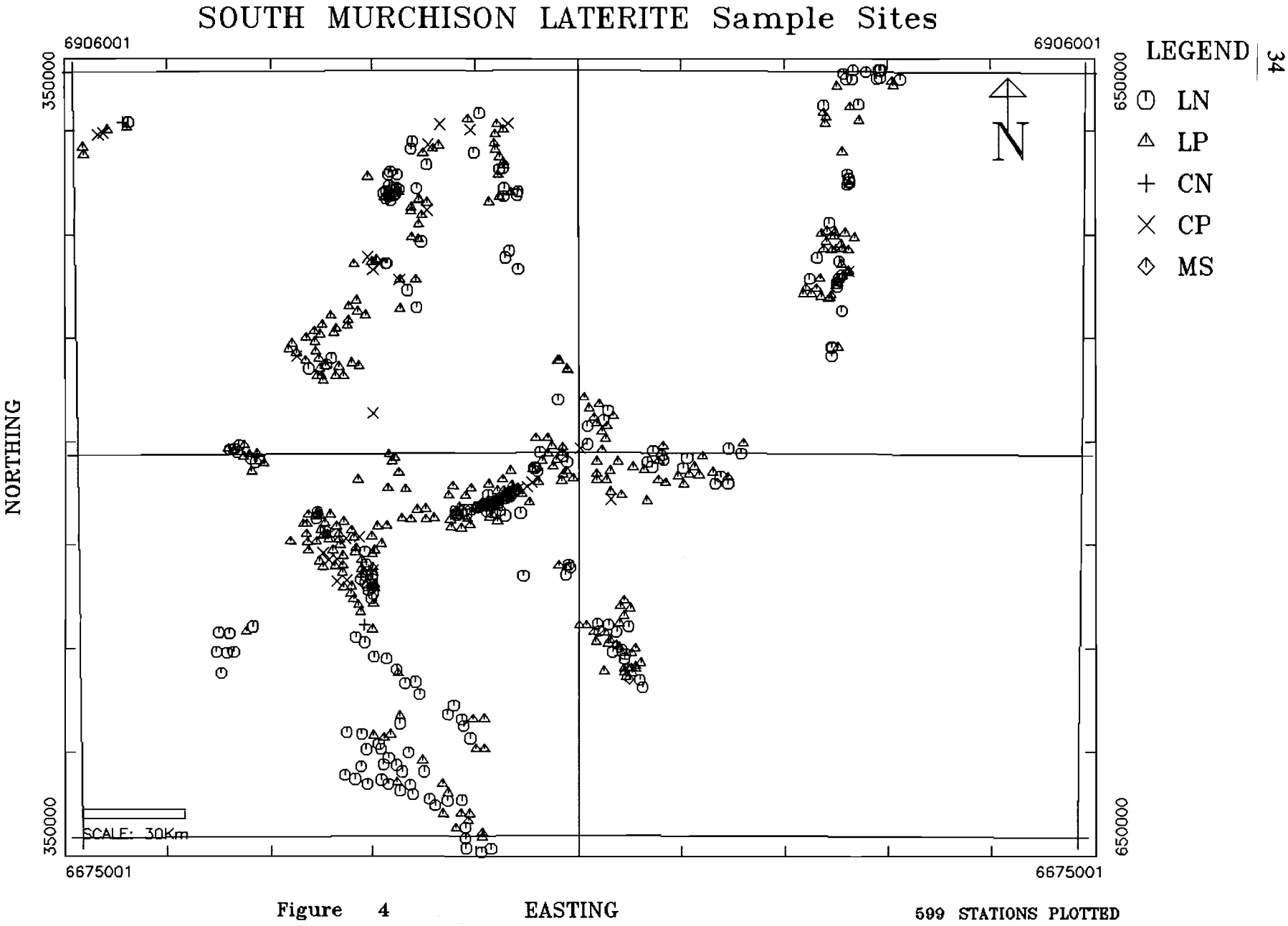
SOUTH MURCHISON LATERITE Sample Sites
6906001
6906001
350000
650000
N
LEGEND
LN
LP
CN
CP
MS
NORTHING
SCALE: 30Km
350000
650000
6675001
6675001
EASTING
599 STATIONS PLOTTED

Figure 4

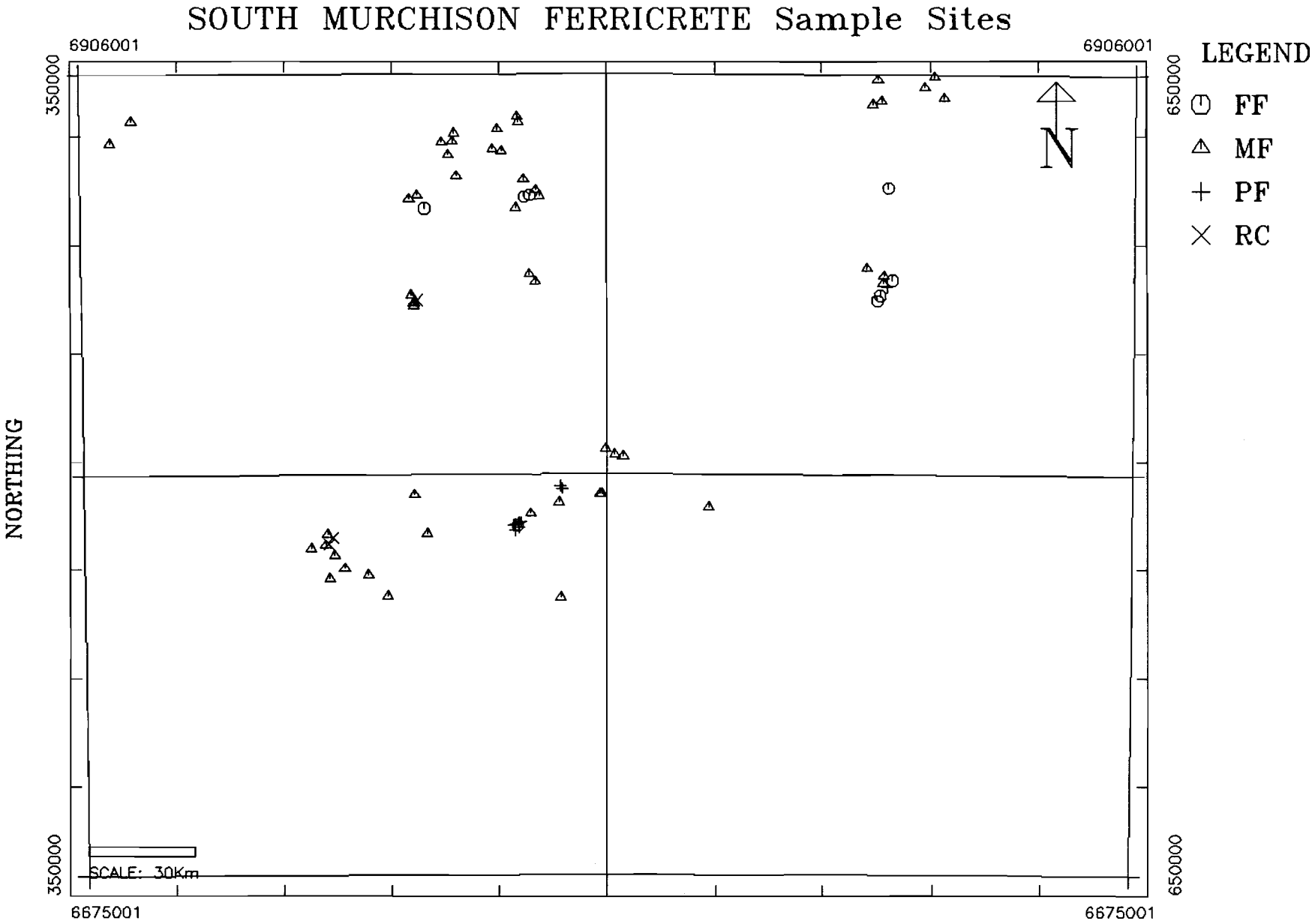
SOUTH MURCHISON FERRICRETE Sample Sites
6906001
6906001
350000
650000
LEGEND
FF
MF
PF
RC
N
NORTHING
SCALE: 30Km
350000
650000
6675001
6675001
EASTING
77 STATIONS PLOTTED

Figure 5

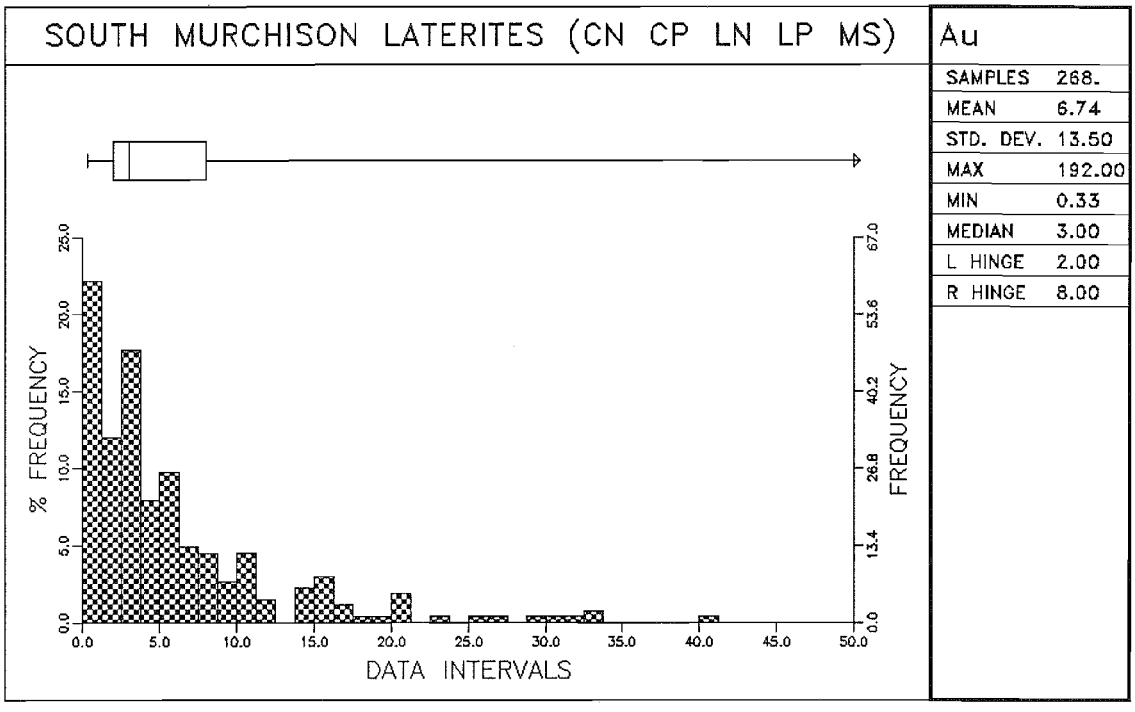

Au	
SAMPLES	268.
MEAN	6.74
STD. DEV.	13.50
MAX	192.00
MIN	0.33
MEDIAN	3.00
L HINGE	2.00
R HINGE	8.00

Figure 6a

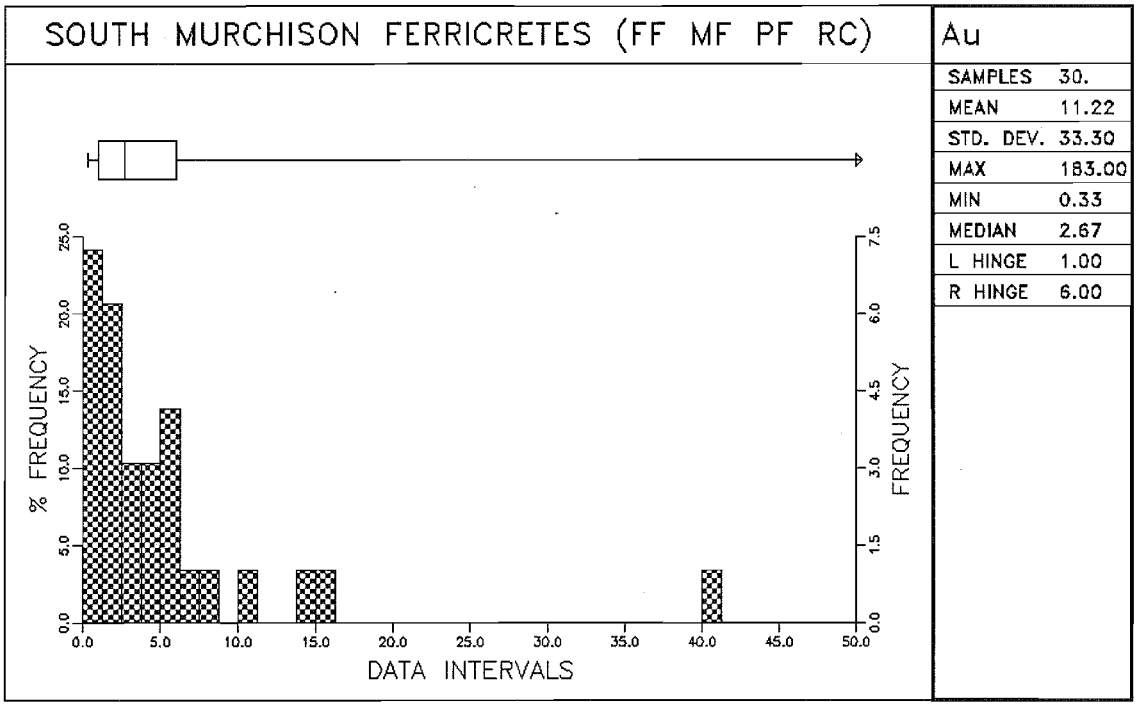

Au	
SAMPLES	30.
MEAN	11.22
STD. DEV.	33.30
MAX	183.00
MIN	0.33
MEDIAN	2.67
L HINGE	1.00
R HINGE	6.00

Figure 6b

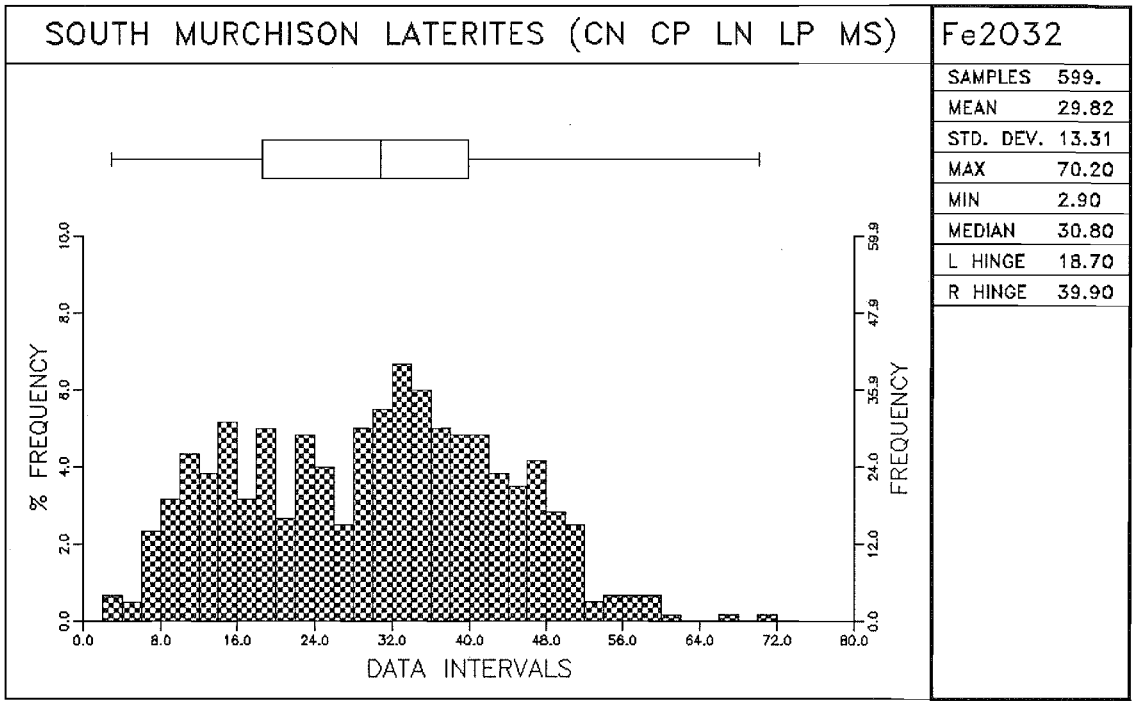

Figure 7a

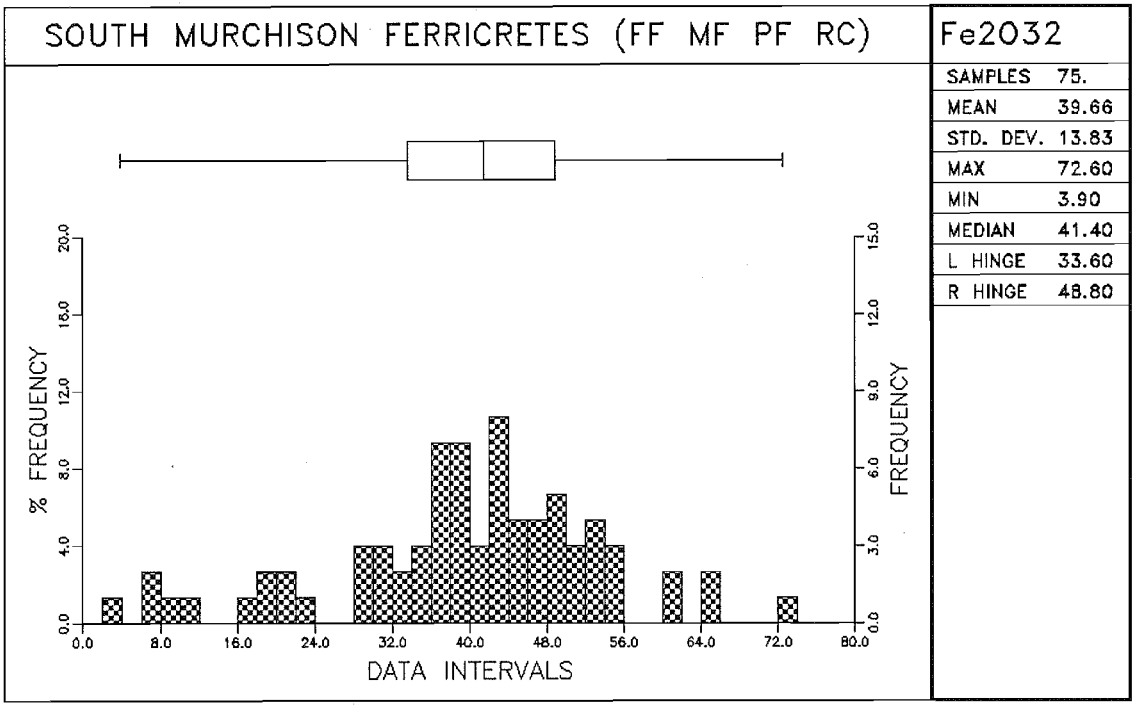

Figure 7b

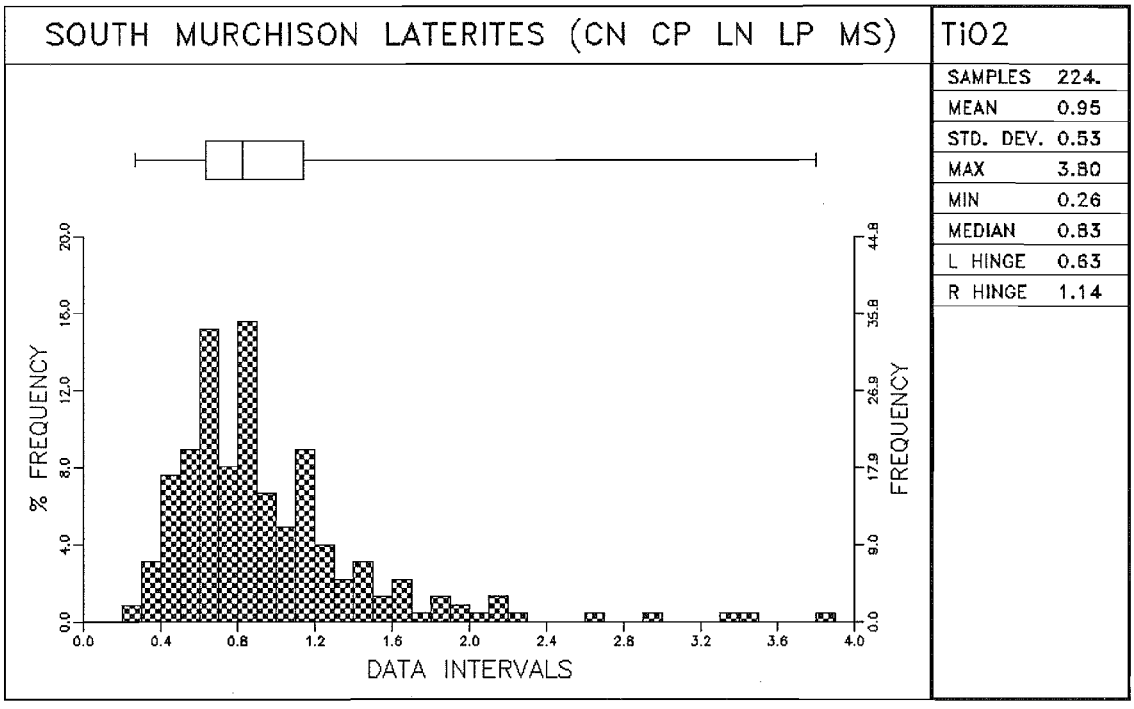

TiO2	
SAMPLES	224.
MEAN	0.95
STD. DEV.	0.53
MAX	3.80
MIN	0.26
MEDIAN	0.83
L HINGE	0.63
R HINGE	1.14

Figure 8a

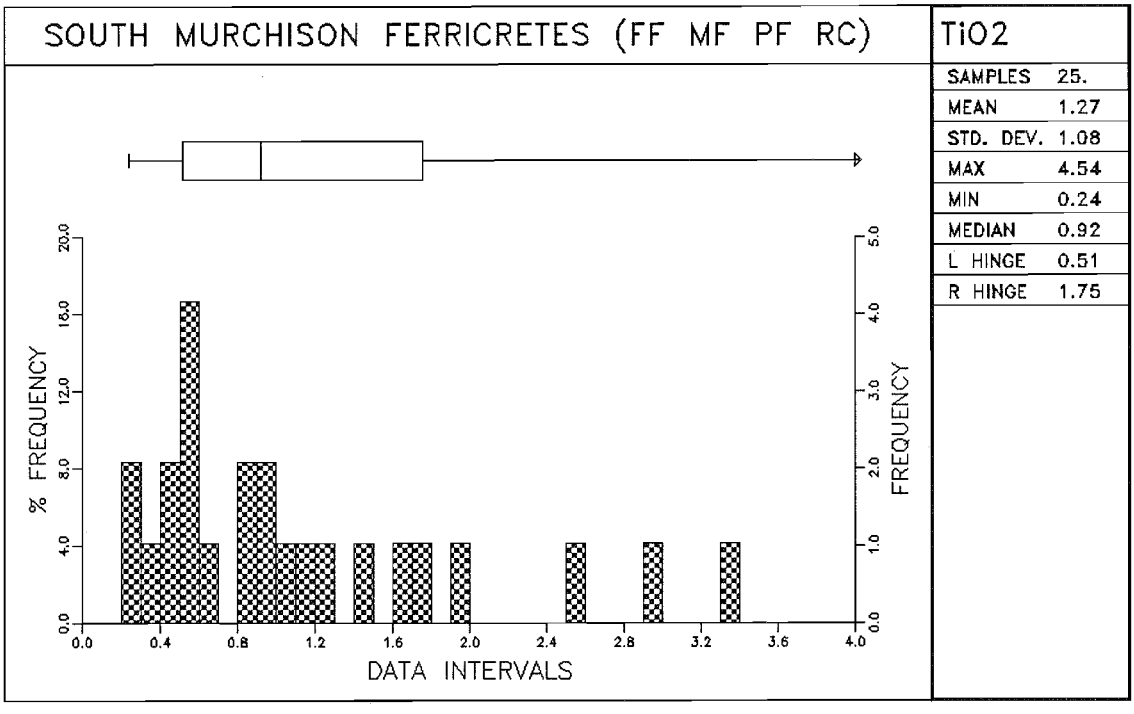

TiO2	
SAMPLES	25.
MEAN	1.27
STD. DEV.	1.08
MAX	4.54
MIN	0.24
MEDIAN	0.92
L HINGE	0.51
R HINGE	1.75

Figure 8b

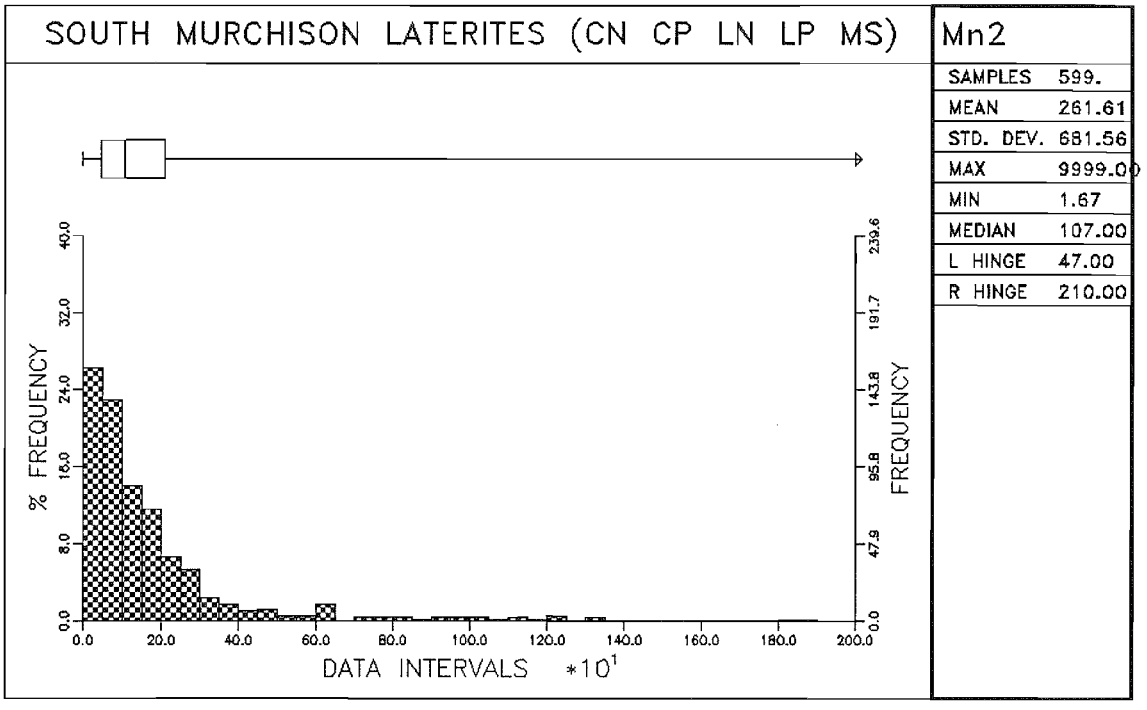

Figure 9a

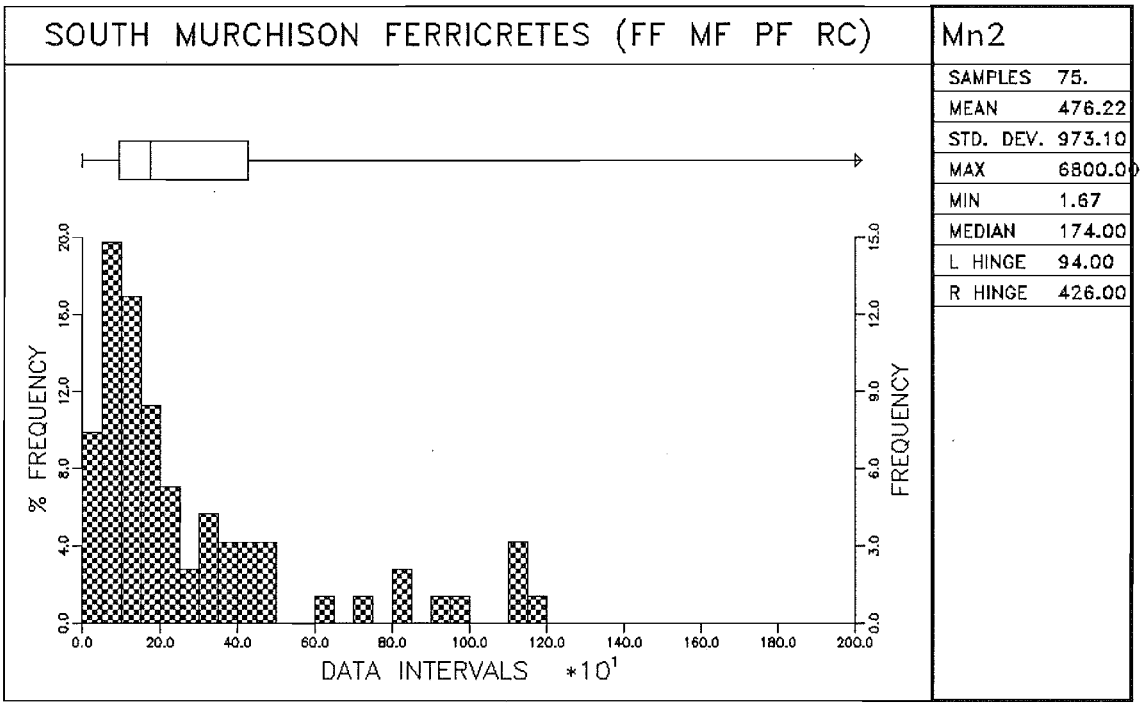

Figure 9b

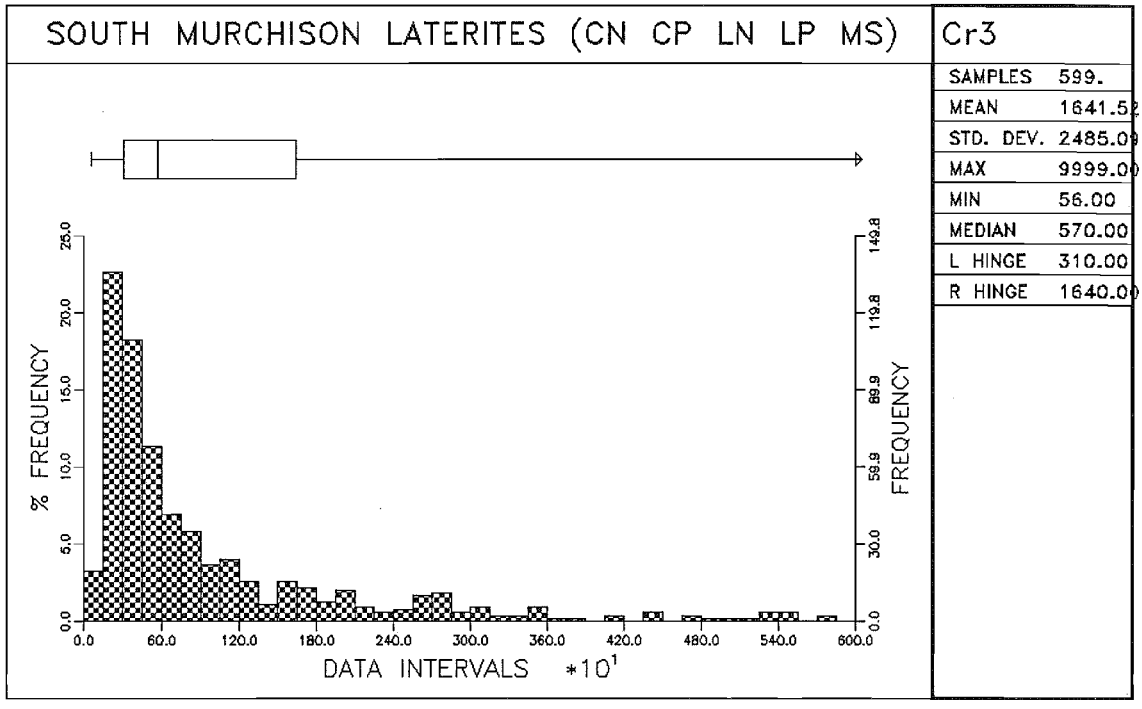

Figure 10a

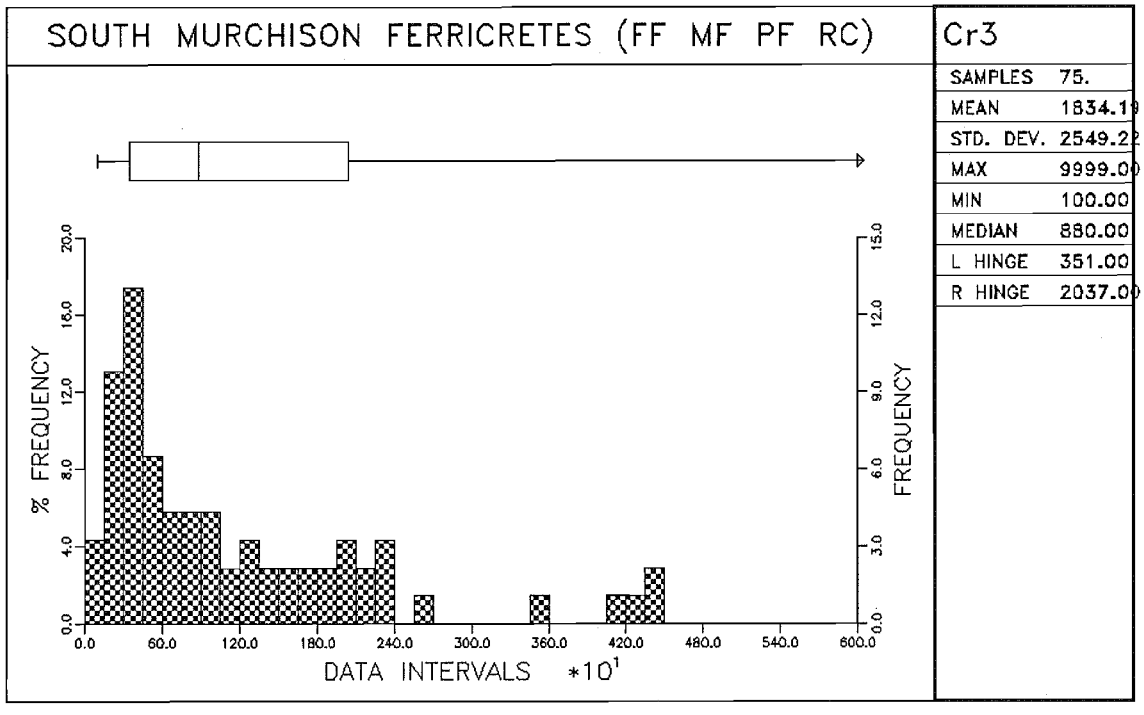

Figure 10b

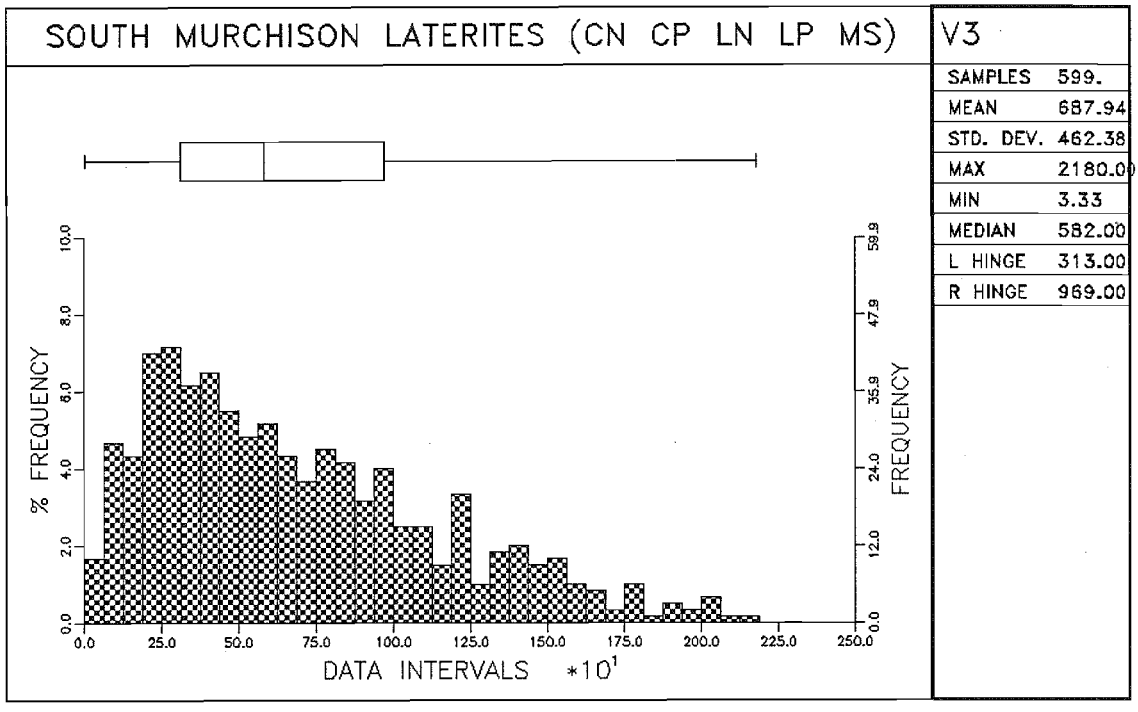

Figure 11a

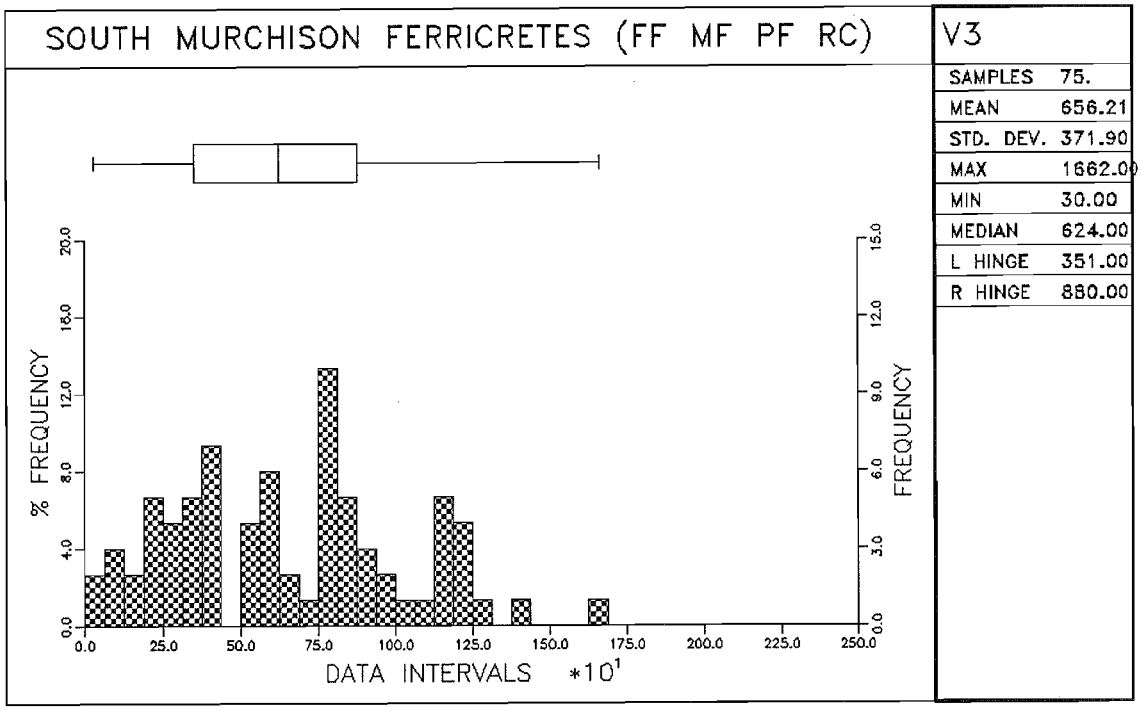

Figure 11b

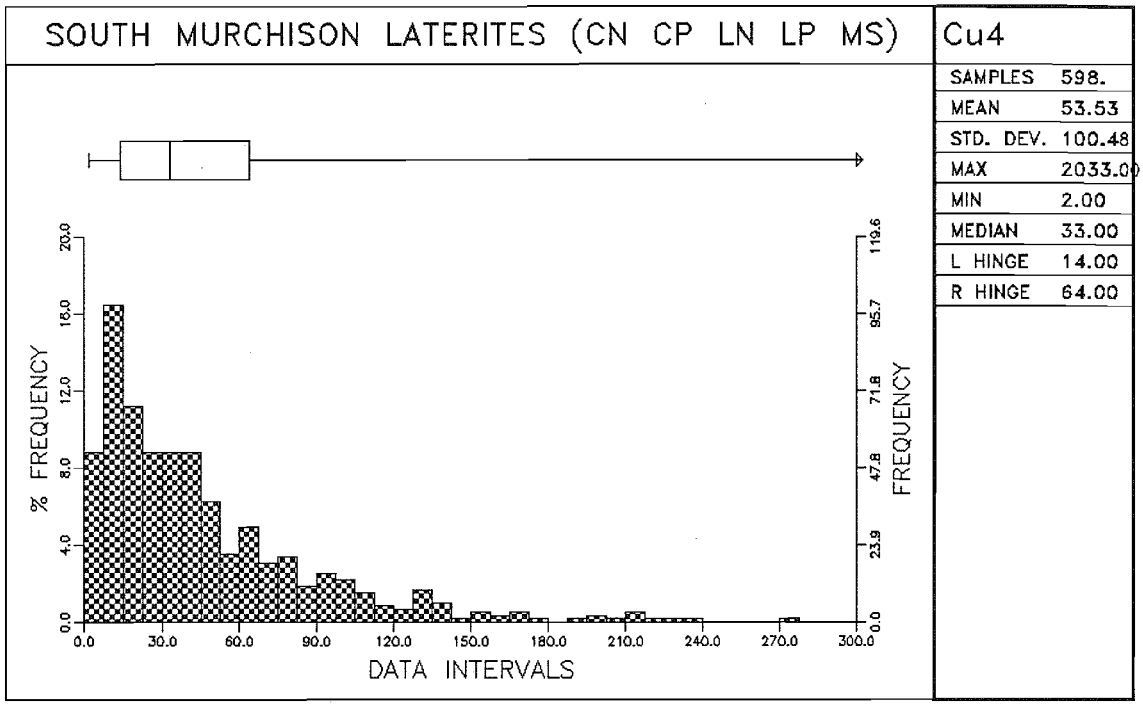

Figure 12a

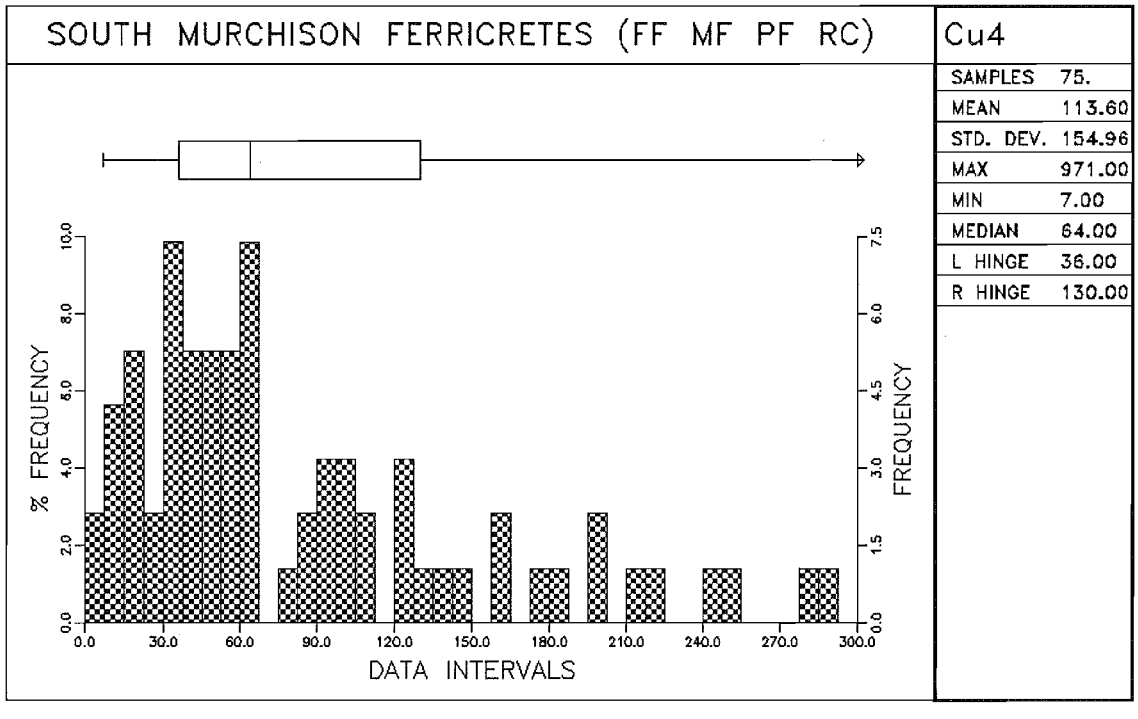

Figure 12b

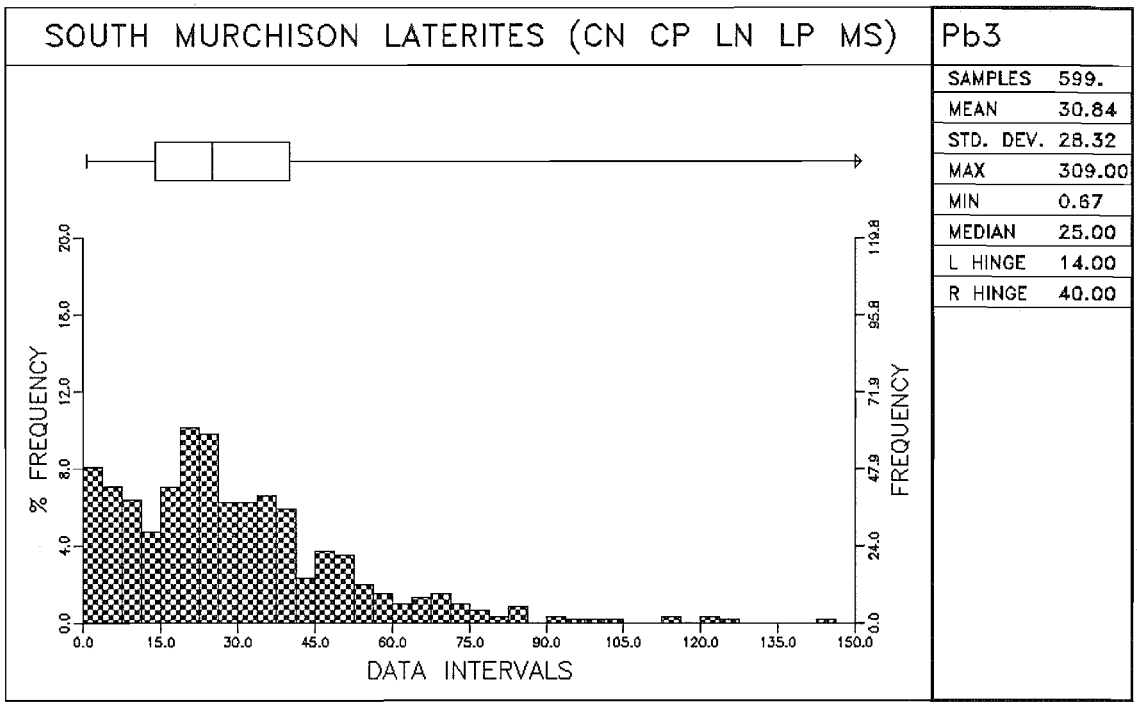

Figure 13a

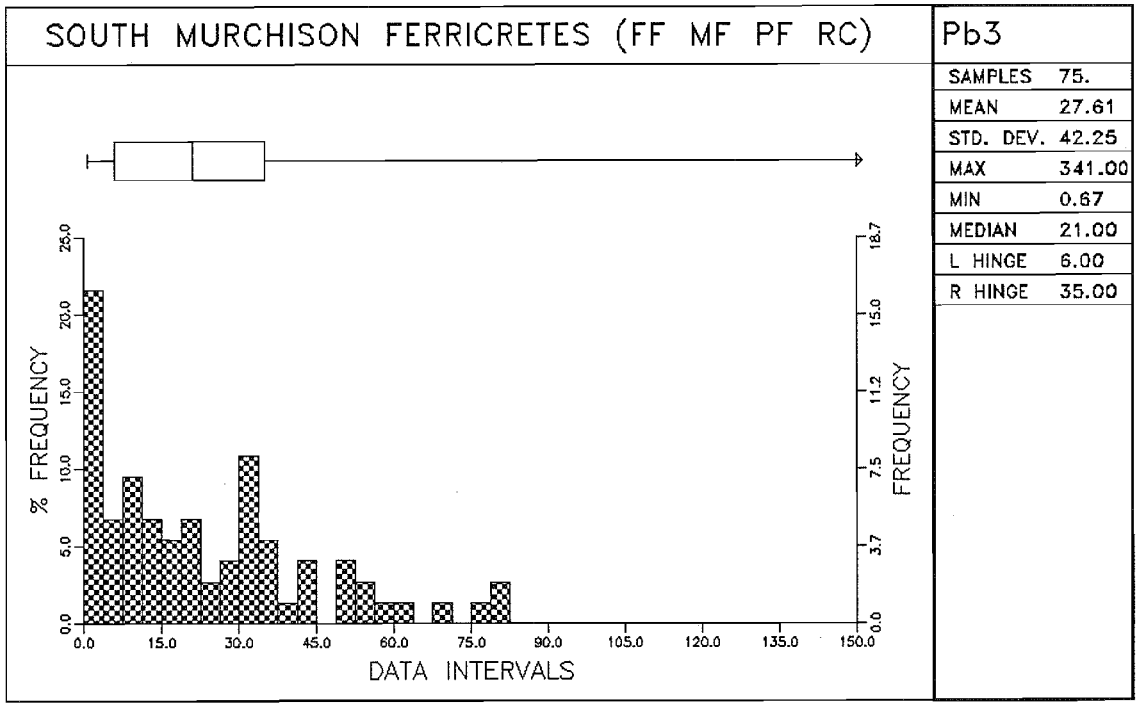

Figure 13b

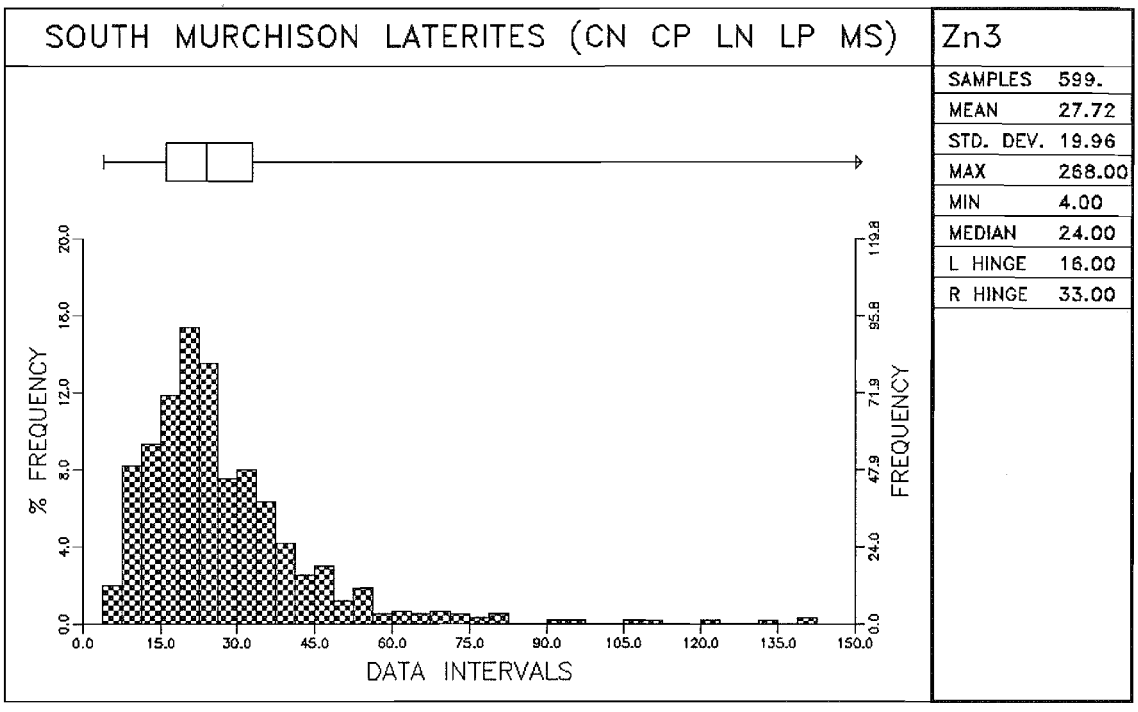

Figure 14a

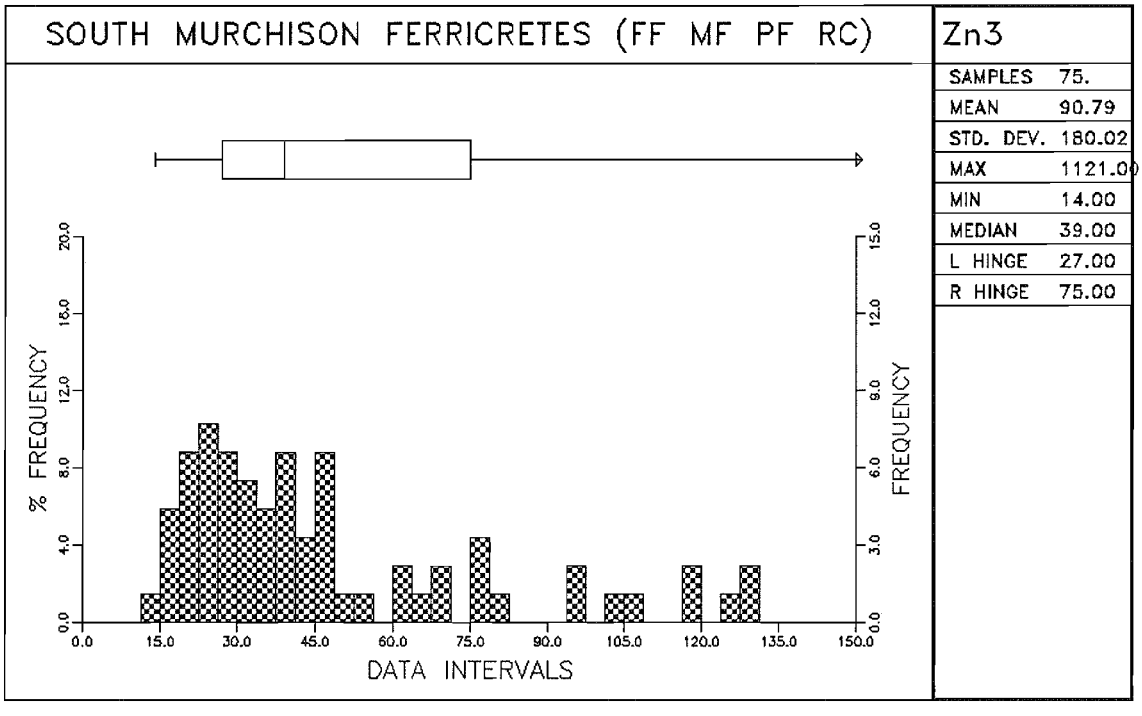

Figure 14b

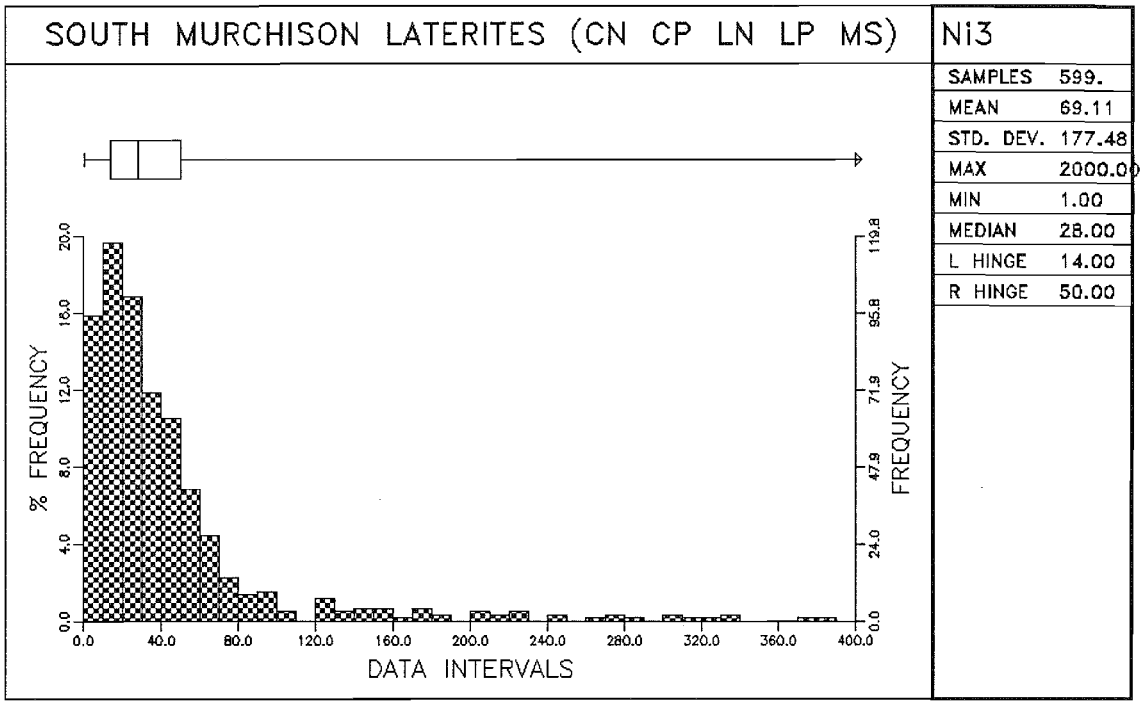

Figure 15a

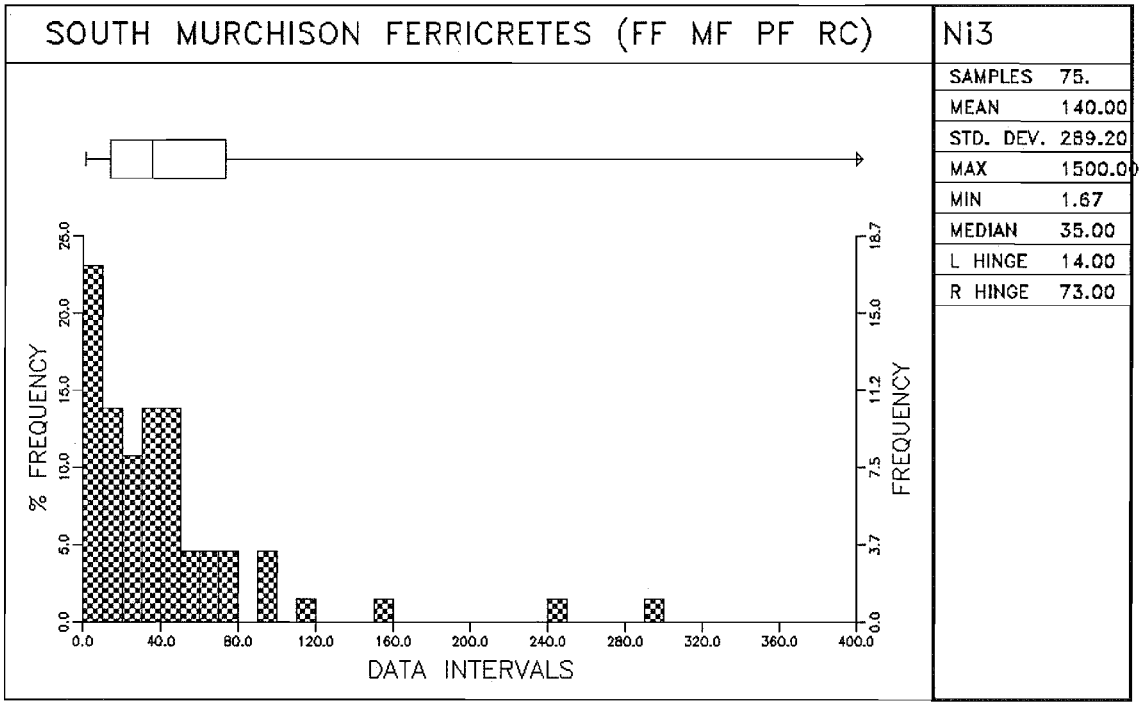

Figure 15b

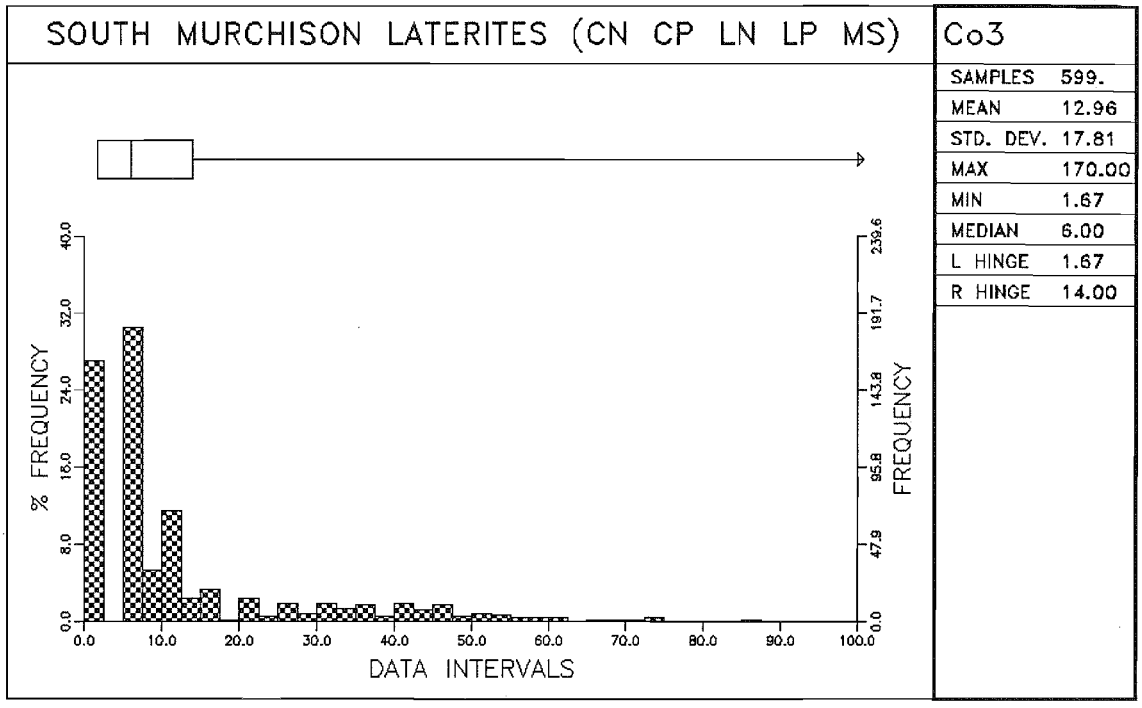

Co3	
SAMPLES	599.
MEAN	12.96
STD. DEV.	17.81
MAX	170.00
MIN	1.67
MEDIAN	6.00
L HINGE	1.67
R HINGE	14.00

Figure 16a

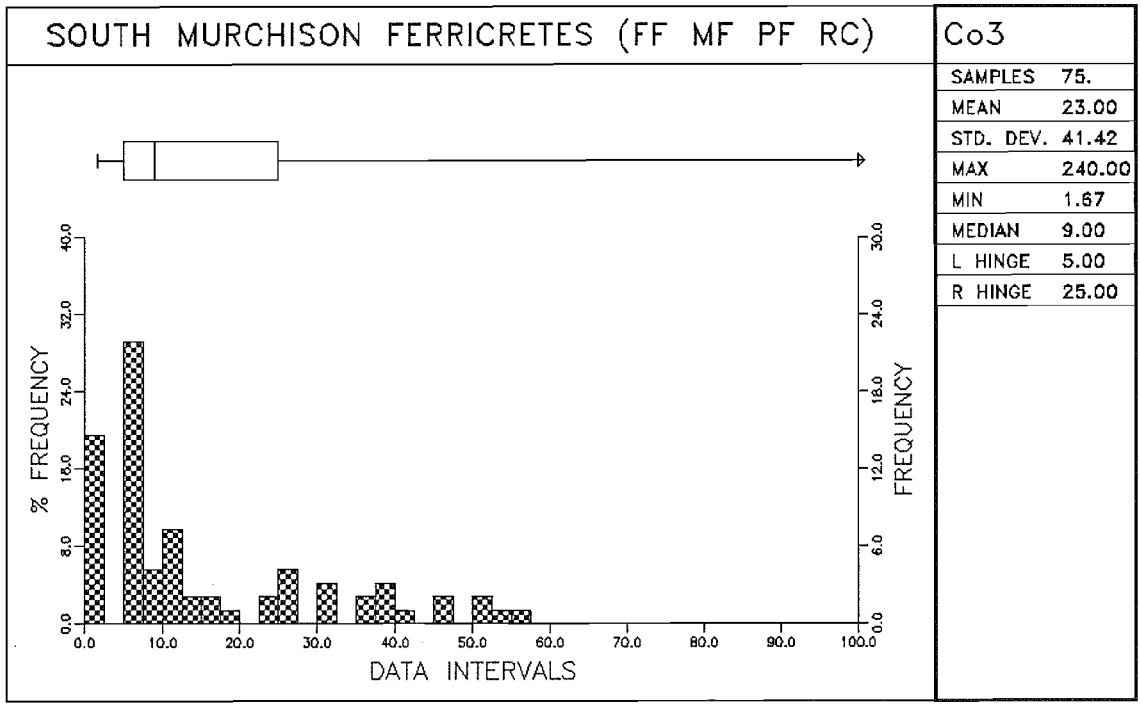

Co3	
SAMPLES	75.
MEAN	23.00
STD. DEV.	41.42
MAX	240.00
MIN	1.67
MEDIAN	9.00
L HINGE	5.00
R HINGE	25.00

Figure 16b

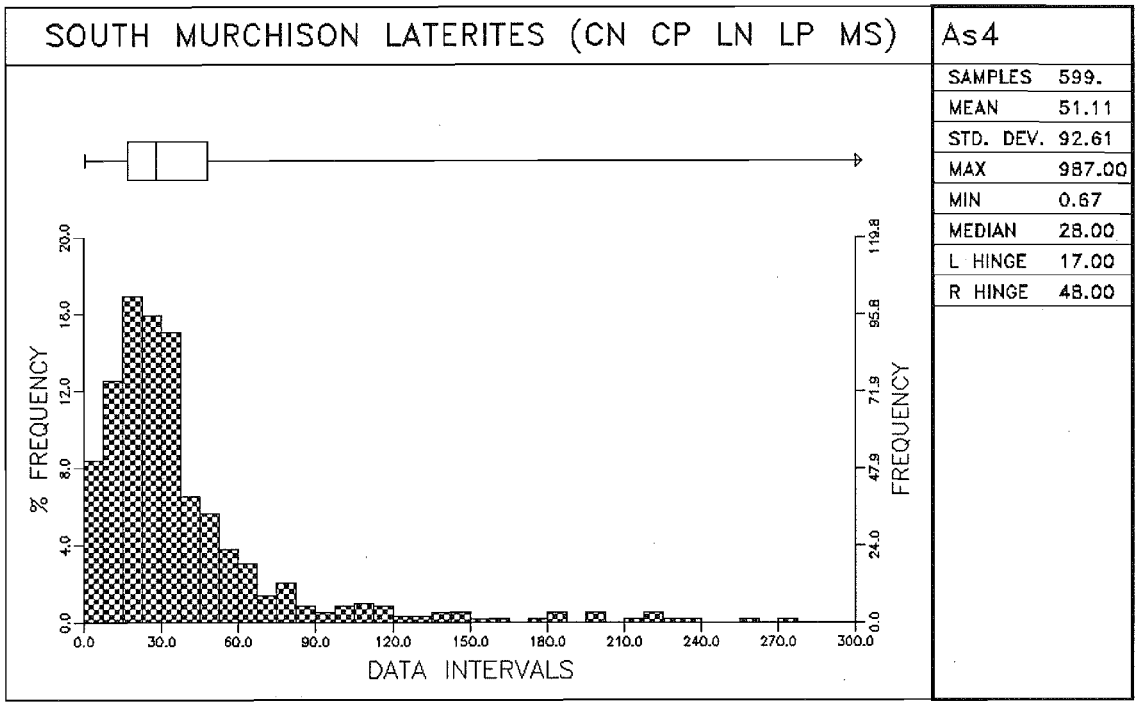

As4	
SAMPLES	599.
MEAN	51.11
STD. DEV.	92.61
MAX	987.00
MIN	0.67
MEDIAN	28.00
L HINGE	17.00
R HINGE	48.00

Figure 17a

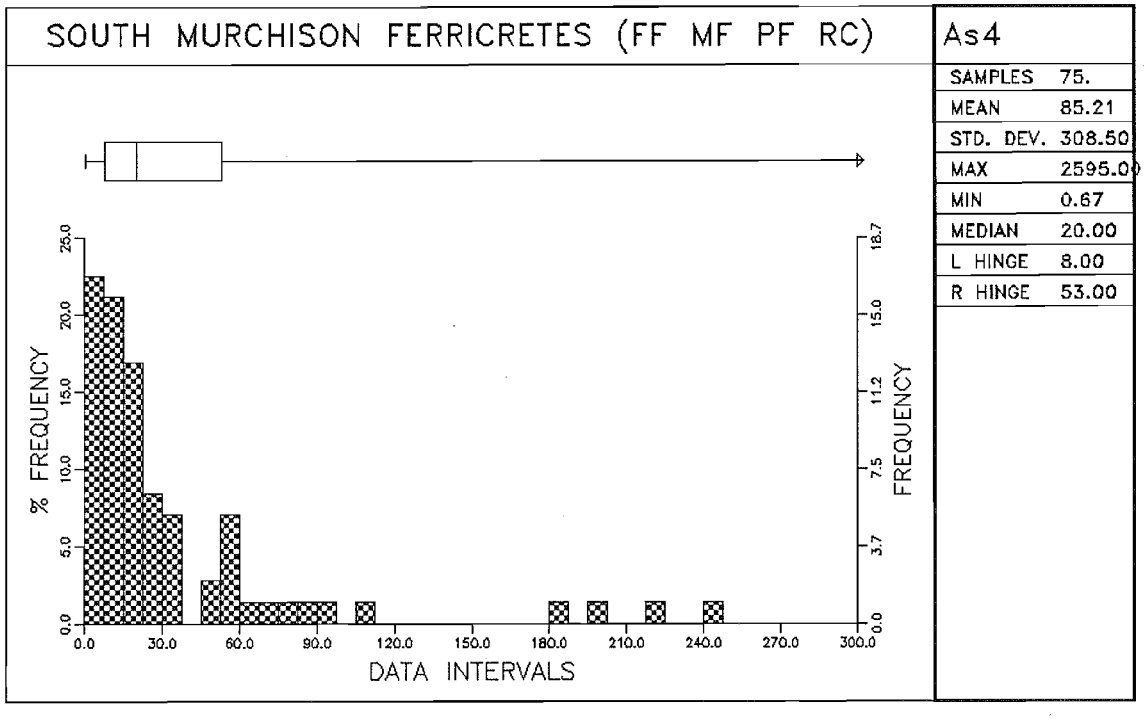

As4	
SAMPLES	75.
MEAN	85.21
STD. DEV.	308.50
MAX	2595.00
MIN	0.67
MEDIAN	20.00
L HINGE	8.00
R HINGE	53.00

Figure 17b

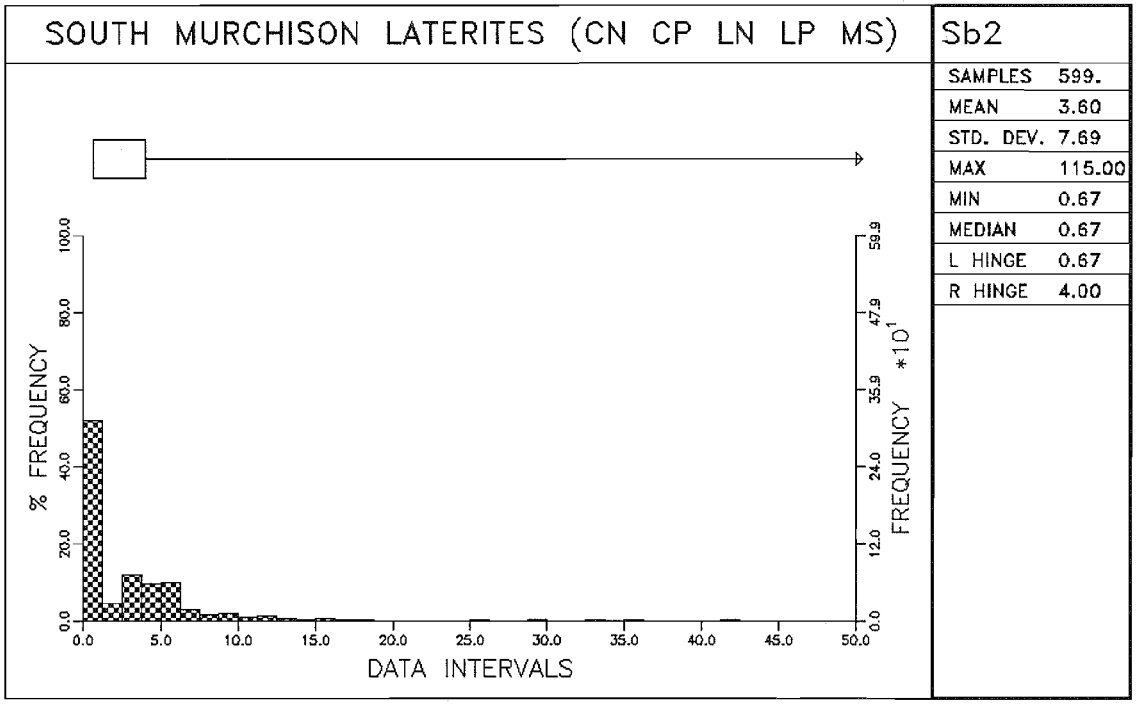

Figure 18a

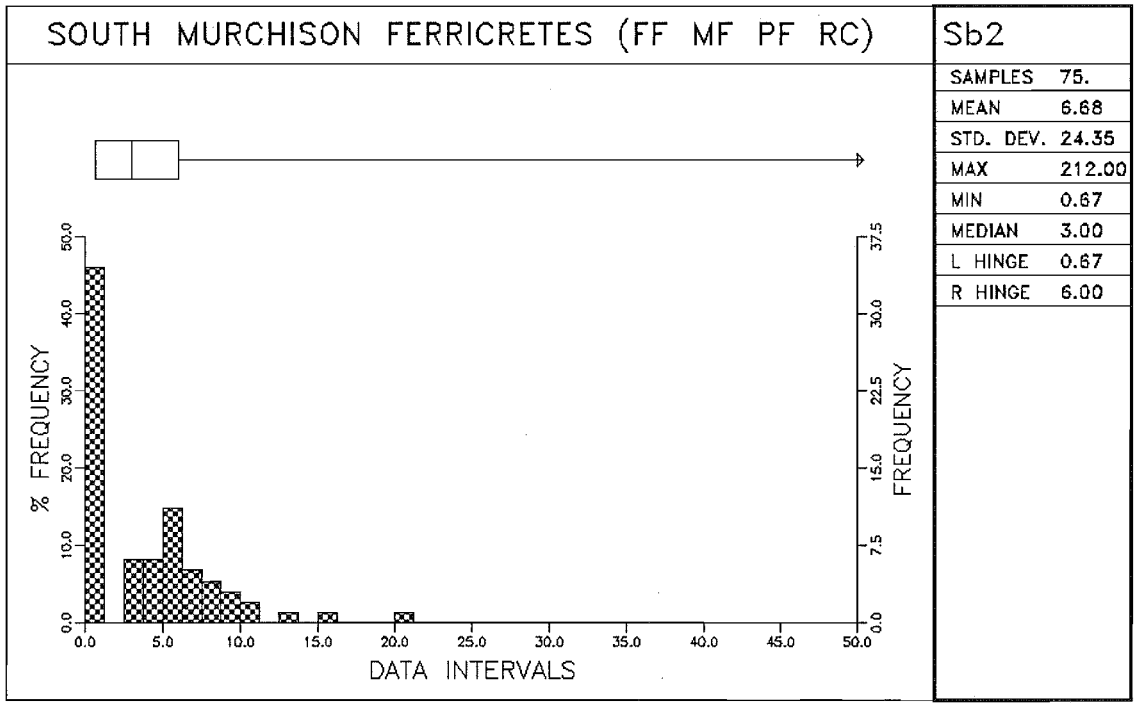

Figure 18b

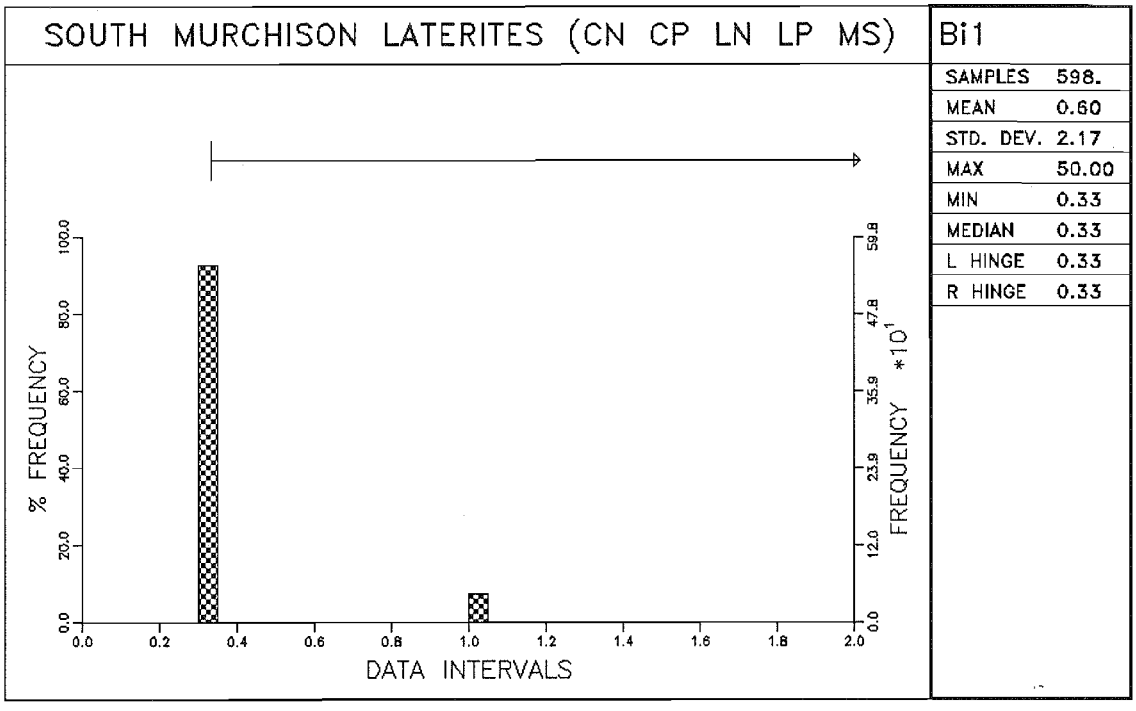

Bi1	
SAMPLES	598.
MEAN	0.60
STD. DEV.	2.17
MAX	50.00
MIN	0.33
MEDIAN	0.33
L HINGE	0.33
R HINGE	0.33

Figure 19a

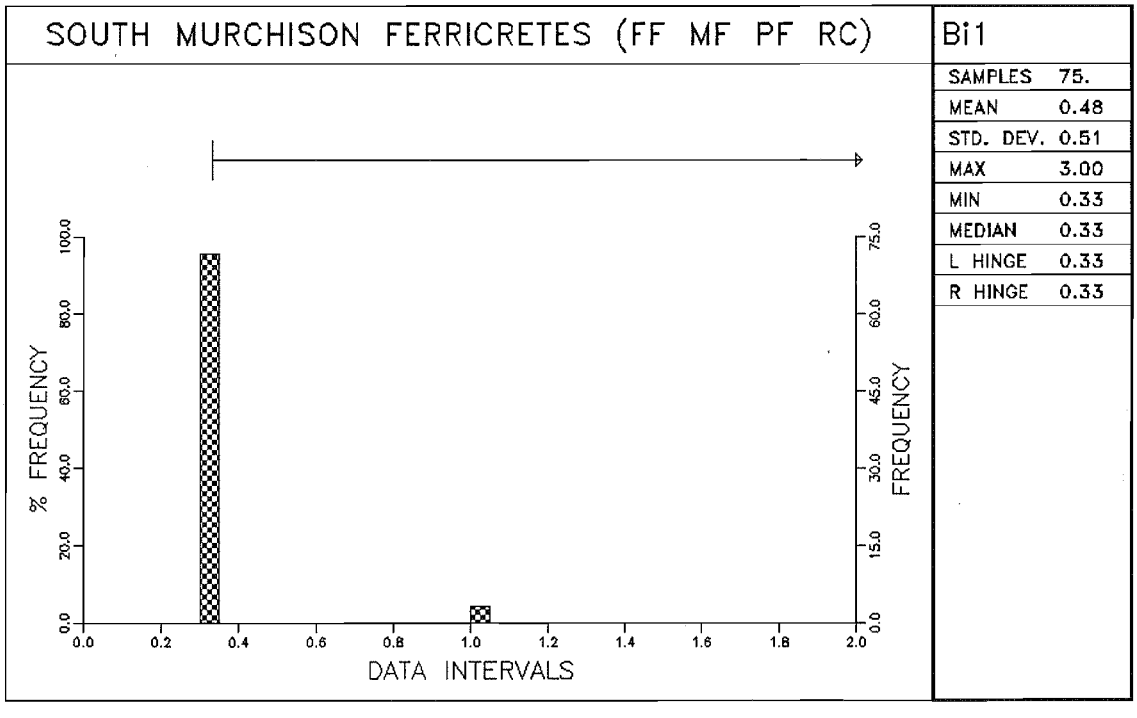

Bi1	
SAMPLES	75.
MEAN	0.48
STD. DEV.	0.51
MAX	3.00
MIN	0.33
MEDIAN	0.33
L HINGE	0.33
R HINGE	0.33

Figure 19b

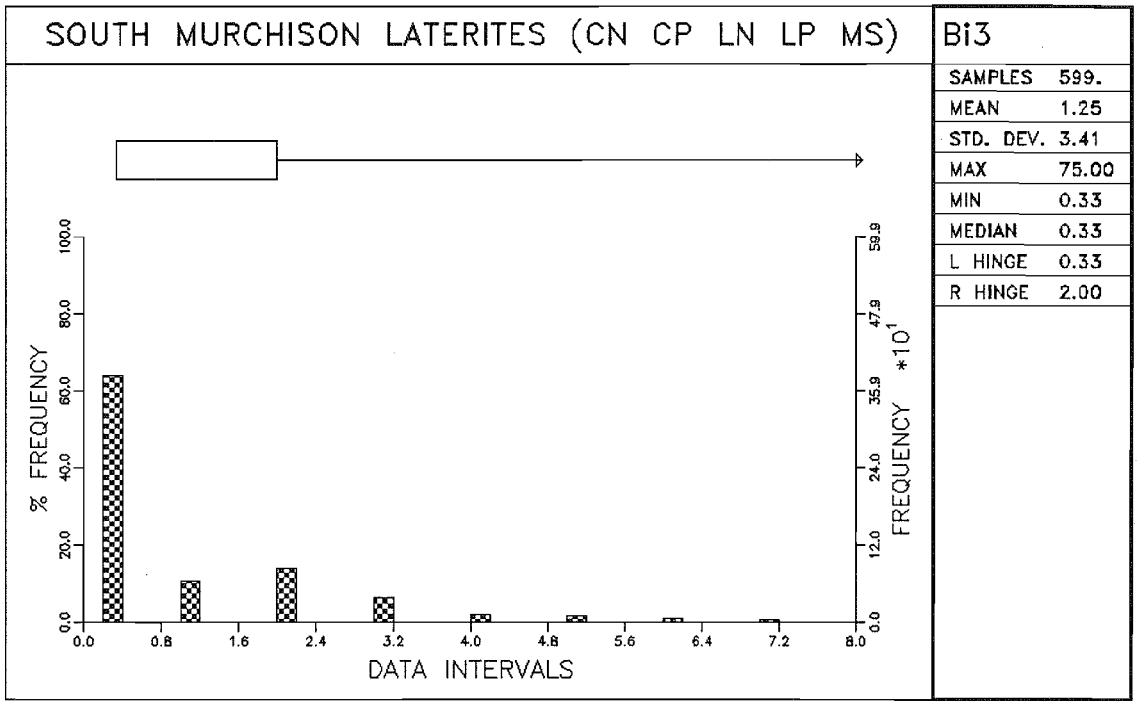

Figure 20a

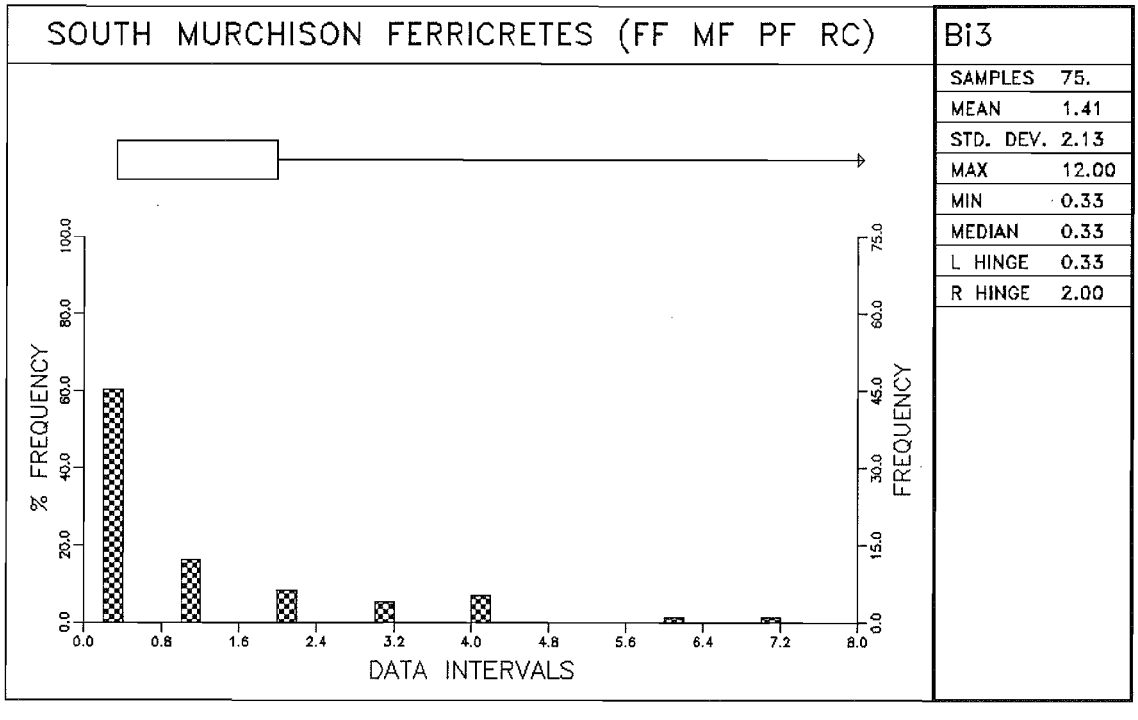

Figure 20b

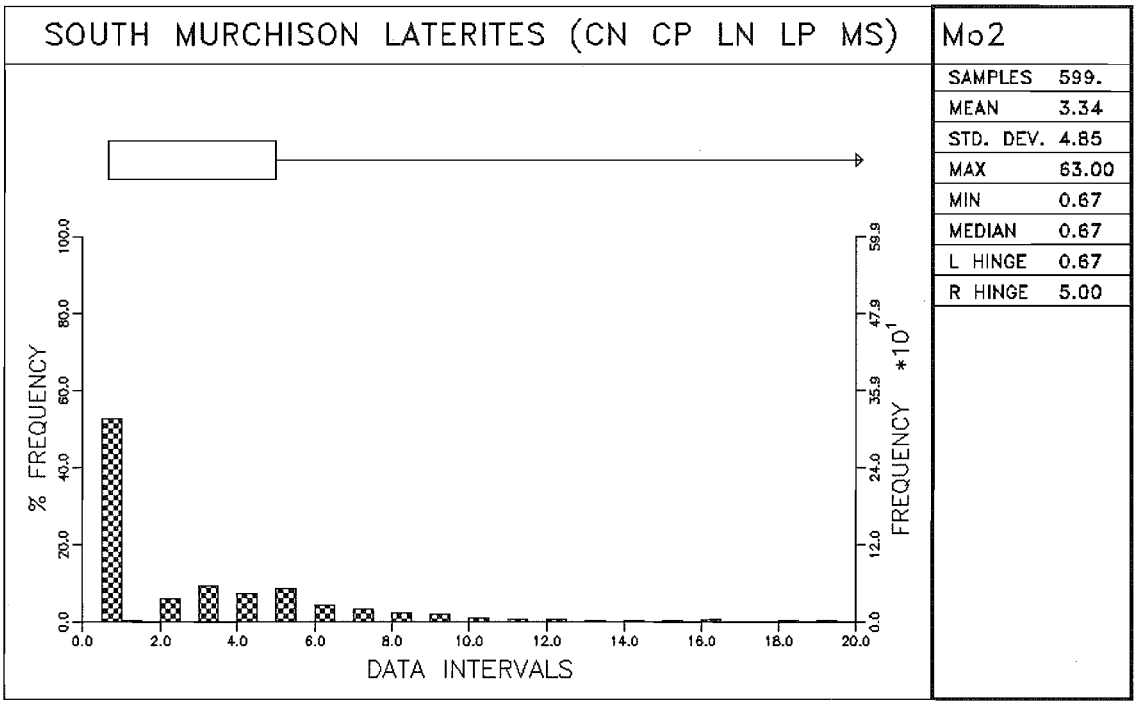

Figure 21a

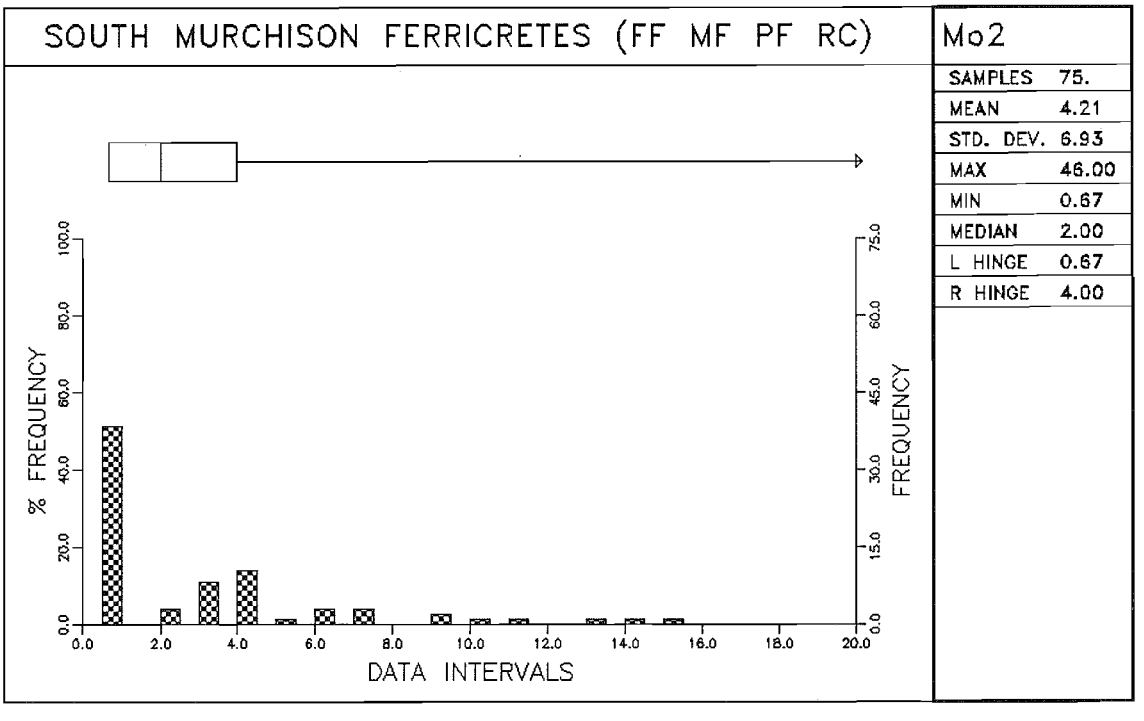

Figure 21b

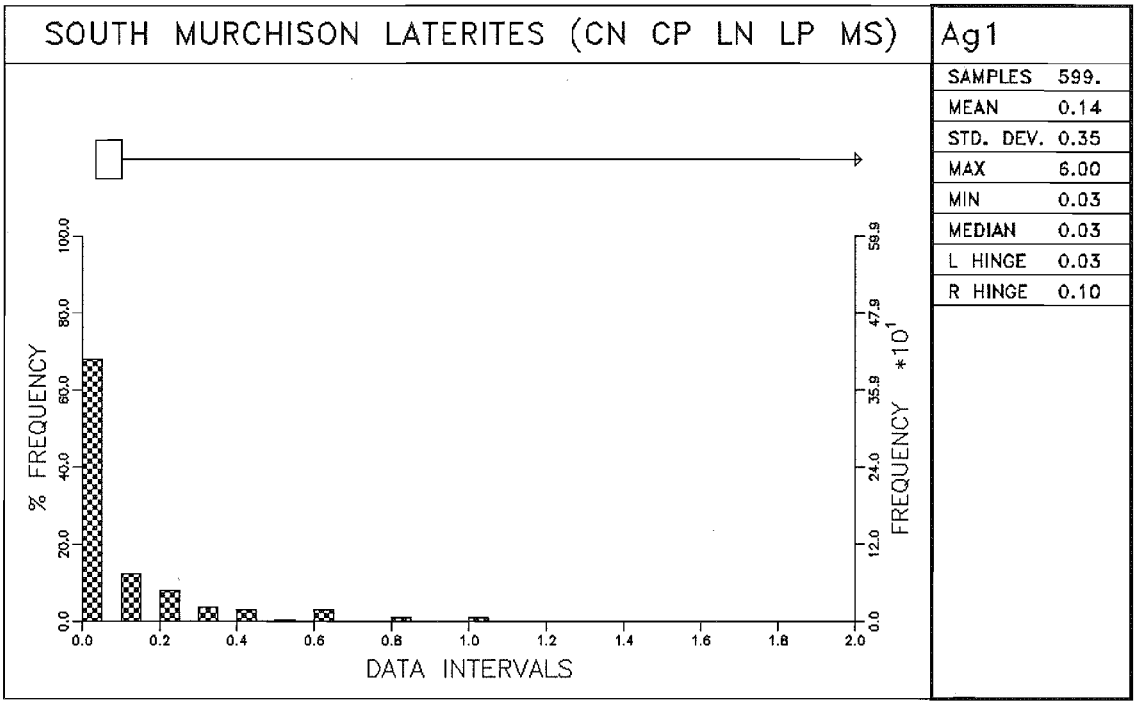

Ag1	
SAMPLES	599.
MEAN	0.14
STD. DEV.	0.35
MAX	6.00
MIN	0.03
MEDIAN	0.03
L HINGE	0.03
R HINGE	0.10

Figure 22a

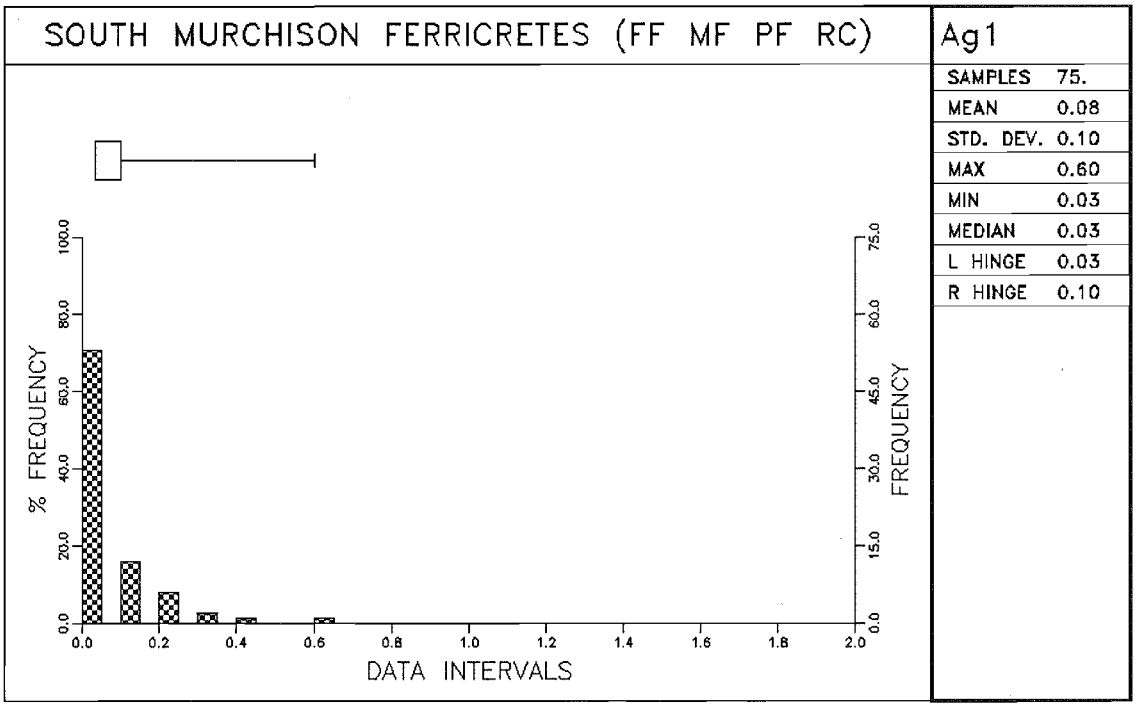

Ag1	
SAMPLES	75.
MEAN	0.08
STD. DEV.	0.10
MAX	0.60
MIN	0.03
MEDIAN	0.03
L HINGE	0.03
R HINGE	0.10

Figure 22b

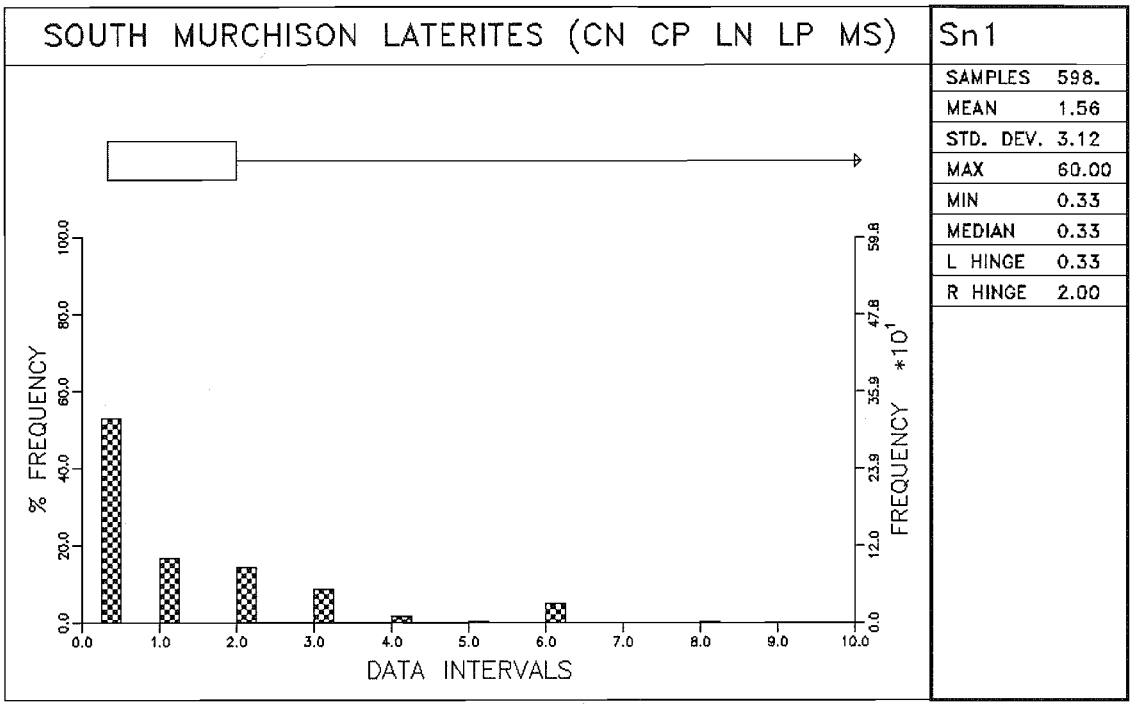

Figure 23a

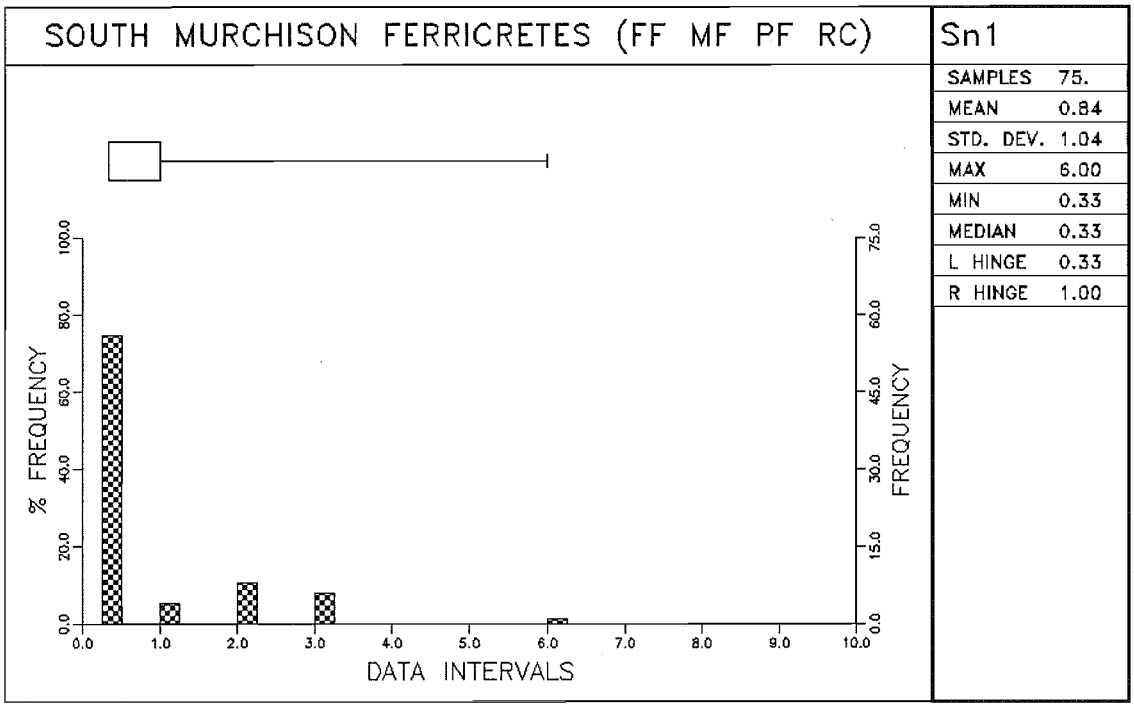

Figure 23b

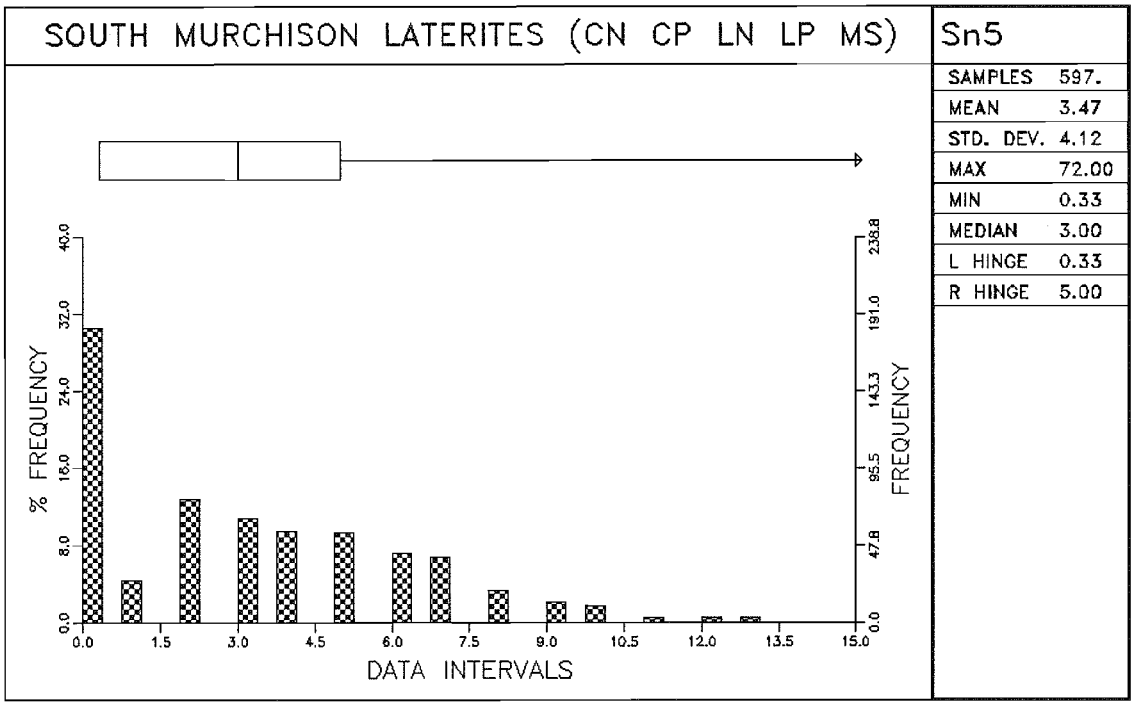

Figure 24a

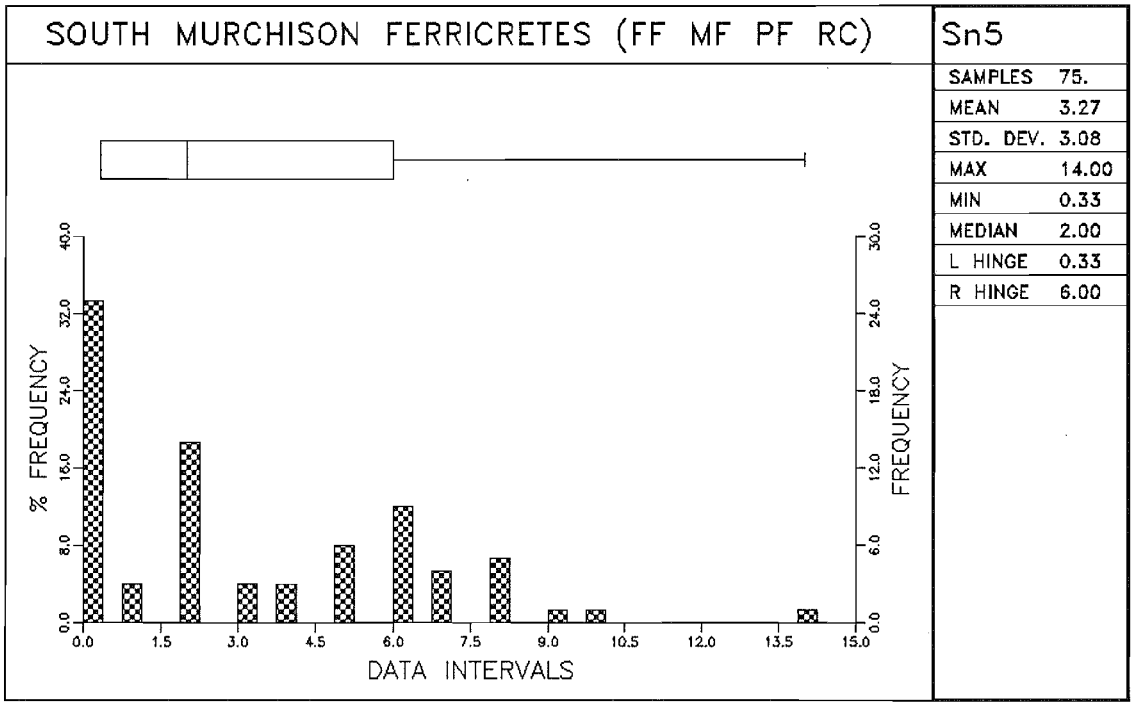

Figure 24b

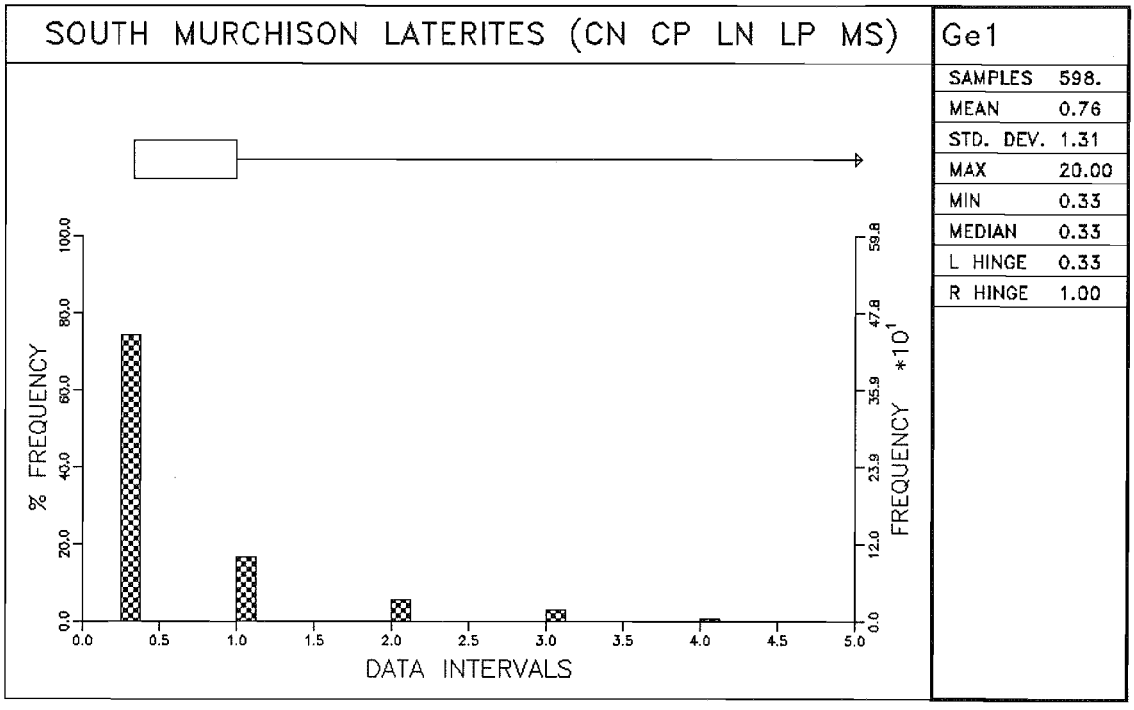

Ge1	
SAMPLES	598.
MEAN	0.76
STD. DEV.	1.31
MAX	20.00
MIN	0.33
MEDIAN	0.33
L HINGE	0.33
R HINGE	1.00

Figure 25a

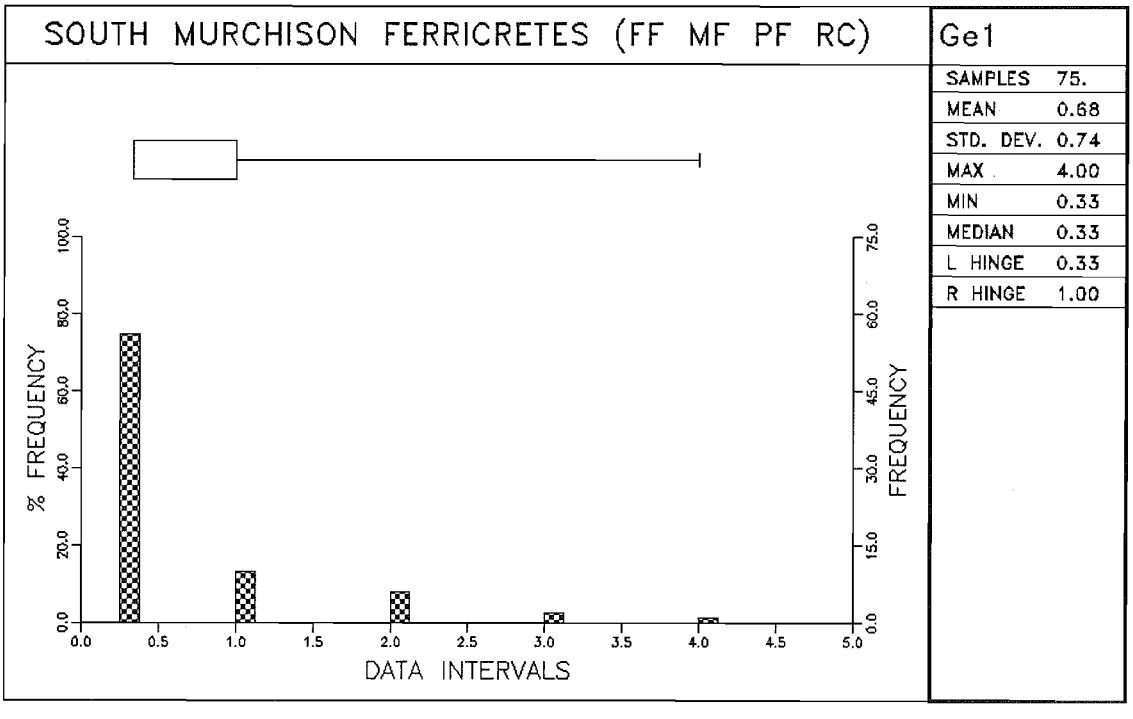

Ge1	
SAMPLES	75.
MEAN	0.68
STD. DEV.	0.74
MAX	4.00
MIN	0.33
MEDIAN	0.33
L HINGE	0.33
R HINGE	1.00

Figure 25b

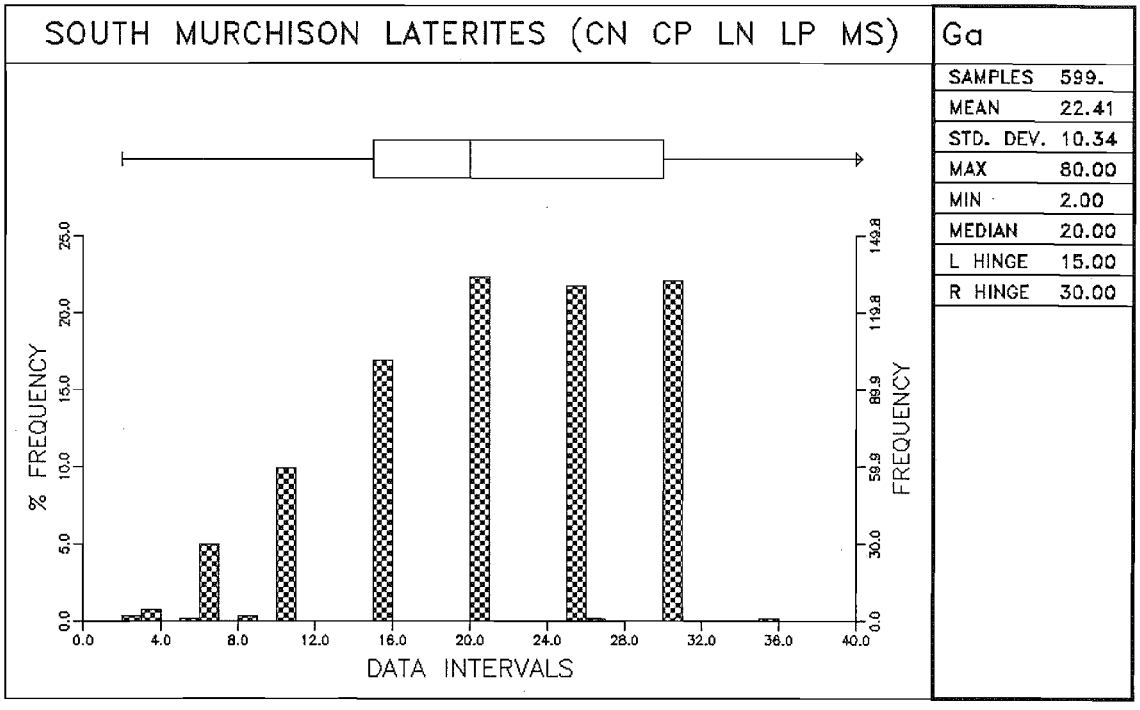

Ga	
SAMPLES	599.
MEAN	22.41
STD. DEV.	10.34
MAX	80.00
MIN	2.00
MEDIAN	20.00
L HINGE	15.00
R HINGE	30.00

Figure 26a

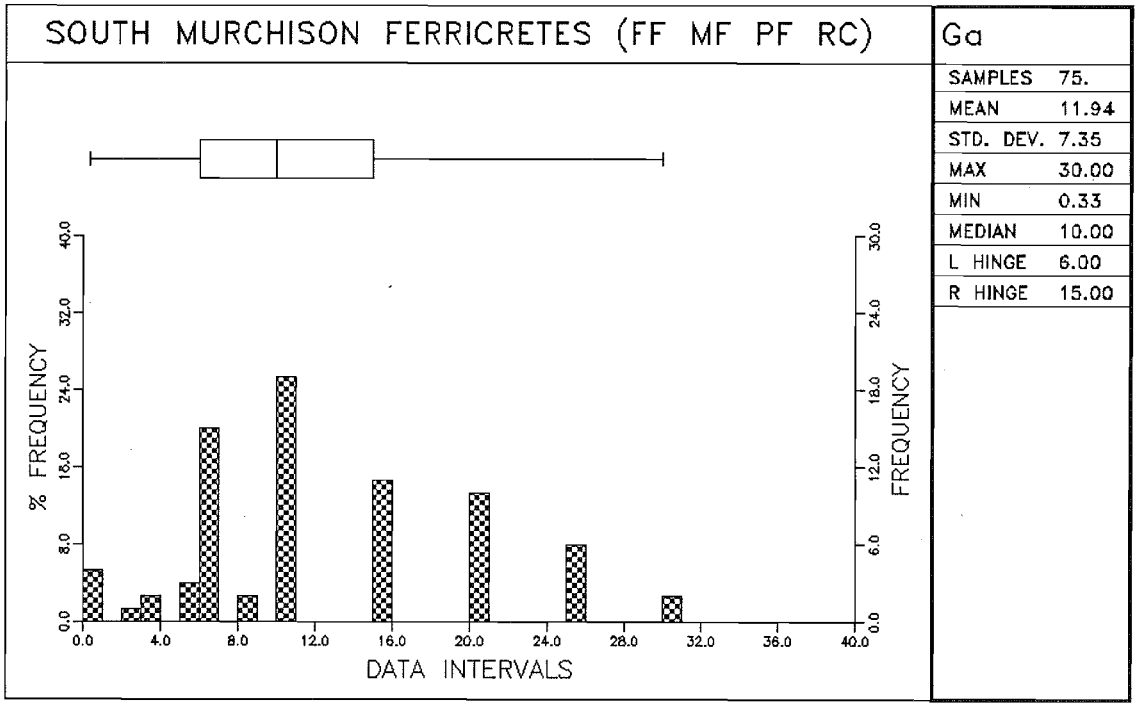

Ga	
SAMPLES	75.
MEAN	11.94
STD. DEV.	7.35
MAX	30.00
MIN	0.33
MEDIAN	10.00
L HINGE	6.00
R HINGE	15.00

Figure 26b

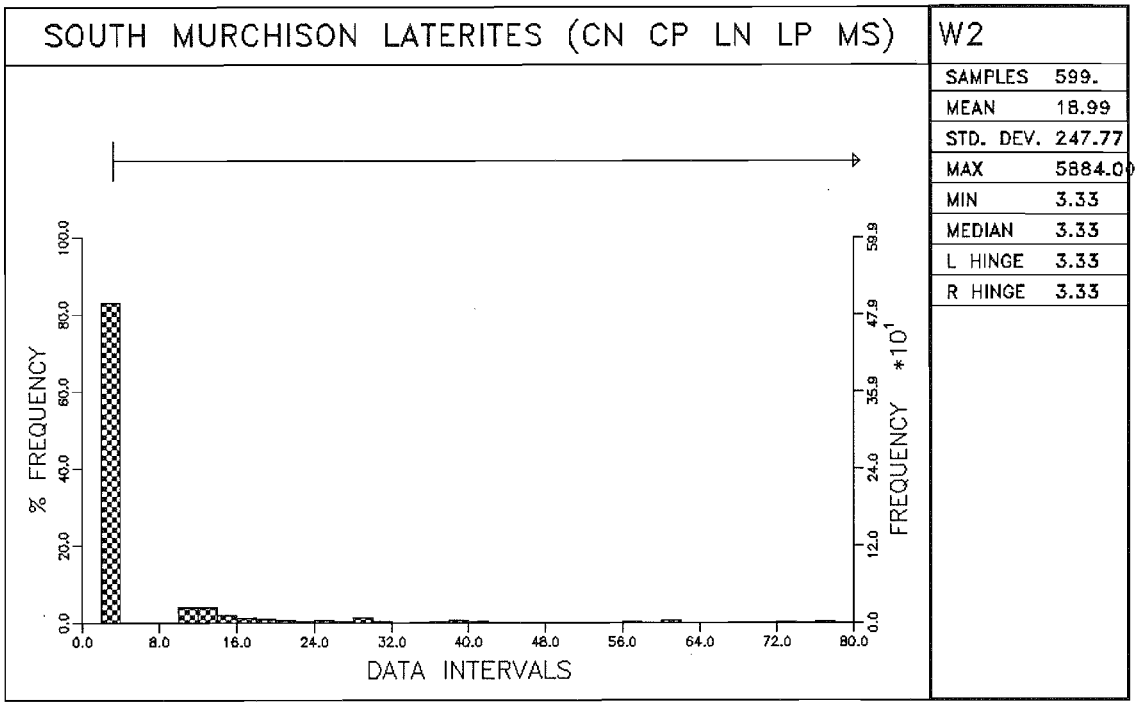

Figure 27a

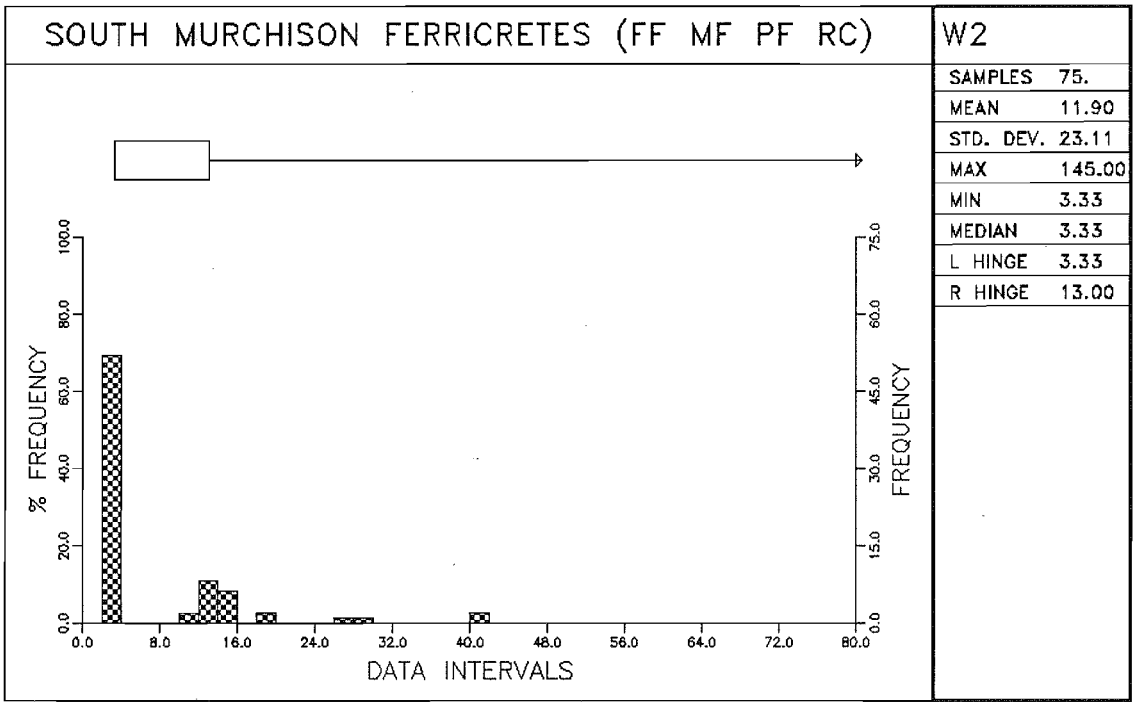

Figure 27b

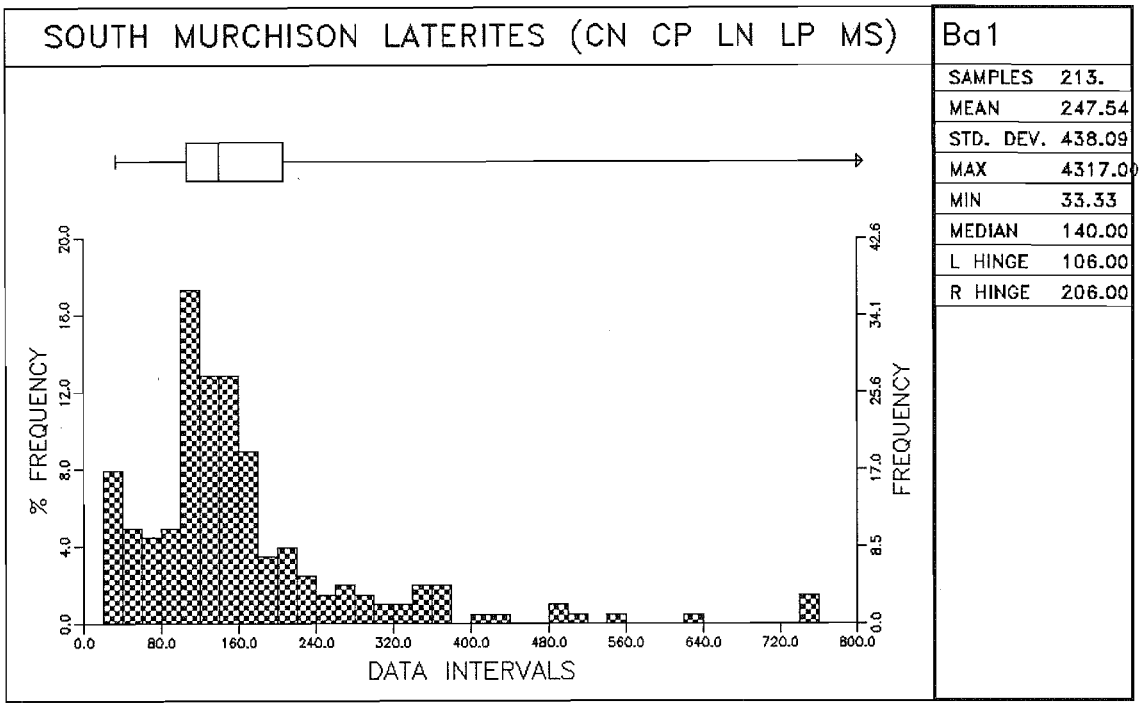

Figure 28a

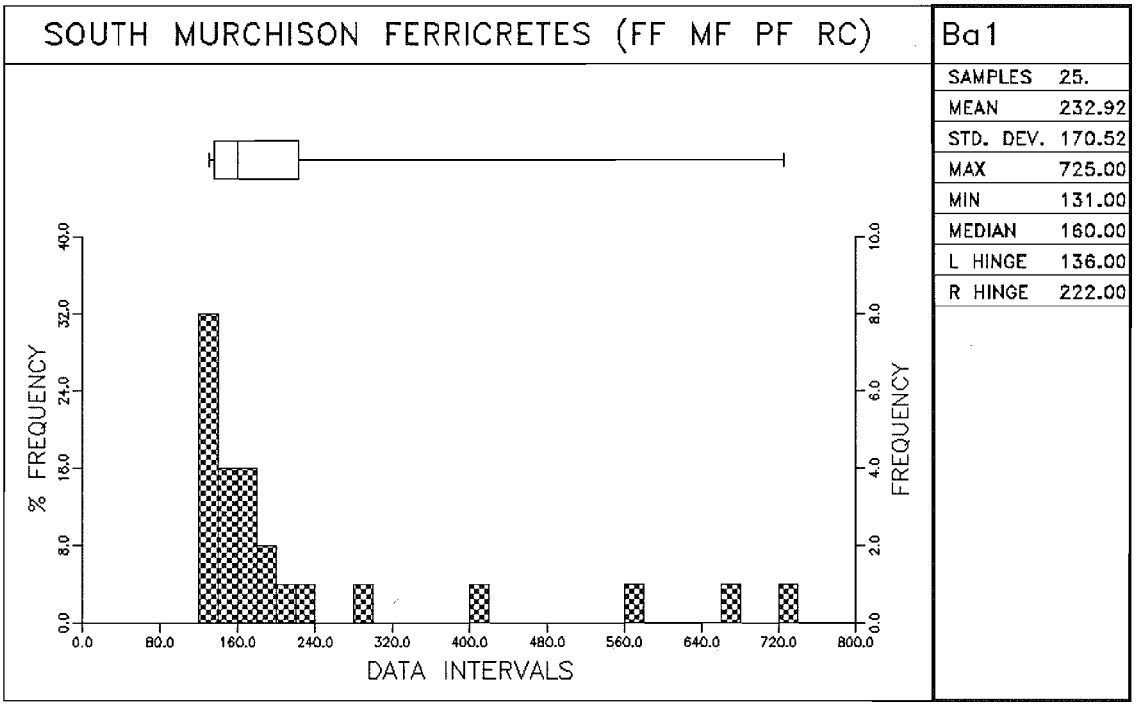

Figure 28b

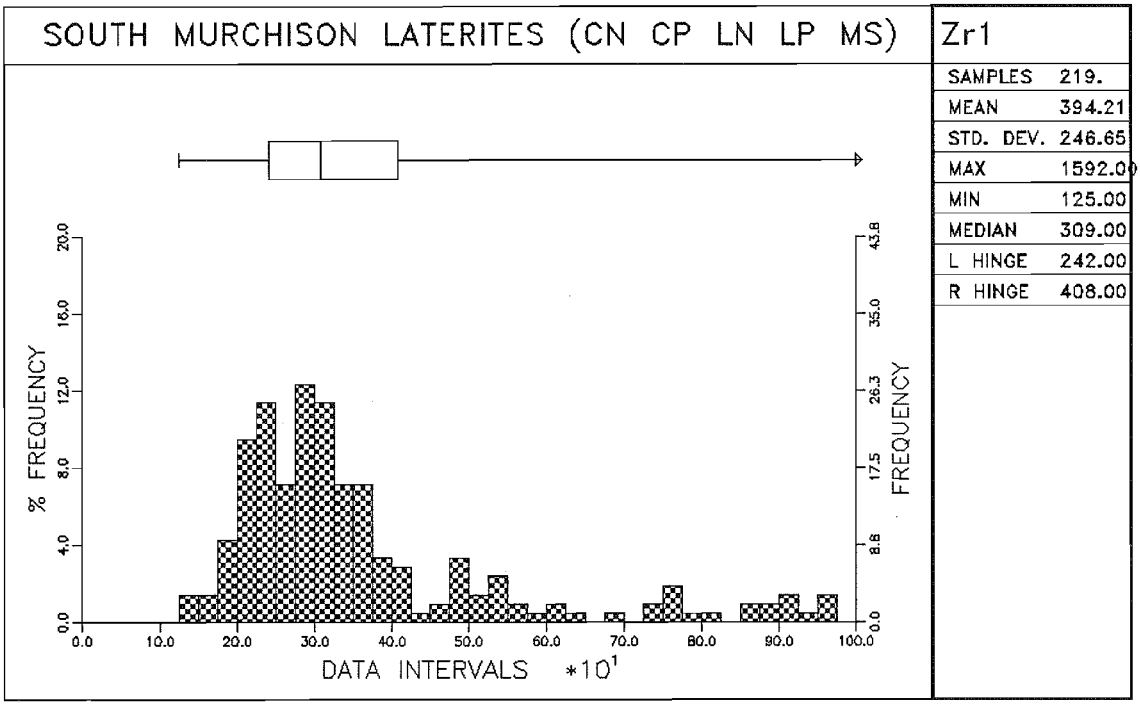

Figure 29a

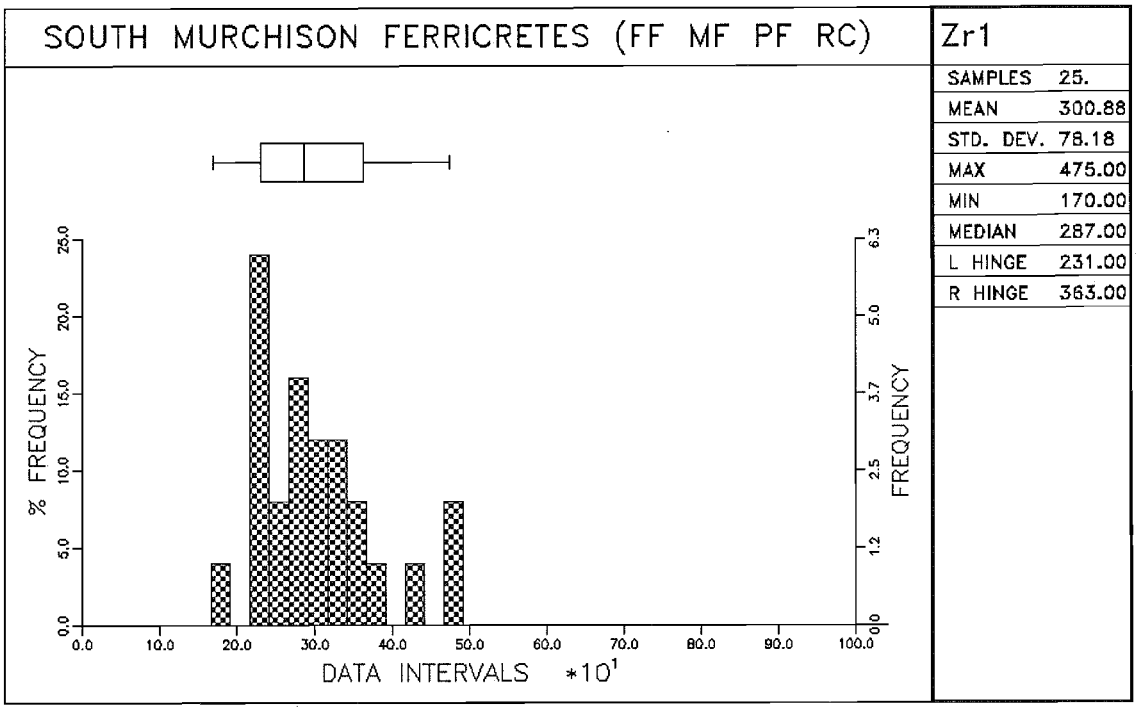

Figure 29b

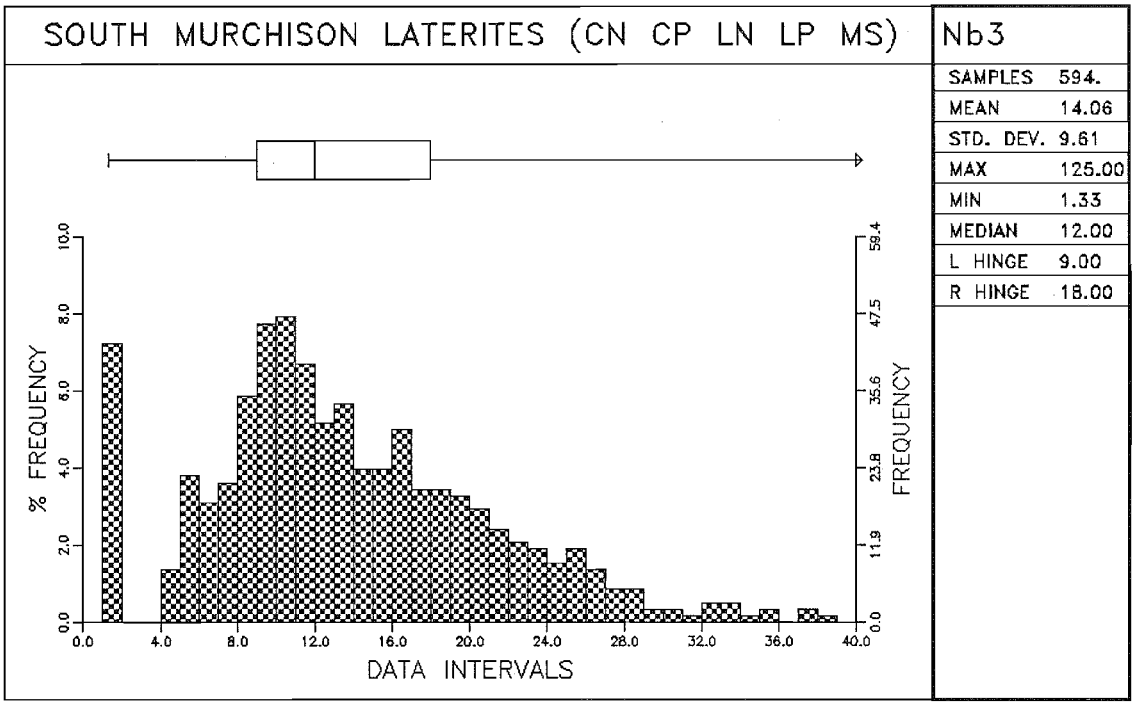

Figure 30a

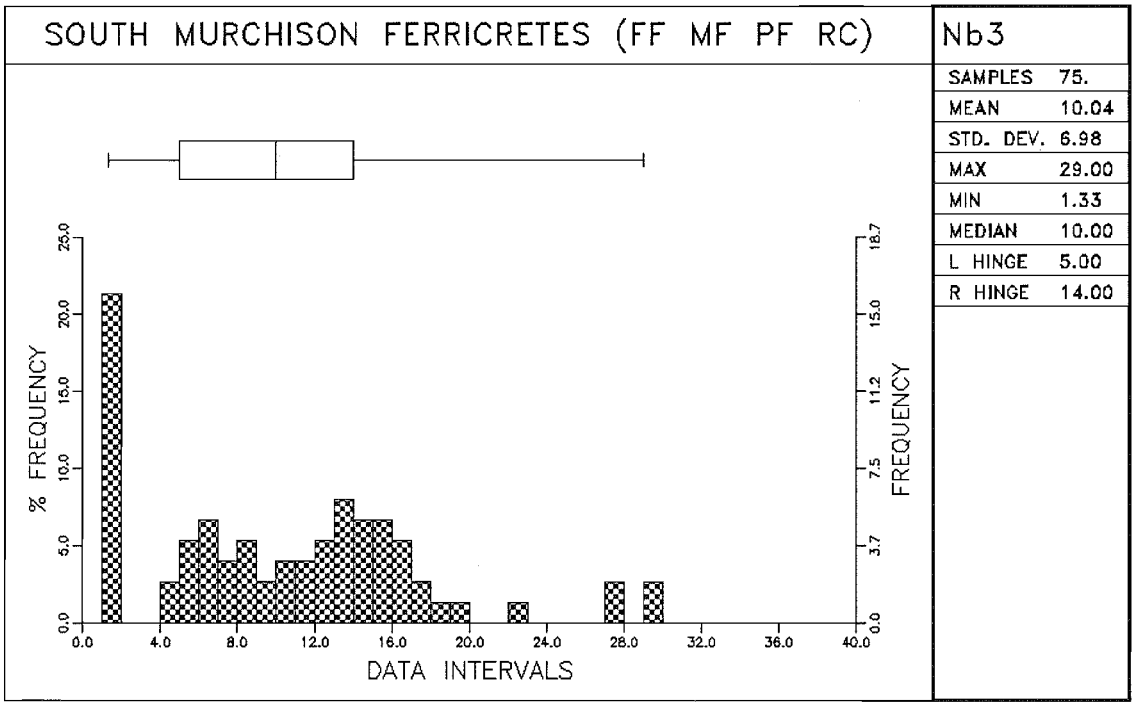

Figure 30b

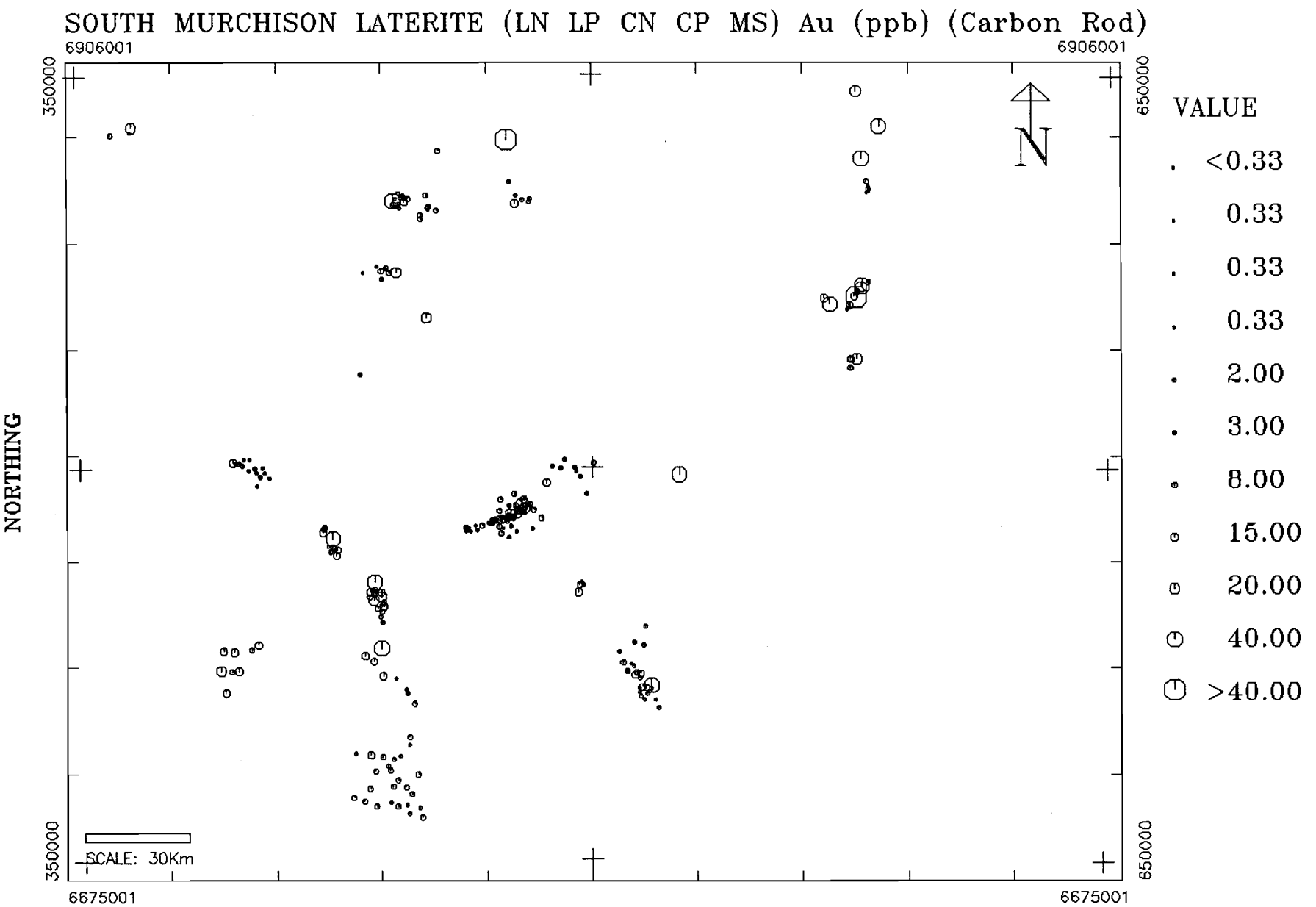
SOUTH MURCHISON LATERITE (LN LP CN CP MS) Au (ppb) (Carbon Rod)
6906001
6906001
350000
650000
N
VALUE
. <0.33
. 0.33
. 0.33
. 0.33
. 2.00
. 3.00
. 8.00
. 15.00
. 20.00
. 40.00
. >40.00
NORTHING
SCALE: 30Km
350000
650000
6675001
6675001
EASTING
268 STATIONS PLOTTED

Figure 31

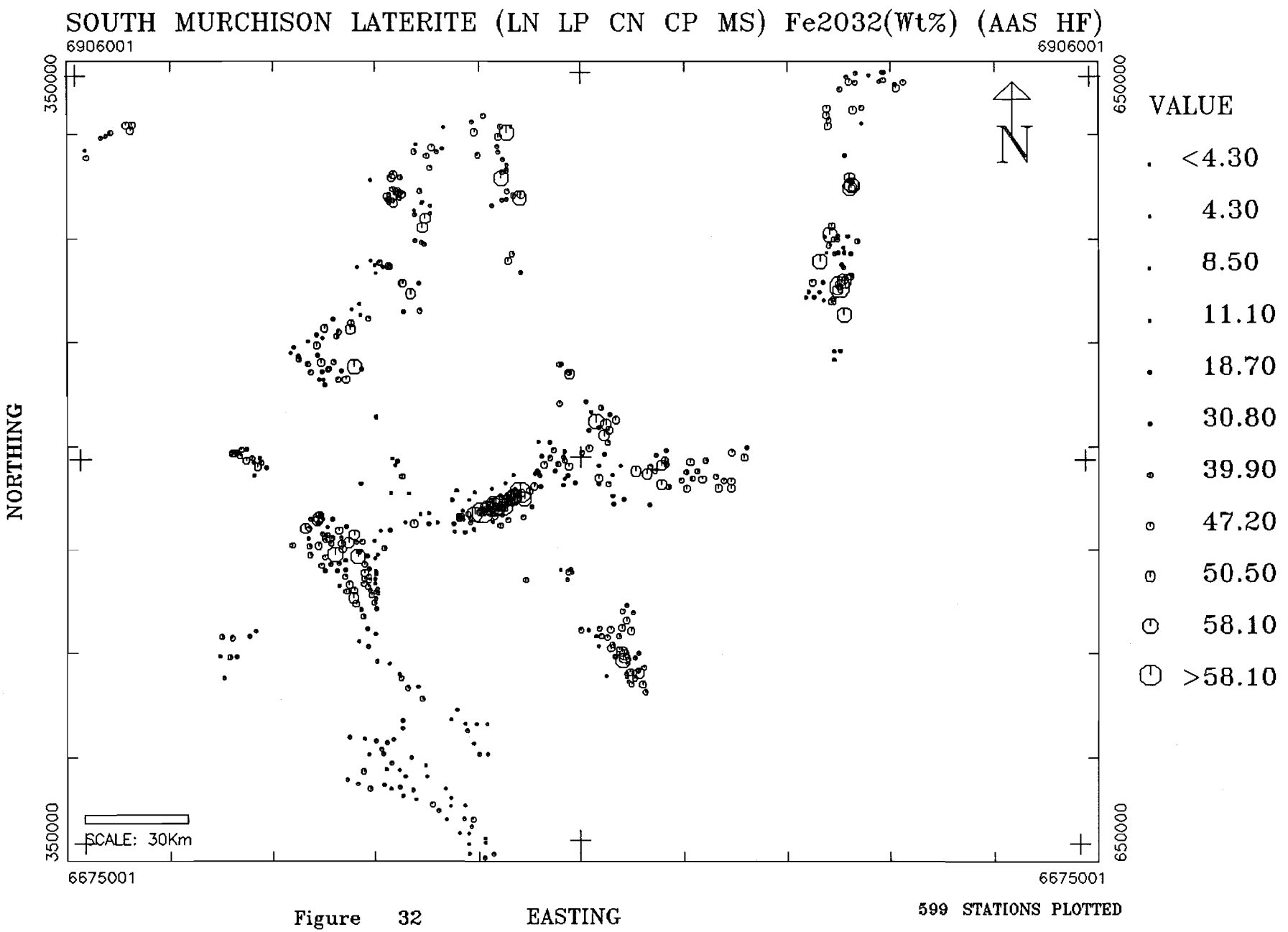
SOUTH MURCHISON LATERITE (LN LP CN CP MS) Fe2032(Wt%) (AAS HF)
6906001
6906001
350000
650000
N
VALUE
. <4.30
. 4.30
. 8.50
. 11.10
. 18.70
. 30.80
. 39.90
. 47.20
. 50.50
. 58.10
. >58.10
SCALE: 30Km
350000
650000
6675001
6675001
NORTHING
EASTING
599 STATIONS PLOTTED

Figure 32

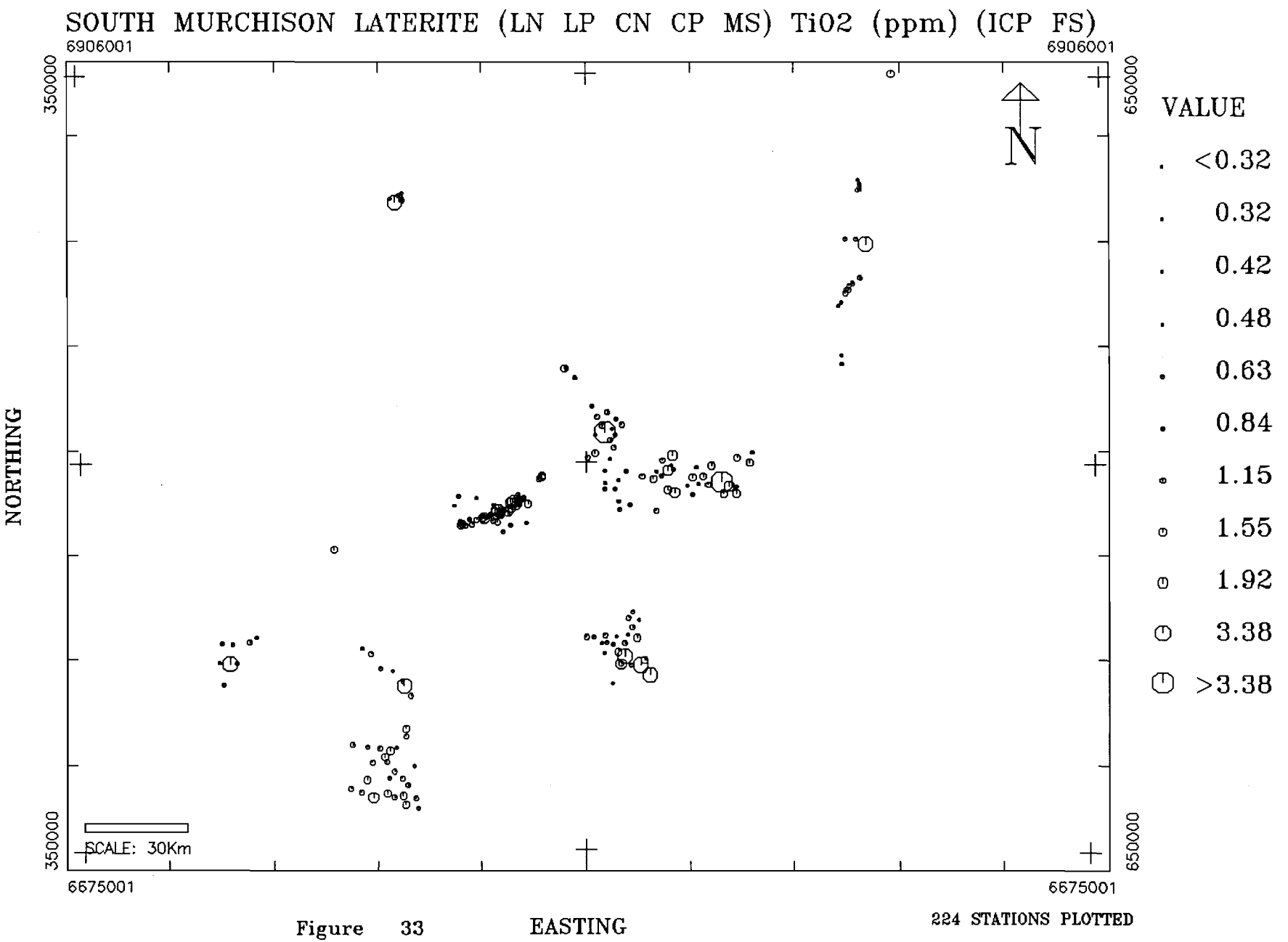
SOUTH MURCHISON LATERITE (LN LP CN CP MS) TiO2 (ppm) (ICP FS)
6906001
6906001
350000
650000
N
VALUE
. <0.32
. 0.32
. 0.42
. 0.48
. 0.63
. 0.84
. 1.15
. 1.55
. 1.92
. 3.38
. >3.38
NORTHING
SCALE: 30Km
350000
650000
6675001
6675001
EASTING
224 STATIONS PLOTTED

Figure 33

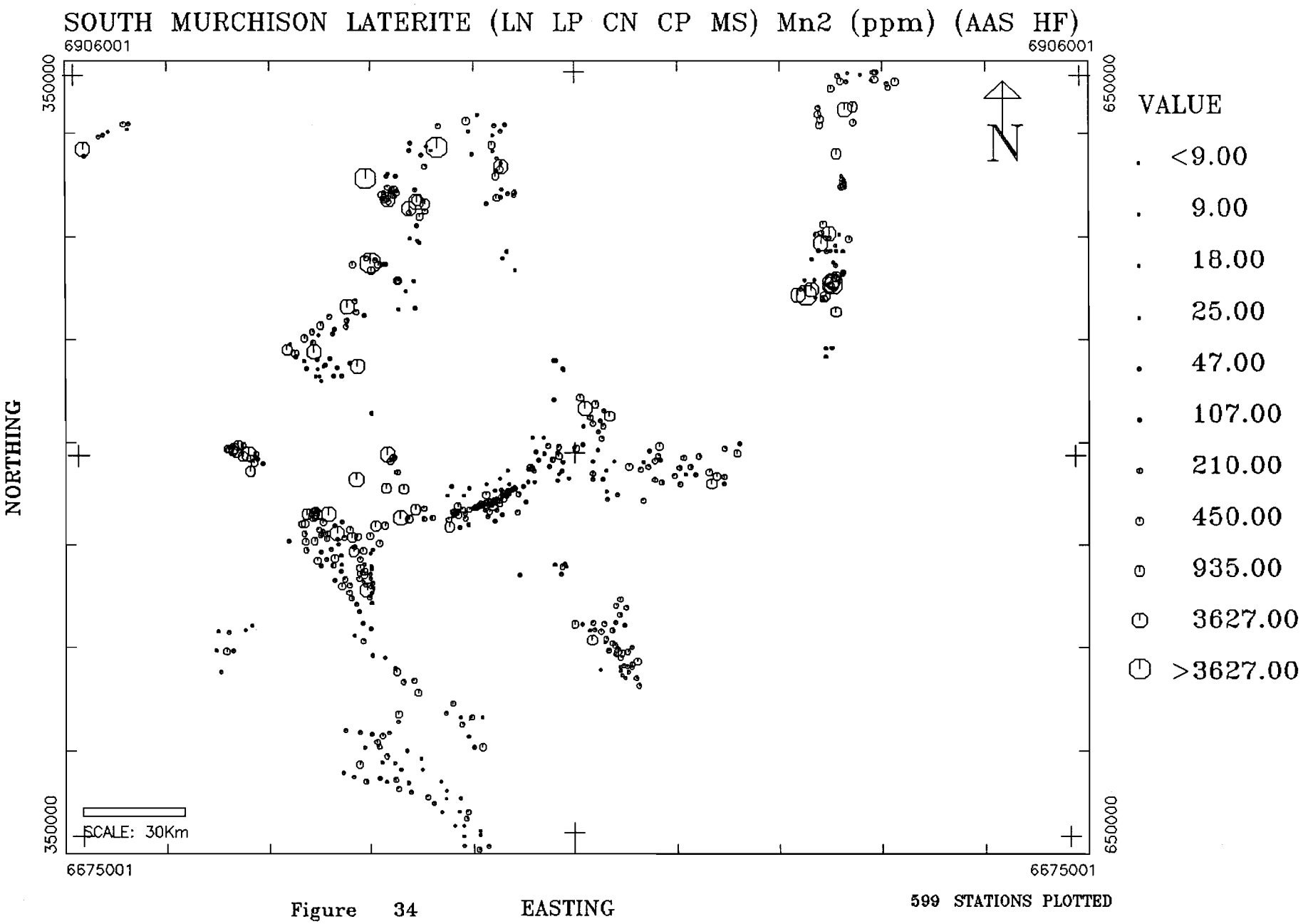
SOUTH MURCHISON LATERITE (LN LP CN CP MS) Mn2 (ppm) (AAS HF)
6906001
6906001
350000
650000
N
VALUE
. <9.00
. 9.00
. 18.00
. 25.00
. 47.00
. 107.00
. 210.00
. 450.00
. 935.00
. 3627.00
. >3627.00
SCALE: 30Km
350000
650000
6675001
6675001
NORTHING
EASTING
599 STATIONS PLOTTED

Figure 34

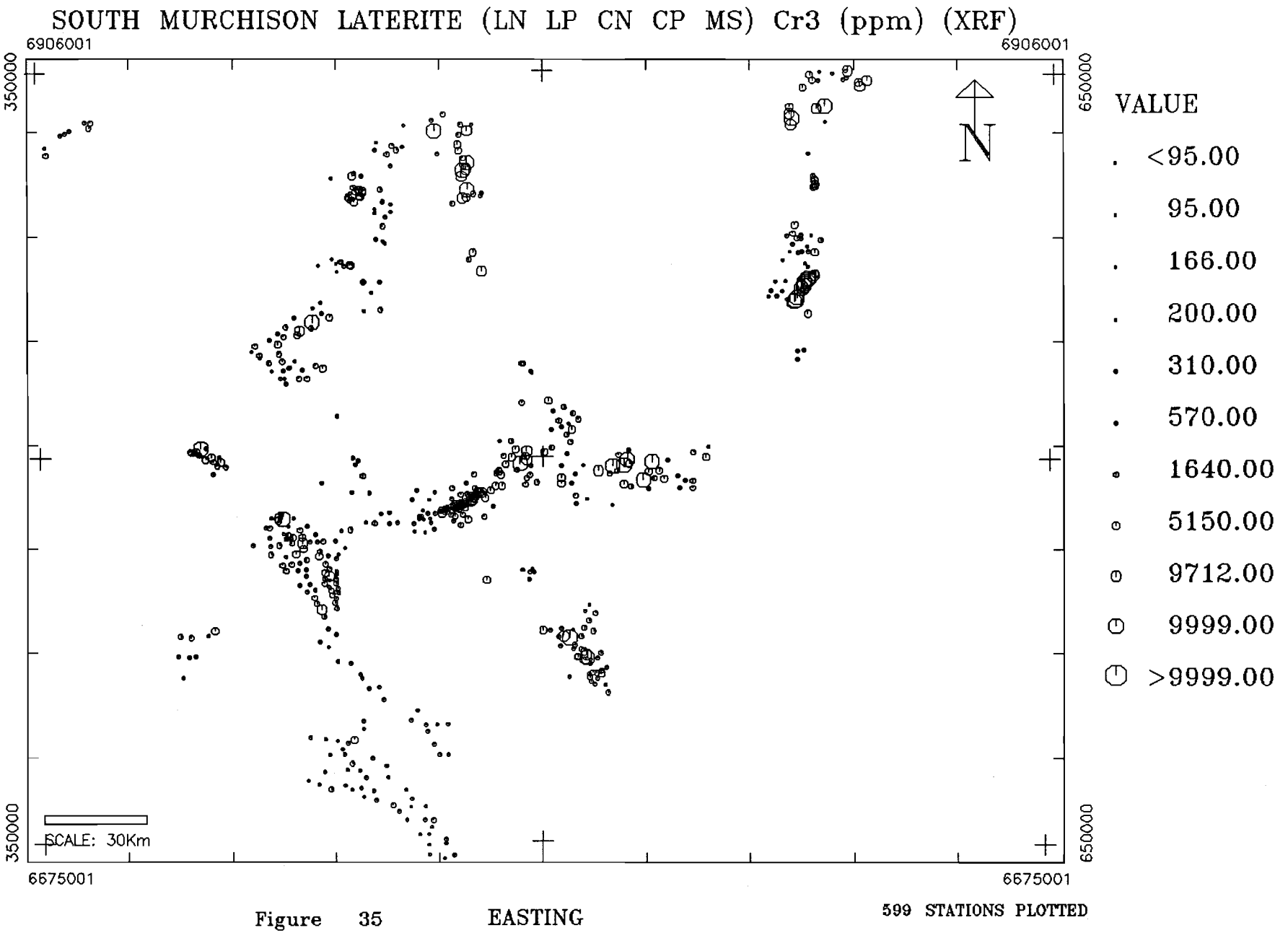
SOUTH MURCHISON LATERITE (LN LP CN CP MS) Cr3 (ppm) (XRF)
6906001
6906001
350000
650000
N
VALUE
. <95.00
. 95.00
. 166.00
. 200.00
. 310.00
. 570.00
. 1640.00
. 5150.00
. 9712.00
. 9999.00
. >9999.00
SCALE: 30Km
350000
650000
6675001
6675001
NORTHING
EASTING
599 STATIONS PLOTTED

Figure 35

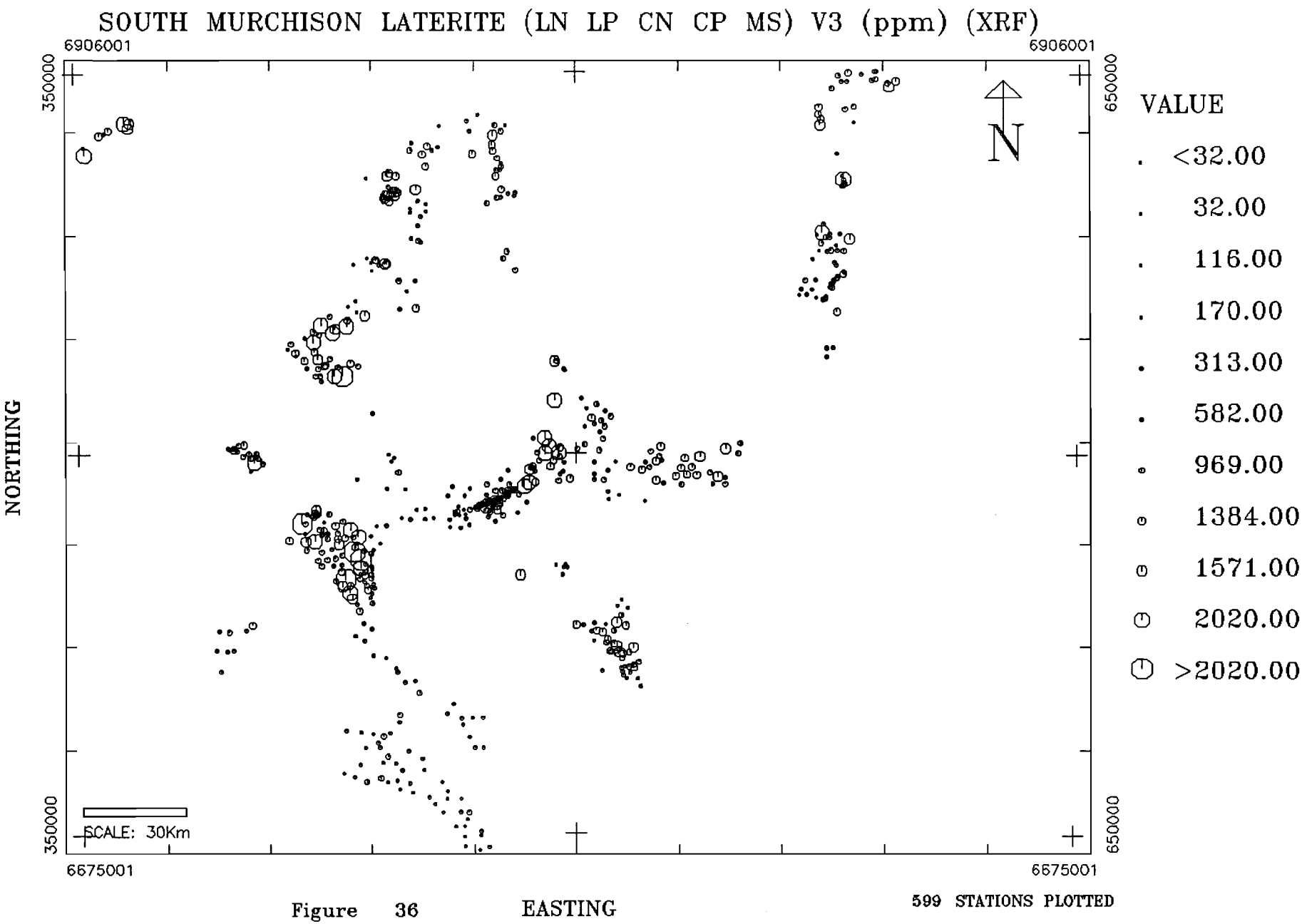
SOUTH MURCHISON LATERITE (LN LP CN CP MS) V3 (ppm) (XRF)
6906001
6906001
350000
650000
N
VALUE
. <32.00
. 32.00
. 116.00
. 170.00
. 313.00
. 582.00
. 969.00
. 1384.00
. 1571.00
. 2020.00
. >2020.00
SCALE: 30Km
350000
650000
6675001
6675001
NORTHING
EASTING
599 STATIONS PLOTTED

Figure 36

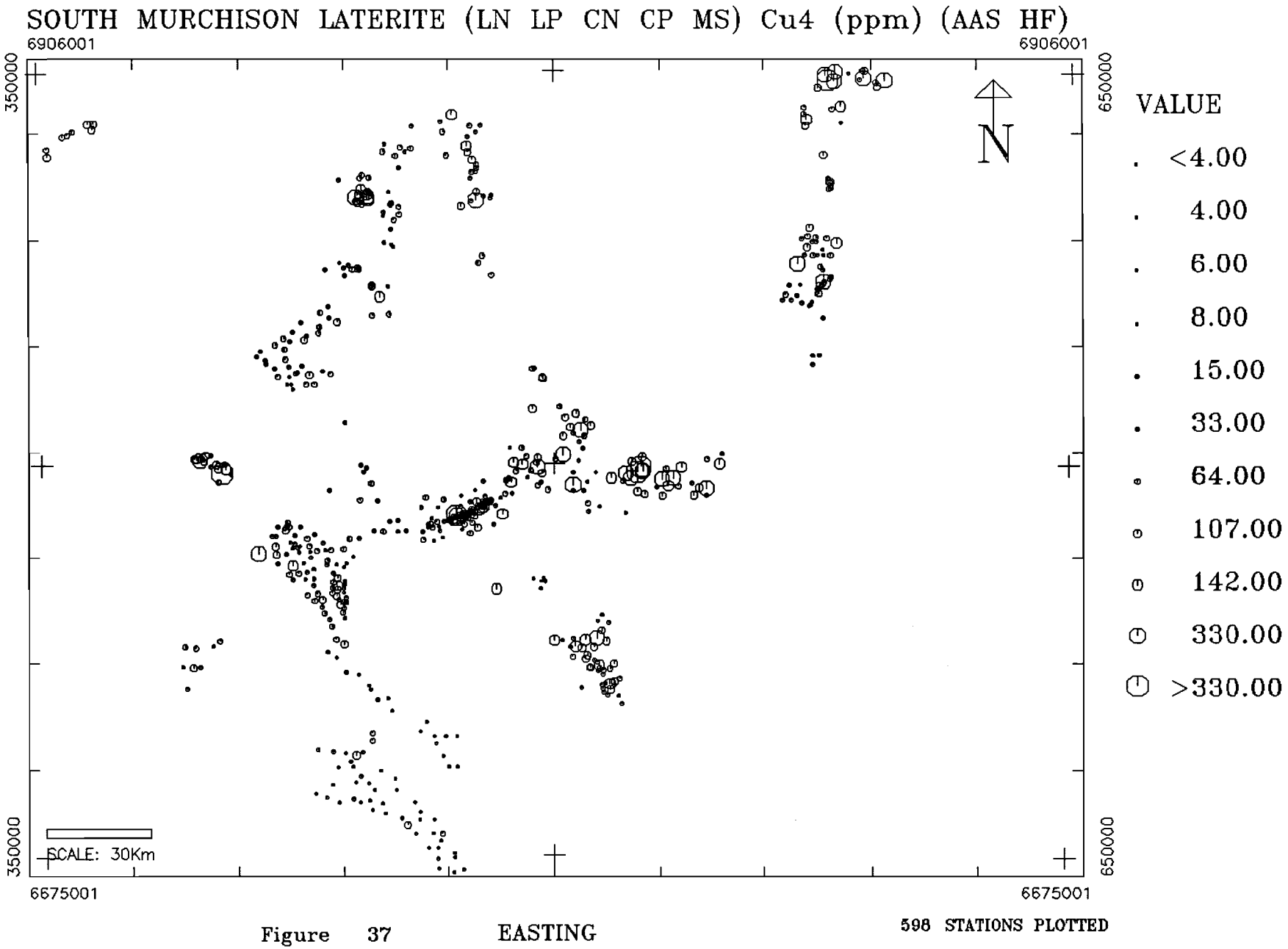
SOUTH MURCHISON LATERITE (LN LP CN CP MS) Cu4 (ppm) (AAS HF)
6906001
6906001
350000
650000
N
VALUE
. <4.00
. 4.00
. 6.00
. 8.00
. 15.00
. 33.00
. 64.00
107.00
142.00
330.00
>330.00
NORTHING
SCALE: 30Km
350000
650000
6675001
6675001
EASTING
598 STATIONS PLOTTED

Figure 37

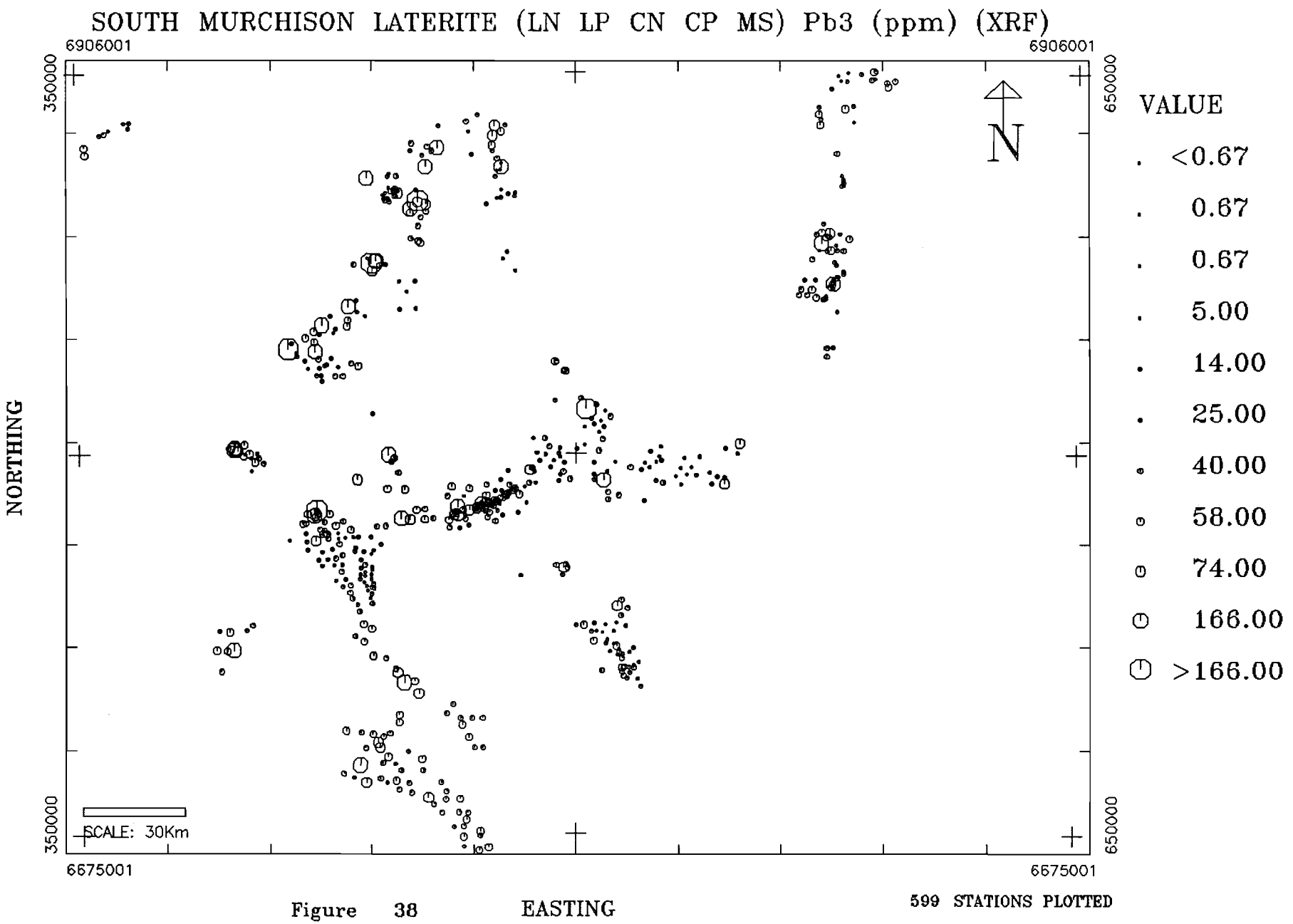
SOUTH MURCHISON LATERITE (LN LP CN CP MS) Pb3 (ppm) (XRF)
6906001
6906001
350000
650000
N
VALUE
. <0.67
. 0.67
. 0.67
. 5.00
. 14.00
. 25.00
. 40.00
. 58.00
. 74.00
. 166.00
. >166.00
NORTHING
SCALE: 30Km
350000
650000
6675001
6675001
EASTING
599 STATIONS PLOTTED

Figure 38

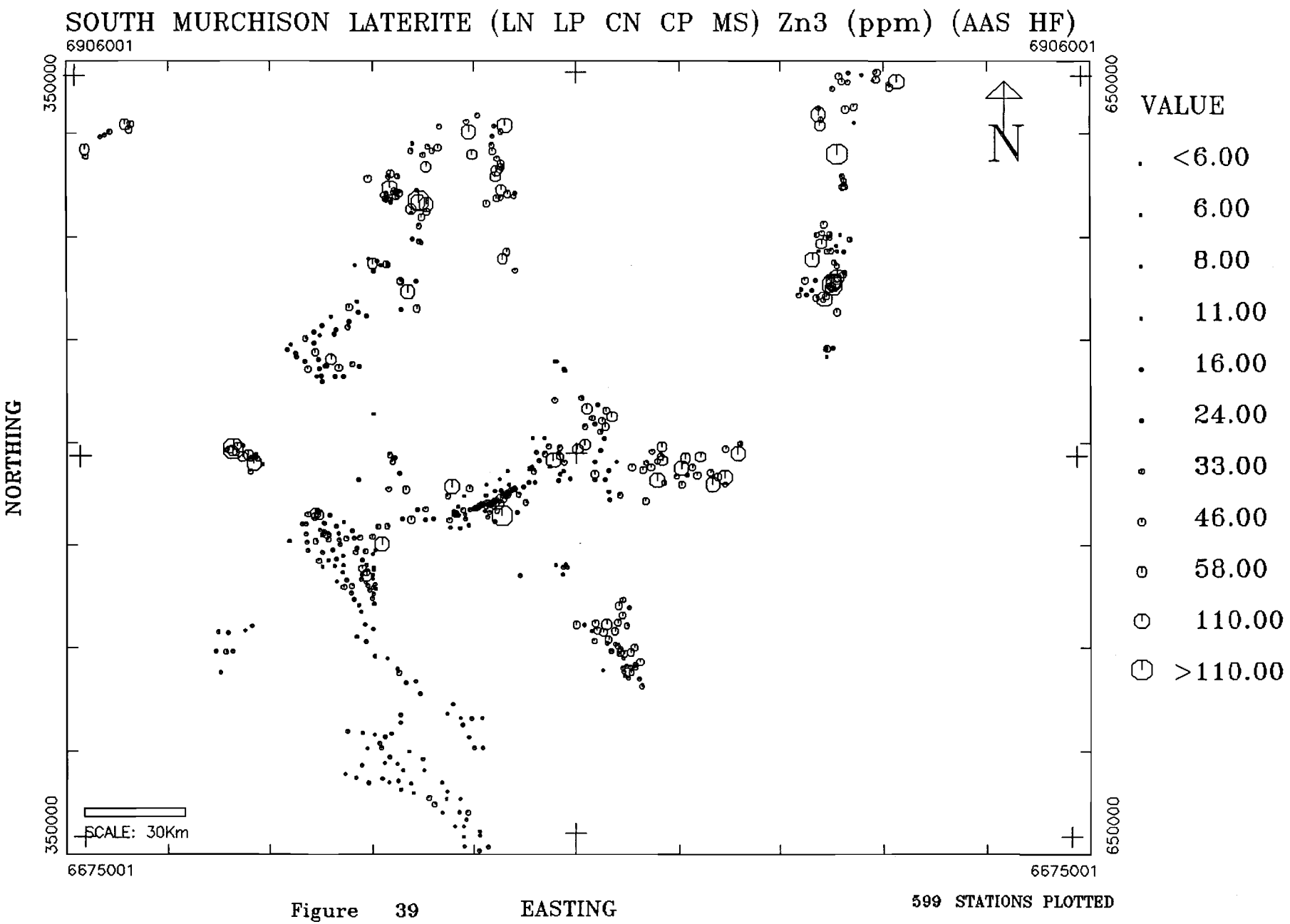
SOUTH MURCHISON LATERITE (LN LP CN CP MS) Zn3 (ppm) (AAS HF)
6906001
6906001
350000
650000
N
VALUE
. <6.00
. 6.00
. 8.00
. 11.00
. 16.00
. 24.00
. 33.00
. 46.00
. 58.00
. 110.00
. >110.00
SCALE: 30Km
350000
650000
6675001
6675001
NORTHING
EASTING
599 STATIONS PLOTTED

Figure 39

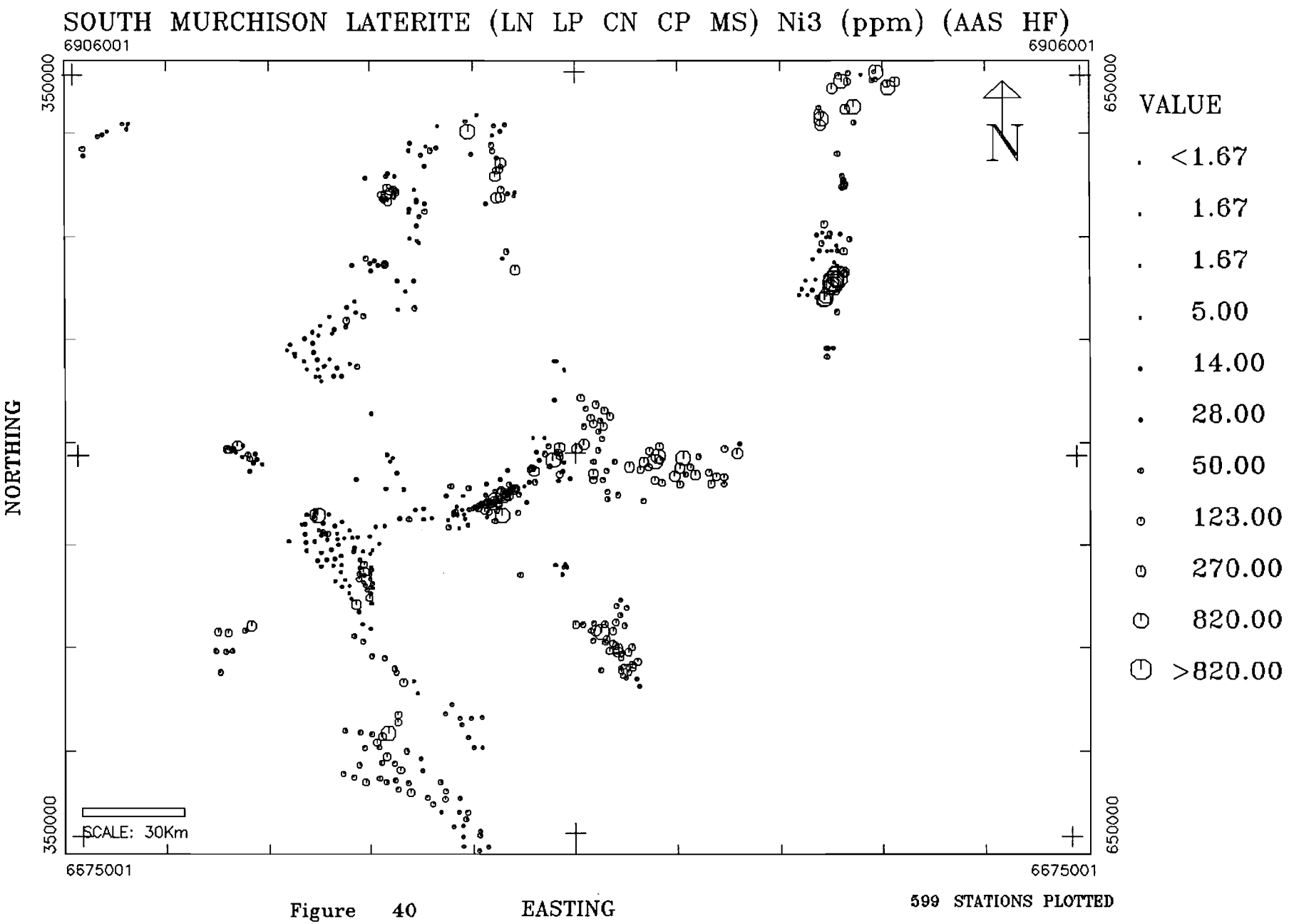
SOUTH MURCHISON LATERITE (LN LP CN CP MS) Ni3 (ppm) (AAS HF)
6906001
6906001
350000
650000
N
VALUE
. <1.67
. 1.67
. 1.67
. 5.00
. 14.00
. 28.00
. 50.00
. 123.00
. 270.00
. 820.00
. >820.00
NORTHING
SCALE: 30Km
350000
650000
6675001
6675001
EASTING
599 STATIONS PLOTTED

Figure 40

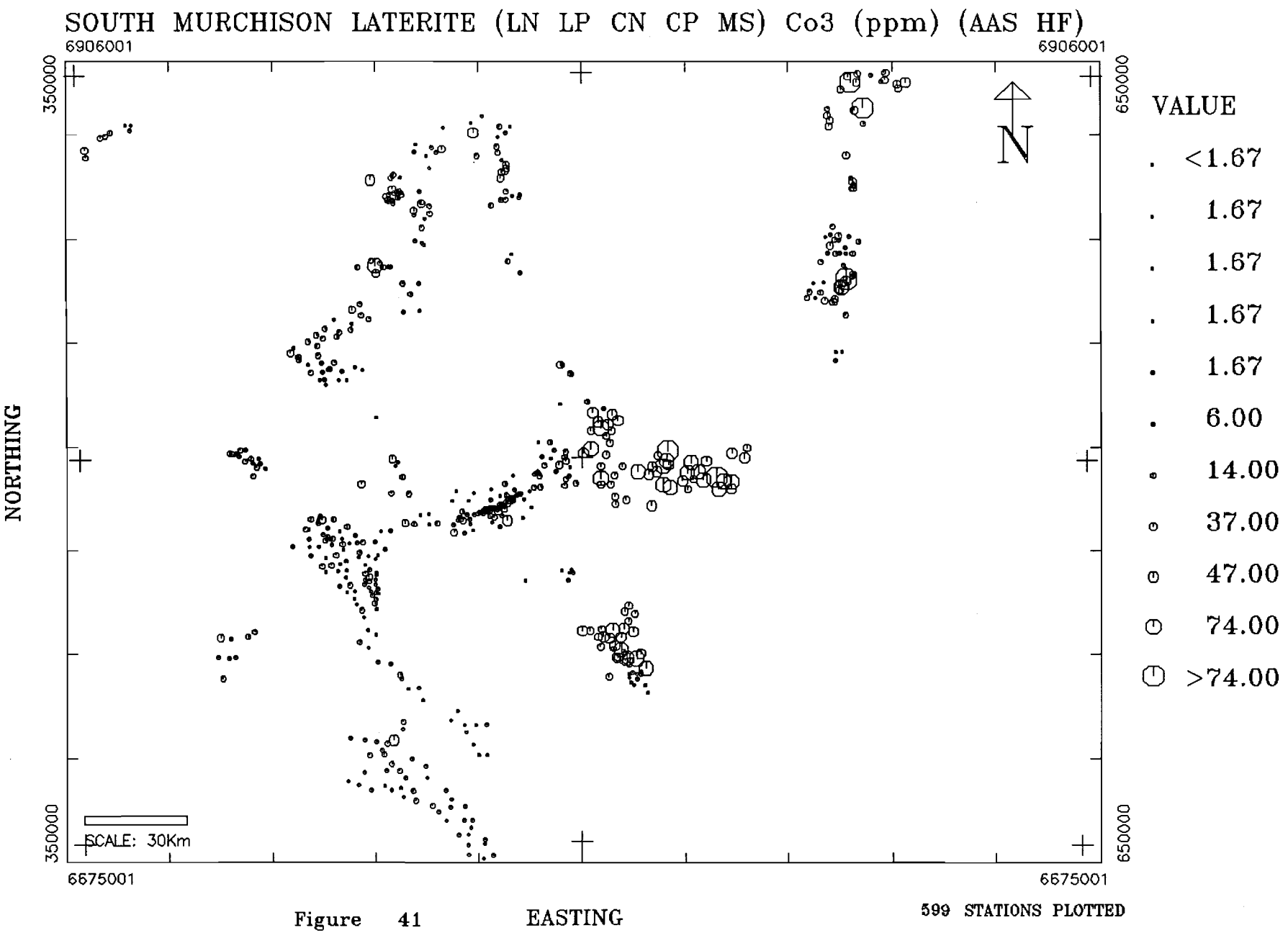
SOUTH MURCHISON LATERITE (LN LP CN CP MS) Co3 (ppm) (AAS HF)
6906001
6906001
350000
650000
N
VALUE
. <1.67
. 1.67
. 1.67
. 1.67
. 1.67
. 6.00
. 14.00
. 37.00
. 47.00
. 74.00
. >74.00
SCALE: 30Km
350000
650000
6675001
6675001
NORTHING
EASTING
599 STATIONS PLOTTED

Figure 41

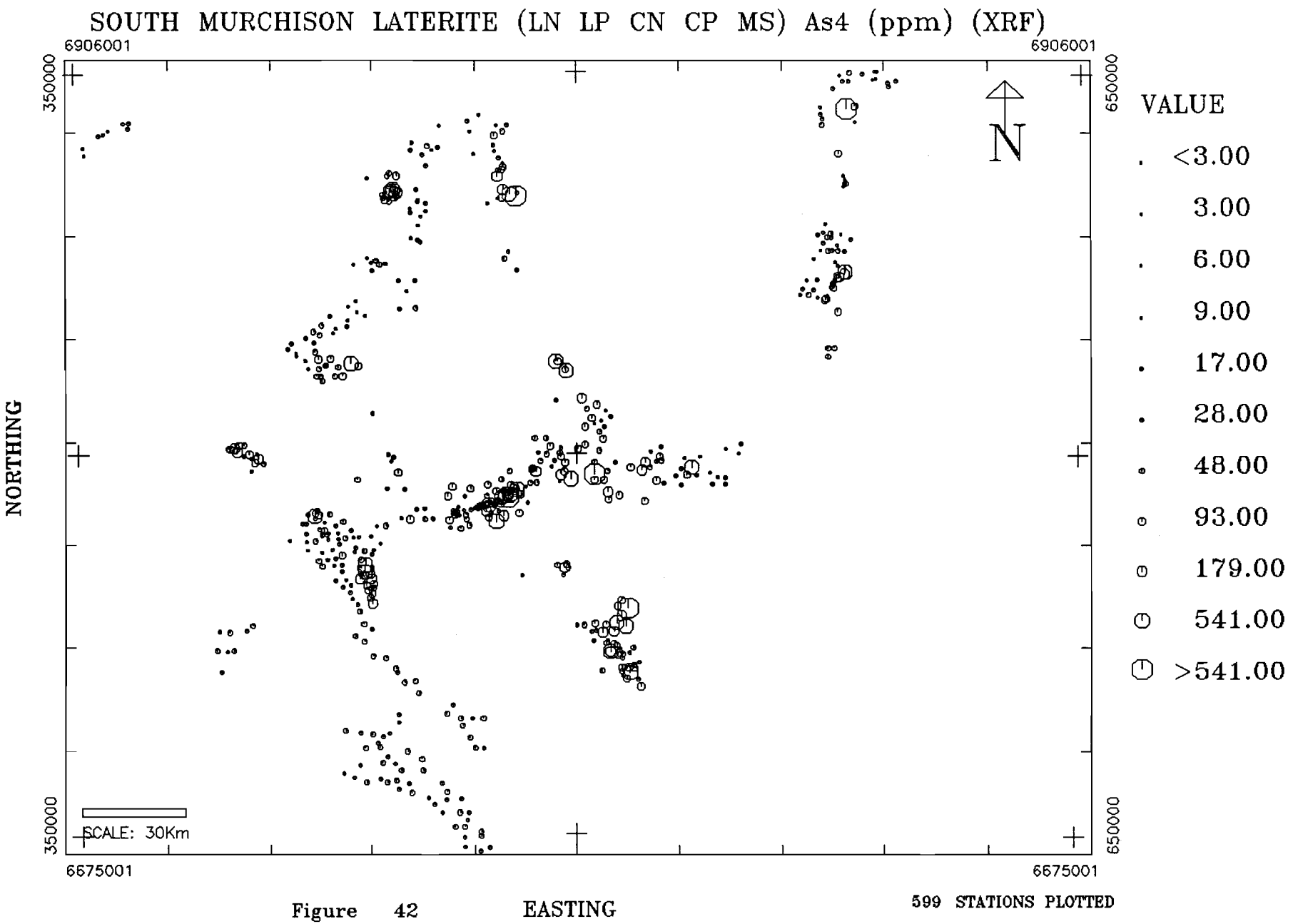
SOUTH MURCHISON LATERITE (LN LP CN CP MS) As4 (ppm) (XRF)
6906001
6906001
350000
650000
N
VALUE
. <3.00
. 3.00
. 6.00
. 9.00
. 17.00
. 28.00
. 48.00
. 93.00
. 179.00
. 541.00
. >541.00
SCALE: 30Km
350000
650000
6675001
6675001
NORTHING
EASTING
599 STATIONS PLOTTED

Figure 42

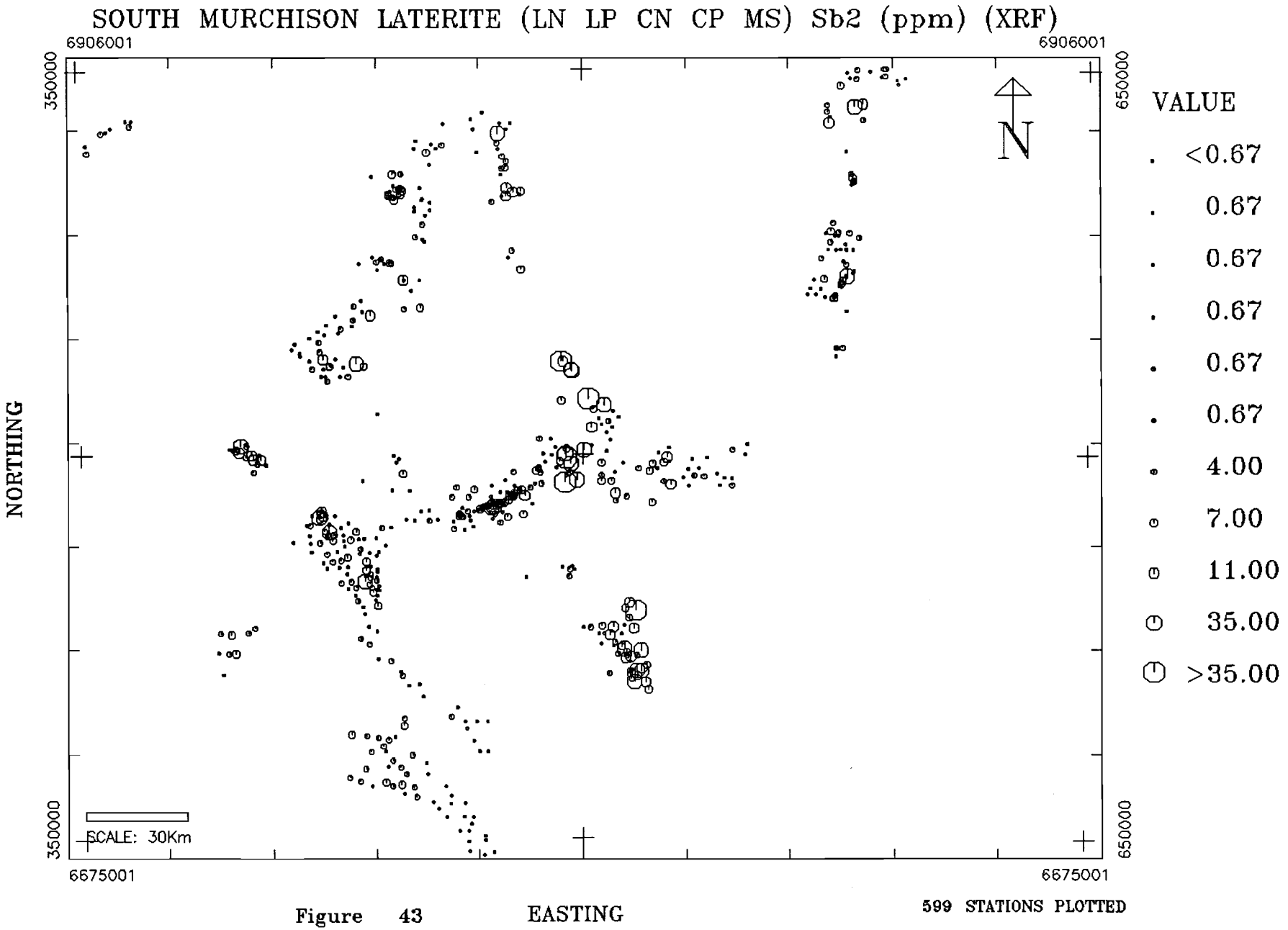
SOUTH MURCHISON LATERITE (LN LP CN CP MS) Sb2 (ppm) (XRF)
6906001
6906001
350000
650000
N
VALUE
. <0.67
. 0.67
. 0.67
. 0.67
. 0.67
. 0.67
. 4.00
7.00
11.00
35.00
>35.00
NORTHING
SCALE: 30Km
350000
650000
6675001
6675001
EASTING
599 STATIONS PLOTTED

Figure 43

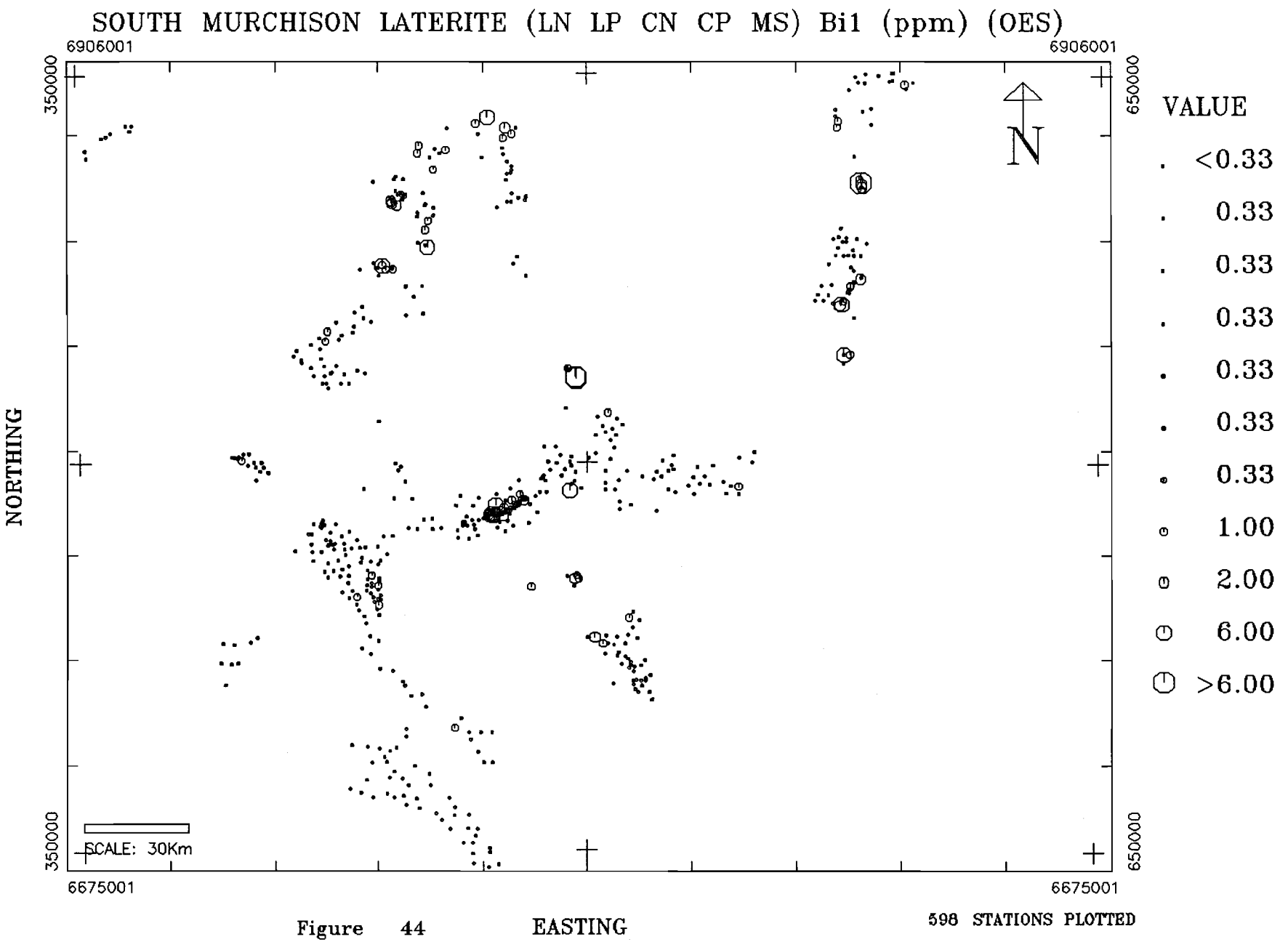
SOUTH MURCHISON LATERITE (LN LP CN CP MS) Bi1 (ppm) (OES)
6906001
6906001
350000
650000
N
VALUE
. <0.33
. 0.33
. 0.33
. 0.33
. 0.33
. 0.33
. 0.33
1.00
2.00
6.00
>6.00
NORTHING
SCALE: 30Km
350000
650000
6675001
6675001
EASTING
598 STATIONS PLOTTED

Figure 44

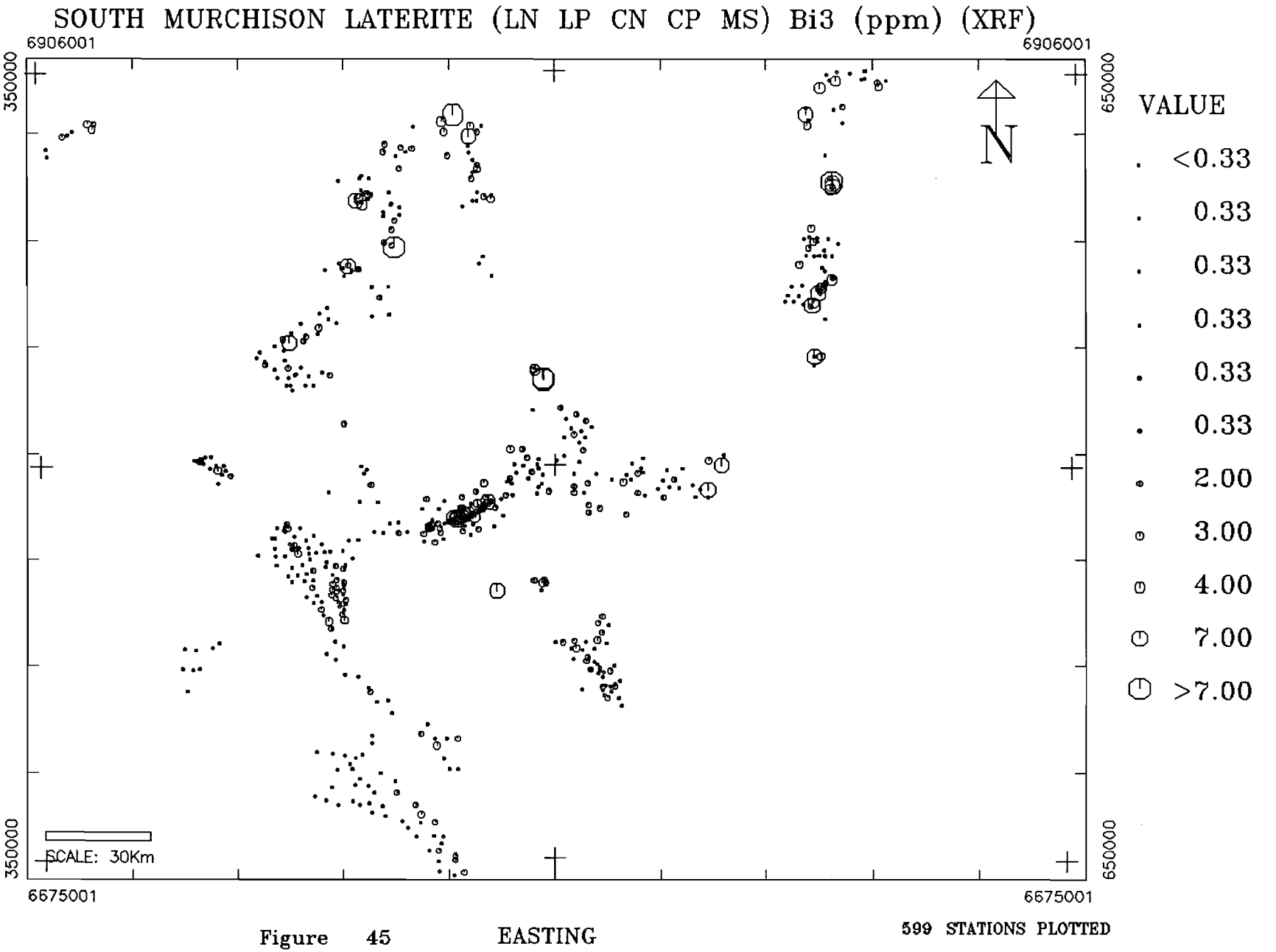
SOUTH MURCHISON LATERITE (LN LP CN CP MS) Bi3 (ppm) (XRF)
6906001
6906001
350000
650000
N
VALUE
. <0.33
. 0.33
. 0.33
. 0.33
. 0.33
. 0.33
. 2.00
. 3.00
. 4.00
. 7.00
. >7.00
NORTHING
SCALE: 30Km
350000
650000
6675001
6675001
EASTING
599 STATIONS PLOTTED

Figure 45

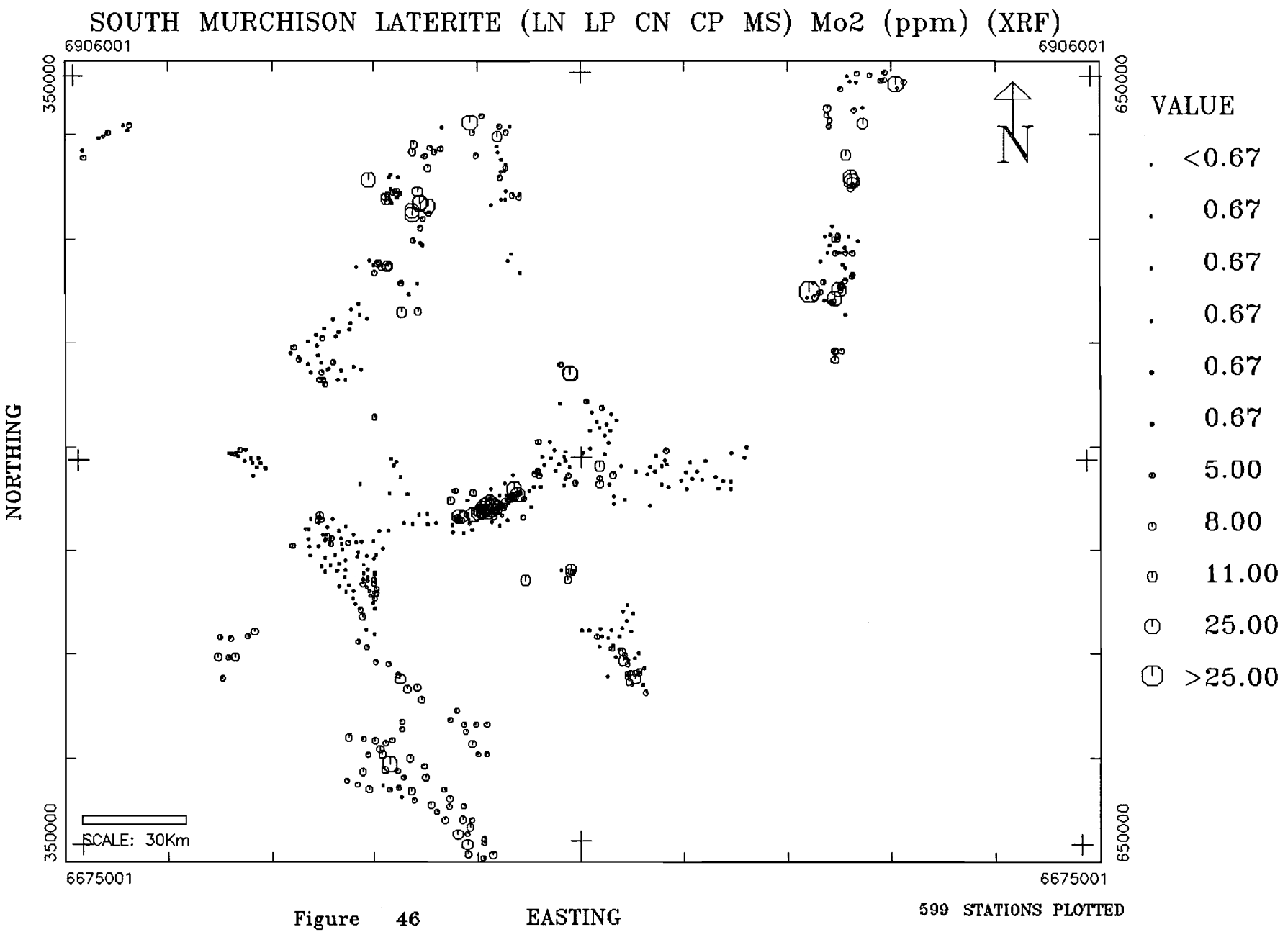
SOUTH MURCHISON LATERITE (LN LP CN CP MS) Mo2 (ppm) (XRF)
6906001
6906001
350000
650000
N
VALUE
. <0.67
. 0.67
. 0.67
. 0.67
. 0.67
. 0.67
. 5.00
8.00
11.00
25.00
>25.00
NORTHING
SCALE: 30Km
350000
650000
6675001
6675001
EASTING
599 STATIONS PLOTTED

Figure 46

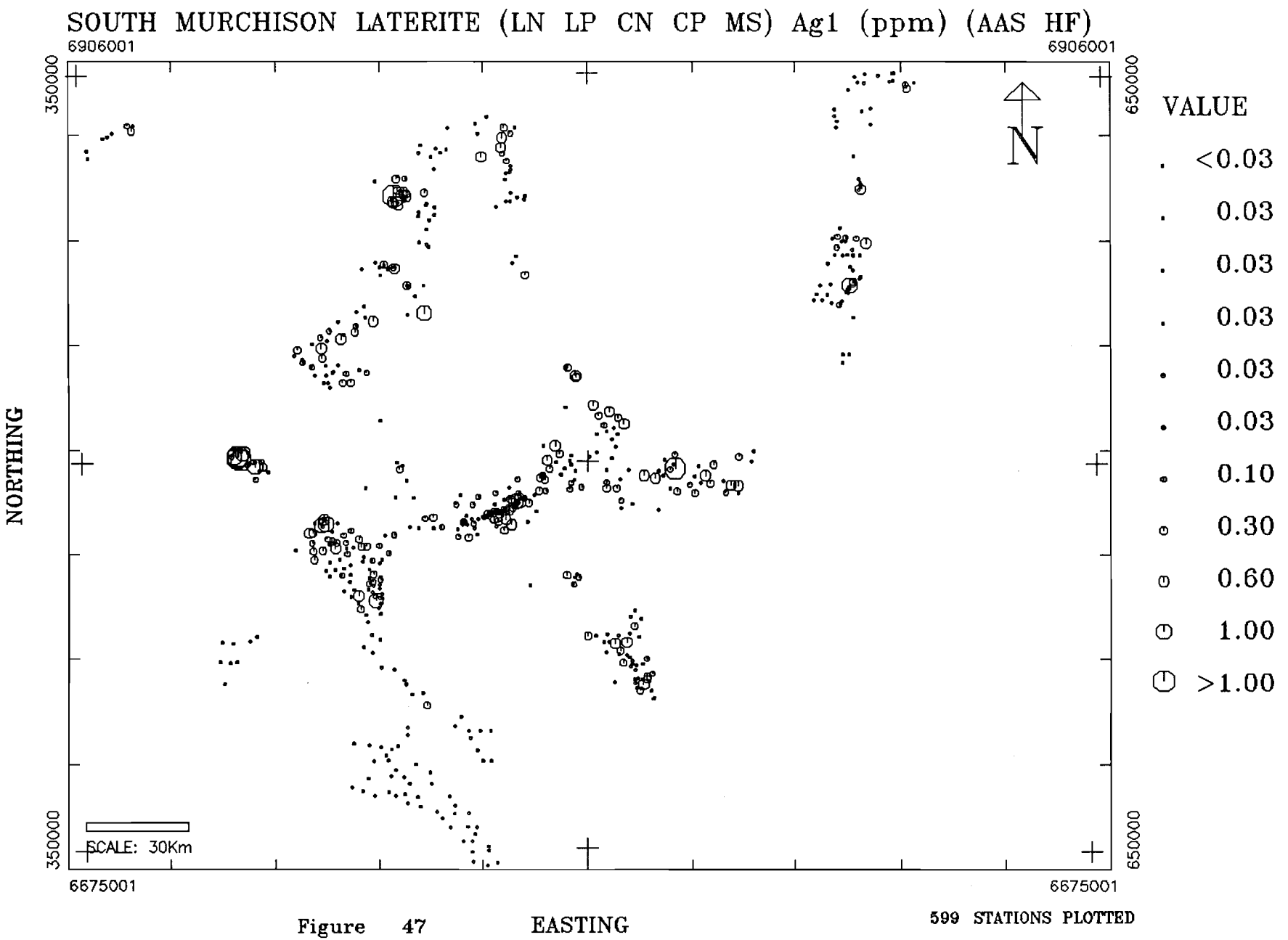
SOUTH MURCHISON LATERITE (LN LP CN CP MS) Ag1 (ppm) (AAS HF)
6906001
6906001
350000
650000
N
VALUE
. <0.03
. 0.03
. 0.03
. 0.03
. 0.03
. 0.03
. 0.10
0.30
0.60
1.00
>1.00
NORTHING
SCALE: 30Km
350000
650000
6675001
6675001
EASTING
599 STATIONS PLOTTED

Figure 47

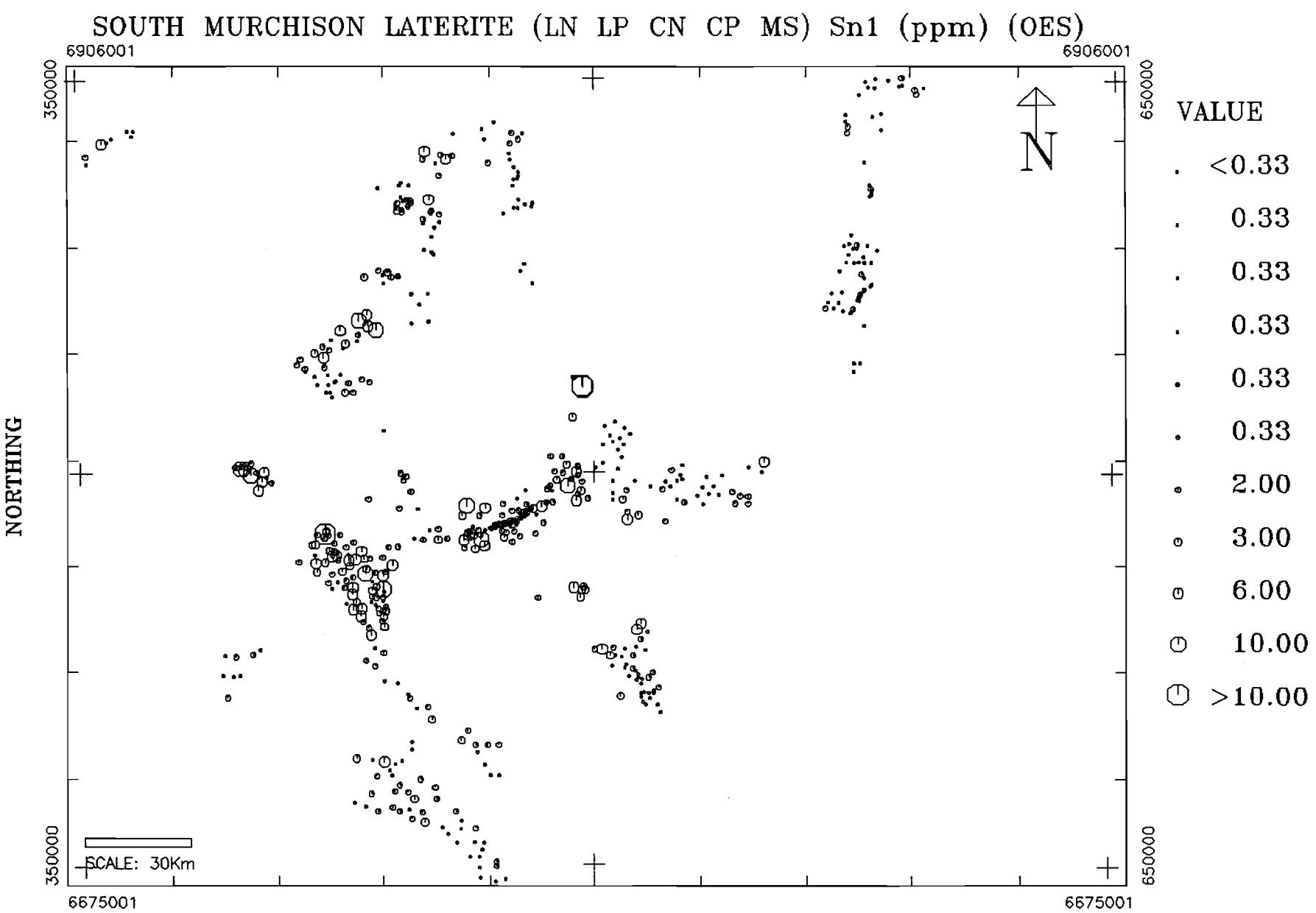
SOUTH MURCHISON LATERITE (LN LP CN CP MS) Sn1 (ppm) (OES)
6906001
6906001
350000
650000
N
VALUE
. <0.33
. 0.33
. 0.33
. 0.33
. 0.33
. 0.33
. 2.00
. 3.00
. 6.00
. 10.00
. >10.00
NORTHING
SCALE: 30Km
350000
650000
6675001
6675001
EASTING
598 STATIONS PLOTTED

Figure 48

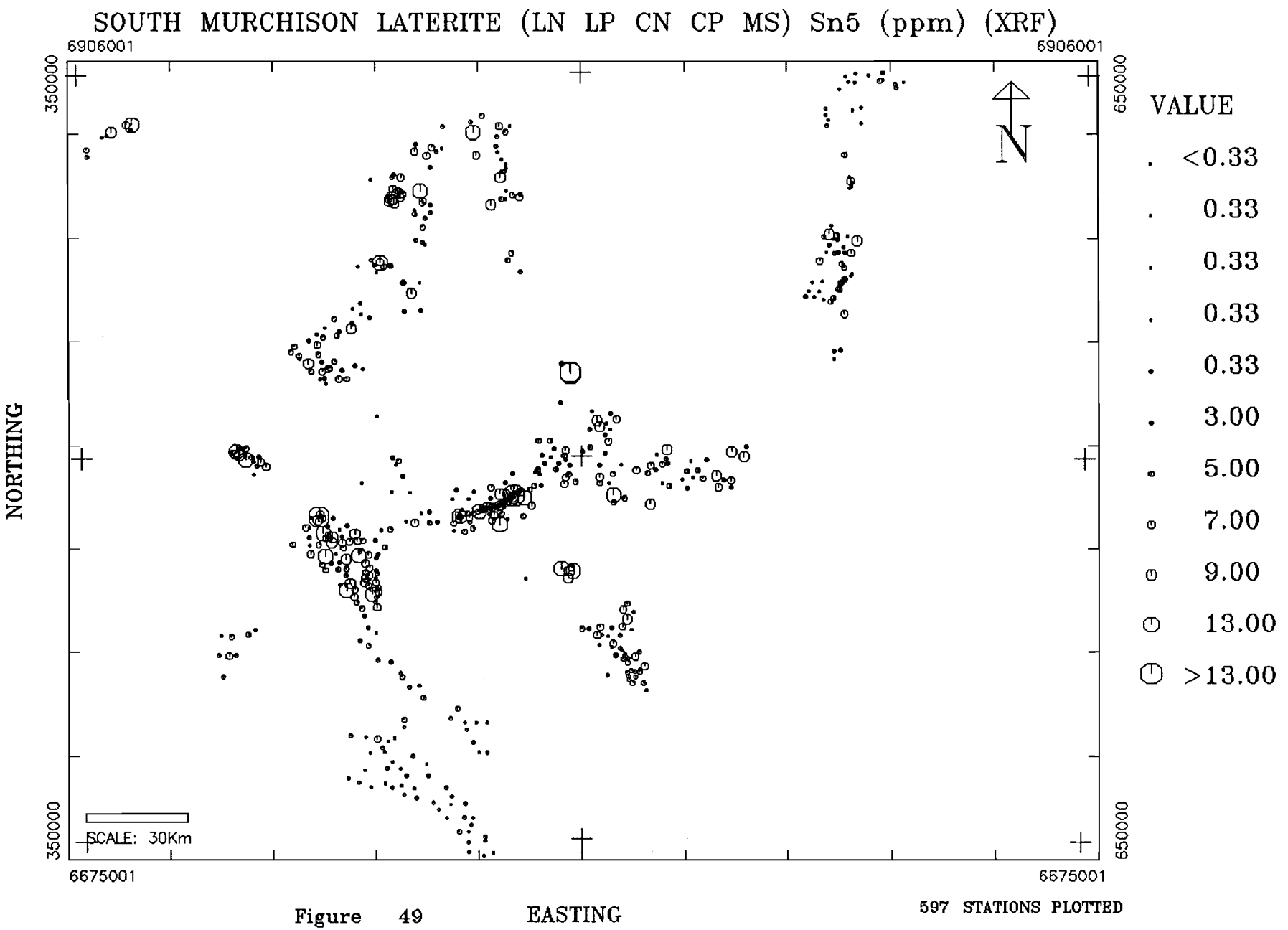
SOUTH MURCHISON LATERITE (LN LP CN CP MS) Sn5 (ppm) (XRF)
6906001
6906001
350000
650000
N
VALUE
. <0.33
. 0.33
. 0.33
. 0.33
. 0.33
. 3.00
. 5.00
. 7.00
. 9.00
. 13.00
. >13.00
NORTHING
SCALE: 30Km
350000
650000
6675001
6675001
EASTING
597 STATIONS PLOTTED

Figure 49

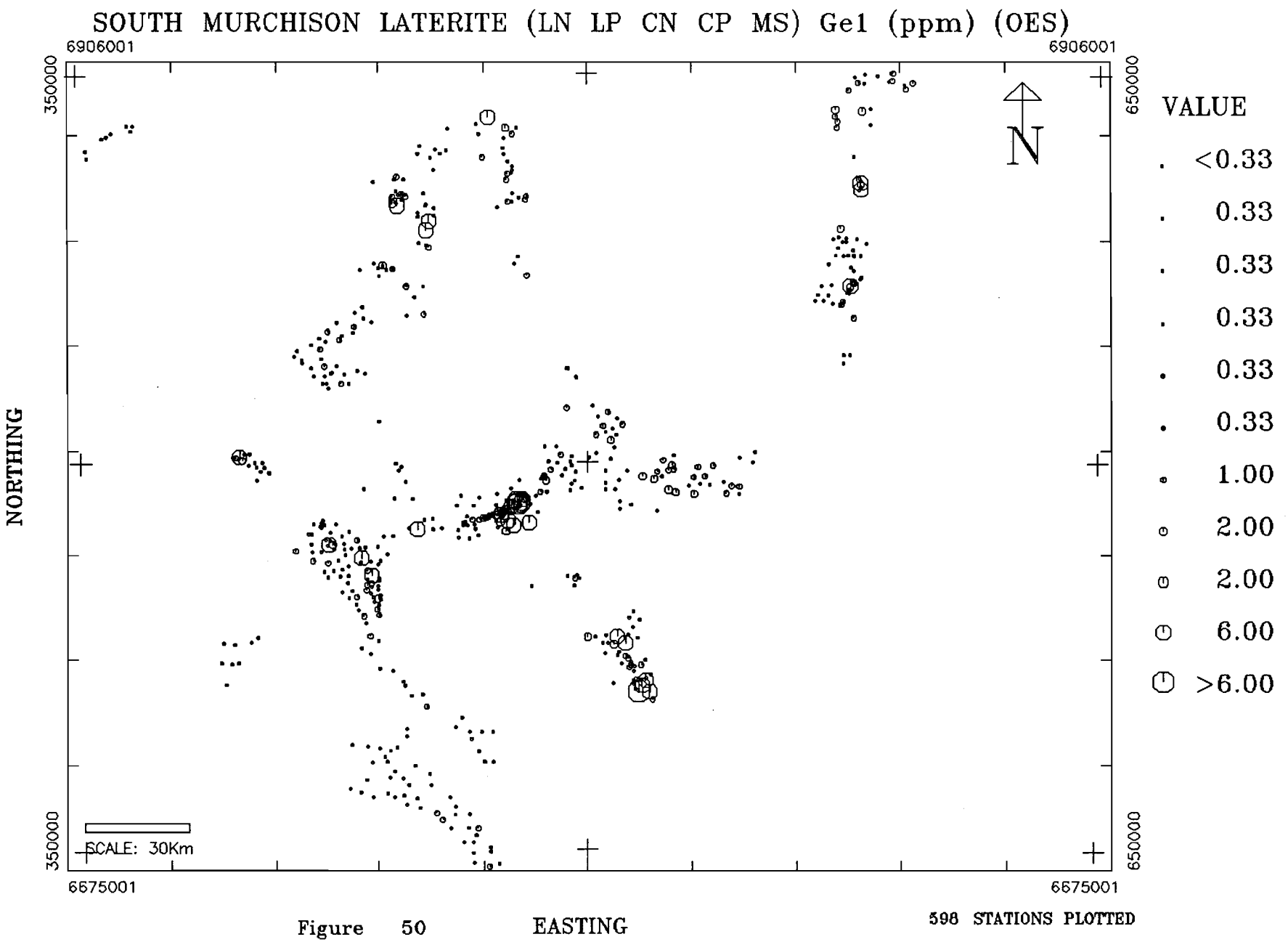
SOUTH MURCHISON LATERITE (LN LP CN CP MS) Ge1 (ppm) (OES)
6906001
6906001
350000
650000
N
VALUE
. <0.33
. 0.33
. 0.33
. 0.33
. 0.33
. 0.33
. 1.00
. 2.00
. 2.00
. 6.00
. >6.00
SCALE: 30Km
350000
650000
6675001
6675001
NORTHING
EASTING
598 STATIONS PLOTTED

Figure 50

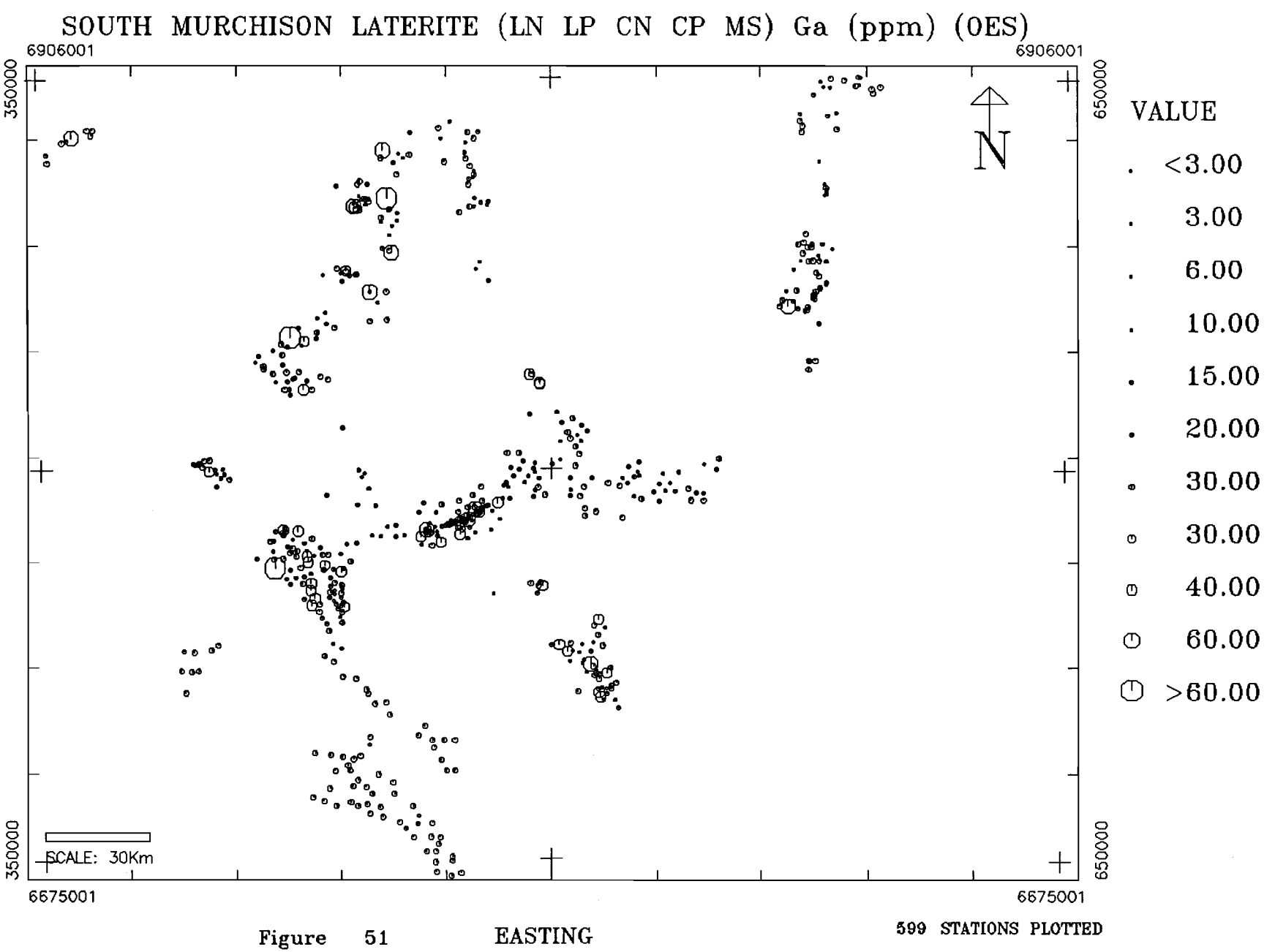
SOUTH MURCHISON LATERITE (LN LP CN CP MS) Ga (ppm) (OES)
6906001
6906001
350000
650000
N
VALUE
. <3.00
. 3.00
. 6.00
. 10.00
. 15.00
. 20.00
. 30.00
. 30.00
. 40.00
. 60.00
. >60.00
NORTHING
SCALE: 30Km
350000
650000
6675001
6675001
EASTING
599 STATIONS PLOTTED

Figure 51

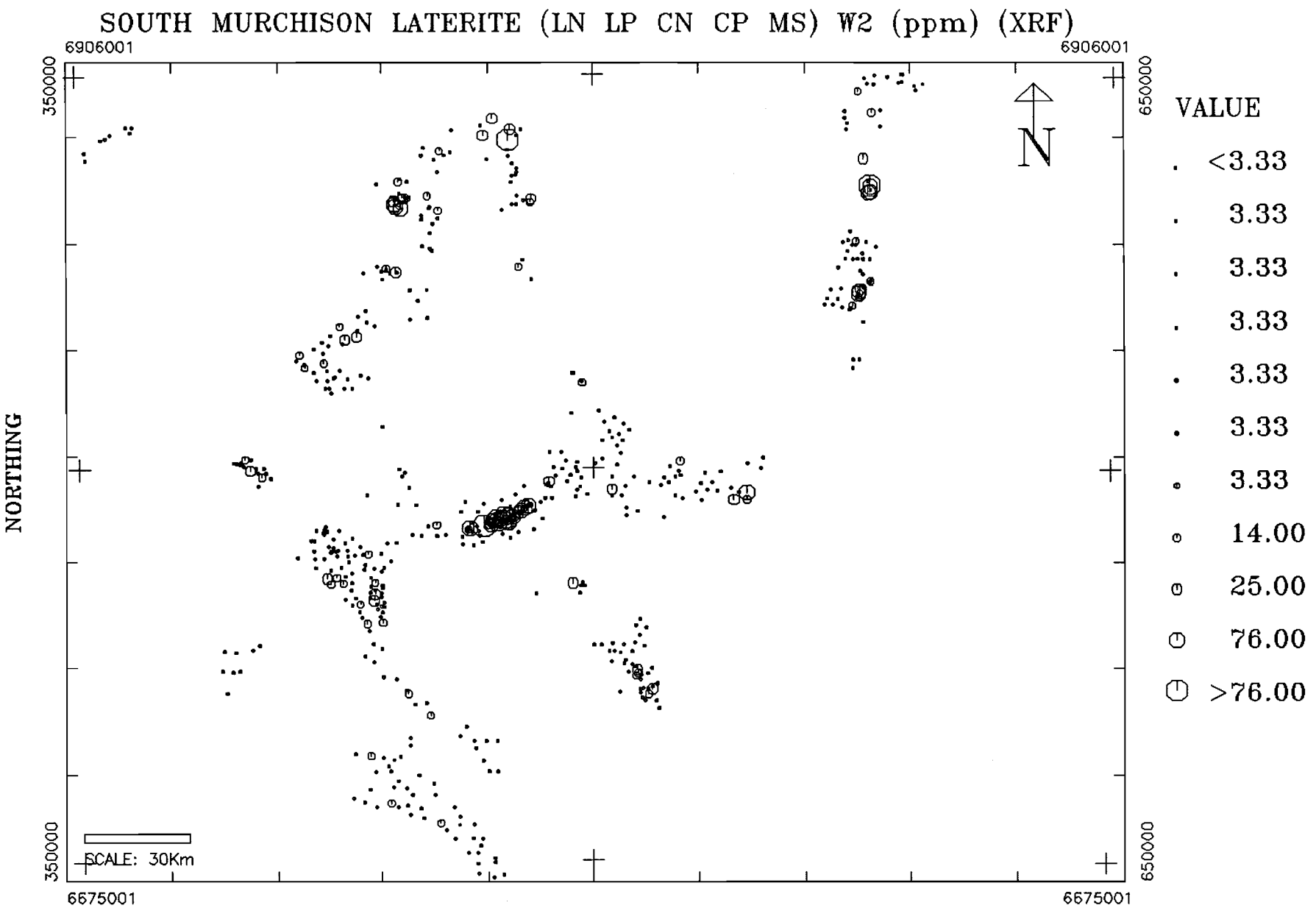
SOUTH MURCHISON LATERITE (LN LP CN CP MS) W2 (ppm) (XRF)
6906001
6906001
350000
650000
N
VALUE
. <3.33
. 3.33
. 3.33
. 3.33
. 3.33
. 3.33
. 3.33
o 14.00
o 25.00
O 76.00
O >76.00
NORTHING
SCALE: 30Km
350000
650000
6675001
6675001
EASTING
599 STATIONS PLOTTED

Figure 52

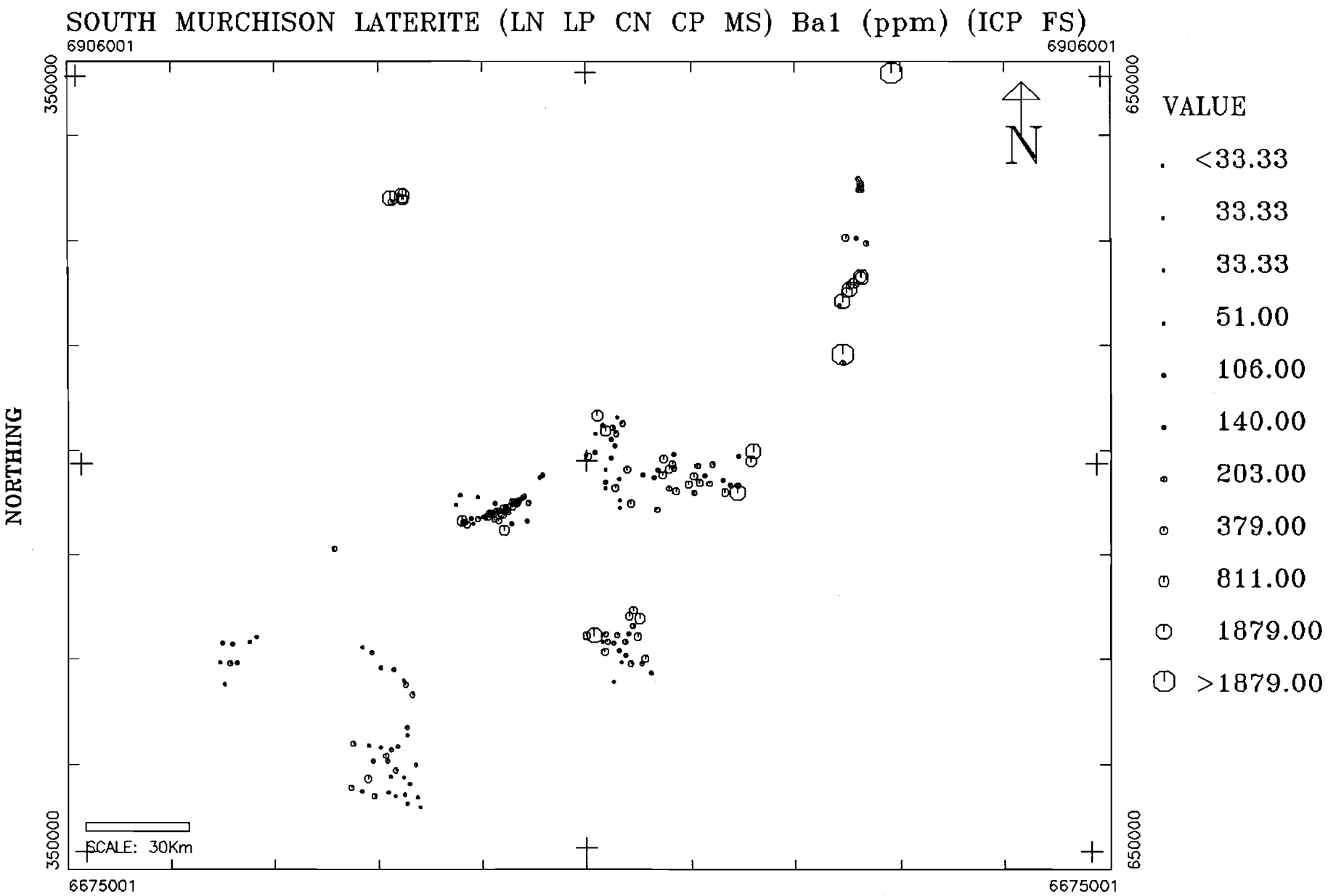
SOUTH MURCHISON LATERITE (LN LP CN CP MS) Ba1 (ppm) (ICP FS)
6906001
6906001
350000
650000
N
VALUE
. <33.33
. 33.33
. 33.33
. 51.00
. 106.00
. 140.00
. 203.00
. 379.00
. 811.00
. 1879.00
. >1879.00
NORTHING
SCALE: 30Km
350000
650000
6675001
6675001
EASTING
213 STATIONS PLOTTED

Figure 53

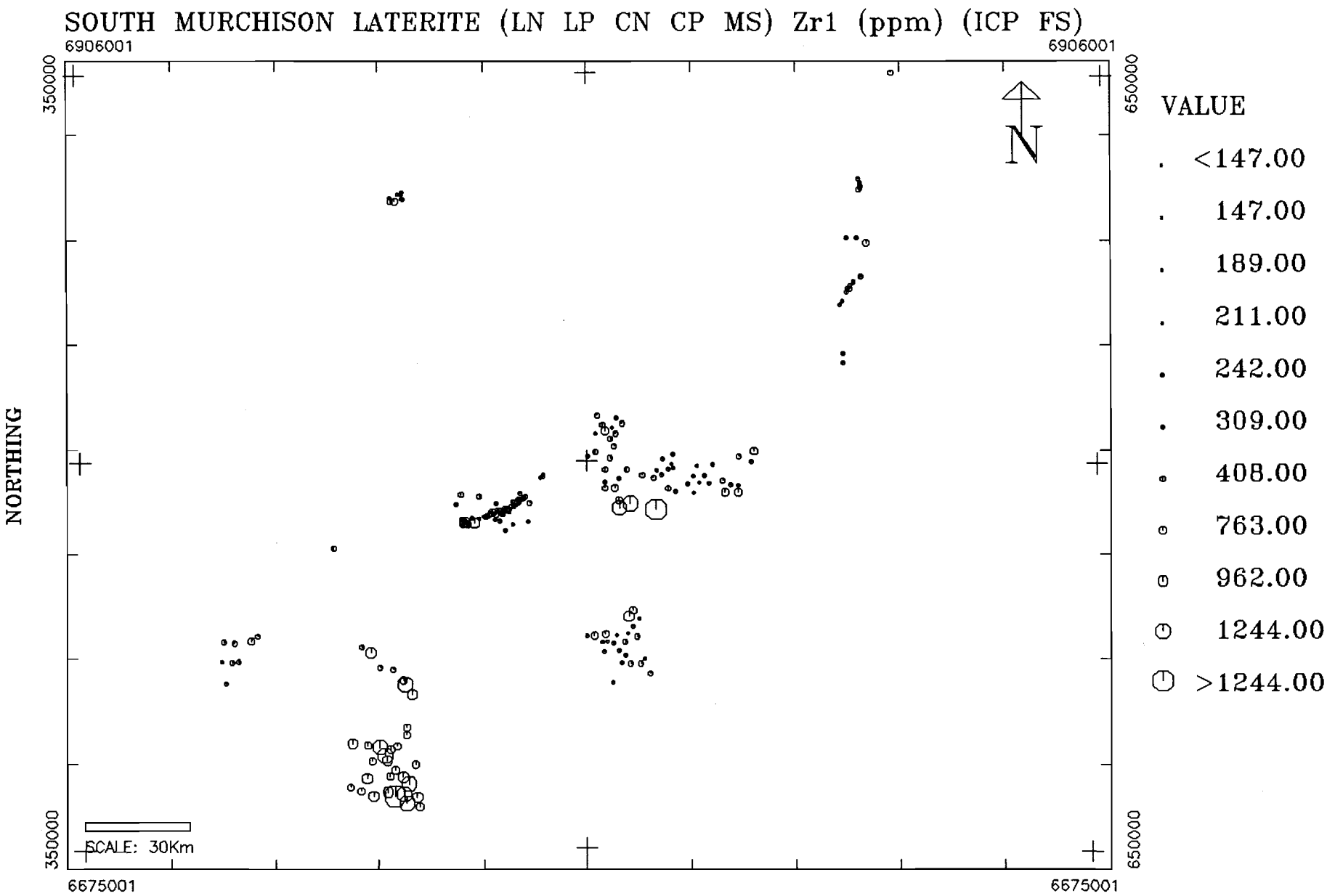
SOUTH MURCHISON LATERITE (LN LP CN CP MS) Zr1 (ppm) (ICP FS)
6906001
6906001
350000
650000
N
VALUE
. <147.00
. 147.00
. 189.00
. 211.00
. 242.00
. 309.00
. 408.00
763.00
962.00
1244.00
>1244.00
NORTHING
SCALE: 30Km
350000
650000
6675001
6675001
EASTING
219 STATIONS PLOTTED

Figure 54

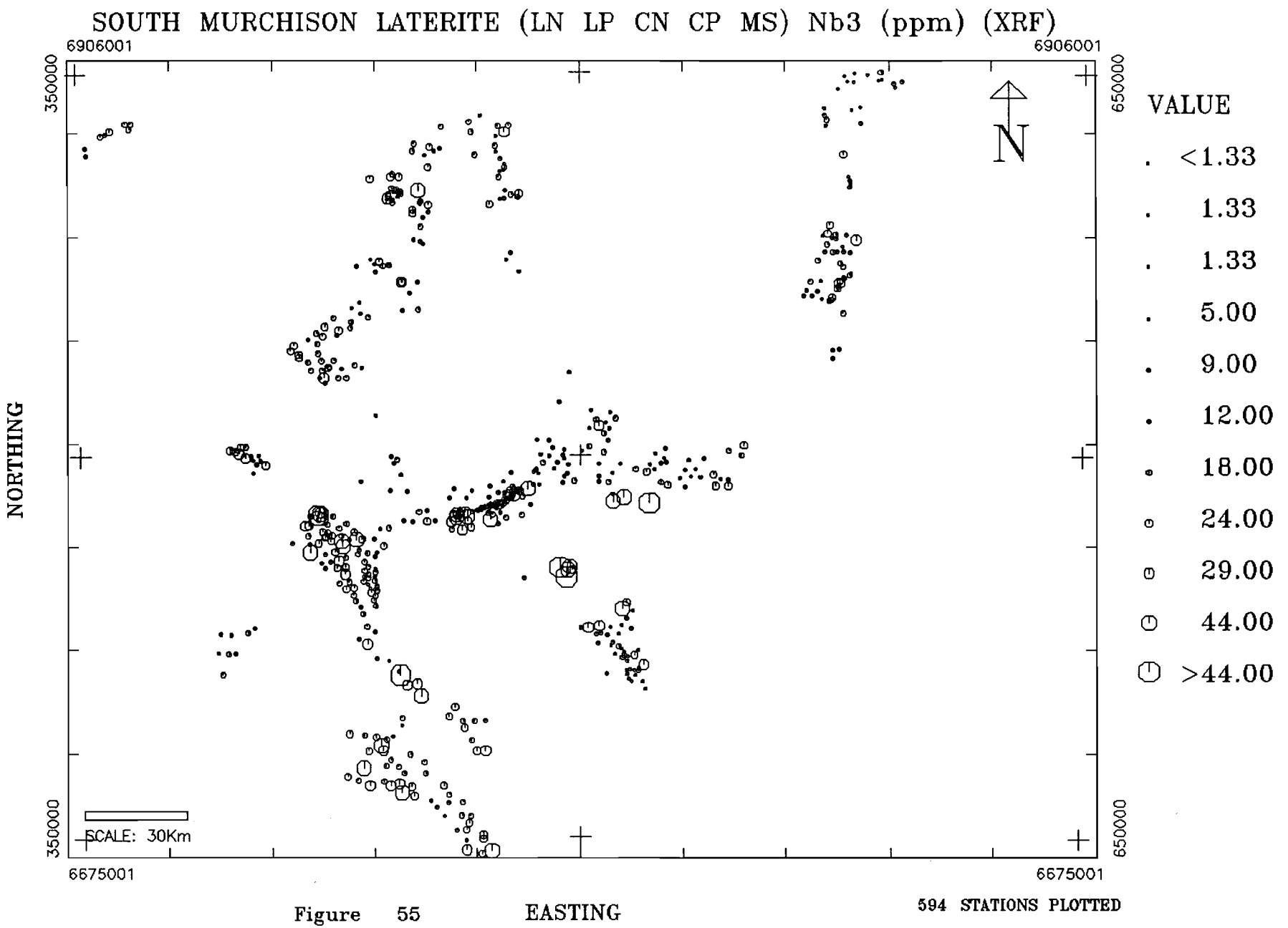
SOUTH MURCHISON LATERITE (LN LP CN CP MS) Nb3 (ppm) (XRF)
6906001
6906001
350000
650000
N
VALUE
. <1.33
. 1.33
. 1.33
. 5.00
. 9.00
. 12.00
. 18.00
. 24.00
. 29.00
. 44.00
. >44.00
NORTHING
SCALE: 30Km
350000
650000
6675001
6675001
EASTING
594 STATIONS PLOTTED

Figure 55

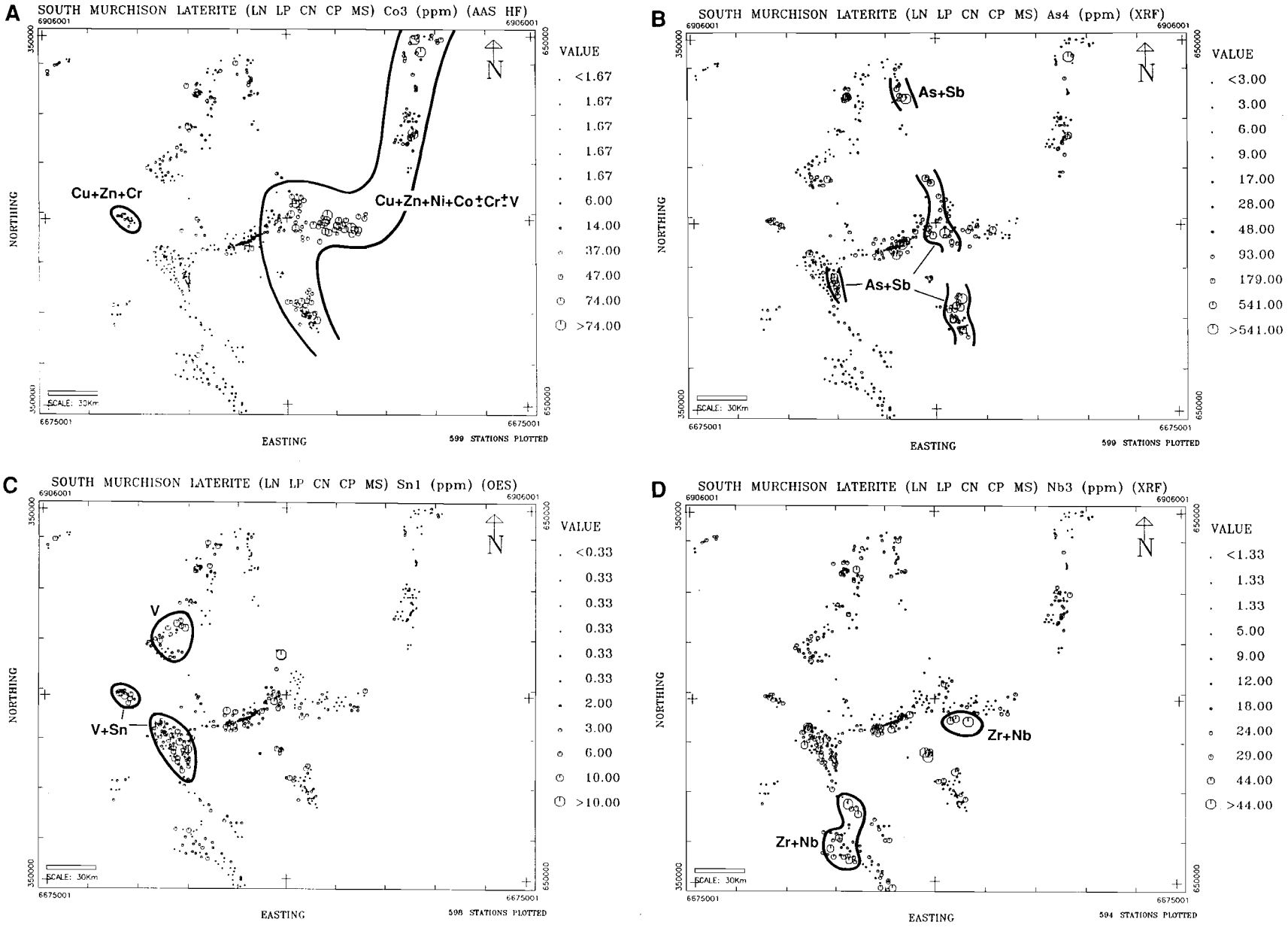
A
SOUTH MURCHISON LATERITE (LN LP CN CP MS) Co3 (ppm) (AAS HF)
6906001
350000
650000
6675001
N
Cu+Zn+Cr
Cu+Zn+Ni+Co±Cr±V
SCALE: 30Km
NORTHING
EASTING
599 STATIONS PLOTTED
VALUE
<1.67
1.67
1.67
1.67
1.67
6.00
14.00
37.00
47.00
74.00
>74.00
B
SOUTH MURCHISON LATERITE (LN LP CN CP MS) As4 (ppm) (XRF)
As+Sb
As+Sb
599 STATIONS PLOTTED
VALUE
<3.00
3.00
6.00
9.00
17.00
28.00
48.00
93.00
179.00
541.00
>541.00
C
SOUTH MURCHISON LATERITE (LN LP CN CP MS) Sn1 (ppm) (OES)
V
V+Sn
598 STATIONS PLOTTED
VALUE
<0.33
0.33
0.33
0.33
0.33
0.33
2.00
3.00
6.00
10.00
>10.00
D
SOUTH MURCHISON LATERITE (LN LP CN CP MS) Nb3 (ppm) (XRF)
Zr+Nb
Zr+Nb
594 STATIONS PLOTTED
VALUE
<1.33
1.33
1.33
5.00
9.00
12.00
18.00
24.00
29.00
44.00
>44.00

Figure 56

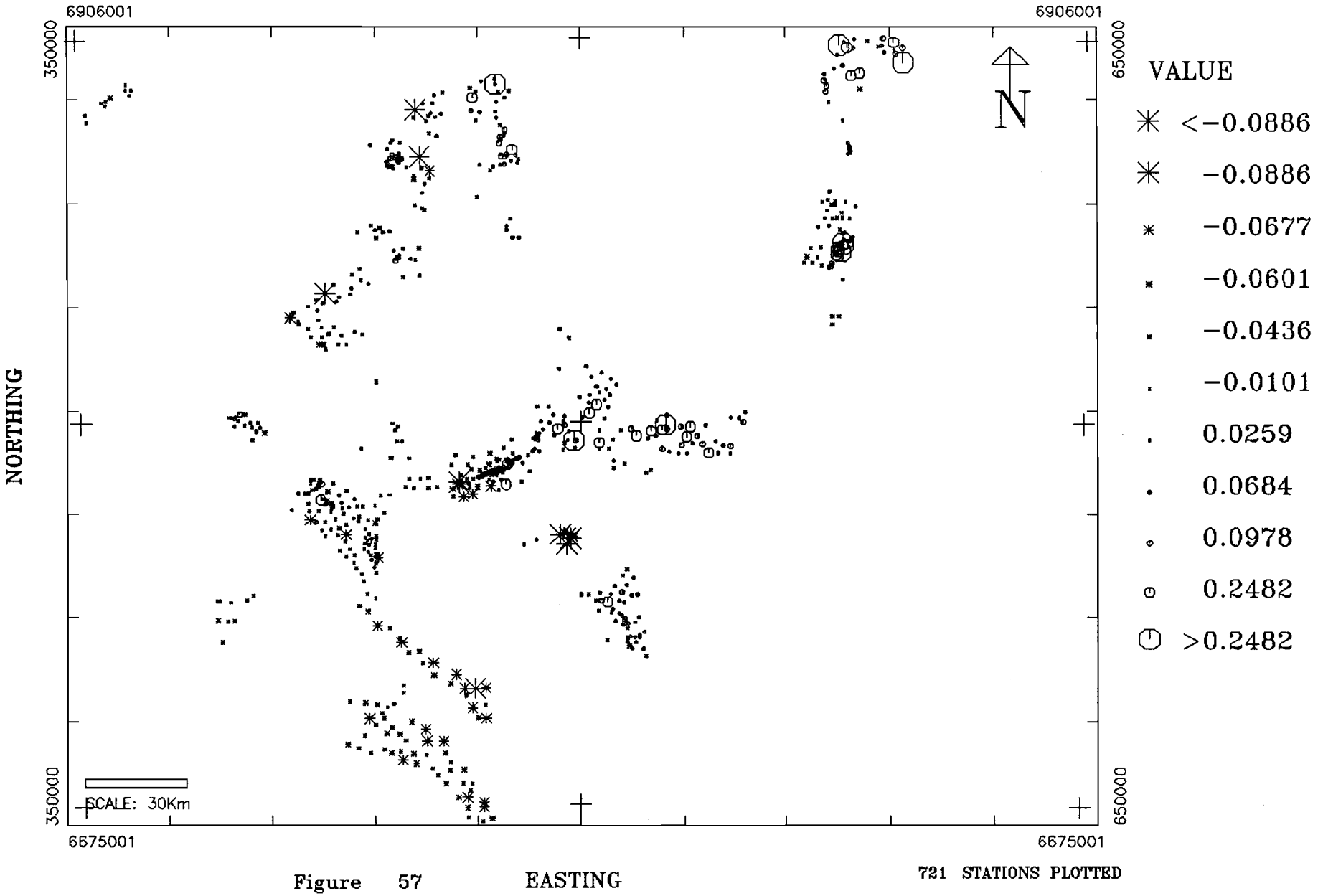
SOUTH MURCHISON LATERITE PRINCIPAL COMPONENT 1
6906001
6906001
350000
650000
N
VALUE
<-0.0886
-0.0886
-0.0677
-0.0601
-0.0436
-0.0101
0.0259
0.0684
0.0978
0.2482
>0.2482
NORTHING
SCALE: 30Km
350000
650000
6675001
6675001
EASTING
721 STATIONS PLOTTED

Figure 57

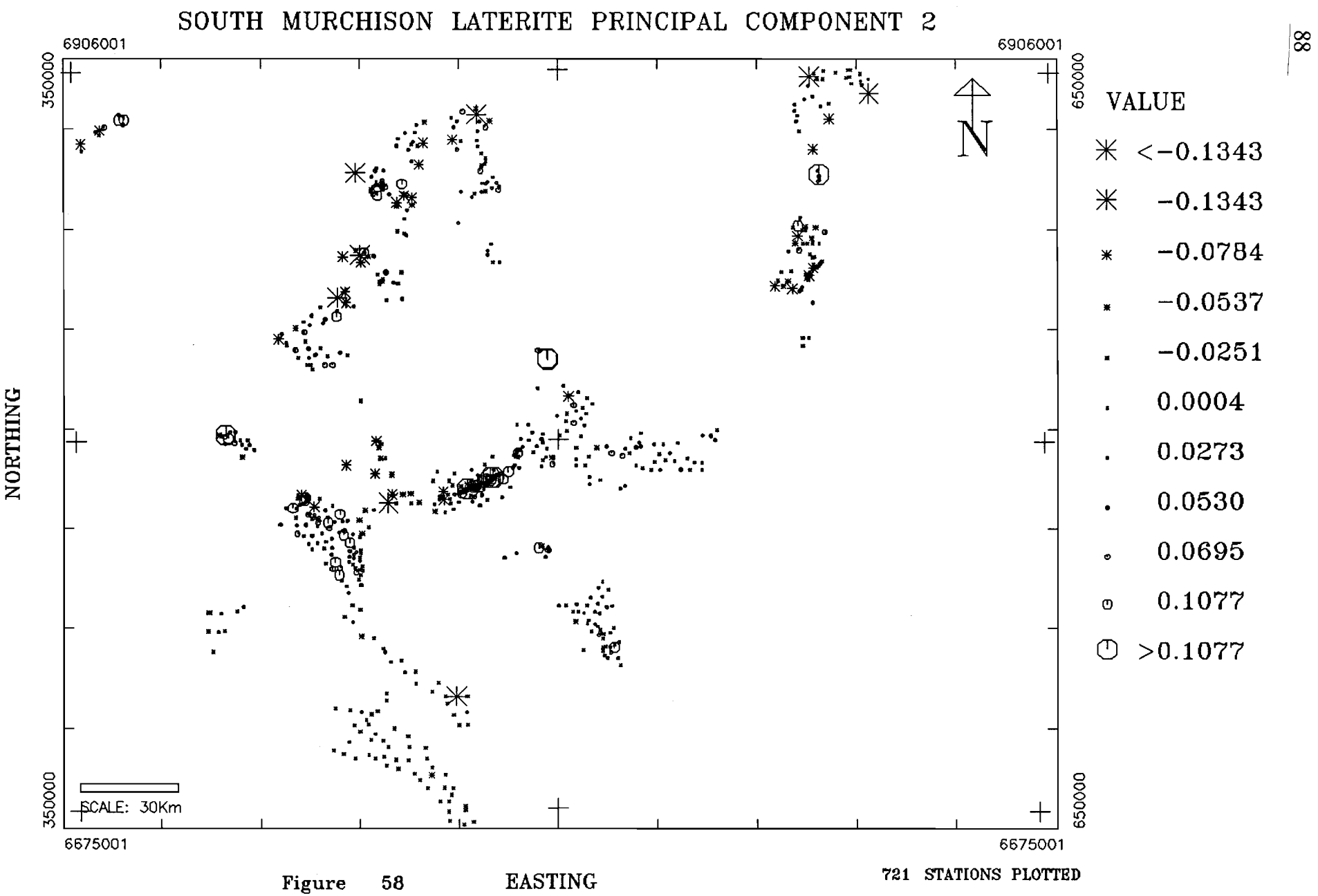
SOUTH MURCHISON LATERITE PRINCIPAL COMPONENT 2
6906001
6906001
350000
650000
N
VALUE
<-0.1343
-0.1343
-0.0784
-0.0537
-0.0251
0.0004
0.0273
0.0530
0.0695
0.1077
>0.1077
NORTHING
SCALE: 30Km
350000
650000
6675001
6675001
EASTING
721 STATIONS PLOTTED

Figure 58

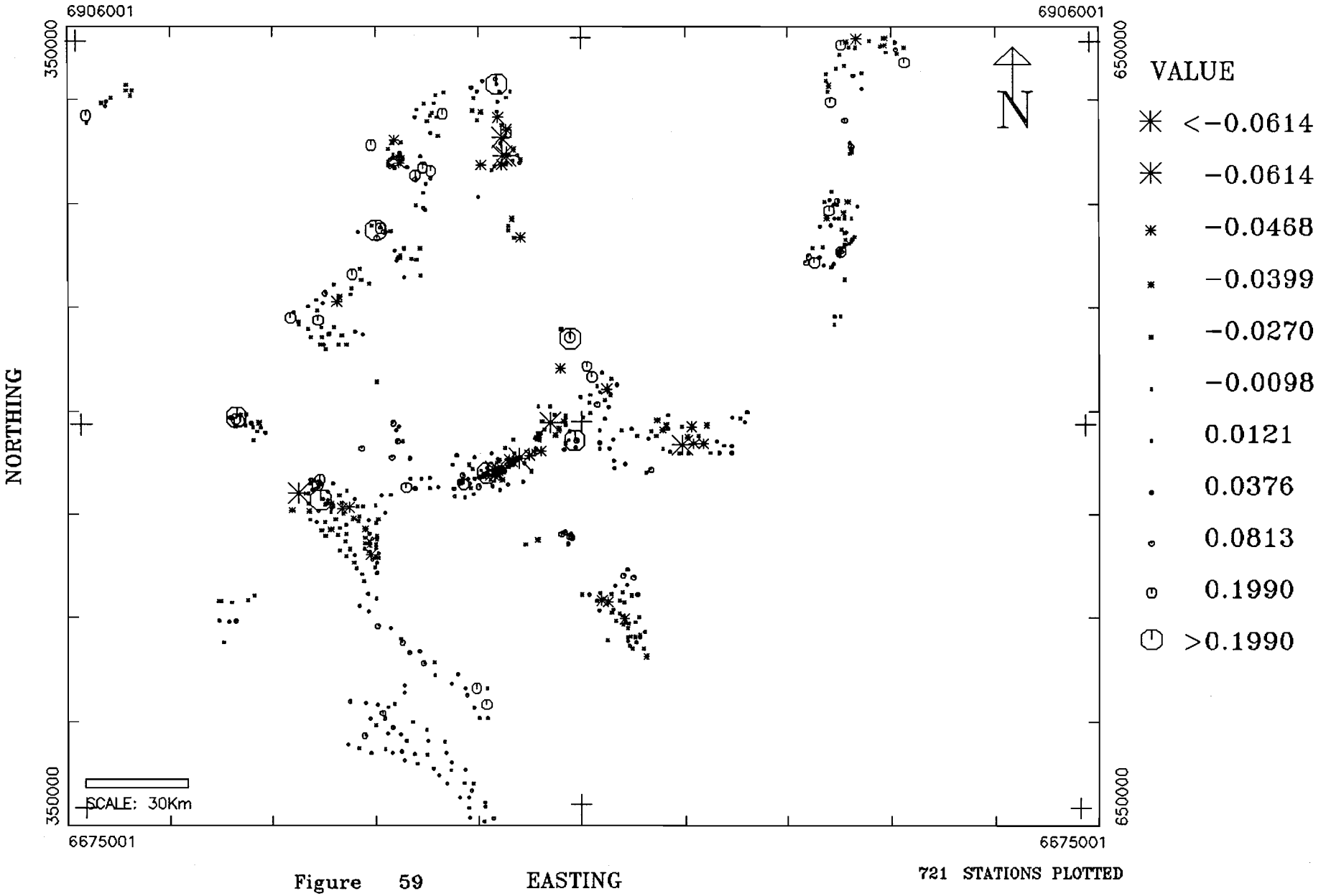
SOUTH MURCHISON LATERITE PRINCIPAL COMPONENT 3
6906001
6906001
350000
650000
N
VALUE
<-0.0614
-0.0614
-0.0468
-0.0399
-0.0270
-0.0098
0.0121
0.0376
0.0813
0.1990
>0.1990
SCALE: 30Km
350000
650000
6675001
6675001
NORTHING
EASTING
721 STATIONS PLOTTED

Figure 59

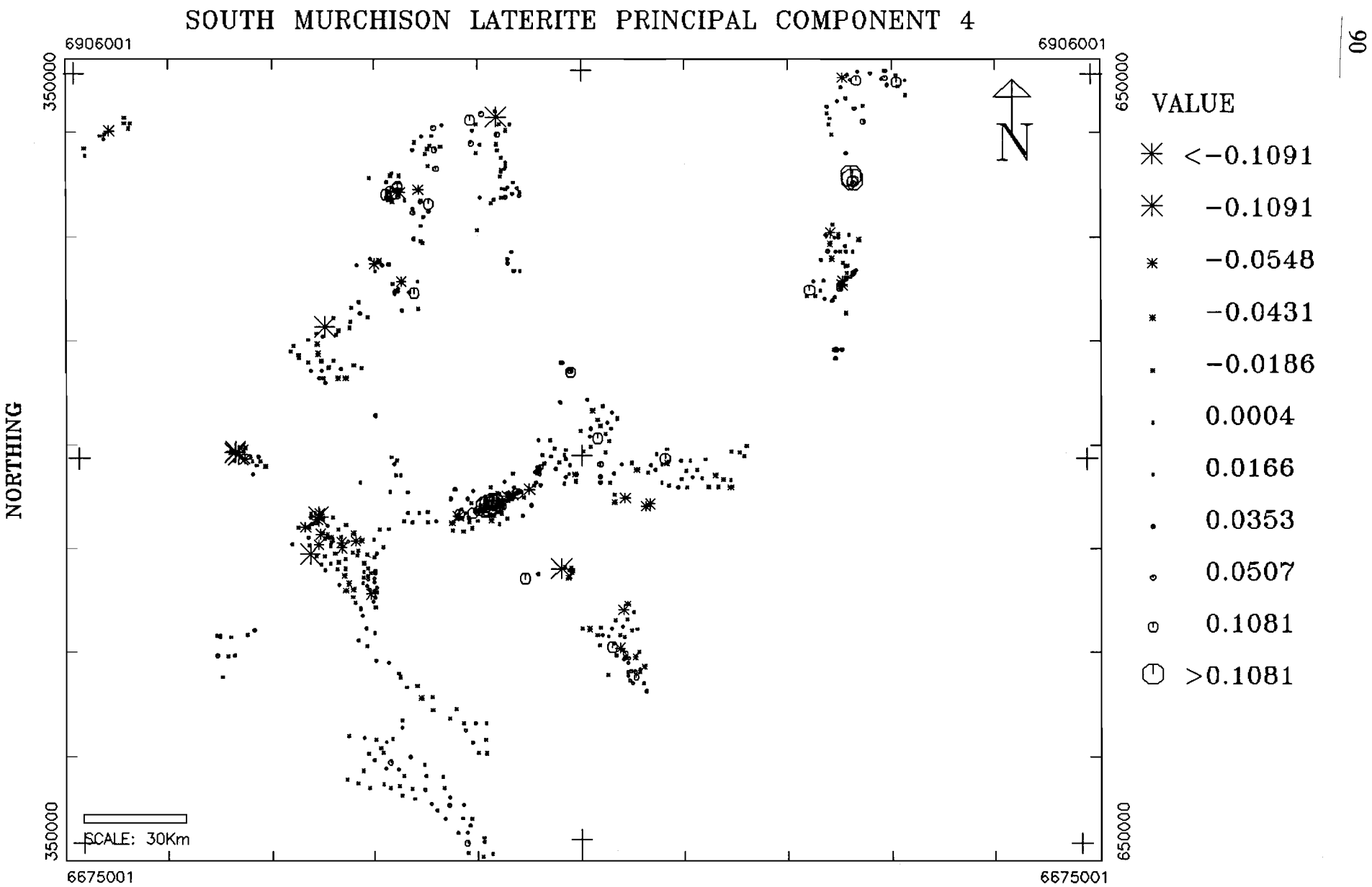
SOUTH MURCHISON LATERITE PRINCIPAL COMPONENT 4
6906001
6906001
350000
650000
N
VALUE
<-0.1091
-0.1091
-0.0548
-0.0431
-0.0186
0.0004
0.0166
0.0353
0.0507
0.1081
>0.1081
NORTHING
SCALE: 30Km
6675001
6675001
EASTING
721 STATIONS PLOTTED

Figure 60

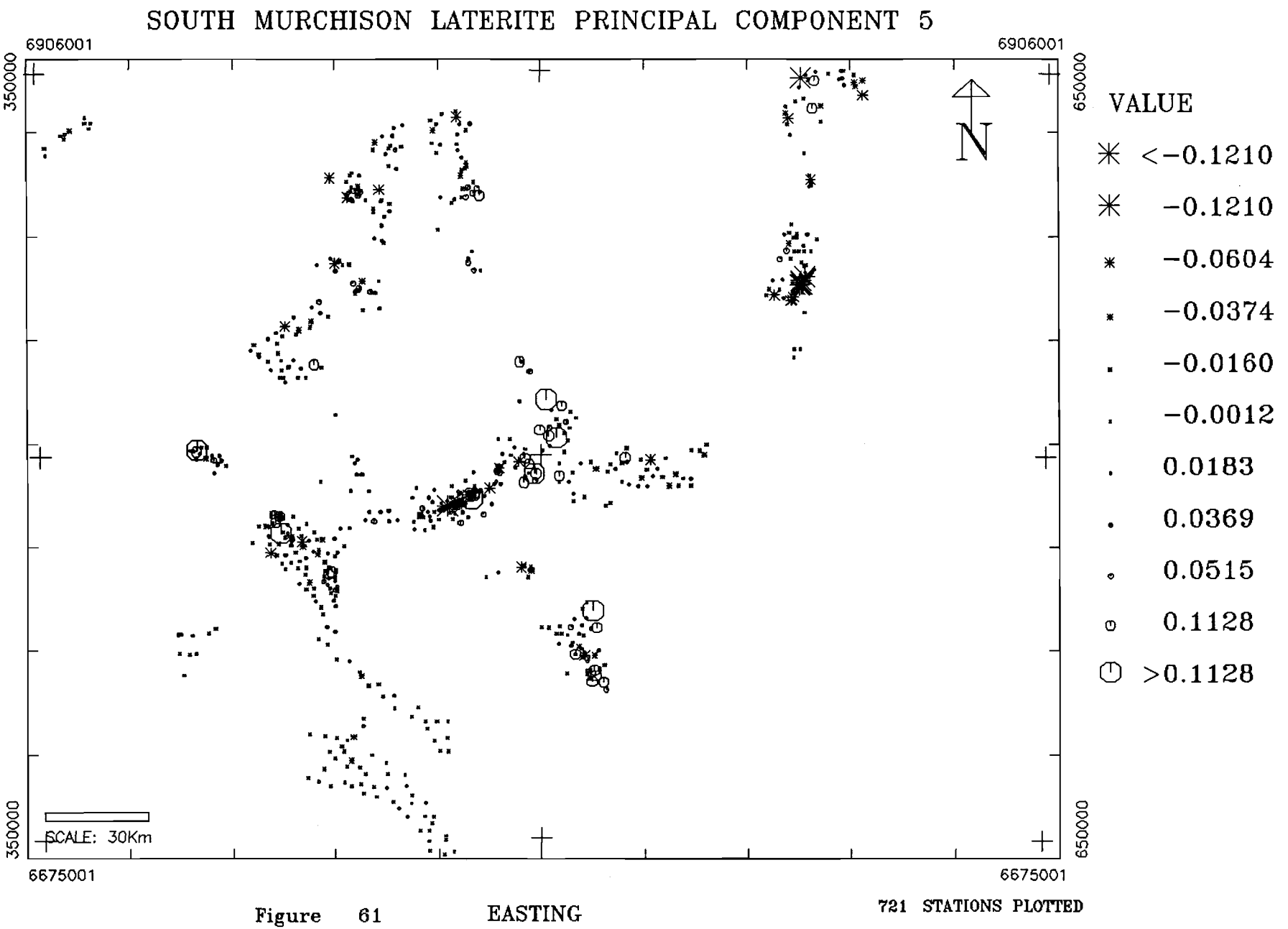
SOUTH MURCHISON LATERITE PRINCIPAL COMPONENT 5
6906001
6906001
350000
650000
N
VALUE
<-0.1210
-0.1210
-0.0604
-0.0374
-0.0160
-0.0012
0.0183
0.0369
0.0515
0.1128
>0.1128
NORTHING
SCALE: 30Km
350000
650000
6675001
6675001
EASTING
721 STATIONS PLOTTED

Figure 61

SOUTH MURCHISON ANOMALY LOCATION MAP

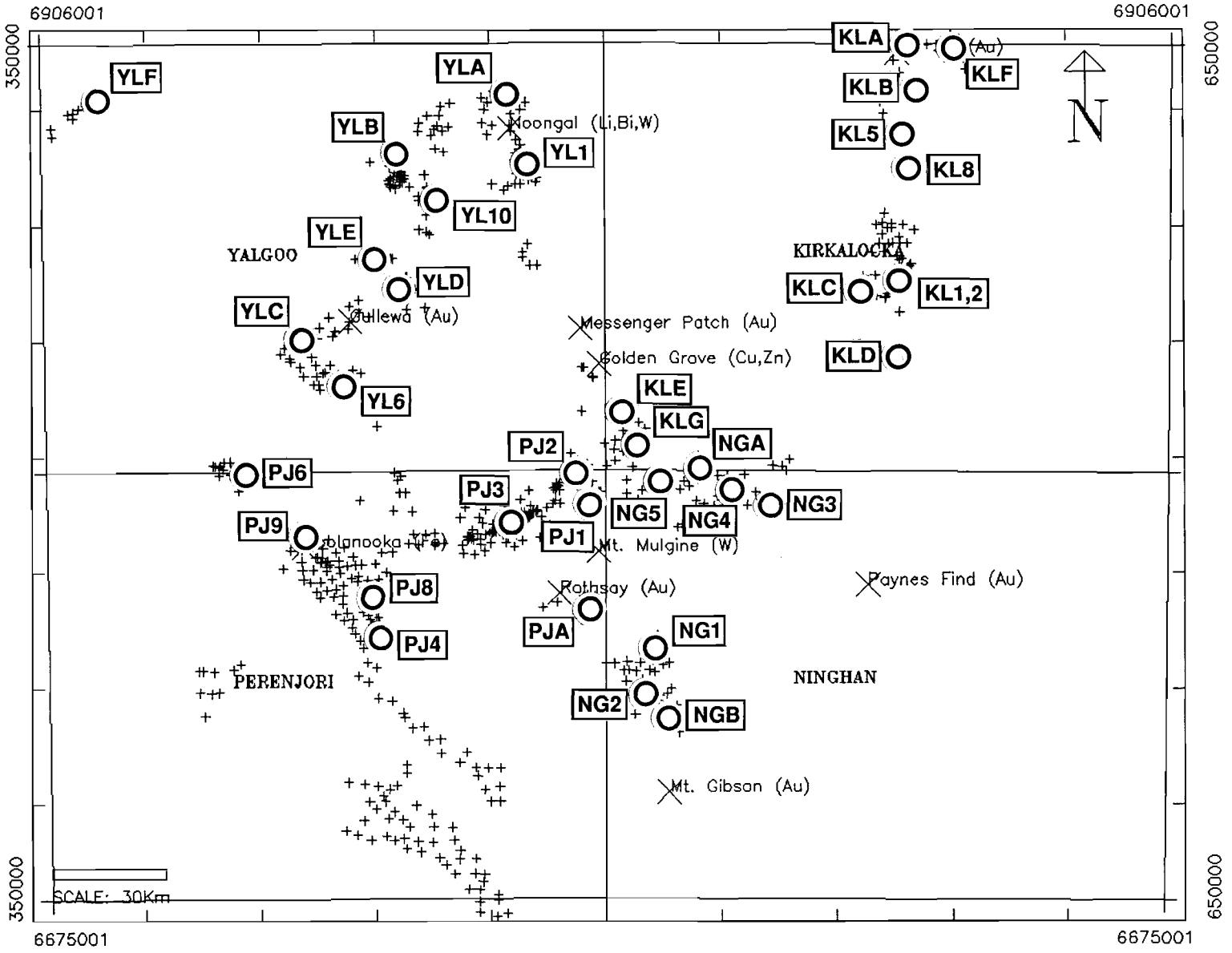

NORTHING

Figure 62

EASTING

721 STATIONS PLOTTED

March 31, 1989

Supplement to:

Exploration Geoscience Report 2R

REPORT ON LATERITE GEOCHEMISTRY IN THE CSIRO-AGE DATABASE FOR THE SOUTHERN MURCHISON REGION

E.C. Grunsky, J. Innes, R.E. Smith, J.L. Perdrix,

CSIRO / AMIRA Laterite Geochemistry Project P240
(Confidential to the sponsors of the project)

Included in this supplement:

Figure 1: Regional Geology of the Southern Murchison Area.

Table 10: Samples with abundance levels > 95 percentile for the elements shown in figures 6-30 and 31-55.

Table 11: Samples with principal component scores < 2 percentile (large negative scores) and principal component scores > 98 percentile (large positive scores) for principal components 1-5.

Figure 1:

This map is a generalisation of the geology of the south Murchison area. It is intended as a general guide for the purpose of placing the element abundances shown in the maps of figures 31-62 in context with the general geology of the area. For more detailed geological relationships, the reader should refer to the section, "Regional Setting and Mineralisation", on page 3.

Table 10:

This table has been prepared in response to requests by some of the sponsors for a list of samples that are associated with the designated anomalies in the area. Table 10 has been prepared for the elements that are represented in figures 6-30 (histograms) and figures 31-55 (percentile maps).

The lists contain sample numbers, designated anomaly association, UTM coordinates, and abundance values for samples with a ranking of >95 percentile. Au was listed for samples with a ranking of >90 percentile.

Samples that rank >95 percentile are considered to be anomalous in that they represent the extreme positive end of the abundance distribution. These values do not necessarily reflect mineralisation for two reasons. One, the maximum value of the distribution for a given element may be less than that associated with any kind of mineralisation. Thus, although the sample is an extreme value, it is does not represent the range of values that might be associated with mineralisation. Second, a high percentile ranking of a single sample does not necessarily define a zone of high mineral potential. Several samples are usually required in order to confirm an anomalous zone.

The number of samples listed for each element vary due to the number of samples used to perform the ranking. For example, there are only 224 samples that were analyzed

for TiO_2. Thus, only 11 samples represent the >95 percentile ranking. For Fe_2O_3, 599 samples were used for ranking, and thus there are 29 samples that represent values greater than the 95 percentile ranking.

More than 5% of the Cr analyses are greater than 9999 ppm, thus the 95 percentile ranking of the data only indicates samples that are > than 9999 ppm.

Not all of the "anomalous" samples area associated with designated labelled anomalies (c.f. figure 62) as shown in the lists of many of the elements. Anomalies that are suffixed by a number (i.e. PJ3, KL1,2) were chosen prior to the current study; not on the basis of any results of this study. Anomalies that are suffixed by a letter (i.e. PJA, NGB) were chosen based on multi-element associations of abundance increases at common sites by percentile ranking (Table 8, p. 24). Within Table 10, samples that are listed in the >95 percentile rankings but have no desinated anomaly associated with them, are samples that are high in abundance but do not have any multi-element associations. These individual samples may or may not have significance in terms of representing zones of alteration or mineralisation.

This study has not used any formal approach in outlining anomalous zones or defining anomalies based on comparison between various reference groups of mineralised and un-mineralised samples. Future work will address this problem specifically; similar to a method outlined by Smith *et al* (1984).

Table 11:

The application of principal components analysis to the south Murchison data resulted in the delineation of some meaningful geological relationships based on the correlations of a selected suite of elements. Large positive scores (>98 percentile ranking) of the first component are associated with Co-Ni-Cr-Cu-Fe-Zn increases. This most probably reflects areas that are underlain by mafic/ultramafic volcanic sequences. The large negative scores (< 2 percentile ranking) are interpreted to represent Ga enriched samples reflecting fractionated materials, most probably, underlying felsic volcanic and felsic intrusive rocks and gneisses. For the first component, the entire range of the scores represents a continuum of compositional variation of the underlying igneous rocks.

Several of the components are not readily interpreted within any kind of meaningful geological context. Further work is required to adequately explain these components. However, many of the extreme values (<2 and >98 percentile rankings) of these components are associated with the designated anomalies of Figure 62 and thus may represent systematic variation associated with some specific geological process. Because the components represent linear combinations of several elements, the significance of the percentile rankings of the samples should not be overlooked.

The >98 percentile ranking of the positive scores of the fifth component appears to be a significant group of samples that outline As-Sb associations as shown in figures 56b and 61. The samples associated with the positive rankings of this component warrant investigation in terms of As-Sb-Au associations and possible Au mineralisation.

References:

Smith, R.E., Campbell, N.A., Litchfield, R.
1984: Multivariate statistical techniques applied to pisolitic laterite geochemistry at Golden Grove, Western Australia, Journal of Geochemical Exploration, vol 22, No. 1-3, pp. 193-216.

Supplement: Table 10
Samples with Abundance Levels > 95 Percentile

SOUTH MURCHISON LATERITE (LN LP CN CP MS)
Au (ppm)

Anomaly	Sample	Easting	Northing	Abundance
KL1,2	G04176	575300.	6840000.	192.0
YLA	G04137	475729.	6884289.	58.0
KL1,2	G04171	576907.	6843135.	40.0
PJ9	G04704	425900.	6771500.	33.0
NGA	G02451	524886.	6789812.	33.0
KL5	G04180	576732.	6878989.	32.0
	G02505	439936.	6740590.	30.0
NGB	G03600	516818.	6730118.	29.0
KLB	G04181	581700.	6888035.	27.0
PJ3	G03717	479998.	6780742.	25.0
KLC	G02593	567773.	6837959.	23.0
YLB	G06937	443400.	6867000.	21.0
PJ8	G04710	438000.	6759350.	21.0
YLE	G04721	444350.	6846900.	20.0
PJ8	G04713	439800.	6755200.	20.0
PJ8	G04709	437700.	6754200.	20.0
YLF	G04160	368788.	6887594.	19.0
KLD	G04179	575415.	6822524.	18.0
	G04684	394100.	6734100.	17.0
KLA	G04189	575215.	6897925.	17.0
YLD	G02543	452955.	6834092.	17.0
KL1,2	G04894	576633.	6842828.	16.0
PJ3	G03719	476624.	6778581.	16.0

SOUTH MURCHISON LATERITE (LN LP CN CP MS)
Fe2O32 (Wt%) (AAS HF)

Anomaly	Sample	Easting	Northing	Abundance
PJ3	G03330	470821.	6775798.	70.20
PJ3	G03711	474734.	6777654.	67.30
PJ3	G03707	476760.	6777966.	61.30
KL1,2	G04893	575262.	6840991.	59.50
PJ3	G03345	482024.	6781668.	58.80
KL8	G04898	578718.	6870359.	58.10
YL1	G02573	482029.	6866760.	58.10
PJ3	G03716	480000.	6780300.	57.90
NG2	G04618	512166.	6733140.	57.80
	G04897	578168.	6869440.	57.30
	G04894	576633.	6842828.	56.00
PJ3	G03349	474463.	6777807.	55.40
PJ3	G03705	472303.	6777186.	55.00
	G04073	434825.	6763030.	54.70
YL1	G02577	476571.	6872444.	54.50
PJ3	G04690	483300.	6779900.	53.90
YLA	G04141	478182.	6885526.	53.20
	G02586	569464.	6848413.	52.60
PJ3	G03714	479864.	6779972.	51.90
	G02601	572230.	6856090.	51.80
PJ3	G04177	576569.	6832981.	51.70
	G04083	428209.	6763606.	51.70
PJ3	G03715	479324.	6779817.	51.40
KL8	G04899	578854.	6870204.	51.30
PJ3	G03720	475813.	6778425.	51.20
PJ3	G03352	468660.	6775330.	51.20
KL1,2	G04694	480250.	6780500.	50.90
YL6	G04107	433835.	6817964.	50.90
KLE	G04025	504468.	6802148.	50.80

SOUTH MURCHISON LATERITE (LN LP CN CP MS)
TiO2 (ppm) (ICP FS)

Anomaly	Sample	Easting	Northing	Abundance
KL6	G04018	505280.	6800455.	3.80
NG3	G02452	539076.	6786233.	3.44
NGB	G02416	518299.	6731039.	3.38
	G02608	580379.	6854191.	2.98
	G02417	515612.	6733813.	2.61
	G04682	397150.	6733850.	2.22
NG2	G02419	511039.	6736281.	2.18
PJ3	G04693	479500.	6780400.	2.15
	G04675	447500.	6727900.	2.12
PJ3	G03711	474734.	6777654.	2.00
	G06939	444850.	6866000.	1.98

Supplement: Table 10
Samples with Abundance Levels > 95 Percentile

SOUTH MURCHISON LATERITE (LN LP CN CP MS)
Mn2 (ppm) (AAS HF)

Anomaly	Sample	Easting	Northing	Abundance
YLE	G02550	439922.	6847234.	9999.0
YLB	G02585	438570.	6871847.	5634.0
KL1,2	G04891	575535.	6841143.	5400.0
KLC	G02593	567773.	6837959.	4902.0
	G02494	459379.	6880860.	3813.0
KLE	G04033	502979.	6804918.	3627.0
	G02598	572076.	6853014.	3625.0
	G04168	355371.	6880359.	3230.0
YL1	G04146	478200.	6875216.	2959.0
YLC	G02533	423237.	6821284.	2344.0
KLC	G02590	565328.	6837973.	2271.0
	G02501	448545.	6772796.	2182.0
	G02523	433062.	6834425.	2155.0
	G02495	435678.	6784119.	2153.0
	G02499	444809.	6791399.	1852.0
YL10	G02584	451274.	6862981.	1812.0
KLC	G02591	569276.	6839489.	1317.0
	G04103	429934.	6768388.	1308.0
YL6	G04106	436008.	6817206.	1207.0
KL1,2	G04893	575262.	6840991.	1200.0
	G04717	453500.	6865000.	1200.0
PJ6	G02516	403683.	6791436.	1164.0
	G04622	575677.	6842219.	1100.0
	G02610	574540.	6855768.	1100.0
PJ9	G04067	427469.	6773913.	1086.0
KL1,2	G04170	575539.	6841759.	1031.0

SOUTH MURCHISON LATERITE (LN LP CN CP MS)
V3 (ppm) (XRF)

Anomaly	Sample	Easting	Northing	Abundance
	G04085	436727.	6760733.	2180.0
PJ9	G04062	419520.	6771089.	2120.0
YL6	G04109	431416.	6814256.	2040.0
	G04089	432309.	6754859.	2040.0
	G04073	434825.	6763030.	2040.0
	G04054	433708.	6769334.	2020.0
PJ2	G02462	490937.	6791682.	1980.0
PJ3	G04046	476356.	6777504.	1960.0
YLF	G04161	367152.	6887576.	1920.0
	G04091	433545.	6751019.	1920.0
PJ2	G02464	494859.	6791992.	1920.0
	G04081	436015.	6767346.	1820.0
	G02525	432688.	6828729.	1800.0
PJ2	G02461	492017.	6793991.	1800.0
	G04050	484862.	6782135.	1780.0
PJ3	G03333	473656.	6776420.	1768.0
PJ8	G04086	436740.	6758270.	1760.0
	G02601	572230.	6856090.	1760.0
YL6	G04110	429112.	6814242.	1740.0
	G02466	490798.	6796298.	1720.0
YLC	G02534	422947.	6824052.	1680.0
	G04100	423334.	6766037.	1660.0
	G04036	486212.	6783367.	1660.0
	G02527	425222.	6828991.	1660.0
	G02536	428629.	6826704.	1640.0
	G04169	355670.	6878208.	1600.0

Supplement: Table 10
Samples with Abundance Levels > 95 Percentile

SOUTH MURCHISON LATERITE (LN LP CN CP MS)
Cr3 (ppm) (XRF)

Anomaly	Sample	Easting	Northing	(XRF) Abundance	(ICP) Abundance
KL1,2	G04896	574714.	6840225.	9999.0	17388.0
KL1,2	G04894	576633.	6842828.	9999.0	14535.0
KL1,2	G04893	575262.	6840991.	9999.0	
KL1,2	G04891	575535.	6841143.	9999.0	10943.0
PJ9	G04706	424200.	6773750.	9999.0	
KL1,2	G04623	576690.	6843351.	9999.0	14324.0
	G04186	572021.	6889020.	9999.0	
KLB	G04182	581595.	6892652.	9999.0	
KL1,2	G04175	573000.	6836800.	9999.0	
KL1,2	G04171	576907.	6843135.	9999.0	
KL1,2	G04170	575539.	6841759.	9999.0	
YL1	G04147	476840.	6874137.	9999.0	
YL1	G04145	478198.	6876293.	9999.0	
YLA	G04129	468637.	6885504.	9999.0	
	G04000	520151.	6789205.	9999.0	10268.0
PJ3	G03718	478649.	6779508.	9999.0	9701.0
PJ6	G03153	400550.	6794000.	9999.0	
	G03066	573400.	6837600.	9999.0	13016.0
YL1	G02574	478213.	6868601.	9999.0	
	G02524	432950.	6830423.	9999.0	
PJ2	G02521	493373.	6789837.	9999.0	
NG4	G02458	529068.	6785185.	9999.0	7688.0
	G02445	531651.	6790411.	9999.0	8033.0
NGA	G02438	524348.	6791044.	9999.0	14098.0
NGA	G02435	523398.	6789507.	9999.0	9057.0
NG2	G02418	512651.	6733817.	9999.0	8350.0
NG1	G02411	507675.	6739669.	9999.0	8516.0
	G03065	572600.	6836500.	9755.0	10800.0
KL1,2	G04622	575677.	6842219.	9735.0	7064.0

SOUTH MURCHISON LATERITE (LN LP CN CP MS)
Cu4 (ppm) (AAS HF)

Anomaly	Sample	Easting	Northing	Abundance
NGA	G02438	524348.	6791044.	2033.0
NGA	G02435	523398.	6789507.	727.0
PJ3	G03705	472303.	6777186.	410.0
KLA	G04192	577959.	6900062.	400.0
PJ6	G02517	405327.	6788987.	345.0
KLA	G04193	579733.	6899896.	330.0
KLA	G04191	577150.	6901606.	310.0
	G04000	520151.	6789205.	293.0
	G04029	502435.	6794455.	273.0
	G04009	505273.	6785836.	238.0
YLB	G06936	446700.	6866650.	232.0
NG3	G02450	543397.	6784832.	218.0
KLG	G04020	507311.	6801377.	217.0
NGA	G02451	524886.	6789812.	215.0
NG1	G02427	511853.	6742436.	213.0
	G02513	399073.	6792628.	208.0
	G04060	415639.	6766136.	199.0
	G04014	521501.	6787818.	197.0
	G02586	569464.	6848413.	191.0
PJ2	G04043	495266.	6790915.	176.0
YLB	G06937	443400.	6867000.	170.0
KLA	G04194	580023.	6902510.	170.0
PJ3	G05816	472450.	6777000.	165.0
KLF	G04197	587930.	6900609.	160.0
YL1	G03174	478081.	6866300.	160.0
	G02444	530561.	6787490.	157.0
KL1,2	G04623	576690.	6843351.	150.0
KLF	G04200	593797.	6899949.	150.0
NG4	G02443	533672.	6787789.	143.0

Supplement: Table 10
Samples with Abundance Levels > 95 Percentile

SOUTH MURCHISON LATERITE (LN LP CN CP MS)
Pb3 (ppm) (XRF)

Anomaly	Sample	Easting	Northing	Abundance
PJ9	G04705	423700.	6774950.	309.0
YL10	G02583	453578.	6865452.	206.0
	G02550	439922.	6847234.	199.0
YLC	G02531	415229.	6821998.	171.0
KLE	G04033	502979.	6804918.	169.0
PJ6	G03152	399300.	6793100.	166.0
PJ6	G02513	399073.	6792628.	143.0
PJ9	G04715	423000.	6773300.	126.0
	G02527	425222.	6828991.	123.0
	G02533	423237.	6821284.	122.0
YLE	G02551	441278.	6847856.	116.0
KL1,2	G04891	575535.	6841143.	114.0
	G04010	508111.	6784142.	104.0
YL1	G04146	478200.	6875216.	101.0
	G04154	459379.	6880860.	96.0
YLB	G02585	438570.	6871847.	91.0
	G02523	433062.	6834425.	91.0
	G02499	444809.	6791399.	86.0
PJ3	G05816	472450.	6777000.	85.0
YLE	G04726	441300.	6848000.	85.0
	G04159	455856.	6875309.	84.0
	G02501	448545.	6772796.	84.0
	G02479	465200.	6776250.	81.0
	G04659	436600.	6701000.	80.0
	G04683	399100.	6734100.	78.0
	G04674	449500.	6725000.	77.0
	G02598	572076.	6853014.	75.0
YL10	G02584	451274.	6862981.	75.0

SOUTH MURCHISON LATERITE (LN LP CN CP MS)
Zn3 (ppm) (AAS HF)

Anomaly	Sample	Easting	Northing	Abundance
	G02583	453578.	6865452.	268.0
KL1,2	G04893	575262.	6840991.	140.0
	G03152	399300.	6793100.	140.0
KL5	G04180	576732.	6878989.	134.0
PJ3	G03145	478400.	6773700.	120.0
KL1,2	G04622	575677.	6842219.	110.0
	G02450	543397.	6784832.	105.0
	G04129	468637.	6885504.	96.0
	G04170	575539.	6841759.	92.0
KL1,2	G04623	576690.	6843351.	80.0
	G04187	571348.	6890409.	80.0
	G04027	523387.	6783967.	80.0
	G02448	547211.	6791742.	77.0
NG3	G02454	539740.	6782845.	75.0
YLD	G02541	450288.	6838973.	74.0
NG4	G02444	530561.	6787490.	74.0
PJ2	G02521	493373.	6789837.	72.0
YL10	G04717	453500.	6865000.	70.0
YL10	G04716	455900.	6864350.	70.0
KLF	G04200	593797.	6899949.	70.0
PJ6	G02517	405327.	6788987.	70.0
KL1,2	G04891	575535.	6841143.	65.0
YLA	G04142	479406.	6887374.	65.0
YLB	G03171	445000.	6869200.	65.0
	G02510	442505.	6765380.	63.0
	G06622	463400.	6782150.	62.0
	G04175	573000.	6836800.	61.0
	G02586	569464.	6848413.	61.0

Supplement: Table 10
Samples with Abundance Levels > 95 Percentile

SOUTH MURCHISON LATERITE (LN LP CN CP MS)
Ni3 (ppm) (AAS HF)

Anomaly	Sample	Easting	Northing	Abundance
	G04622	575677.	6842219.	2000.0
	G04623	576690.	6843351.	1900.0
KL1,2	G04171	576907.	6843135.	1688.0
KL1,2	G04893	575262.	6840991.	1500.0
	G04170	575539.	6841759.	1198.0
KL1,2	G04894	576633.	6842828.	820.0
KL1,2	G04891	575535.	6841143.	780.0
KL1,2	G04896	574714.	6840225.	690.0
NGA	G02438	524348.	6791044.	616.0
KL1,2	G03066	573400.	6837600.	600.0
PJ2	G02521	493373.	6789837.	573.0
PJ3	G03718	478649.	6779508.	550.0
	G04650	445250.	6710200.	520.0
KLA	G04192	577959.	6900062.	510.0
	G04182	581595.	6892652.	480.0
KL1,2	G04892	574991.	6841146.	470.0
PJ3	G03145	478400.	6773700.	450.0
NGA	G02435	523398.	6789507.	400.0
YLA	G04129	468637.	6885504.	399.0
	G04196	588219.	6902761.	380.0
KL1,2	G04175	573000.	6836800.	372.0
PJ9	G04706	424200.	6773750.	330.0
KL1,2	G03065	572600.	6836500.	330.0
NGA	G02445	531651.	6790411.	328.0
PJ3	G03708	476354.	6778119.	310.0
KLF	G04198	591736.	6898272.	300.0
	G02411	507675.	6739669.	300.0
	G04186	572021.	6889020.	280.0

SOUTH MURCHISON LATERITE (LN LP CN CP MS)
Co3 (ppm) (AAS HF)

Anomaly	Sample	Easting	Northing	Abundance
KL1,2	G04623	576690.	6843351.	170.0
KLA	G04192	577959.	6900062.	150.0
KLB	G04182	581595.	6892652.	110.0
	G02452	539076.	6786233.	109.0
NGA	G02439	524760.	6793813.	85.0
NGA	G02435	523398.	6789507.	74.0
	G02445	531651.	6790411.	73.0
	G04891	575535.	6841143.	70.0
	G04029	502435.	6794455.	68.0
NGA	G02438	524348.	6791044.	66.0
KL1,2	G04893	575262.	6840991.	60.0
	G04009	505273.	6785836.	60.0
NG3	G02454	539740.	6782845.	59.0
	G02444	530561.	6787490.	59.0
NG4	G04027	523387.	6783967.	56.0
	G02429	508620.	6741977.	56.0
	G02441	541235.	6784994.	54.0
NG2	G02418	512651.	6733817.	54.0
	G04026	515957.	6787827.	53.0
NG2	G02419	511039.	6736281.	53.0
NG4	G02457	525413.	6783194.	52.0
	G02450	543397.	6784832.	52.0
KLG	G04018	505280.	6800455.	50.0
YLE	G02550	439922.	6847234.	50.0
	G02416	518299.	6731039.	50.0
	G02440	535152.	6785476.	49.0
	G02443	533672.	6787789.	48.0
	G02417	515612.	6733813.	48.0

Supplement: Table 10
Samples with Abundance Levels > 95 Percentile

SOUTH MURCHISON LATERITE (LN LP CN CP MS)
As4 (ppm) (XRF)

Anomaly	Sample	Easting	Northing	Abundance
PJ3	G03343	479595.	6779202.	987.0
KLB	G04183	579152.	6891894.	889.0
	G04009	505273.	6785836.	740.0
YL1	G02573	482029.	6866760.	690.0
NG1	G02409	515091.	6746741.	612.0
	G06084	496750.	6816000.	541.0
PJ8	G04711	437900.	6757200.	510.0
NG2	G02420	509960.	6734128.	498.0
YL6	G04107	433835.	6817964.	493.0
PJ3	G03344	480270.	6779973.	405.0
NGB	G03601	515738.	6727965.	370.0
YLB	G06934	445700.	6868000.	328.0
PJ9	G04715	423000.	6773300.	319.0
PJ1	G04041	498243.	6784453.	319.0
NG1	G02428	514545.	6741509.	297.0
YL1	G02572	480121.	6867373.	274.0
PJ3	G04049	482300.	6781500.	255.0
PJ3	G04698	480100.	6779500.	239.0
KL1,2	G04885	578683.	6844661.	227.0
PJ3	G03718	478649.	6779508.	223.0
PJ8	G04710	438000.	6759350.	220.0
	G06086	493800.	6818750.	218.0
PJ3	G03721	477704.	6779045.	211.0
NG4	G02443	533672.	6787789.	201.0
NG1	G02427	511853.	6742436.	200.0
KL1,2	G04888	578818.	6844507.	196.0
PJ3	G03144	476200.	6772000.	186.0
PJ3	G02473	474061.	6776883.	186.0
YLB	G03172	446300.	6868600.	185.0

SOUTH MURCHISON LATERITE (LN LP CN CP MS)
Sb2 (ppm) (XRF)

Anomaly	Sample	Easting	Northing	Abundance
KLE	G06083	501500.	6808000.	115.0
NG1	G02409	515091.	6746741.	74.0
	G04043	495266.	6790915.	64.0
NG5	G04034	494863.	6783836.	58.0
	G06086	493800.	6818750.	42.0
	G06084	496750.	6816000.	35.0
KLE	G06082	506000.	6806100.	35.0
	G02415	516691.	6735197.	33.0
NG5	G04041	498243.	6784453.	29.0
PJ9	G04715	423000.	6773300.	26.0
PJ3	G04044	496484.	6789223.	18.0
NGB	G03603	516816.	6729348.	18.0
NGB	G03607	515471.	6729504.	17.0
KLB	G04183	579152.	6891894.	16.0
PJ3	G03334	474331.	6776729.	16.0
	G06085	496580.	6816350.	15.0
PJ2	G04030	500270.	6793224.	14.0
	G04702	425900.	6769100.	13.0
YLA	G04137	475729.	6884289.	13.0
YL6	G04107	433835.	6817964.	13.0
PJ8	G04712	436450.	6755100.	12.0
	G04617	511845.	6735664.	12.0
KL1,2	G04171	576907.	6843135.	12.0
NGB	G03606	514794.	6726273.	12.0
PJ3	G03333	473656.	6776420.	12.0
PJ6	G03153	400550.	6794000.	12.0
	G02464	494859.	6791992.	12.0

Supplement: Table 10
Samples with Abundance Levels > 95 Percentile

SOUTH MURCHISON LATERITE (LN LP CN CP MS)
Bi1 (ppm) (OES)

Anomaly	Sample	Easting	Northing	Abundance
	G06084	496750.	6816000.	50.0
	G06085	496580.	6816350.	10.0
KL8	G02612	578589.	6871437.	8.0
YLA	G04139	471216.	6890281.	6.0
NG5	G04034	494863.	6783836.	6.0
	G02558	454307.	6853146.	6.0
YLE	G02551	441278.	6847856.	6.0
PJ3	G05816	472450.	6777000.	3.0
KLD	G04178	573651.	6822381.	3.0
KL1,2	G04175	573000.	6836800.	3.0
PJ3	G03132	472700.	6776700.	3.0
PJ3	G03130	473500.	6779600.	3.0

SOUTH MURCHISON LATERITE (LN LP CN CP MS)
Bi3 (ppm) (XRF)

Anomaly	Sample	Easting	Northing	Abundance
	G06084	496750.	6816000.	75.0
	G02612	578589.	6871437.	16.0
	G06085	496580.	6816350.	15.0
YLA	G04139	471216.	6890281.	11.0
	G02558	454307.	6853146.	8.0
KL8	G04899	578854.	6870204.	7.0
PJ3	G03350	473923.	6777806.	7.0
PJ3	G03348	473383.	6777497.	7.0
	G02469	483682.	6756280.	7.0
KLD	G04178	573651.	6822381.	6.0
PJ3	G03706	472170.	6776417.	6.0
YLB	G02556	443637.	6866179.	6.0
YLE	G02551	441278.	6847856.	6.0
PJ3	G02478	471359.	6776877.	6.0
KL1,2	G04896	574714.	6840225.	5.0
	G04187	571348.	6890409.	5.0
KL1,2	G04175	573000.	6836800.	5.0
	G04137	475729.	6884289.	5.0
PJ3	G03712	481213.	6781359.	5.0
PJ3	G03705	472303.	6777186.	5.0
KL8	G03321	578723.	6871129.	5.0
YLC	G02535	424561.	6826217.	5.0
NG3	G02450	543397.	6784832.	5.0
	G02448	547211.	6791742.	5.0

SOUTH MURCHISON LATERITE (LN LP CN CP MS)
Mo2 (ppm) (XRF)

Anomaly	Sample	Easting	Northing	Abundance
PJ3	G05816	472450.	6777000.	63.0
PJ3	G03348	473383.	6777497.	29.0
KLC	G02589	566152.	6839661.	26.0
KLF	G04199	591400.	6899400.	25.0
PJ3	G03705	472303.	6777186.	25.0
KL8	G03322	578188.	6872517.	25.0
PJ3	G03347	481349.	6781052.	23.0
YLA	G04128	467947.	6888426.	21.0
PJ3	G03354	464745.	6774703.	21.0
PJ3	G03352	468660.	6775330.	20.0
PJ3	G03350	473923.	6777806.	20.0
KLB	G02612	578589.	6871437.	20.0
PJ3	G05813	470300.	6775900.	19.0
YL10	G04716	455900.	6864350.	19.0
	G04671	444700.	6703400.	18.0
KL1,2	G04896	574714.	6840225.	16.0
YLB	G02585	438570.	6871847.	16.0
YL10	G02583	453578.	6865452.	16.0
	G06084	496750.	6816000.	15.0
PJ3	G03349	474463.	6777807.	15.0
KL1,2	G03066	573400.	6837600.	14.0
YL10	G02584	451274.	6862981.	14.0
YL10	G04717	453500.	6865000.	13.0
PJ3	G03329	471090.	6776260.	13.0
	G06085	496580.	6816350.	12.0
YL10	G04720	451350.	6861850.	12.0
PJ3	G04697	480400.	6782700.	12.0

Supplement: Table 10
Samples with Abundance Levels > 95 Percentile

SOUTH MURCHISON LATERITE (LN LP CN CP MS)
Ag1 (ppm) (AAS HF)

Anomaly	Sample	Easting	Northing	Abundance
PJ6	G03152	399300.	6793100.	6.0
PJ6	G03148	400100.	6792100.	3.0
PJ6	G02513	399073.	6792628.	3.0
YLB	G03170	444000.	6867600.	2.0
NGA	G02451	524886.	6789812.	2.0
PJ3	G04693	479500.	6780400.	1.0
PJ4	G03164	438800.	6751850.	1.0
PJ6	G03154	404200.	6790200.	1.0
PJ6	G03153	400550.	6794000.	1.0
PJ6	G03151	398100.	6792800.	1.0
YLD	G02543	452955.	6834092.	1.0
PJ9	G04715	423000.	6773300.	.80
PJ9	G04706	424200.	6773750.	.80
PJ3	G04694	480250.	6780500.	.80
KL1,2	G04622	575677.	6842219.	.80
PJ3	G03333	473656.	6776420.	.80

SOUTH MURCHISON LATERITE (LN LP CN CP MS)
Sn1 (ppm) (OES)

Anomaly	Sample	Easting	Northing	Abundance
	G06084	496750.	6816000.	60.0
PJ9	G04105	423279.	6774193.	20.0
	G06085	496580.	6816350.	15.0
	G06622	463400.	6782150.	10.0
	G04073	434825.	6763030.	10.0
	G02526	438000.	6831836.	10.0
	G02523	433062.	6834425.	10.0
PJ2	G02520	492427.	6787990.	10.0
PJ6	G02513	399073.	6792628.	10.0
PJ6	G02512	402000.	6790800.	10.0
PJ8	G02508	439976.	6758596.	8.0
PJ3	G02477	467500.	6772700.	8.0

SOUTH MURCHISON LATERITE (LN LP CN CP MS)
Sn5 (ppm) (XRF)

Anomaly	Sample	Easting	Northing	Abundance
	G06084	496750.	6816000.	72.0
	G06085	496580.	6816350.	18.0
PJ3	G04694	480250.	6780500.	16.0
PJ9	G04105	423279.	6774193.	15.0
PJ3	G04690	483300.	6779900.	13.0
	G04005	509325.	6780602.	13.0
PJA	G02471	494065.	6759214.	13.0
	G04160	368788.	6887594.	12.0
	G04090	431377.	6752853.	12.0
YLE	G02551	441278.	6847856.	12.0
	G04073	434825.	6763030.	11.0
PJ6	G03164	438800.	6751850.	11.0
PJ6	G02512	402000.	6790800.	11.0
PJ3	G05813	470300.	6775900.	10.0
PJ3	G04718	452900.	6868500.	10.0
YLA	G04129	468637.	6885504.	10.0
	G04075	425245.	6762818.	10.0
	G04058	424526.	6769431.	10.0
PJ3	G04047	479595.	6779510.	10.0
PJA	G03156	497400.	6758600.	10.0
PJ6	G03152	399300.	6793100.	10.0
	G03144	476200.	6772000.	10.0
PJ3	G02480	464341.	6774395.	10.0

Supplement: Table 10
Samples with Abundance Levels > 95 Percentile

SOUTH MURCHISON LATERITE (LN LP CN CP MS)
Ge1 (ppm) (OES)

Anomaly	Sample	Easting	Northing	Abundance
PJ3	G04694	480250.	6780500.	20.0
PJ3	G04693	479500.	6780400.	10.0
PJ3	G03714	479864.	6779972.	10.0
NGB	G03606	514794.	6726273.	10.0
PJ3	G03715	479324.	6779817.	8.0
PJ3	G04082	435087.	6764263.	6.0
PJ6	G03152	399300.	6793100.	6.0
NGB	G03608	518022.	6726115.	5.0
NGB	G03601	515738.	6727965.	5.0
PJ3	G03713	480943.	6781051.	4.0
PJ3	G03344	480270.	6779973.	4.0
NG1	G02429	508620.	6741977.	4.0
PJ8	G04710	438000.	6759350.	3.0
PJ3	G04703	425500.	6768150.	3.0
KL1,2	G04622	575677.	6842219.	3.0
YLA	G04139	471216.	6890281.	3.0
PJ3	G03721	477704.	6779045.	3.0
NGB	G03603	516816.	6729348.	3.0
PJ3	G03335	474871.	6776731.	3.0
YLB	G03168	445300.	6865000.	3.0
PJ3	G03147	476800.	6775100.	3.0
PJ3	G03146	482900.	6774500.	3.0
PJ3	G03145	478400.	6773700.	3.0
KL8	G02612	578589.	6871437.	3.0
KL8	G02611	578713.	6869590.	3.0
YL10	G02561	453607.	6858067.	3.0
YL10	G02559	454414.	6860686.	3.0
	G02489	451112.	6772499.	3.0
NG1	G02412	511042.	6739974.	3.0

SOUTH MURCHISON LATERITE (LN LP CN CP MS)
Ga (ppm) (OES)

Anomaly	Sample	Easting	Northing	Abundance
	G04718	452900.	6868500.	80.0
	G04068	420923.	6763404.	80.0
YLC	G02527	425222.	6828991.	80.0
PJ3	G04696	478400.	6780250.	60.0
YLF	G04164	362675.	6885370.	60.0
	G04157	451741.	6882063.	60.0
PJ3	G04046	476356.	6777504.	60.0
YLB	G02556	443637.	6866179.	60.0
YLD	G02544	447964.	6842040.	60.0
PJ3	G02480	464341.	6774395.	60.0
	G02419	511039.	6736281.	50.0
KLC	G02593	567773.	6837959.	45.0
	G02558	454307.	6853146.	45.0

Supplement: Table 10
Samples with Abundance Levels > 95 Percentile

SOUTH MURCHISON LATERITE (LN LP CN CP MS)
W2 (ppm) (XRF)

Anomaly	Sample	Easting	Northing	Abundance
PJ3	G05816	472450.	6777000.	5884.0
KL8	G02612	578589.	6871437.	1483.0
YLA	G04137	475729.	6884289.	162.0
PJ3	G03352	468660.	6775330.	86.0
PJ3	G03349	474463.	6777807.	86.0
YLB	G02556	443637.	6866179.	76.0
PJ3	G03354	464745.	6774703.	72.0
KL8	G03321	578723.	6871129.	61.0
PJ3	G03350	473923.	6777806.	60.0
PJ3	G03348	473383.	6777497.	60.0
PJ3	G03720	475813.	6778425.	57.0
YLB	G03169	444000.	6865500.	40.0
YLB	G06938	443600.	6865900.	38.0
KL1,2	G04893	575262.	6840991.	38.0
PJ3	G03339	475682.	6776425.	38.0
YLB	G03168	445300.	6865000.	38.0
KL1,2	G04170	575539.	6841759.	36.0
PJ3	G03707	476760.	6777966.	36.0
PJ3	G03330	470821.	6775798.	31.0
PJ3	G03347	481349.	6781052.	30.0
PJ3	G03715	479324.	6779817.	29.0
PJ3	G03711	474734.	6777654.	29.0
PJ3	G02478	471359.	6776877.	29.0
NG3	G02450	543397.	6784832.	29.0
KL8	G04897	578168.	6869440.	28.0
PJ3	G04694	480250.	6780500.	28.0
KL8	G02611	578713.	6869590.	28.0
PJ3	G03705	472303.	6777186.	27.0

SOUTH MURCHISON LATERITE (LN LP CN CP MS)
Ba1 (ppm) (ICP FS)

Anomaly	Sample	Easting	Northing	Abundance
KLD	G04625	573515.	6822474.	4317.0
KLF	G02613	587673.	6902765.	3067.0
KL1,2	G04888	578818.	6844507.	1879.0
YLB	G06935	446750.	6867800.	1802.0
KL1,2	G03066	573400.	6837600.	1620.0
YLB	G06937	443400.	6867000.	1564.0
	G02447	547900.	6794663.	1174.0
NG3	G02453	543390.	6782832.	1152.0
	G02434	502155.	6741826.	1076.0
KL1,2	G04891	575535.	6841143.	857.0

SOUTH MURCHISON LATERITE (LN LP CN CP MS)
Zr1 (ppm) (ICP FS)

Anomaly	Sample	Easting	Northing	Abundance
	G04664	444600.	6696000.	1592.0
	G04028	519997.	6777972.	1438.0
	G04673	447250.	6696500.	1244.0
	G04665	448000.	6694000.	1204.0
	G04675	447500.	6727900.	1140.0
	G04668	448700.	6699500.	1124.0
	G04006	509458.	6778447.	1071.0
	G04004	512567.	6779676.	991.0
	G04656	441800.	6707500.	973.0
	G04652	440300.	6709900.	967.0

SOUTH MURCHISON LATERITE (LN LP CN CP MS)
Nb3 (ppm) (XRF)

Anomaly	Sample	Easting	Northing	Abundance
	G02471	494065.	6759214.	125.0
	G04028	519997.	6777972.	55.0
PJ9	G04105	423279.	6774193.	53.0
PJA	G03161	496000.	6756500.	53.0
	G04675	447500.	6727900.	49.0
PJ3	G02480	464341.	6774395.	44.0
PJ3	G03139	464050.	6773750.	42.0
	G03124	453700.	6721850.	42.0
	G04055	434396.	6767183.	41.0
	G04004	512567.	6779676.	41.0
	G04006	509458.	6778447.	40.0
	G03158	496900.	6759500.	40.0
	G04665	448000.	6694000.	39.0
	G04057	430079.	6766696.	38.0
PJ3	G04694	480250.	6780500.	37.0
PJ3	G04050	484862.	6782135.	37.0
	G04656	441800.	6707500.	35.0
	G04084	430358.	6765159.	35.0
NG1	G02408	512127.	6747360.	34.0
	G04718	452900.	6868500.	33.0
	G04659	436600.	6701000.	33.0
	G04068	420923.	6763404.	33.0
PJ3	G03136	467300.	6774000.	32.0
	G03090	474350.	6677200.	32.0
PJ3	G02472	473994.	6773188.	32.0
PJ9	G04715	423000.	6773300.	31.0
PJ9	G08079	423600.	6774600.	30.0
PJA	G03160	496300.	6758600.	30.0

Supplement: Table 11
Lower (<2) and Upper (>98) Percentiles of
Principal Component Scores

SOUTH MURCHISON LATERITE
(LN LP CN CP MS)
PRINCIPAL COMPONENT #1

Ga, Nb Association
< 2 Percentile

Anomaly	Sample	Easting	Northing	PCA Score
PJA	G02471	494065.	6759214.	-.1654
	G03119	469300.	6714700.	-.1082
	G03159	497000.	6758100.	-.0986
	G04157	451741.	6882063.	-.0961
PJ3	G02480	464341.	6774395.	-.0917
YLC	G02527	425222.	6828991.	-.0899
PJA	G03161	496000.	6756500.	-.0893
PJ3	G04718	452900.	6868500.	-.0886
	G04068	420923.	6763404.	-.0880
PJ3	G02472	473994.	6773188.	-.0843
YLC	G02531	415229.	6821998.	-.0832
PJA	G03156	497400.	6758600.	-.0817
	G03140	465400.	6773700.	-.0805
	G02504	440682.	6752444.	-.0787
	G03157	495100.	6759800.	-.0785

Co, Cr, Ni, Cu, Fe, Zn Association
> 98 Percentile

Anomaly	Sample	Easting	Northing	PCA Score
KLB	G04182	581595.	6892652.	.1914
KL1,2	G04171	576907.	6843135.	.2115
NGA	G02435	523398.	6789507.	.2218
KLA	G04192	577959.	6900062.	.2300
	G04622	575677.	6842219.	.2398
KL1,2	G04893	575262.	6840991.	.2406
	G04023	504466.	6796916.	.2482
	G04890	576078.	6841139.	.2574
KL1,2	G04623	576690.	6843351.	.3345
	G04203	593899.	6895639.	.3525
	G04190	575642.	6900754.	.3567
	G04040	497972.	6786515.	.3639
NGA	G02438	524348.	6791044.	.3988
	G04133	475447.	6889367.	.4454

SOUTH MURCHISON LATERITE
(LN LP CN CP MS)
PRINCIPAL COMPONENT #2

Mn, Be Association
< 2 Percentile

Anomaly	Sample	Easting	Northing	PCA Score
YLE	G02550	439922.	6847234.	-.2679
	G04133	475447.	6889367.	-.1983
	G04190	575642.	6900754.	-.1940
	G03119	469300.	6714700.	-.1736
YLB	G02585	438570.	6871847.	-.1474
	G02501	448545.	6772796.	-.1461
	G02523	433062.	6834425.	-.1421
	G04203	593899.	6895639.	-.1343
YL10	G04716	455900.	6864350.	-.1327
YLC	G02531	415229.	6821998.	-.1310
	G04168	355371.	6880359.	-.1302
KL1,2	G04891	575535.	6841143.	-.1254
	G02479	465200.	6776250.	-.1185
	G04154	459379.	6880860.	-.1147
	G02494	444451.	6781487.	-.1141

Sn, Fe, V, Bi Association
> 98 Percentile

Anomaly	Sample	Easting	Northing	PCA Score
	G04073	434825.	6763030.	.0956
PJ3	G03714	479864.	6779972.	.0956
PJ3	G04047	479595.	6779510.	.1007
PJ6	G03148	400100.	6792100.	.1013
PJ9	G04105	423279.	6774193.	.1032
PJ3	G04046	476356.	6777504.	.1041
PJ3	G04718	452900.	6868500.	.1077
PJ3	G04693	479500.	6780400.	.1204
	G06085	496580.	6816350.	.1644
KL8	G02612	578589.	6871437.	.1665
PJ6	G03152	399300.	6793100.	.1803
PJ3	G05816	472450.	6777000.	.1882
KL1,2	G04694	480250.	6780500.	.2155
	G06084	496750.	6816000.	.7081

Supplement: Table 11
Lower (<2) and Upper (>98) Percentiles of
Principal Component Scores

SOUTH MURCHISON LATERITE
(LN LP CN CP MS)
PRINCIPAL COMPONENT #3

Cr, V, Fe Association
< 2 Percentile

Anomaly	Sample	Easting	Northing	PCA Score
PJ2	G02462	490937.	6791682.	-.0811
PJ3	G03711	474734.	6777654.	-.0747
YL1	G02574	478213.	6868601.	-.0702
YL1	G04147	476840.	6874137.	-.0674
NG4	G02458	529068.	6785185.	-.0670
	G03346	481754.	6781206.	-.0624
	G03176	477100.	6868750.	-.0620
	G04061	417493.	6771075.	-.0614
PJ3	G03716	480000.	6780300.	-.0586
KLG	G04020	507311.	6801377.	-.0582
	G04035	488104.	6783369.	-.0579
	G04616	512517.	6734740.	-.0575
YL1	G04145	478198.	6876293.	-.0574
	G02445	531651.	6790411.	-.0571
	G02436	532283.	6785600.	-.0561

Pb, Mn Association
> 98 Percentile

Anomaly	Sample	Easting	Northing	PCA Score
KL1,2	G04891	575535.	6841143.	.1507
KLE	G04033	502979.	6804918.	.1635
YLB	G02585	438570.	6871847.	.1847
YLC	G02531	415229.	6821998.	.1887
PJ9	G04705	423700.	6774950.	.1963
	G04190	575642.	6900754.	.1986
YL10	G02583	453578.	6865452.	.1990
	G04040	497972.	6786515.	.2012
PJ6	G03152	399300.	6793100.	.2260
	G04133	475447.	6889367.	.2710
PJ3	G05816	472450.	6777000.	.3150
YLE	G02550	439922.	6847234.	.3496
	G04066	423988.	6769119.	.4229
	G06084	496750.	6816000.	.4461

SOUTH MURCHISON LATERITE
(LN LP CN CP MS)
PRINCIPAL COMPONENT #4

Nb, Ag Association
< 2 Percentile

Anomaly	Sample	Easting	Northing	PCA Score
PJ6	G03152	399300.	6793100.	-.2222
PJA	G02471	494065.	6759214.	-.1953
PJ6	G03148	400100.	6792100.	-.1284
PJ9	G04105	423279.	6774193.	-.1244
	G02513	399073.	6792628.	-.1228
	G04068	420923.	6763404.	-.1134
YLC	G02527	425222.	6828991.	-.1120
	G04133	475447.	6889367.	-.1091
PJ3	G02480	464341.	6774395.	-.1082
YLE	G02550	439922.	6847234.	-.0943
PJ3	G04718	452900.	6868500.	-.0883
PJ3	G04046	476356.	6777504.	-.0869
	G04055	434396.	6767183.	-.0814
PJ9	G04715	423000.	6773300.	-.0796
	G04057	430079.	6766696.	-.0771

Mo, W Association
> 98 Percentile

Anomaly	Sample	Easting	Northing	PCA Score
PJ3	G03350	473923.	6777806.	.0895
PJ3	G03354	464745.	6774703.	.0907
	G06084	496750.	6816000.	.0945
PJ3	G03347	481349.	6781052.	.0955
	G05801	446900.	6869500.	.0987
KLC	G02589	566152.	6839661.	.1071
	G05807	475300.	6778300.	.1081
PJ3	G03348	473383.	6777497.	.1289
KL8	G03322	578188.	6872517.	.1338
	G05806	474700.	6778000.	.1369
PJ3	G03705	472303.	6777186.	.1440
	G05805	474450.	6777900.	.1900
KL8	G02612	578589.	6871437.	.2028
PJ3	G05816	472450.	6777000.	.7663

15

Supplement: Table 11
Lower (<2) and Upper (>98) Percentiles of
Principal Component Scores

SOUTH MURCHISON LATERITE
(LN LP CN CP MS)
PRINCIPAL COMPONENT #5

Ni, Ga Association
< 2 Percentile

Anomaly	Sample	Easting	Northing	PCA Score
PJ3	G05816	472450.	6777000.	-.2879
KL1,2	G04623	576690.	6843351.	-.1819
	G04190	575642.	6900754.	-.1629
	G04622	575677.	6842219.	-.1568
KL1,2	G04893	575262.	6840991.	-.1446
KL1,2	G04891	575535.	6841143.	-.1426
	G04890	576078.	6841139.	-.1230
KL1,2	G04170	575539.	6841759.	-.1210
	G04895	575254.	6839760.	-.1139
	G04203	593899.	6895639.	-.1132
KL1,2	G04171	576907.	6843135.	-.1115
	G03066	573400.	6837600.	-.1110
KL1,2	G04896	574714.	6840225.	-.1091
KL8	G02612	578589.	6871437.	-.1016
PJ3	G04718	452900.	6868500.	-.0979

As, Sb Association
> 98 Percentile

Anomaly	Sample	Easting	Northing	PCA Score
NGB	G03601	515738.	6727965.	.0810
YL1	G02573	482029.	6866760.	.0922
	G04009	505273.	6785836.	.0929
PJ2	G04043	495266.	6790915.	.0957
NGA	G02438	524348.	6791044.	.0973
NGB	G03606	514794.	6726273.	.0988
KLB	G04183	579152.	6891894.	.1128
PJ6	G03152	399300.	6793100.	.1146
	G04040	497972.	6786515.	.1150
PJ3	G03343	479595.	6779202.	.1446
KLE	G06083	501500.	6808000.	.1967
NG1	G02409	515091.	6746741.	.2086
	G04023	504466.	6796916.	.4142
	G04066	423988.	6769119.	.4556

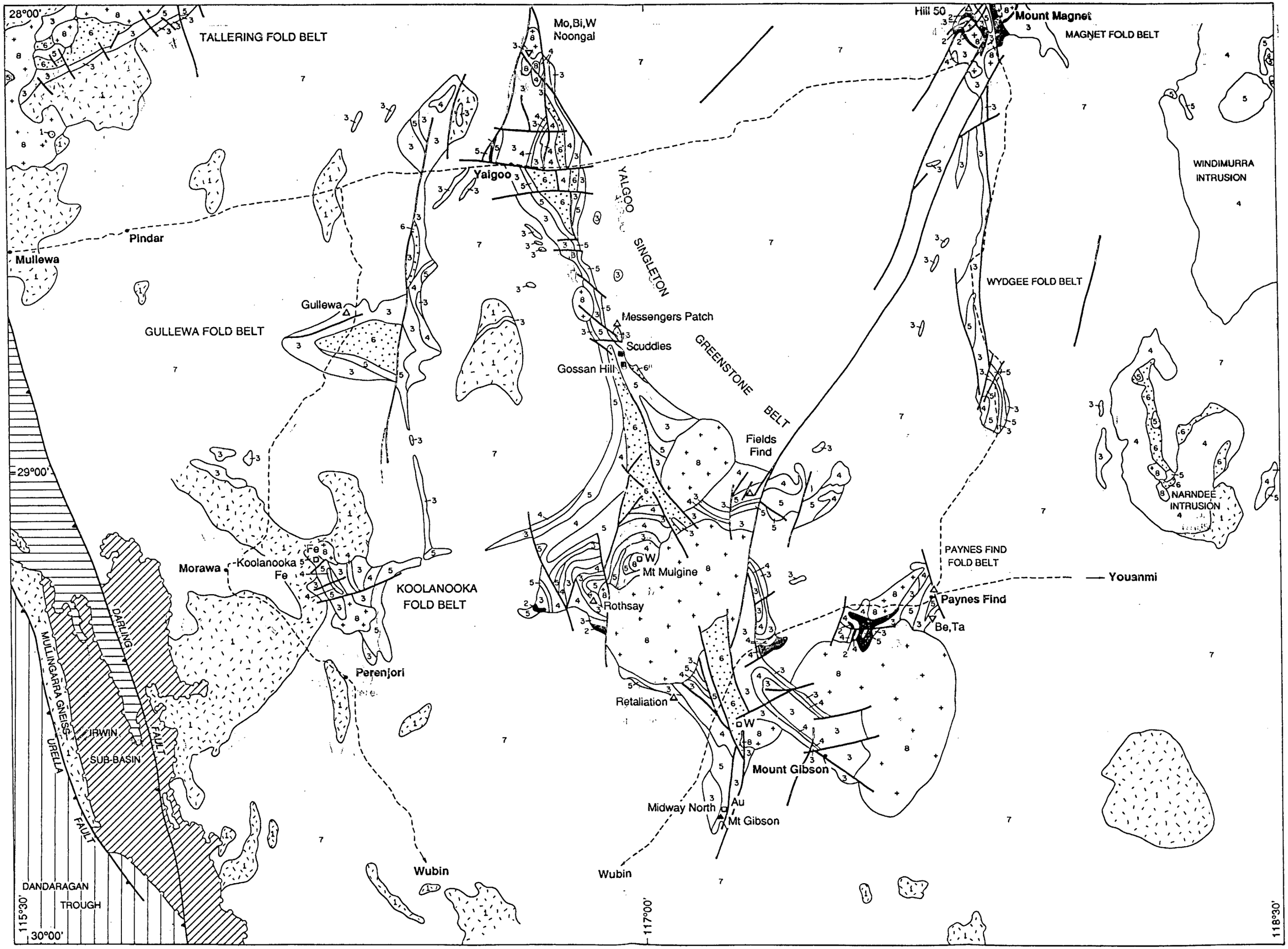

CRC LEME Open File Report 8 - **Figure 1**